Appendix F.

AIMS Regional Shoals and Shelf Assessment (Heyward et al. 2017)

Includes Addendum:
Regional Biodiversity Patterns and Connectivity Amongst the Submerged Shoals and Banks in Relation to the Area of Influence from a Hypothetical Uncontrolled Release

BAROSSA ENVIRONMENTAL BASELINE STUDY 2015
AIMS FINAL REPORT

Regional Shoals & Shelf Assessment 2015

Authors:
Andrew Heyward, Ben Radford, Mike Cappo, Mary Wakeford, Rebecca Fisher, Jamie Colquhoun, Mark Case, Marcus Stowar, Karen Miller

PRODUCED FOR
ConocoPhillips Australia Pty Ltd
Contract No. 251834.0-MSA-COMP-2.0

Australian Government | Australian Institute of Marine Science

PERTH
April 2017
Rev 1

BAROSSA ENVIRONMENTAL BASELINE STUDY 2015
AIMS FINAL REPORT

Australian Institute of Marine Science
PMB No 3
Townsville MC Qld 4810

University of Western Australia Oceans Institute (M096)
35 Stirling Hwy
Crawley WA 6009

PO Box 41775
Casuarina NT 0811

This report should be cited as: A Heyward *et al.* 2017; Barossa Environmental Baseline Study, Regional Shoals and Shelf Assessment 2015 Final Report. A report for ConocoPhillips Australia Exploration Pty Ltd by the Australian Institute of Marine Science, Perth 2017. 143pp

Corresponding Author: Dr Andrew Heyward a.heyward@aims.gov.au

Revision History
Issue Rev 1 Apr 2017
Issue Rev 0 Oct 2016
Draft Rev B Sept 2016
Draft Rev A June 2016

Acknowledgments: This survey relied on the professionalism and support of RV Solander's Master & crew. We gratefully acknowledge Anne Kennedy for exemplary use of the multibeam system and Shaun Hahn for maintenance of the towed video system. Olwyn Hunt provided administrative support for the field program and report production.

DISCLAIMER

Contents

List of Figures

List of Tables

Summary

This report presents final results from seabed biodiversity surveys of benthos and associated fish, by the Australian Institute of Marine Science (AIMS) in collaboration with ConocoPhillips, that were undertaken as part of the Barossa marine studies program. The surveys, conducted in October 2015, sampled five principle locations of regional interest, consisting of Evans, Tassie and Blackwood Shoals, the closest shoals to the Barossa Field, as well as two mid-shelf seabed locations adjacent to Goodrich Bank and Cape Helvetius, relevant to a potential gas export pipeline route.

The submerged shoals featured habitats consistent with other outer shelf shoals in the North and North-west marine regions, including the Margaret Harries Banks, the Sahul Banks and the Karmt Shoals. Analysis of the full benthic data set available from Evans, Tassie and Blackwood Shoals, including data from 9,961 high resolution still images of the seabed, provided a detailed, quantitative characterisation of the habitats encountered. The major elements of shoal plateau regions were light-dependent algal and coral assemblages, interspersed with sand and rubble areas which varied in extent between shoals. Average coral cover was similar between Evans and Tassie Shoals at around 9% of the total plateau area surveyed, but higher at Blackwood Shoal, where coral habitat was a consistent feature across the very small shoal plateau, with a mean of 25%. The three shoals closest to the Barossa Field support diverse tropical reef biota, with many species in common, but with each shoal somewhat different in character. All three appeared to be in healthy condition at the time of the survey.

The fish fauna on Evans and Tassie Shoals comprises a mix of shelf-based species normally found on Indo-Pacific reefs and some "oceanic" species. Economically important fishes, such as red emperor and gold-band snapper were encountered in deeper waters, but not in the large numbers we expected from such habitats remote from Australian ports. Shovelnose rays and hammerhead sharks, known to be prized in the shark-fin trade, were also relatively rare. In addition, the behaviour of large-bodied cods, snappers and emperors seemed shy in relation to approaching the bait, based on our experience in the North-West Shelf (NWS) and Great Barrier Reef. These observations are consistent with a fish community exposed to fishing pressure.

Species richness in the fish community was influenced most by the calcareous reef composition of the substratum, and the percentage cover of hard coral on this substratum type. Depths shallower than approximately 30 m had higher, steeply rising, richness, and bare seabeds had lower than average richness. Fish abundance was influenced most by the presence of any epibenthos on the seafloor (not just coral) and by calcareous reef composition of the substratum. Total fish abundance was above average for Stereo Baited Remote Underwater Videos (SBRUVS) where there was more than 20% of the seabed in the field of view covered by any category of epibenthos. Depth had a lesser influence, but fish abundance was below average in deeper waters and above average in shallows under 30 m.

It was clear that most of the "pattern" in diversity and abundance in the fish dataset was concentrated in the one-third of the SBRUVS set in shallow shoal waters where coral cover was highest. However, species accumulation curves for the five assemblages were far short of an

asymptote – implying that more SBRUVS sets in all habitats would produce more species. Where repeat surveys have been conducted on other shoals by AIMS, additional species have been observed, with total recorded fish species incrementing around 10% with each additional survey. Tassie Shoal is much smaller than Evans Shoal, yet they both supported only three distinct fish assemblages in the analysis. This is perhaps a function of the number of samples taken, with additional sampling possibly able to resolve finer scale differences in assemblages, but it supports further the notion that diversity increases sharply with coral cover and with decreasing depth. Tassie Shoal has outstanding fish diversity and abundance in comparison with shoals and reef bases at similar depths around Australia. It has the highest median species richness yet recorded by AIMS using the same sampling techniques. There were three new species records for Australia for fish known to occur in Indonesia.

The mid-shelf areas adjacent to Goodrich Bank and Cape Helvetius were turbid, typically had large areas of bare seabed, but supported patchy filter feeders habitats associated with limited areas of consolidated substrate. Sponges tended to be the dominant fauna, consistent with other studies in turbid shelf areas in this region, with gorgonian soft corals generally making lesser contributions to the mixed filter feeder communities. The sediment data collected during this project and a review of sediment data for the region suggest a complex spatial pattern of reworked old terrigenous sediments, likely related to the drowned coastal features across this region, and in situ production of carbonates, which may increase in importance in shallow waters as well as with distance from the coast.

Regional context

The shoals biodiversity and habitat data were assessed in the context of AIMS regional database covering 20 shoals located from west to east across the North and North-west marine regions.

The patterns of benthic habitat at Goodrich Bank and Cape Helvetius were consistent with the regional community analysis and regional spatial model where the majority of the area modelled consisted of predominantly bare areas, with insufficient biota to allow a discrete category to be modelled as a habitat class (Model Category "None" -69.24%), interspersed with areas where infauna, epibenthic fauna (Burrows/ Crinoids; 22.91%) and to a lesser extent filter feeding sessile organisms like sponges and seafans (6.44%) were the dominant contributors to benthic communities. Coral reef communities were associated with the shallower reefs, shoals and banks particularly as they moved away from the turbid coastal fringe. However these habitats made up a small proportion of the model spatial extent. Caution should be used interpreting the regional model beyond the extent of the surveyed data. There are large areas where there is no validation information available so estimates of model accuracy and error are not possible to calculate without additional field data. It should also be noted with caution that while over the entire regional model performed well for most habitat categories, the "None" category had the poorest performance most frequently under predicting filter feeder and Halimeda communities which by their nature can be discrete, stochastic and challenging to model.

The benthic habitats at all three shoals were consistent with other outer-shelf shoals. Both Evans and Tassie Shoals were similar in terms of coral cover and mid-ranking in a regional context, having similar coral community composition on their shallow plateaus but with Evans featuring a greater

abundance of foliaceous hard coral below 30 m depths. In contrast, Blackwood Shoal, although the smallest of the three shoals studied, featured some of the highest levels of coral yet observed. Coral cover on Blackwood was on par with outer shelf shoals in the central area of the Oceanic Shoals bioregion, such as Kepah and Krill, situated 370 km west near the western lateral boundary of the Joint Petroleum Development Area (JPDA).

Cluster analysis of quantitative benthic data indicated similarities among shoals close together for some habitat attributes, but also found that some benthic community components, for example hard coral assemblages, could be shared by shoals at opposite ends of the bioregion. The quantitative measures of major habitat types and fine scale detail of coral abundance and diversity point to strong regional similarities among shoals. The available information indicates that each shoal has its own benthic community character, but that many coral species occur on shoals across the region. The abundance of particular coral species varied with depth and location. A dense band of foliaceous coral, approximately 300 m wide in places, was a notable feature in 40-60 m depths at Evans Shoal, but has also been observed elsewhere, including a small amount on Tassie Shoal at shallower depth and on reefs further west. The presence of an isolated very large colony of the coral *Pavona clavus* on Evans Shoal was unusual in terms of its size, but a smaller example was present on Tassie Shoal and another large example was previously observed by AIMS at Seringapatam Reef. The fish abundance and diversity at Evans and Tassie Shoals was most similar to shoals in the Margaret Harries Banks group, 100 km away, and other shoals >600 km to the southwest. Given the strong ocean currents throughout this bioregion, including the Indonesian Throughflow, connectivity between shoal features may be shaping the broad similarity in community composition. The status of the biota on each shoal may reflect varying connectivity, to some degree, but also varying disturbance event histories, such as cyclone or storm related damage and coral bleaching.

Conclusion

This report provides the final results from the October 2015 study and establishes baseline information relevant to the Barossa Field. It provides a general characterisation of habitat distributions and dominant biota on shoals and mid-shelf areas surveyed, within the context of similar studies throughout the region. The mid-shelf areas display limited amounts of macro-epibenthic life, restricted in distribution to locations with abrupt changes in bathymetry or the availability of suitable consolidated substrate to support the dominant filter feeders such as sponges and soft corals. This patchy distribution is consistent with other surveys in the region and is likely to be a widespread, repeated pattern linked to the underlying geology and complex bathymetry that are a legacy of the drowned coastal shelf area.

The submerged shoals closest to the Barossa Field were further offshore in much clearer water. While filter feeding communities exist there in the deeper zones on the sides of the shoals, their most striking attribute is a rich biodiversity more similar to coral reefs, driven by light in the upper regions and across the plateaux. This is also consistent with many other shoals in the same bioregion, although each individual shoal has its own character.

While the survey recorded the major habitat types and a large portion of the species present, it is clear that the biodiversity will continue to be further defined as part of additional regional survey efforts over time. Future repeats of this survey would likely produce a very similar broad characterisation of the

seabed biodiversity, although change in abundance of dominant species and distribution of habitats is possible, with variability over time likely to be a natural attribute of these ecosystems. These systems, particularly the shallower habitats, may also be subject to larger scale changes from acute, but less predictable, natural disturbances such as a severe storms or elevated seawater temperature anomalies.

Background

ConocoPhillips Australia Exploration Pty Ltd (ConocoPhillips), as proponent on behalf of current and future joint venturers, are proposing to develop the gas and condensate reserves in the Barossa field and surrounds located approximately 300 kilometers (km) north of Darwin, Northern Territory (NT).

The retention lease permits NT/RL5 (Barossa) and NT/RL6 (Caldita) are located in the Bonaparte Basin, in Commonwealth waters offshore of the Northern Territory (NT). If results from the appraisal campaign support the business case for commercialisation of the Caldita-Barossa field, ConocoPhillips will evaluate a number of conceptual development options.

To facilitate the environmental approvals process for any development concept, a robust understanding of the existing state of the key environmental values of the Barossa field and surrounds will be necessary. This understanding will be gained from a series of studies and surveys to assess and monitor the baseline state of environmental factors such as water quality, sediment quality, underwater noise, metocean conditions and benthic habitats within the Barossa field and across a broader geographical area. Phased studies assessing these factors commenced in June 2014.

As part of that marine studies program, this study surveyed the seabed and associated biota at a number of submerged shoals near the edge of the continental shelf, with Evans Shoal 60 km to the west of the Barossa field, Tassie Shoal 70km to the southwest and at more distant, bathymetrically complex areas of the mid-continental shelf, through which a potential pipeline would pass.

Based on other shoals further west in the same bioregion, the shallow shelf-edge shoals closest to the Barossa field have the potential to support diverse tropical reef life, with significant benthic primary producer habitat, including reef building corals, macroalgae and seagrass. Following shoal assessments related to the Montara uncontrolled release the submerged shoals of this bioregion have been regarded as sensitive, key environment features (see Heyward et al. 2011). Shoreward from the shoals, the much more extensive seabed of the mid-continental shelf is structurally complex, with numerous ridges, shoals, valleys and plains. A number of studies conducted jointly in this more turbid region by Geoscience Australia and AIMS (e.g. Anderson et al, 2011; Nichol et al, 2013) have shown that the complex mid-shelf region supports patchily distributed filter feeders more than primary producer habitats seen on the clearer water shoal areas.

Submerged shoals assessments by AIMS began using a variety of data sources in the 1990s (Heyward et al, 1997). A more consistent methodology and quantitative analysis of the shoal benthic communities has been implemented by AIMS since 2009, beginning with survey of nine shoals at the western end of the bioregion following the Montara uncontrolled release (Heyward et al, 2012). Subsequently, additional shoals across the bioregion have been assessed using consistent methods, providing comparable information spanning the region.

1 Methods

The field survey methods are described in full in the December 2015 Interim Report (Heyward et al, 2015), with description of key aspects repeated below.

In support of the marine studies program, a research cruise was undertaken by AIMS during September-October, 2015. Areas identified for assessment included two mid-shelf regions and two submerged shoals. Multibeam and towed video were used at all locations to map the seabed and classify seabed habitats. Replicate sediment samples (collected using a Smith McIntyre Grab) and Conductivity Temperature Depth (CTD) casts were taken within each mid-shelf area to provide additional environmental data. At the shoals, sampling also included the fish communities, which was undertaken using stereo Baited Remote Underwater Video Stations (SBRUVS).

The mid-shelf locations were separate areas along a potential cross-shelf pipeline route from the Barossa field to the existing ConocoPhillips operated Bayu-Undan to Darwin pipeline. The southernmost of these was to the west of Cape Helvetius, at the southwest corner of Bathurst Island. The second area was midway to the shelf break, adjacent to and off the western side of Goodrich Bank. Evans and Tassie Shoals, lying further northwest on the outer shelf, were selected for investigation as larger submerged shoals, closest to the Barossa field. An initial towed video inspection was also undertaken at the much smaller Blackwood Shoal, lying a few kilometres to the west of Evans Shoal. In total the survey sampled in five principle locations, consisting of Evans, Tassie and Blackwood Shoals, open shelf adjacent to Goodrich Bank and open shelf adjacent to Cape Helvetius. The location of study areas and the vessel track for the voyage are shown in Figure 1.

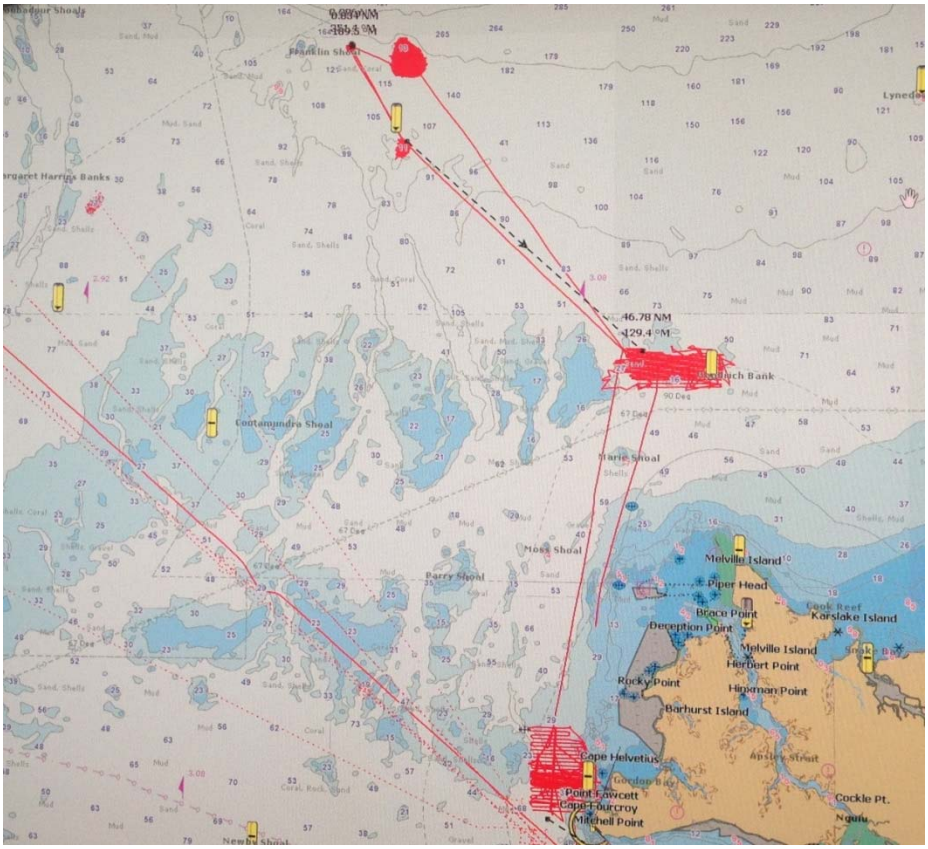

Figure 1: Location of shoal and shelf study sites. Track of the RV Solander during AIMS cruise 6251.

1.1 Field sampling – Benthic habitats

1.1.1 Sampling design

The location of seabed video transects was based on the textural analysis of existing LIDAR (Royal Australian Navy), single beam bathymetry (Geosciences Australia) and side-scan datasets (ConocoPhillips) using Generalized Random-Tessellation Stratified (GRTS) Survey Design (Stevens and Olsen 2004). This provided a habitat-stratified, spatially weighted sampling design covering the area of interest. Maps showing sampling completed on the three shoals are in Figures 15, 21 and 27. Maps showing sampling completed on the two mid-shelf areas are in Figures 7 and 9. Details of all sampling events are provided in Appendix 1.

1.1.2 Multibeam

The bathymetric and terrain surveys of the five study areas were conducted in September 2015 using a shipborn Reason 7125v2 multibeam with a POSMV-V5 motion reference unit. Setup of the multibeam echosounder, realtime field data and preparation of derived datasets are described in Heyward et al (2015).

For areas bisecting the planned pipeline route, multibeam was captured at 500m spacing and interpolated to a 50m pixel. For Tassie, Evans and Blackwood shoals, multibeam was captured allowing for a 20% overlap in beam, resulting in full coverage across the three shoals. The data was post processed in CARIS HIPS/SIPS to a two metre pixel size

1.1.3 Towed video

The AIMS towed video system comprises a towed camera platform sending a live camera feed to a vessel-based, realtime image classification system (see Heyward et al. 2011). The towed platform supports a forward-facing video camera with lights, together with a downward-facing high resolution still camera and strobe system programmed to take sequential still images at fixed time intervals of 10 seconds. The towed platform was deployed over the stern of the vessel, maintained within a metre of the seabed and towed at 1-2 knots (1.5 nominal) until a minimum distance of 1.5 km was covered in a continuous line transect. On the vessel, a computer-based towed video program managed collation of position, depth, and operator-derived habitat classification data, which was captured in real time as an operator interpreted the live video feed, and then archived for subsequent spatial analysis. At the completion of a transect, the tow platform was retrieved to the vessel deck, still camera images downloaded and the camera systems serviced as required while the vessel steamed to the next transect station.

1.1.4 Still photo analysis

The downward-looking still images were geo-referenced during post-processing then analysed using a point-intercept approach. The number of images collected and used in the analysis was proportional to the size of the shoal and total length of towed video transect conducted. After sorting and discarding poor quality photos, a total of 9,921 images from the three shoals were analysed for this report (Evans = 7,673; Tassie = 1,963; Blackwood = 285; Table 1). Still images from Cape Helvetius and Goodrich Bank towed video transects were not scored.

Information on benthic biota at each shoal was extracted from images using a point intercept approach with the AIMS Reefmon software (Jonker et al., 2008). All images were analysed using the Reefmon database system, with five overlaid points classified per photo and data logged against transect, depth and position. The benthos under each superimposed point was identified to the highest possible taxonomic classification and/or morphotype. Categories of benthos include: hard corals, soft corals, algae, seagrass, sponges, abiotic and other animals (Table 2). Hard corals were

potentially identified to species but more typically to genus or genus morphotype, e.g. *Acropora* tabulate. Reefmon has added classification categories appropriate to the region or habitat, e.g. sponge morphotypes categories were expanded to include the common sponge morphologies encountered in deeper water tropical shoals i.e. hollow massive, simple massive, erect branching, simple erect, erect laminar and clathrate. Benthos was classified as seagrass only when the point fell on a seagrass leaf, rhizome or stalk. Crustose coralline algae (CCA) was regularly encountered during the classification process. When CCA was observed on rocks, consolidated pavement or reef-type substrate it was classified as CCA. However when CCA occurred on free rubble and small stones, with a nodule appearance, it was classified as Rhodoliths.

Table 1. Summary of the number of images used to quantify benthic community composition at Evans, Tassie and Blackwood Shoals across the three depth ranges.

Depth Range	Evans	Tassie	Blackwood	
<20m	1134	898	88	
20-40m	5105	330	166	
>40m	1434	735	31	
Totals	7673	1963	285	9921

Table 2. Benthic broad-scale and fine-scale image classification categories used for analysis of Evans, Tassie and Blackwood Shoals still images.

Broad-scale category	Fine-scale category	Benthic groups included
Algae	Macroalgae	Brown, green and red algae; any other algae described as macroalgae. Genera include: *Lobophora, Peyssonnelia, Dichotomaria, Caulerpa, Dictyota*
	Halimeda	Mostly *Halimeda* spp., small amounts of other unidentified articulated calcareous algae
	Rhodolith	Rhodoliths
	Padina	*Padina* spp.
Consolidated Reef		Consolidated substrate, reefal substrate, turf and crustose coralline algae (algal turf community), filamentous algae on consolidated substrate
Hard Coral	*Acropora* – branching, digitate, corymbose and table	Branching, digitate, corymbose and table forms of coral from the genera *Acropora*
	Branching	All non-*Acropora* branching scleractinian corals. Genera include: *Duncanopsammia* (Dendrophylliidae); *Hydnophora* (Merulinidae); *Seriatopora* (Pocilloporidae); *Porites* (Poritidae)
	Encrusting	Encrusting growth forms from all scleractinian corals. Genera include : *Montipora, Astreopora, Isopora* (Acroporidae); *Pavona* (Agariciidae); *Turbinaria* (Dendrophylliidae),

Broad-scale category	Fine-scale category	Benthic groups included
		Cyphastrea, Goniastrea, Echinopora, Favia, Platygyra, Favites (Faviidae); *Hydnophora, Merulina* (Merulinidae); *Galaxea* (Oculinidae); *Mycedium, Echinophyllia, Oxypora* (Pectiniidae); *Porites* (Poritidae)
	Foliose	Foliose growth forms from all scleractinian corals. Genera include: *Montipora* (Acroporidae); *Pachyseris, Leptoseris, Pavona* (Agaridiidae); *Turbinaria* (Dendrophylliidae); *Echinopora* (Faviidae); *Podabacia* (Fungiidae); *Merulina* (Merulinidae); *Echinophyllia, Mycedium, Oxypora, Pectinia* (Pectiniidae); *Porites* (Poritidae)
	Massive	Massive growth forms from all scleractinian corals. Genera include: *Astreopora* (Acroporidae); *Pavona* (Agariciidae); *Euphyllia, Physogyra, Plerogyra* (Euphyllidae); *Cyphastrea, Diploastrea, Favia, Favites, Goniastrea, Leptoria, Oulophyllia, Platygyra* (Faviidae); *Lobophyllia, Symphyllia (Mussidae);* *Alveopora, Goniopora, Porites* (Poritidae)
	Solitary/ free-living	All solitary and free-living corals including the genera: *Heteropsammia* (Dendrophylliidae); *Ctenactis, Diaseris, Fungia, Halomitra, Herpolitha, Polyphyllia, Sandalolitha, Zoopilus* (Fungiidae); *Cynarina* (Mussidae)
	Submassive/ columnar	Submassive and columnar growth forms from all scleractinian corals. Genera include: *Acropora, Isopora, Montipora* (Acroporidae); *Pavona* (Agariciidae); *Caulastrea, Favites* (Faviidae); *Hydnophora* (Merulinidae); *Galaxea* (Oculinidae); *Pocillopora, Stylophora* (Pocilloporidae); *Alveopora, Porites* (Poritidae); *Psammocora* (Siderastreidae)
Other	Ascidian	Ascidians
	Other organisms	All other non-ascidian animals, including: Anenomes, annelids, bryozoans, corallimorpharians, crinoids, gastropods, holothurians, hydroids, *Millepora* spp., seastars, *Tridacna* spp., urchins, zoanthids
Sand/silt		Sand and silt
Seagrass	Elliptical leaf	Seagrass with elliptical leaves from the genera *Halophila*

Broad-scale category	Fine-scale category	Benthic groups included
		(Hydrocharitaceae)
Soft Coral	Gorgonian	Members of the Gorgoniidae and Ellisellidae family including the genera *Rumphella* and *Junceella*
	Soft coral	All other non-gorgonian soft corals. Genera include: *Lobophytum, Sarcophyton, Sinlularia* (Alcyoniidae); *Erythropodium* (Anthothelidae); *Briareum* (Briareidae); *Clavularia* (Clavulariinae); *Heliopora* (Helioporidae); *Isis* (Isidae); *Capnella* (Nephtheidae); (Pennatulacea); *Plumarella* (Primnoidea); *Tubipora* (Tubiporidae); *Asterospicularia, Xenia* (Xeniidae)
Sponge	Sponge – encrusting	Encrusting growth forms
	Sponge – erect/ branching	Erect growth forms. Includes branching, fallacious, stalked, erect laminar and erect simple types
	Sponge – massive	All massive-like sponges, including both simple and hollow massive, barrel or ridge like, cup and vase shaped sponges
Unconsolidated substrate		Rubble, shells/skeletal rubble, turf algae on *Halimeda* spp., turf algae on sand

1.2 Fish Communities

Non-destructive, "video-fishing" techniques were used to survey fish communities at two shoals, Evans and Tassie.

Remotely operated, video-based monitoring techniques are emerging rapidly in the field of marine ecology. Video image quality has improved markedly whilst camera size and cost has reduced rapidly. Baited and unbaited video units are now widely used to identify, count and measure fish (see Cappo et al. 2007b, Mallet & Pelletier 2014 for reviews). A fleet of Baited Remote Underwater Video Stations (BRUVS™) was developed at AIMS to identify fish-habitat associations (eg Cappo et al. 2011, Fitzpatrick et al. 2012), measure the effects of marine protected areas (eg Denny et al. 2004, Cappo et al. 2012, Malcolm et al. 2007, McLean et al. 2010) and explore faunal boundaries at broad scales (eg Cappo et al. 2007a, Colton & Swearer 2012, Harvey et al. 2013). The BRUVS technique has proven useful to survey sharks (Espinoza et al. 2014) and sea snakes (Udyawer et al. 2013) as well as fish.

The Stereo Baited Remote Underwater Video Stations (SBRUVS) used in this study comprised a galvanised steel frame onto which two camera housings, an arm bearing a flashing diode and bait canister, ballast weights, ropes and floats were attached. A flexible bait arm held a plastic mesh bait bag containing 1 kg of crushed pilchards (*Sardinops sagax neopilchardus*) at a distance of approximately 1.5 m in front of the camera lens. SBRUVS frames were ballasted according to the prevailing sea-state and current conditions to ensure stability on the seabed. An 8mm diameter polypropylene rope with surface floats attached enabled the SBRUVS to be deployed and later retrieved from the

surface with a pot-hauler (Figure 2). The scope of the rope length was selected to be approximately twice the water depth.

Each camera housing contained a Sony HDR-CX110E 'handicam' video camera fitted with a x0.6 wide conversion lens. The cameras were set to record at full high definition resolution (1920 x 1080 pixels), with focus set to infinity in manual focus mode. Camera footage was recorded onto a 16GB SD card, with recording initiated manually immediately prior to deployment. At the end of each deployment (60 minutes duration at the seabed) footage was downloaded from the cameras via Picture Motion Browser (Sony, 2010) software and stored on portable hard drives in .m2ts file format. The footage was converted to .avi format and is hitherto referred to as a "tape".

The allocation of deployment positions across each shoal was done using a "regular/random" design within the bounds of the 60 m depth contour whilst maintaining a minimum distance of 250 m between each SBRUVS unit. Once the positions were derived, the sequence of deployments, in sets of eight replicate units, was determined by proximity and prevailing sea conditions on the day. A total of 72 SBRUVS deployments were conducted at Evans Shoal, and 23 deployments at Tassie Shoal.

1.2.1 Video Analysis

The left-hand camera in each stereo pair was interrogated using custom software designed by AIMS ("BRUVS2.2.6.mdb) to capture and store the timing of events, reference images and counts of fish in the field of view. Records were made, for each species, of the time of first sighting, stage (adult or juvenile), time of first feeding at the bait, the maximum numbers seen together in progression of the whole tape (MaxN) and updated times at which each MaxN occurred. The use of MaxN has been reviewed by Schobernd et al. (2014) and Willis and Babcock (2000). It is the most widely accepted metric of relative abundance used in baited video studies.

Species identifications were made according to the Australian CAABCodes national standard (Yearsley et al. 1997). As some taxa were indistinguishable from each other on video footage, these were pooled either at the level of taxa, genus, family or order. These pooled taxa, hitherto referred to as species, were signified by the use of 'sp'. The MaxN data were then summed over adults and juveniles for each species. The term 'fish' hitherto refers to any marine vertebrate seen in the field of view, including sharks, rays and sea snakes.

A standardised classification scheme for the seabed in the SBRUVS field of view was developed for shoals of north-western Australia by AIMS for a previous study of the effects of the Montara uncontrolled release (Heyward et al. 2011). This same scheme was applied here by reviewing all images of the seafloor collected from all 95 SBRUVS deployments from Tassie and Evans shoals, and assigning habitats to one of eight qualitative categories of "bedform" (flat sand or gravel or silt, sand ripples, sand dunes, rubble field, Halimeda bank, low reef/outcrop, high reef/outcrop, or boulder field) with percentage cover (to the nearest 10%) estimated for six categories within these bedforms (mud, sand, gravel, rubble, bedrock and boulder, calcareous reef). In addition, the benthos in the SBRUVS images was assigned to one of six "habitat categories" (open sandy seabed, seagrass bed, macroalgal bed, low-relief rubble field, coral reef, gorgonian and seawhip gardens) with percentage cover (to the nearest 10%) estimated for 12 categories of epibenthos (gorgonian fans, sponges, sea whips, soft corals, hard corals, macroalgae, seagrass, Halimeda, bryozoans and encrusting animals, zoanthids, hydroids and "Bare").

Figure 2: Stereo-BRUVS units ready for deployment, during the process of retrieval, and in action capturing video on the seabed.

1.3 Statistical analysis

1.3.1 Benthic Spatial Models

Local scale

To infer spatial distributions of marine biota and abiotic substrate within each of the five study areas, we characterised environmental relationships in detail using a combination of forward facing towed video footage, downward facing digital stills and multibeam hydroacoustic surveys in conjunction with a statistical modelling approach. Towed video and digital images provide data on benthic diversity and cover on different scales. Secondary (textural) datasets correlated with seafloor properties were developed from the multibeam bathymetry (Table 3) to provide information on environmental characteristics, and give full coverage of the field area.

To model the relationship between physical and biological parameters, we implemented the most recent development in boosted regression methods "xgboost". This method provides very comparable accuracy to boosted regression trees and its computationally efficient making it suitable for spatial prediction of large multibeam datasets. A detailed description of the application of boosted regression method with ecological data is outlined in De'ath at al. (2007) and Elith et al. (2006, 2009, 2011). Boosted regression methods are very commonly used in ecological analysis as they provide accurate and robust predictions with complex data containing non-linear responses and interactions. A detailed description of xgboost method is outlined in Chen and He (2015) and was implemented using the r package xgboost 0.3. (http://xgboost.readthedocs.io/ en/latest/python/index.html). Model accuracy is based on testing the models against a 20% blind validation dataset (checked and adjusted for spatial autocorrelation with the testing dataset).

Regional model

To infer a regional scale distribution of course benthic categories a habitat model was produced covering both the study area and the broader Bonaparte Basin. The regional habitat model was developed based on the Oceanic Shoals Commonwealth Marine Reserve benthic habitat model produced as part of the Australian National Environmental Science Programme (http://northwestatlas.org/node/1710). Both the Oceanic Shoals Commonwealth Marine Reserve benthic habitat model and the regional habitat model were developed as part of the National Environmental Research Project D1 (as descripted here http://maps.northwestatlas.org/files/montara/html_popups_oceanic_shoals/Spatial_benthic_habitat_model_for_the_Oceanic_Shoals_CMR_6dec16.pdf). The extension of the model included additional benthic habitat data help by AIMS and collected as part of this report which extending beyond the Oceanic Shoals Commonwealth Marine Reserve in some areas see outlined below.

The regional model was at a much coarser resolution than the local scale model and based on Geosciences Australia 250 m bathymetry grid (http://www.ga.gov.au/metadata-gateway/metadata/record/gcat_67703) combined with a regional database of AIMS towed video real time classification (http://www.aims.gov.au/docs/research/monitoring/seabed/video-monitoring.html). As with the local scale models, secondary textural datasets were developed (Table 3) providing environmental characteristics information over the whole of the regional model domain.

Multivariate models expressing the relationship between physical and biological parameters were developed using randomForest classification trees (Breiman et al. 1984, Breiman 2001, Cutler et al.

2007). This method has the same general advantages of boosted regression trees and is also commonly used in ecological analysis. randomForest classification has efficiency advantages for modelling large datasets and can model multiple classes simultaneously (producing a map of maximum likelihood for habitat found in each pixel). The randomForest classification was performed using the Python programing language (Python library scikit-learn 0.18.1 with Python version 3.5 http://scikit-learn.org/stable/). Model accuracy and Kappa statistics were calculated by testing the models against a 33% blind validation dataset (checked and adjusted for spatial autocorrelation with the testing dataset).

Table 3. Datasets derived from multibeam bathymetry that were used as environmental surrogate variables for modelling biota, substrate and fish abundance/richness.

Dataset prefixes	Predictor datasets	Definition
depth	Bathymetry	Elevation relative to the Australian Height Datum (AHD)
asp	Aspect	Azimuthal direction of the steepest slope, calculated on a 3 x 3 pixel area
slp	Slope	First derivative of elevation: Average change in elevation / distance calculated on a 3 x 3 pixel area
prof	Profile curvature	Second derivative of elevation: concavity/convexity parallel to the slope, calculated on a 3 x 3 pixel area
plan	Plan curvature	Second derivative of elevation: concavity/convexity perpendicular to the slope, calculated on a 3 x 3 pixel area
curv	Curvature	Combined index of profile and plan curvature
mean	mean depth[a]	Mean depth local neighbourhood
rng	Local relief (Range) [a,b]	Maximum minus the minimum elevation in a local neighbourhood
std	Std Dev [a,b]	Standard deviation of elevation

[a] Local scale models neighbourhood analysis: run on circles of kernel pixel radius 5, 10, 25, 50 original cell size is 2.5 m
[b] Local neighbourhood analysis: run on circles of kernel pixel radius 3 and 5 with original cell size is 250 m

1.3.2 Benthic composition within and between shoals

All benthic codes from the scored images from Tassie, Evans and Blackwood Shoals were aggregated to broad- and fine-scale taxonomic groupings that were considered robust to observer variation and included pooling of some rare categories to avoid issues with zero inflation.

Data were analysed at the image level and compared among the three shoals, as well as across three depth bands within each shoal (<20 m, 20-40 m, >40 m, Table 2). Bar and pie charts were constructed to examine differences in community composition, and represented the proportion of scored points for each category for a given shoal and tow combination, or shoal and depth combination.

1.3.3 Fish community composition within and between shoals

Fish communities were analysed using techniques identical to those applied for the same types of exploration of the Great Barrier Reef Marine Park (Cappo et al. 2007a), James Price Point (Cappo et al. 2011), and the Montara shoals (Heyward et al 2011).

They are based on boosted regression introduced to the ecological literature relatively recently by De'ath (2002; 2007). This approach derives from both classification and regression trees starting with a data model (De'ath & Fabricius 2000) and from 'machine learning' where no data model is specified and algorithms are used to learn the relationship between a predictor and its response (Breiman 2001). Boosted regression trees are therefore an 'ensemble' method, whereby models are

improved by first fitting many simple models and then combining them for prediction, using an algorithm from classification and a 'boosting' algorithm, which combines a collection of models (Elith et al. 2008).

Boosted regression trees are complex, but can be summarised in ways that give powerful ecological insight by representing complex information in a visual way that is easily interpretable. They are robust and flexible, because explanatory (predictor) variables can be numeric, categorical, binary, or of any other type, and model outcomes are unaffected by transformations and different scales of measurement of the predictors. They are not sensitive to outliers, and handle missing data in predictors by applying best surrogates with little loss of information. Trees are hierarchical structures, and input variables at the tree leaves are dependent on input variables at higher nodes. This allows simple modelling of complex, non-linear interactions that simply cannot be handled by other approaches (see examples in De'ath 2007).

A mixture of 32 explanatory covariates (Table 4) were used to predict univariate responses using aggregated boosted regression trees (abt; De'ath 2007, Ridgeway 2007). The responses were:

1. species richness (raw total number of species on 95 SBRUVS drops),
2. total fish abundance (∑MaxN ; 4th root transformed)

The models were run for interaction depths of 1, 3 and 5 m, and the results show the relative influence of all covariates explaining and predicting the response. They are best portrayed as partial dependency plots, which show the effect of one particular covariate with the effects of all others held constant. Interactions are viewed using partial interaction plots.

To explore similarities and differences in the fish community composition between four nominal depth categories (<=23m, 23-42m, 42-60m and >60m), we used clustering and ordination of the fish genera without any constraints by environmental covariates. Relative fish abundance data (MaxN) was transformed by 4th root to down weigh the influence of rarely occurring but abundant fish such as schooling fusiliers and trevallies, and raise the influence of common species that occur in low numbers.

We avoided rare species and singletons by aggregating fish counts at the level of 98 fish genera in this preliminary clustering and ordination. The transformed abundance (4th root MaxN) data for these genera was converted to a matrix of Bray-Curtis dissimilarities and we computed agglomerative hierarchical clustering of the matrix. The distance between two clusters was the average of the dissimilarities between the points in one cluster and the points in the other cluster. We then conducted an unconstrained principal coordinates analysis (PCoA) on the matrix of Bray-Curtis dissimilarities. The site scores were plotted to reveal trends by depth, and the longest vectors were also plotted to show high correlations between principal coordinates and the abundance of genera.

To define fish assemblages in terms of depth, shoal location, seabed composition and epibenthic cover we used multivariate prediction and regression trees (mvpart). This approach uses the abundances of a large number of species at each SBRUVS site as a multivariate response (see De'ath 2002). We selected 179 species that occurred on at least three individual SBRUVS (~3% of samples) for this analysis and 32 explanatory covariates. As some of the %cover and % composition categories of substratum or epibenthos were absent, or poorly represented, in the dataset, these were pooled with other, larger categories to derive the list of covariates in Table 4. Abiotic covariates were derived using seafloor maps produced from multibeam acoustics (Table 4). From this analysis, links between environmental characters and fish assemblages can be visualised in a tree structure. Each split in the tree minimises the "distance" of sites from the centroids of nodes to which they belong.

This is equivalent to maximising the distance between node centroids. Each terminal node of the tree (leaf) can be defined by the multivariate mean of its sites, the predictors that define it, the number of sites that were grouped there, and by Dufrêne-Legendre species indicators (DLI). Nodes represent fish assemblages.

Indicator values (DLI; Dufrêne and Legendre 1997) were calculated for each species for each upper (branch) and terminal (leaf) node of the tree. For a given species and a given group of sites, the DLI is defined as the product of the mean species abundance occurring in the group divided by the sum of the mean abundances in all other groups (specificity), times the proportion of sites within the group where the species occurs (fidelity), multiplied by 100. Each species can be associated with the tree node (assemblage) where its maximum DLI value occurred. The index distinguishes between ubiquitous species that dominate many groups in absolute abundance, and species that occur consistently within single groups but have low abundance (Dufrêne and Legendre 1997). The DLI for species at the root node are simply the prevalence of those species in the entire dataset. Species with high DLI can be used as characteristic representatives of each fish assemblage, and the spatial extent of the assemblages was mapped onto diagrams of each shoal.

Species accumulation curves were derived for each assemblage to identify how much latent biodiversity remained after the completion of the single visit to Tassie and Evans shoals. The location of sites within each assemblage were mapped for each shoal.

All analyses used the open-source "R" statistical package (R.Development.Core.Team 2006). We used the public libraries mvpart, vegan, and abt (Ridgeway 2007). The use of common and scientific names follows those reported in Allen & Swainston (1988).

Table 4 Definition of the 32 explanatory covariates used in univariate and multivariate models to examine the relative effect of "habitat" on the univariate and multivariate responses for the fish sighted on SBRUVS at Tassie and Evans shoals. Covariate types included those estimated in the SBRUVS field of view (substratum, epibenthos) and those derived using multibeam acoustic maps. Brief definitions of each covariate are given in the right hand column.

Covariate abbreviation		Covariate type	Covariate Definition
name		spatial	Shoal name
depth		spatial	Depth (m) measured under the hull when the SBRUVS were deployed
latitude		spatial	SBRUVS GPS position
longitude		spatial	SBRUVS GPS position
BRUVS field-of-view			
% composition of seafloor by 6 pooled categories of substratum			
bdrck		substratum	% substratum classified as "bedrock"
calc.rf		substratum	% substratum classified as "calcareous reef"
grvl		substratum	% substratum classified as "gravel"
rbbl		substratum	% substratum classified as "rubble"
snd		substratum	% substratum classified as "sand"
mud		substratum	% substratum classified as "mud"

% coverage of 7 pooled categories of epibenthos			
bare		epibenthos	% coverage of seafloor with no epibenthos
encr		epibenthos	% coverage of the seafloor by "encrusting organisms"
fltrs		epibenthos	% coverage of the seafloor by "fans", "sponges", "sea whips", "zoanthids"
hlmda		epibenthos	% coverage of the seafloor by "*Halimeda*"
alg		epibenthos	% coverage of the seafloor by "algae
crl		epibenthos	% coverage of seafloor by "massive corals" and "solitary corals"
sft.crl		epibenthos	% coverage of seafloor by "soft corals"
Multibeam acoustic derivatives			
asp.dir		spatial	Azimuthal direction of the steepest slope, calculated on a 3 x 3 pixel area
curv		spatial	Combined index of profile and plan curvature {concavity/convexity parallel to and perpendicular to the slope), calculated on a 3 x 3 pixel area
hyp5		topography	Hypsometric index - Indicator of whether a cell is a high or low point within the local neighbourhood (kernel pixel radius of 5) original cell size 4m
hyp10		topography	Hypsometric index (kernel pixel radius of 10)
hyp25		topography	Hypsometric index (kernel pixel radius of 25)
hyp50		topography	Hypsometric index (kernel pixel radius of 50)
rng5		topography	Maximum minus the minimum elevation in a local neighbourhood (5 pixels)
rng10		topography	Maximum minus the minimum elevation in a local neighbourhood (10 pixels)
rng25		topography	Maximum minus the minimum elevation in a local neighbourhood (25 pixels)
rng50		topography	Maximum minus the minimum elevation in a local neighbourhood (50 pixels)
std5		topography	Standard deviation of elevation (5 pixels)
std10		topography	Standard deviation of elevation (10 pixels)
std25		topography	Standard deviation of elevation (25 pixels)
std50		topography	Standard deviation of elevation (50 pixels)
slp		topography	First derivative of elevation: Average change in elevation / distance calculated on a 3 x 3 pixel area

1.3.4 Analysis of regional patterns in benthic and fish communities.

To provide a regional context for the data collected during this survey, an analysis based on coarse-scale habitat data for major benthic groups (greater than 3% total cover) was conducted using data from 28 sites covering the Sahul shelf and Timor Sea. The analysis was done based on percentage total of each benthos group at each site and was conducted using a "distance average" paired hierarchical cluster analysis and heat-map plot (see R library vegan and gplots). The results from the hierarchical analysis dissimilarity measure was use to delimit seven groups of similar sites and these groups were subsequently mapped in order to examine geographical trends.

In addition, the benthic community of Evans, Tassie and Blackwood Shoals was compared with 17 other shoals from the NW Shelf based on the data derived from point-intercept analysis of still images. Bar plots of percentage cover for broad–scale benthic categories and hard coral categories were summarised for each shoal. The bar plots aggregate the data as "All data <60 m", which was then split into two depth bands, <=30 m and >30-60 m. Multivariate differences in community types based on point intercept data were also examined using a "distance average" paired hierarchical cluster analysis and heatmap plot (see R library vegan and gplots).

A regional comparison of fish species richness and abundance (as transformed 4th root) was undertaken to compare fish communities at Tassie and Evans Shoals with reefs and shoals of the

Great Barrier Reef, as well as six reefs and shoals on the NW Shelf. Sites included in the comparison were selected to have similar depths and habitats as the BRUVS imagery analysed from Evans and Tassie Shoals.

1.4 Data management

All data was collated and archived on the AIMS server, under the control of the Perth AIMS Data Manager (m.case@aims.gov.au). The resulting derived files were added to the ConocoPhillips archive.

2. Results

2.1 Spatial coverage of sampling

Work was completed as planned, using all methods, with the exception of a small number of towed video stations in the mid-shelf areas that were unable to be surveyed due to strong tidal currents. Additional benthic transects were completed with the towed video system across Blackwood Shoal. CTD casts, sampling the water column for conductivity, temperature, depth and light, were made twice a day throughout the voyage. A small number of sediment grabs were collected at the shelf locations adjacent to Cape Helvetius and Goodrich Bank. A summary of all sampling locations is included as Appendix 1. The spatial coverage of all sampling is summarised in Figures 7, 9, 15, 21 & 27.

2.2 Shelf area characteristics

Benthic communities at the two survey locations on the continental shelf were strikingly different from those observed on the shoals. Our general observations revealed the shelf areas contained complex bathymetry which to a large degree is likely a legacy of past sea level stands. The resulting plateaus and channels provide various depths and aspects, likely to influence the presence/absence of different benthic biota, with strong tidally driven currents bringing at times highly turbid water over the ridges and valleys. Both shelf locations were much more turbid than the shoals, resulting in greatly reduced amount of light reaching the seabed and an associated shift from primary producer dominated habitats to those featuring sessile filter feeders. Initial review of a subset of water column light profiles indicated progressive drops in water clarity from the outer shelf shoals shorewards, with surface light (corrected PAR) attenuated to <5% at around 45 m depths on the shoals, 30 m at Goodrich Bank and 10m near Cape Helvetius. From the real-time towed-video classifications, it was apparent that phototrophic species such as hard corals were rare and only encountered on the shallowest survey transects to depths of less than 30 m (Figure 3) near Goodrich Bank. Macroscopic biota was generally sparse, but low-medium density filter feeder habitats were encountered in both the Goodrich Bank and Cape Helvetius areas (Figures 5 & 6). Sponges tended to dominate the filter feeder habitats, with various small to medium sized soft corals contributing less biomass. In all cases these communities were associated with small scale patches of consolidated substrate, either sandy pavement or minor rocky outcrops.

Figure 3: Goodrich Bank area examples – limited partial hard coral habitat at 25 m depth (left image) was rare and only encountered at the shallowest sites, while coarse sandy substrate and sparse filter feeders (right image) were more typical.

Figure 4: Goodrich Bank area examples - medium density mixed filter feeder community associated with patches of low relief outcropping rock.

2.2.1 Shelf Area Modelling results

Goodrich Bank and Cape Helvetius were modelled separately from Blackwood, Evans and Tassie shoal because multibeam variables were collected, interpolated and derived at different spatial scales). Accuracy estimates for major benthic modelling results based onoblique forward-facing real time towed video modelled against interpolated multibeam transects (50 m pixel) are shown in Table 7. Model accuracy is based on testing the models against a 20% blind validation dataset (checked and adjusted for spatial autocorrelation with the testing dataset). Real time towed benthic video model test indicated very high accuracy results with AUC values all greater than 0.95.

Spatial representations of probabilistic models for real time video modelled with interpolated multibeam are shown for Goodrich Bank in Figure 6 and Cape Helvetius in Figure 8. A heat map with Euclidian distance based cluster analysis was used to summarise the relative variable importance (scaled model accuracy "Gain" index) for the prediction of biotic groups from multibeam (Figure 9) and more detailed information on model accuracy (AUC plot), variable importance (plot of gain index for all multibeam variables) and the partial responses of each biotic group to the most important six variables are detailed in Appendix 3 (Figures A3.15-A3.19).

For habitat models based on real time towed video, analysis of the relationships between multibeam variables and each biotic group identified two major clusters (based on the first break in the dendogram y-axis, Figure 9). The first cluster contains the "Dense filter feeders" and "Burrowers" communities, where the most important predictor variable is broad scale depth (mean50). Both communities in this cluster show distinctive broad depth responses (probability declining with depth to 50m in Burrowers, and probability increasing with depth to 85 m in dense filter feeders; Appendix 3 Figures A3.15 and A3.16). Both profiles show non-linear responses in mean50 which also indicates that landscape scale topography may influence distribution (for example sloping areas)(Appendix 3 Figures A3.15 and A3.16). The second major cluster contains "medium" and "sparse filter feeder communities" as well as habitats with no benthos (Figure 9). Membership of this second clusteris most highly correlated with the slope and rugosity measure rng50, and depth. As for dense filter feeders, the occurrence of medium and sparse filter feeder communities increases where there is change in topology (indicated by rng50 a measure of change in depth) and where water depth increases (Appendix 3 Figures A3.17 and A3.18

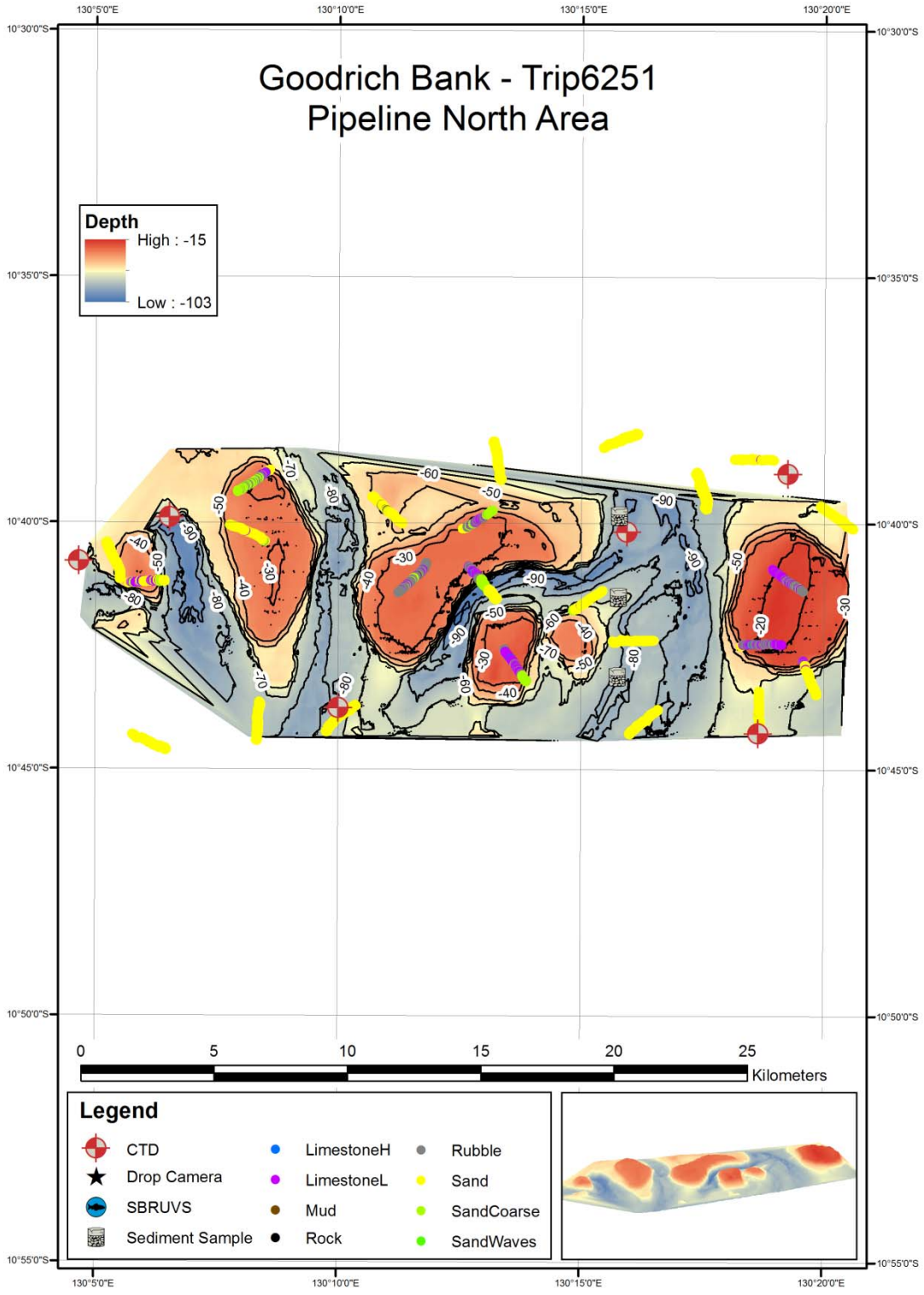

Figure 5: Towed video sampling completed adjacent to Goodrich Bank. The bathymetric representation of the shoal was produced from the expedition's multibeam data. A 3D representation of the shoal is shown in the lower right box. Warmer colours associated with shallower depths. The multi-coloured "worms" summarise the benthos as observed from the real-time towed video.

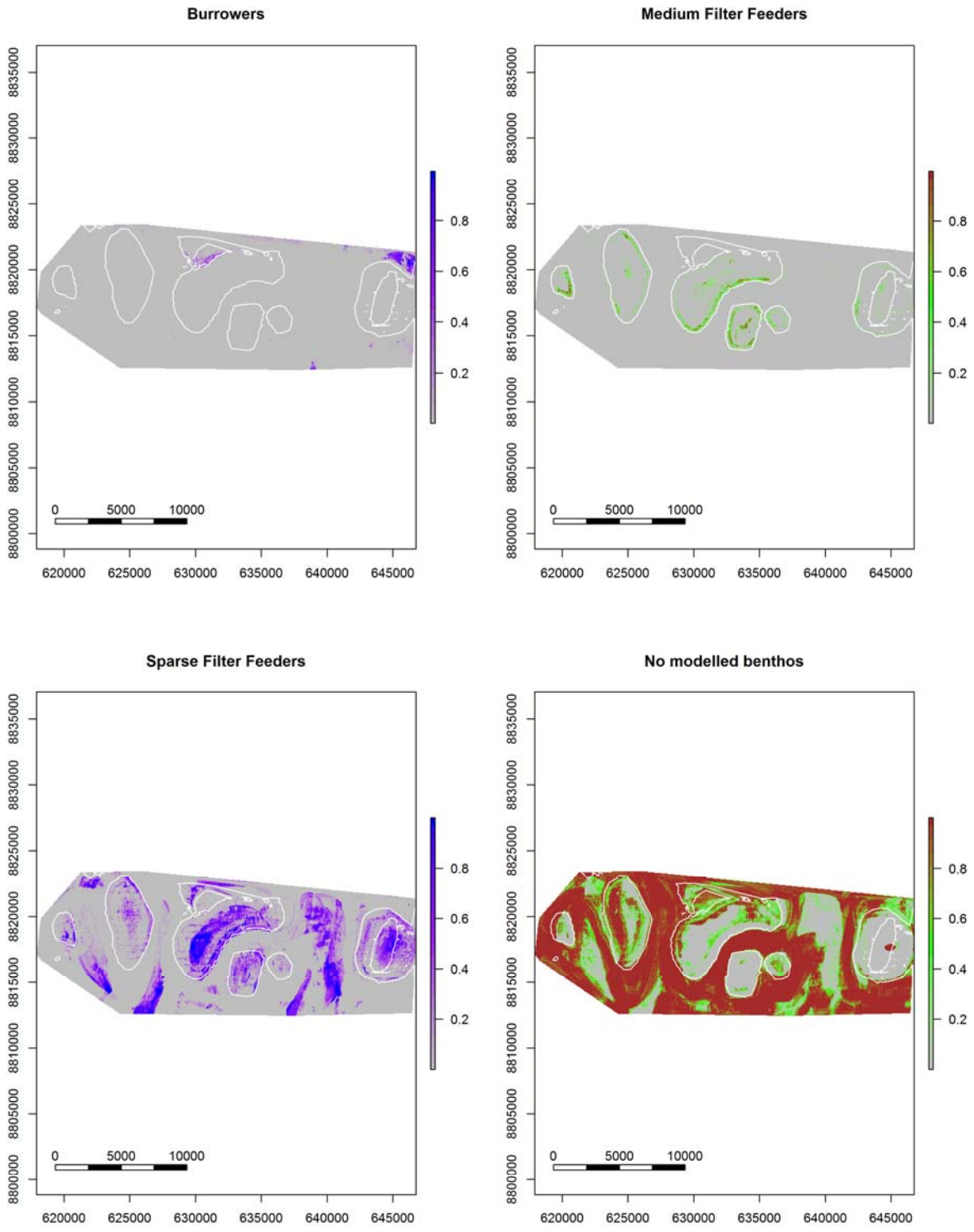

Figure 6: Goodrich bank survey area - modelled spatial distributions describing the presence/absence probabilities for major benthic habitat classes generated using oblique forward facing real-time scored towed video. The 30 and 50m depth contours are shown in white.

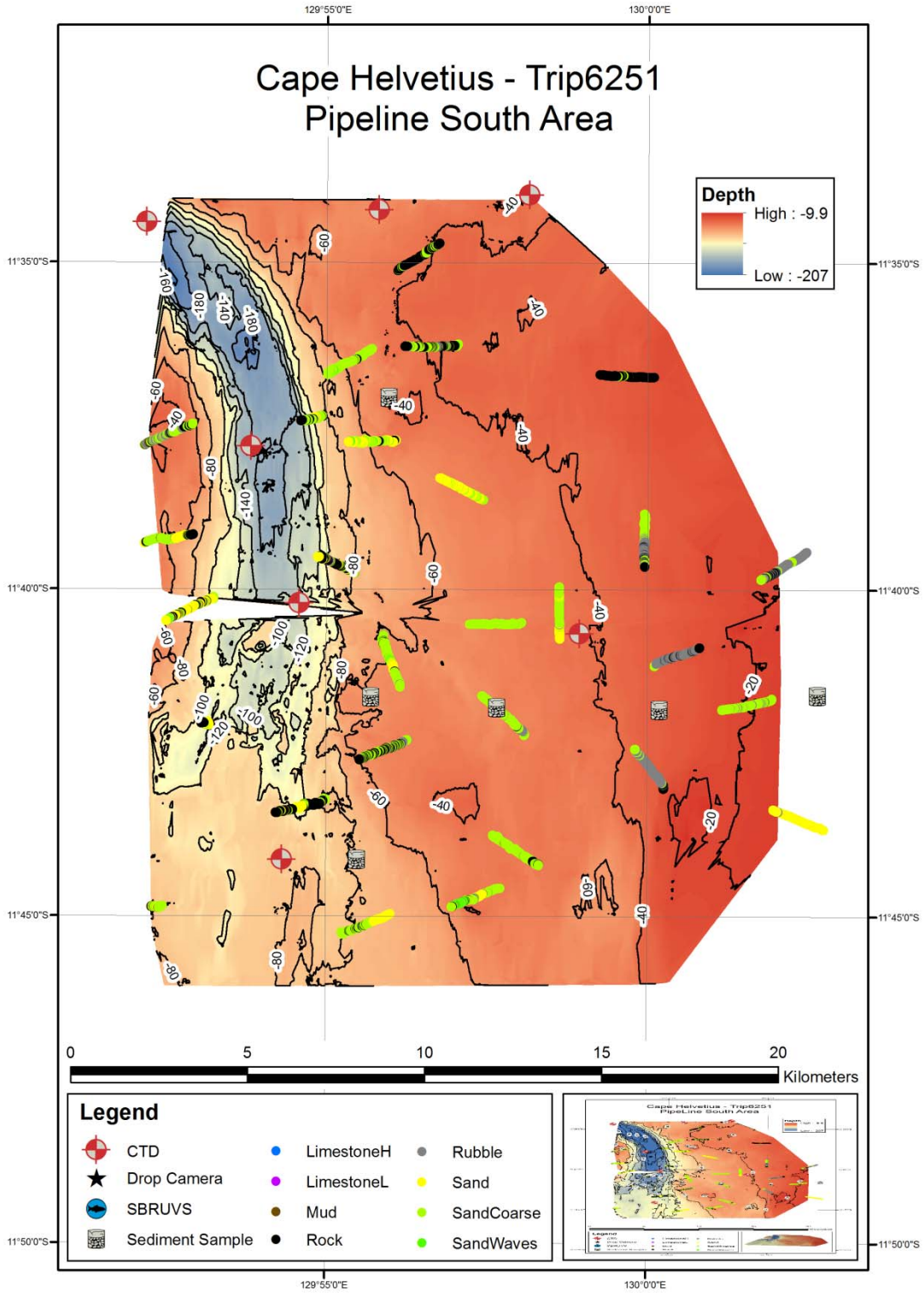

Figure 7: Towed video sampling completed adjacent to Cape Helvetius. The bathymetric representation of the shoal was produced from the expedition's multibeam data. A 3D representation of the shoal is shown in the lower right box. Warmer colours associated with shallower depths. The multi-coloured "worms" summarise the benthos as observed from the real-time towed video.

Modelling of habitat distributions in both shelf areas (Figures 6 & 8) confirms the limited and patchy distribution of the filter feeding habitats and points to associations of filter feeders with high spots and regions of steep bathymetry. In both cases this likely reflects the availability of exposed consolidated substrates for recruitment and subsequent growth.

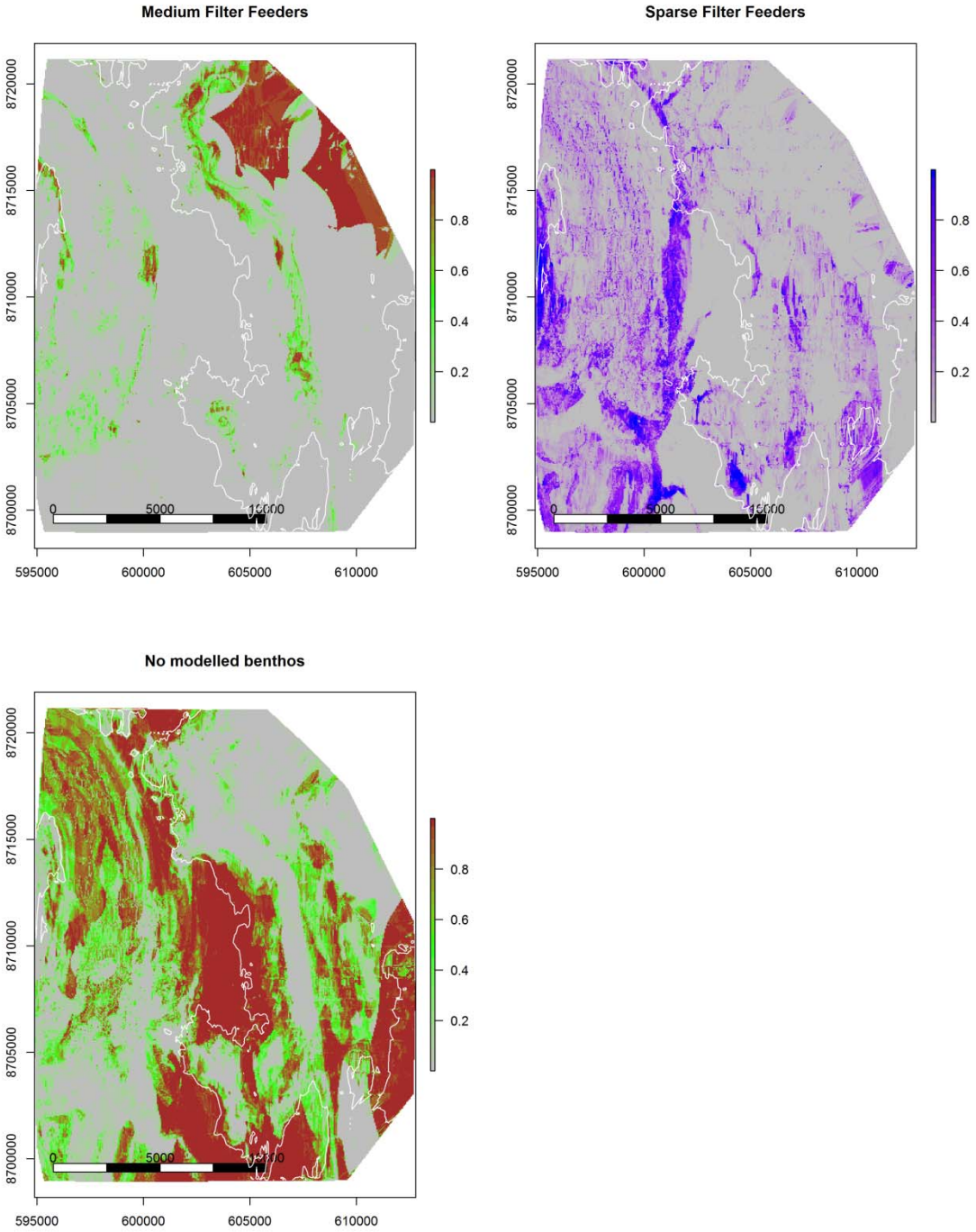

Figure 8: Cape Helvetius survey area modelled spatial distributions describing the presence/absence probabilities for major benthic habitat classes generated using oblique forward facing real-time scored towed video. The 50 m depth contour is shown in white.

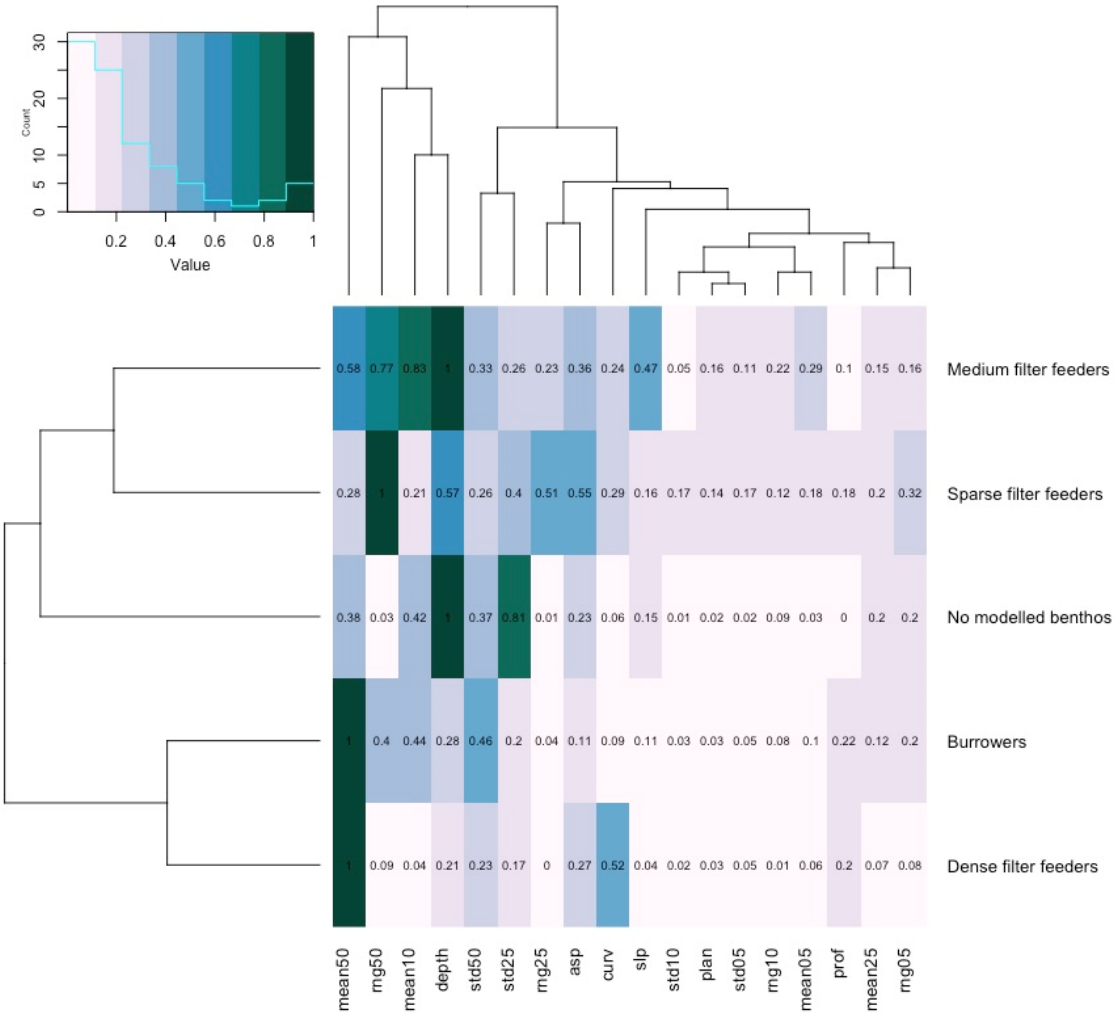

Figure 9: Heatmap with Euclidean distance cluster analysis showing the relative importance of predictor variables (0-1 from least to most important) for towed video real-time classification based on benthic habitat for Cape Helvetius and Goodrich Bank areas. Benthic groups are on the y-axis and 50m interpolated multibeam depth and derivatives are on the x-axis (see Table 3 for variable descriptions).

2.3 Shelf Sediments

Analysis of a limited number (n= 9) of sediment samples, collected with Smith-McIntyregrab within the sampling region near Goodrich Bank and Cape Helvetius (Figures 5, 7, Appendix 1), found that carbonate estimates averaged 48.2% near Goodrich Bank and 39.6% near Cape Helvetius, based on sample weight differences between initial weight and that after hydrochloric acid treatment (Table 5). This is consistent with increasing carbonate contribution to the sediment at locations further offshore. Whilst most of the samples were made up of coarse sand (>2mm), sand (2mm-63 µm) or silty sand (<63µm) (Table 6), some of the samples collected near Cape Helvetius also contained small pebble-sized (5-10mm) mudstone-like pieces, plus some shells.

Table 5 Carbonate fraction, based on the change in sample weights after 10% HCl treatment, for grab samples collected near Goodrich Bank and Cape Helvetius. Sample locations are listed in Appendix 1.

Sample location	% Carbonate	
	2mm-63µm	< 63µm
01 Goodrich Bank	61.59718534	36.23739118
02 Goodrich Bank	56.92279367	40.21009241
03 Goodrich Bank	56.16877229	38.08362577
04 Cape Helvetius	41.23585938	38.73897419
05 Cape Helvetius	38.65095729	39.21727944
06 Cape Helvetius	54.20339849	36.47874184
07 Cape Helvetius	25.83954667	39.68263963
08 Cape Helvetius	55.53110234	37.71587041
09 Cape Helvetius	44.91093347	23.4668703

Table 6 Grain size distribution for grain samples collected near Goodrich Bank and Cape Helvetius. Sample locations are listed in Appendix 1.

Sample location	Grainsize - Percent of total sample		
	>2mm	2mm-63µm	<63µm
01 Goodrich Bank	4.908129877	40.24666499	54.84520513
02 Goodrich Bank	22.26778392	51.72044928	26.0117668
03 Goodrich Bank	33.3007335	29.76365118	36.93561532
04 Cape Helvetius	31.85715964	51.00434629	17.13849407
05 Cape Helvetius	33.10485516	53.08853529	13.80660955
06 Cape Helvetius	26.53565938	60.71118241	12.75315821
07 Cape Helvetius	21.70781893	66.96673525	11.32544582
08 Cape Helvetius	35.34838766	45.83077058	18.82084175
09 Cape Helvetius	54.91081906	30.04576391	15.04341704

2.3.1 Regional comparisons - sediment

At the regional scale, using the Geosciences Australia MARS sediment characteristic database, co-cluster analysis and heatmap results (Figure 10) show the majority of on-shelf locations have a high degree of heterogeneity with respect to broad sediment characteristics, although sand particles (63 µm to 2mm) make up the majority of sediment samples (75% or greater) by weight. The remaining proportion of the sample is made up either of silts (> 63µm) or gravels (> 2mm). The exceptions are a) Eugune McDermott which is located on the shelf edge, surrounded by deeper water, were bottom sediments are subject to less hydrodynamic disturbance and turbulence which corresponds to a sediment sample where 87% is silt and the rest is gravel; b) Heywood, Echuca and Goeree shelf edge shoals where sediment samples are dominated by gravel (>77% by weight). These gravels may be a result of scouring of past land and present biogenic reef present on these shoals.

Overall the grain size data shows no consistent trends with distance from shore, longitude or latitude (Figure 11). Local hydrodynamic factors will have a large influence on the grain sizes reported, but with present knowledge it would seem difficult to predict the grain size composition form one location to another. The more predictable gradient may be an increasing carbonate

component of the sediments with distance from shore, but the presence of underlying ancient coastal features in many locations means there is likely to be widespread terrigenous component in many locations throughout the region.

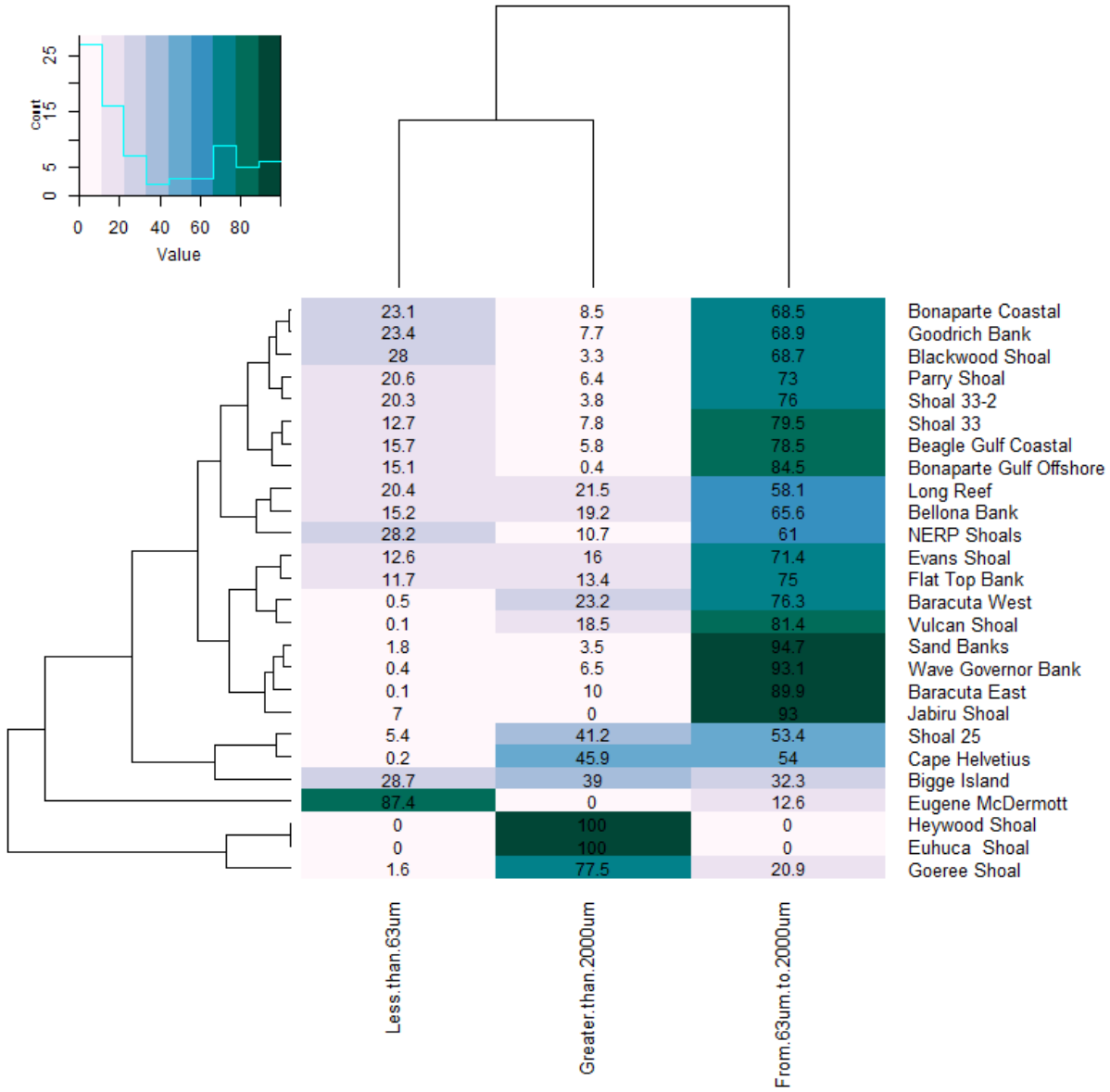

Figure 10: A heat map and co-cluster comparative analysis of the proportion of the three sediment classes represented at sites across the NW Shelf. This was completed using Euclidean distance based hierarchical co-cluster analysis of locations and sediment classes (Mardia et al. 1979, Becker et al., 1988). The sites are on the y-axis and sediment classes on the x-axis. The heat map cell values show the percent by weight of sediment in each class.

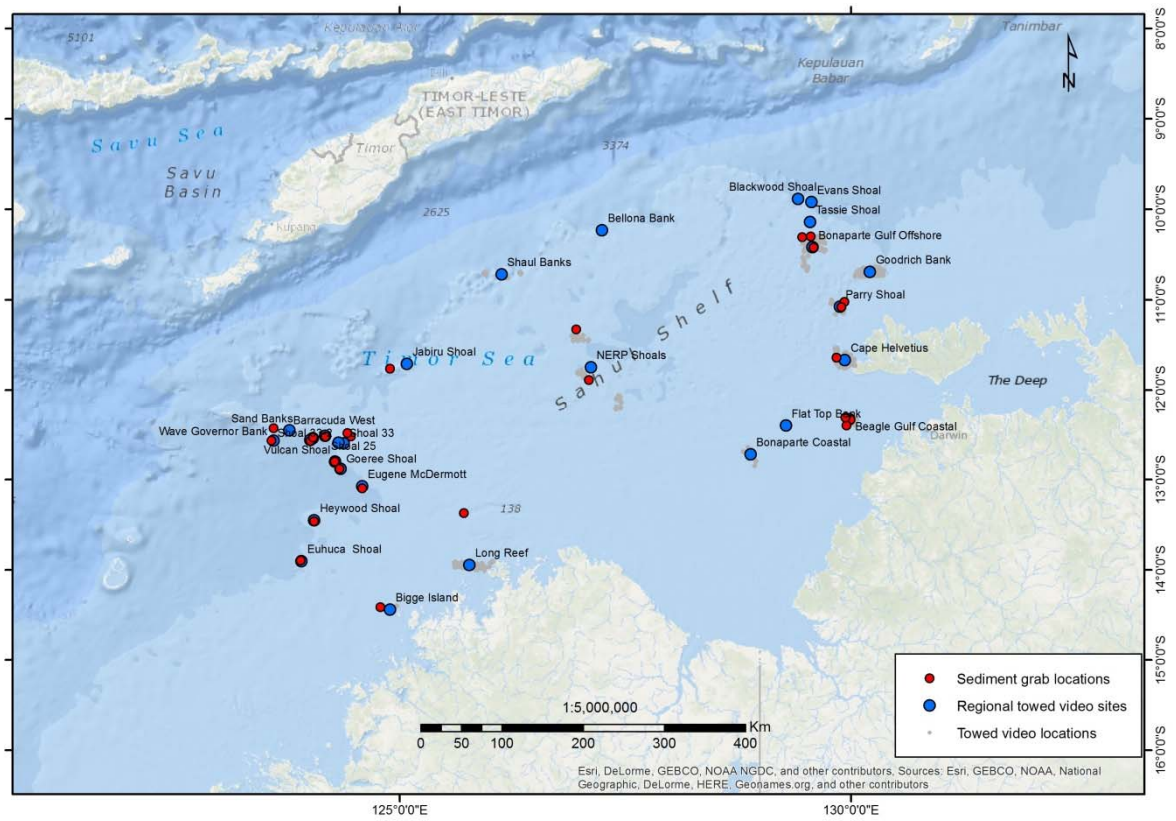

Figure 11: Regional sediment grain size analysis: location of regional comparison centroid locations, general habitat classifications from towed video data and the nearest corresponding location of sediment grabs extracted from the Geosciences Australia MARS sediment database.

2.4 Shoal characteristics

2.4.1 Benthic habitats

2.4.1.1 Broadscale Shoal features

The three submerged shoals surveyed all supported light-dependent benthic communities across the shallower regions of the shoal plateaus down to depths of around 60 m.

Evans Shoal had by far the largest plateau area, much of which had low vertical relief and extensive sand and rubble. The central plateau did support a variety of biota including varying densities of erect *Halimeda* and a few extensive fields with the solitary coral *Heteropsammia*, but was dominated by sandy bare substrates or various forms of low relief algae. Rugosity increased with a greater frequency of small isolated bommies and outcropping reef, along the outer margins of the plateau. Multibeam data suggest a crescent-shaped distribution of more fine-scale rugosity from north to south and along the eastern side of the plateau. These areas of hard substrate supported corals, often mixed with algae, red crustose coralline or green erect calcareous algae such as the widespread *Halimeda*. In localised areas these coral and algal communities included moderate densities of mixed filter feeding organisms, such as sponges and soft corals. Hard coral density was sparse or absent across large areas of Evans Shoal plateau but increased noticeably towards the outer edges of the horizontal section of the plateau. At the northern and southern ends of the shoal coral cover was variable as the seabed slope and depth started to increase, but at 40 m a band of

dense foliaceous coral was encountered on multiple transects. Where it did occur, the foliaceous coral habitat extended down the slope until it transitioned to mostly sparse filter feeder areas, generally occurring on coarse sandy substrates with occasional, isolated small rocky outcrops. This habitat is notable and accounts for dense coral in a narrow depth band at the northern and southern ends of the shoal. It did not occur all the way around the shoal, being noticeably absent from the western margin, where a sandy slope, possibly associated with sediment transported off the plateau, had accumulated. To a lesser extent this was also observed in similar depths at Tassie Shoal and similar mesophotic coral communities have been observed elsewhere in the North and North-west marine regions at around 40-50 m, including at Barton Shoal and in the deeper lagoon at South Scott Reef.

Tassie Shoal plateau covers 5.3km^2 in depths down to 30 m, much smaller than the 43 km^2 on Evans Shoal. Across the shallower region on the top of the plateau Tassie Shoal had a more complex arrangement of low relief ridges and small bommies, interspersed with patches of sand and rubble, but lacking the extensive, low cover sand and rubble dominated fields seen on Evans Shoal. The benthic communities of the two shoals appeared to be very similar in composition, but coral cover on Tassie Shoal was more commonly medium density rather than sparse. Overall, the density of benthic biota was higher on Tassie than Evans Shoal and it was common to encounter mixed coral-algae-filter feeder communities. Slightly more fine scale vertical relief in the reef habitat was seen on Tassie Shoal across the plateau, supporting medium to high coral cover in general and often clearly associated with bommies or ledges. It should be noted however, that although both Evans and Tassie Shoals had very similar coral cover of around 9%, the shoal plateau of Evans is almost nine times bigger. The seabed at Tassie Shoal typically had gentle transition over plateau rim and down slope. This was particularly noticeable along the western margin, where the edge and slope of the shoal were very sandy (see Figure 34) with the sandy slope areas appearing to include fine sand, coarse sand and gravel. These plateau margins often supported very low epibenthic cover at greater depths (60-100 m), though occasional patches of medium density and larger sized filter feeders, including medium sized sponges and gorgonian fans, were encountered.

An unusual feature on both Evans and Tassie Shoals was the presence of single large bommies of the coral *Pavona clavus* on the southwestern quadrant of each plateau. The *Pavona* bommie on Evans Shoal was by far the largest of the two and may be the largest example yet recorded worldwide (Figure 12).

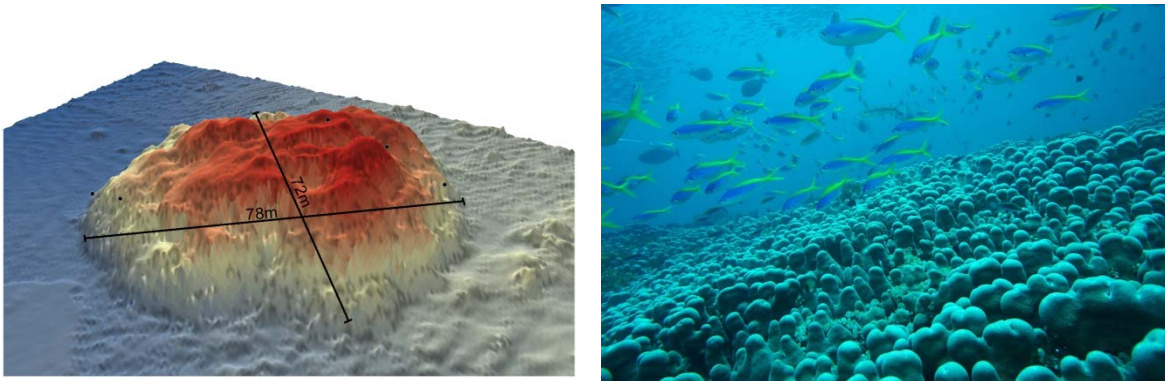

Figure 12: Very large <u>Pavona clavus</u> bommie on Evans Shoal. Left image is multibeam rendering, showing the bommie diameter of approximately 75 m. Right is a drop camera image showing a close up of the bommie and associated fish aggregation

Blackwood Shoal is further from the Barossa field than Evans or Tassie Shoals. It was the smallest and shallowest shoal plateau investigated, with only 0.7km^2 of the central plateau lying within the 30 m depth contour. Two towed video transects oriented perpendicular to each other across the top of the plateau revealed medium to high density of coral habitat throughout. Low relief reef supported mostly high coral cover, especially of the genus *Acropora*, represented by branching, tabulate and corymbose forms. Beyond the plateau rim the slope increased and supported mixed *Halimeda* and corals. The multibeam revealed a slight step down from the shallow plateau to a deeper sloping apron surrounding it, before the slope increased and dropped away (Figure 27). On one tow over the slightly deeper apron a narrow band of foliaceous coral habitat, similar to that seen at Evans and Tassie Shoals, was observed at 45-50 m depth, which then transitioned, as observed on the other shoals, into sand/rubble with greater depth.

The most distinguishing feature of the shoals was the presence of hard corals, which occurred at varying densities but with percentage cover in the most dense coral habitat patches not dissimilar to that found on healthy, emergent coral reefs. Evans and Tassie Shoals at a qualitative level show similar, though not identical assemblages, featuring sparse to medium density coral, sparse filter feeders and a comparable percentage of bare substrate. Blackwood Shoal differs in the dominance of the medium to high density coral habitat, along with other mixed habitats including coral and the algae *Halimeda*.

The shoal locations were noticeably less turbid than the mid-shelf, with sand sediments featuring on extensive bare areas across the shoal plateaus. Bare sand was observed on Evans Shoal to continue over the plateau edges and down the shoal slopes, along a NE-SW axis, suggestive of sediment transport off the plateau regions. The orientation may relate to prevailing patterns of wave energy and tidal currents. In contrast the northern and southern slope regions on Evan Shoal supported dense patches of foliose coral.

2.4.1.2 Fine scale image analysis of Evans, Tassie and Blackwood Shoals

Quantitative analysis of the high resolution images along each towed video transect allowed for fine scale discrimination of the abundance and distribution of benthic components at each shoal. Evans Shoal features large areas of sand, with turf and macroalgae covered consolidated reef representing the most abundant organisms (Figure 14). Coral abundance is highly variable with location and the average cover of 9% is in the mid-range for coral cover observed on other shoals. The relative proportions of the major benthic categories varies with depth, for example hard corals are most abundant in the shallow areas (<20 m depth) and also beyond 40 m (Figure 15). This deep coral communitiy is dominated by dense foliaceous species packed in a narrow band between 40-60 m. Figures 16, 17 & 19 provide additional detail on the composition of algal, hard coral and other invertebrates and variation between depth zones.

Mean coral cover on Tassie Shoal (8.6%) was similar to Evans Shoal (Figure 20), but no hard coral was observed below 40 m depth, and areas below 40 m at Tassie Shoal were predominantley sand (Figure 21). The shallow plateau area of Tassie Shoal had a similar mix of coral species to Evans Shoal (Figures 17 & 23), but there was more reefy substrate and small bommies with encrusting coral and algae were common. Figures 21-24 summarise the relative abundance of the major biotic groups and changes in their relative contribution to the benthos with depth.

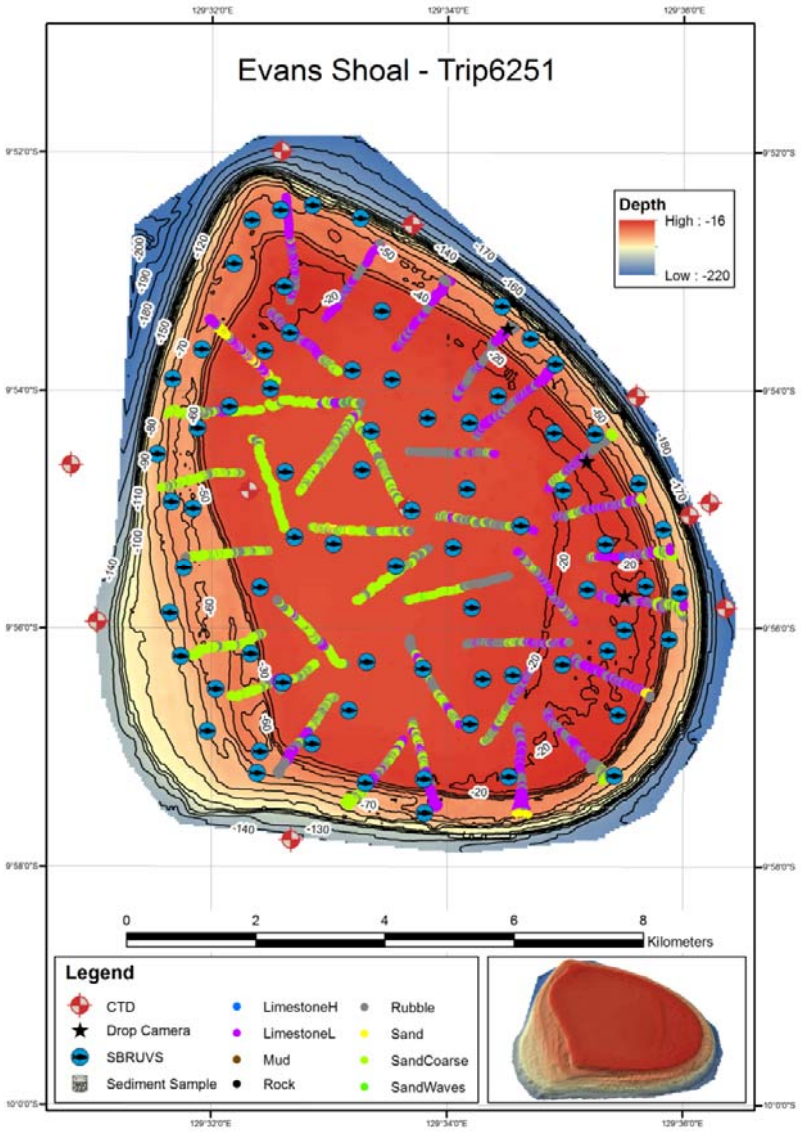

Figure 13: Sampling completed at Evans Shoal. Towed video and SBRUVS stations are overlaid on bathymetry of the shoal produced from the expedition's multibeam data. A 3D representation of the shoal is shown in the lower right box. Warmer colours associated with shallower depths. The multi-coloured "worms" summarise the benthos as observed from the real-time towed video.

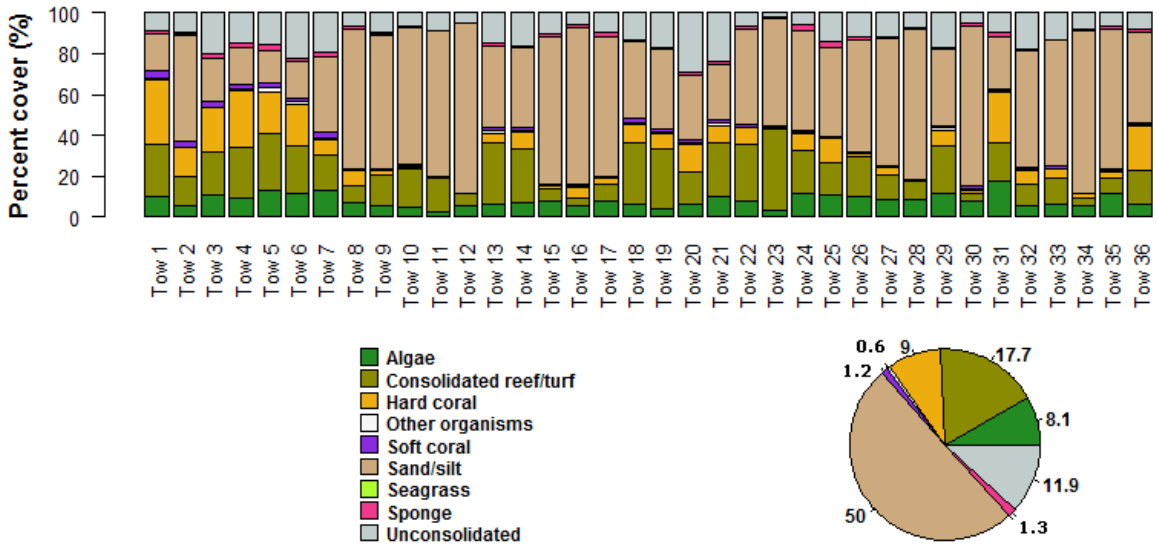

Figure 14:. Summary of the abundance (% cover) of the broad-scale categories of benthos at Evans Shoal, derived from image analysis of high resolution still photos taken using the AIMS towvideo system. Data for individual transects are shown in the bar plots and overall image level percentages for the shoal in the pie diagram.

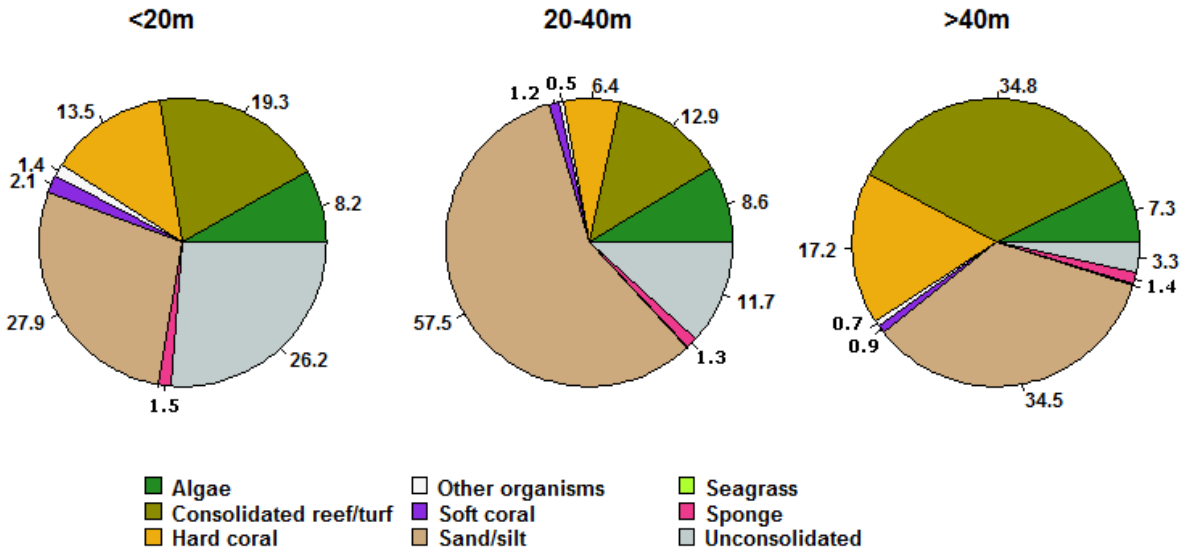

Figure 15: Summary of the relative proportion of each of the broad-scale categories of benthos across depths at Evans Shoal.

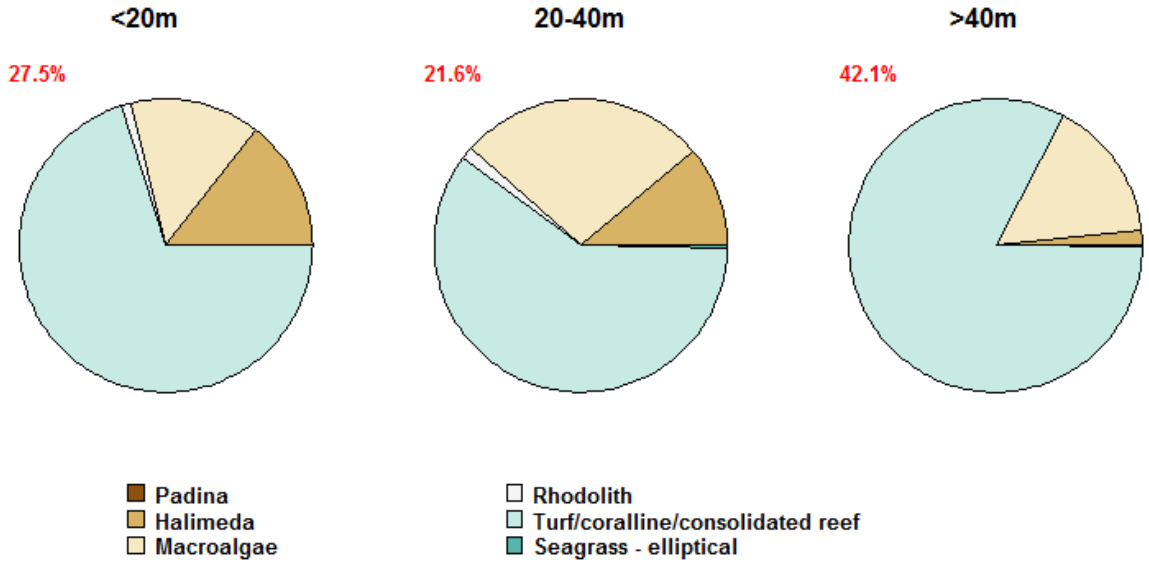

Figure 16: Summary of the proportion of each of the fine-scale categories of algae and seagrass occurring across Evans Shoal grouped by depth. The proportion of all benthos within each grouping that was represented by alage and seagrass is denoted alongside each pie diagram.

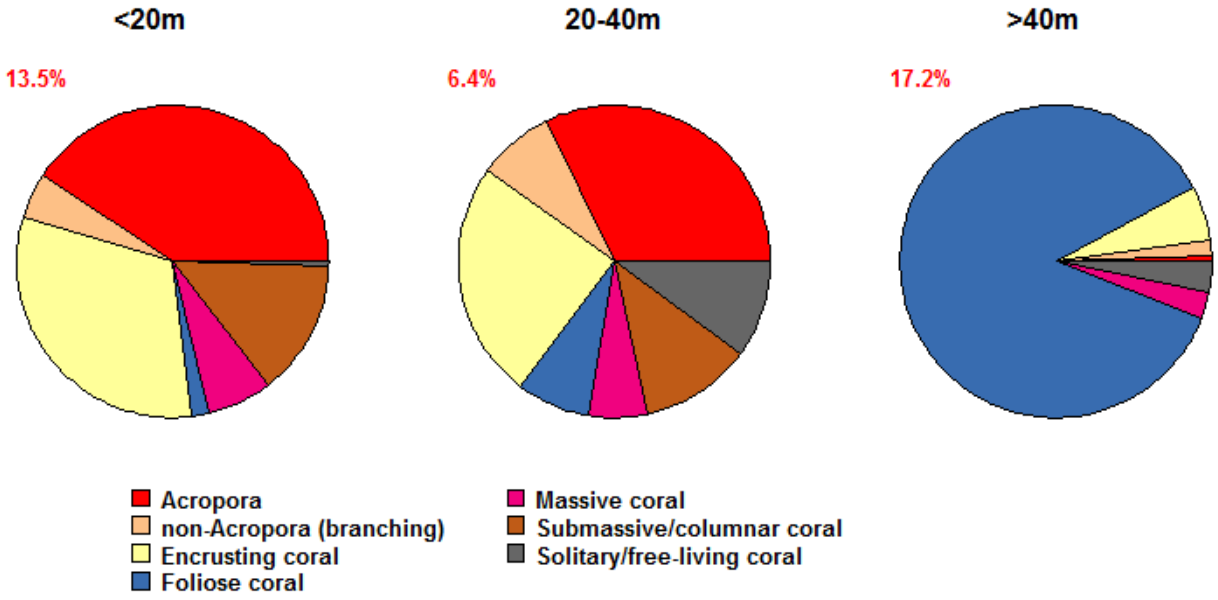

Figure 17: Summary of the proportion of each of the fine-scale categories of hard coral occurring across Evans Shoal grouped by depth. The proportion of all benthos within each grouping that was represented by hard coral is denoted alongside each pie diagram.

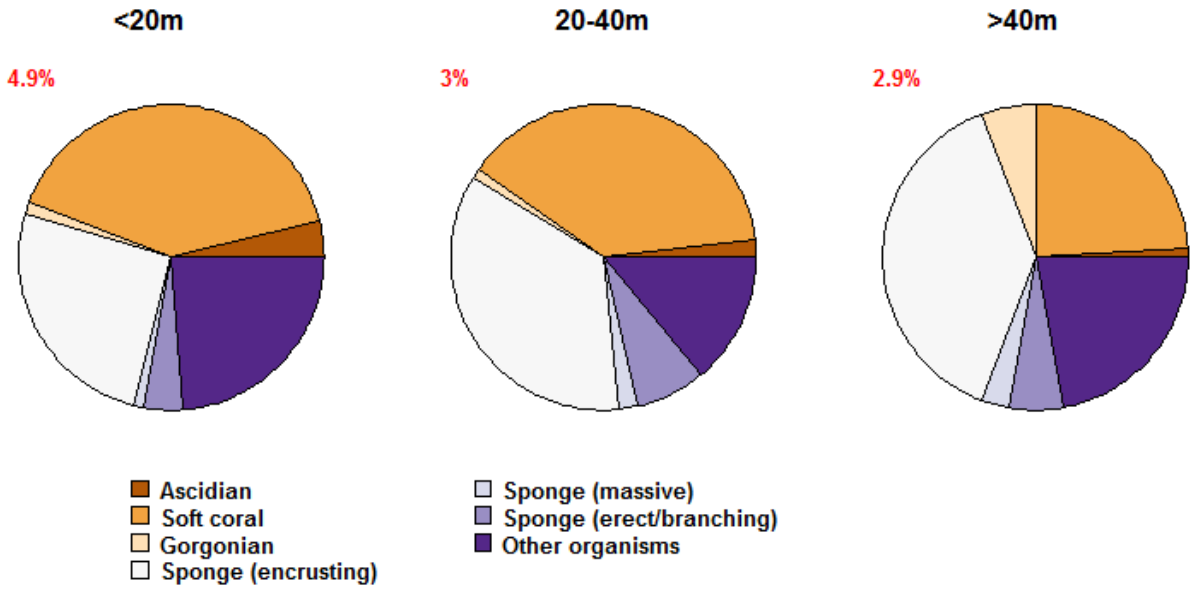

Figure 18: Summary of the proportion of each of the fine-scale categories of other organisms occurring across Evans Shoal grouped by depth. The proportion of all benthos within each grouping that was represented by other organisms is denoted alongside each pie diagram.

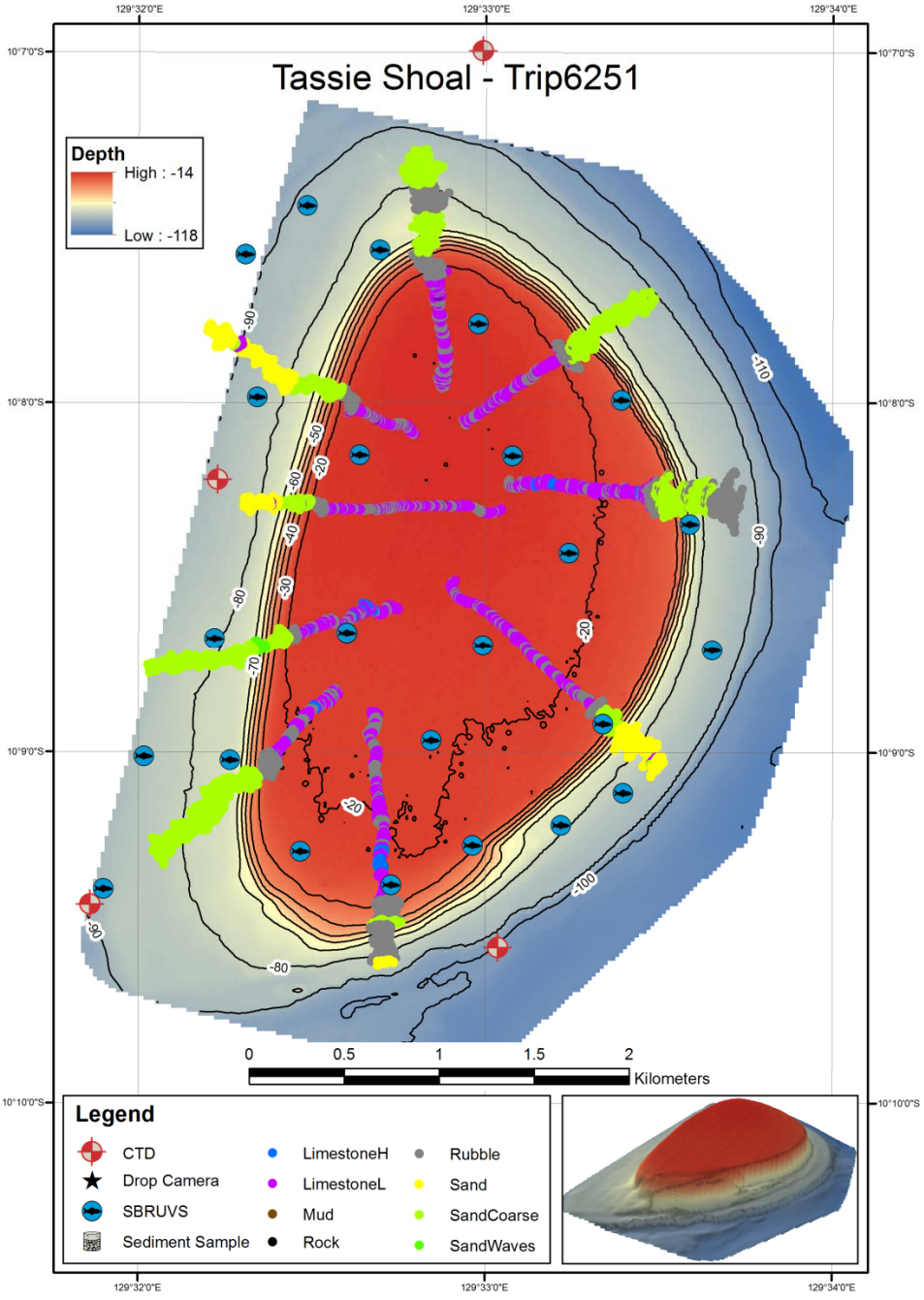

Figure 19: Sampling completed at Tassie Shoal. Towed video and SBRUVS stations are overlaid on bathymetry of the shoal produced from the expedition's multibeam data. A 3D representation of the shoal is shown in the lower right box. Warmer colours associated with shallower depths. The multi-coloured "worms" summarise the benthos as observed from the real-time towed video.

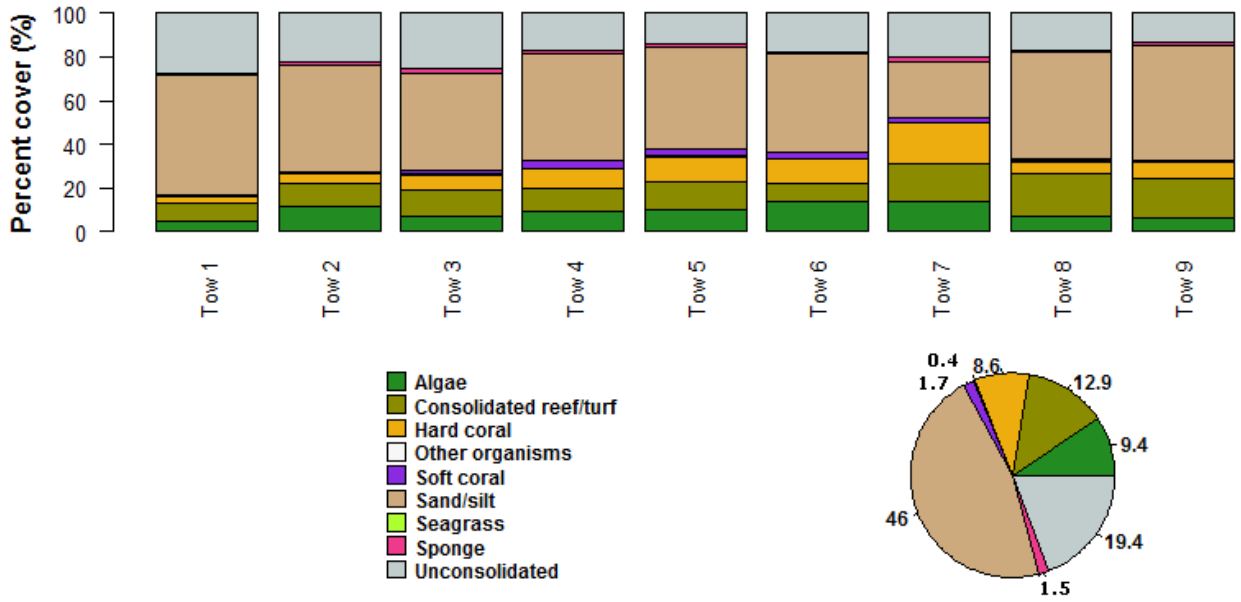

Figure 20: Summary of the abundance (% cover) of the broad-scale categories of benthos at Tassie Shoal, derived from image analysis of high resolution still photos taken using the AIMS towvideo system. Data for individual transects are shown in the bar plots and overall image level percentages for the shoal in the pie diagram.

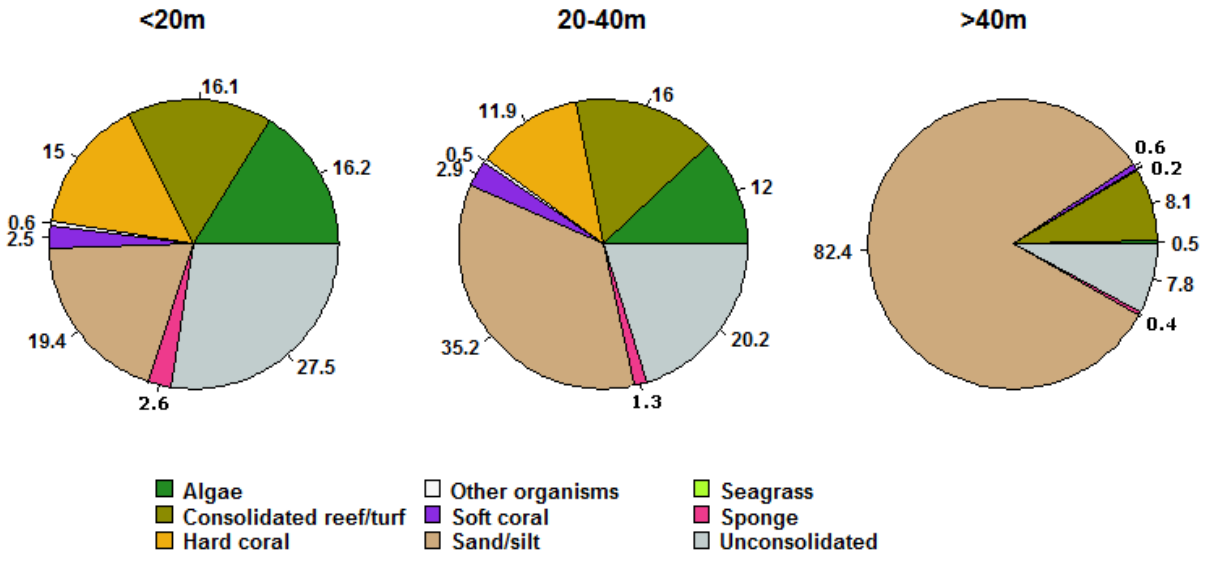

Figure 21: Summary of the relative proportion of each of the broad-scale categories of benthos across depths at Tassie Shoal.

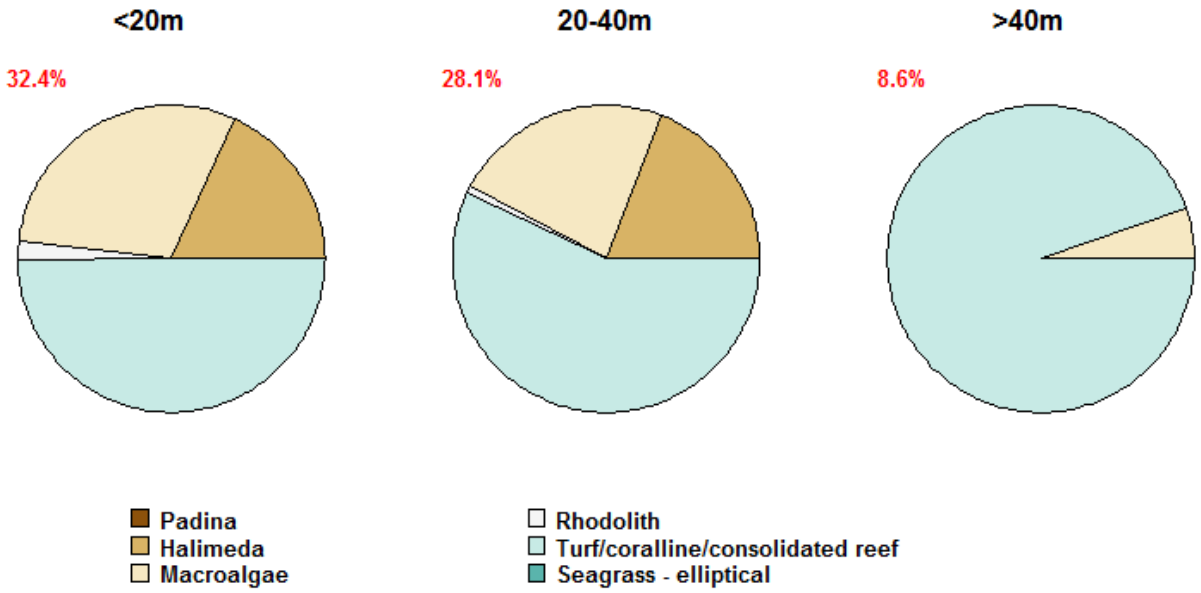

Figure 22: Summary of the proportion of each of the fine-scale categories of algae and seagrass occurring across Tassie Shoal grouped by depth. The proportion of all benthos within each grouping that was represented by alage and seagrass is denoted alongside each pie diagram.

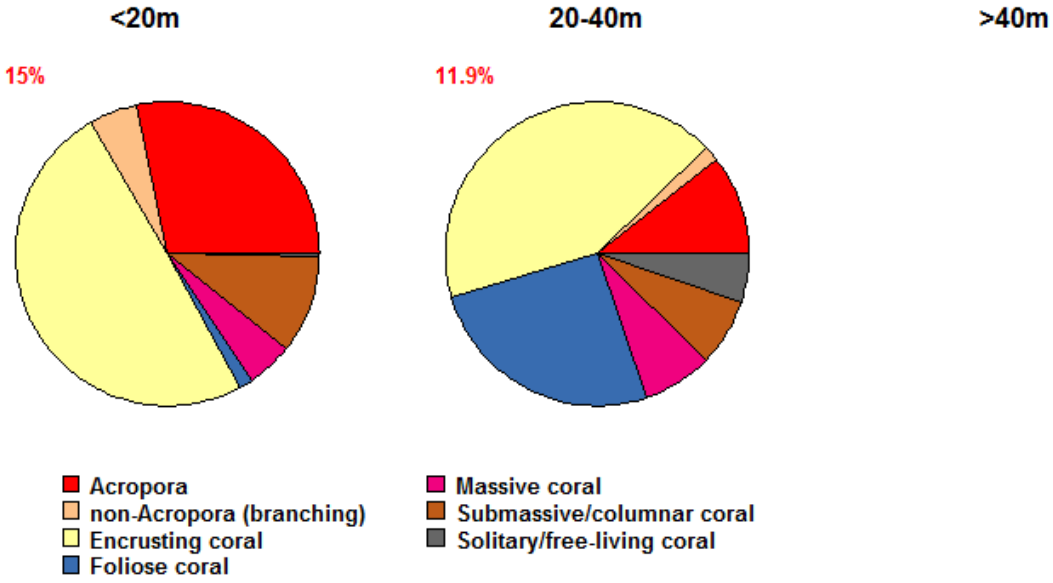

Figure 23: Summary of the proportion of each of the fine-scale categories of hard coral occurring across Tassie Shoal grouped by depth. The proportion of all benthos within each grouping that was represented by hard coral is denoted alongside each pie diagram.

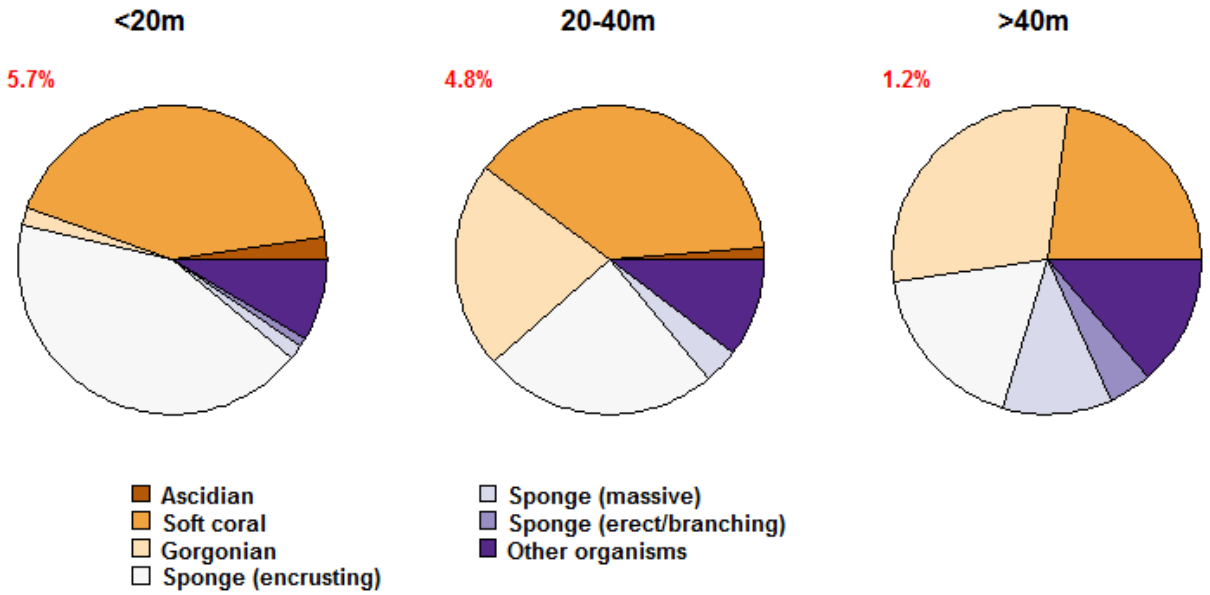

Figure 24: Summary of the proportion of each of the fine-scale categories of other organisms occurring across Tassie Shoal grouped by depth. The proportion of all benthos within each grouping that was represented by other organisms is denoted alongside each pie diagram.

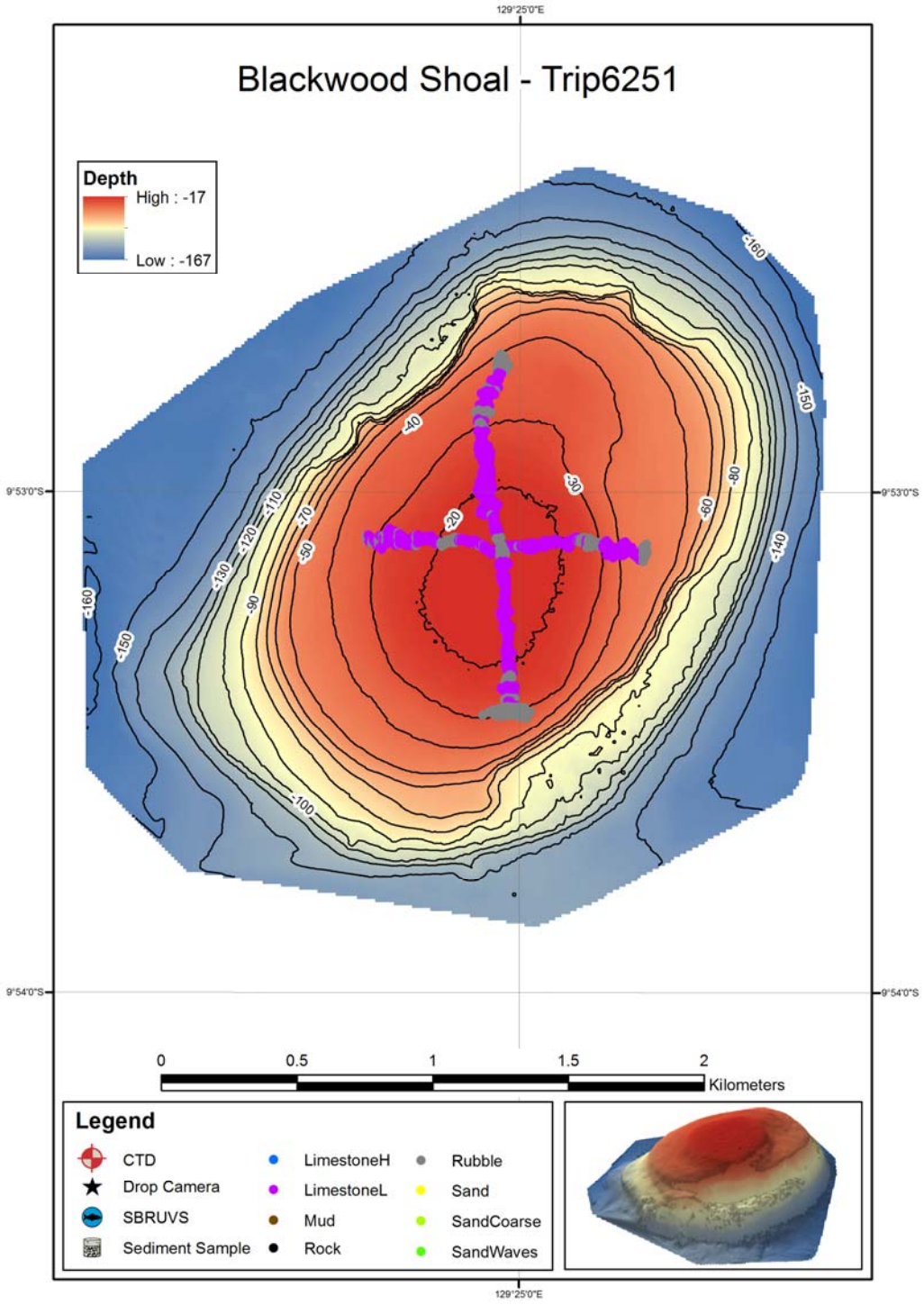

Figure 25: Sampling completed at Blackwood Shoal, which consisted of multibeam mapping and two towed video transects across central plateau region. The bathymetric representation of the shoal was produced from the expedition's multibeam data. A 3D representation of the shoal is shown in the lower right box. Warmer colours associated with shallower depths. The multi-coloured "worms" summarise the benthos as observed from the real-time towed video.

Blackwood Shoal was the smallest and shallowest shoal visited, with only two towed video transects captured representing the broad north-south and east-west axes of the plateau. It was a coral dominated shoal plateau (Figure 26), particularly accross the shallowest area, where coral cover reached 40% in depths <20 m (Figure 27). Coral cover declined to 20% beyond 20 m depth and contributed 17% beyond 40 m depth, where the shallow Acroporid species gave way to a foliaceous dominated assemblage (Figure 29). In contrast the contribution of plants, particularly Halimeda and macroalgae was highest below 20 m depth (Figure 28). Changes with depth in other invertabrate contributions to the benthic ocmmunity, such as soft corals, was also recorded (Figure 30).

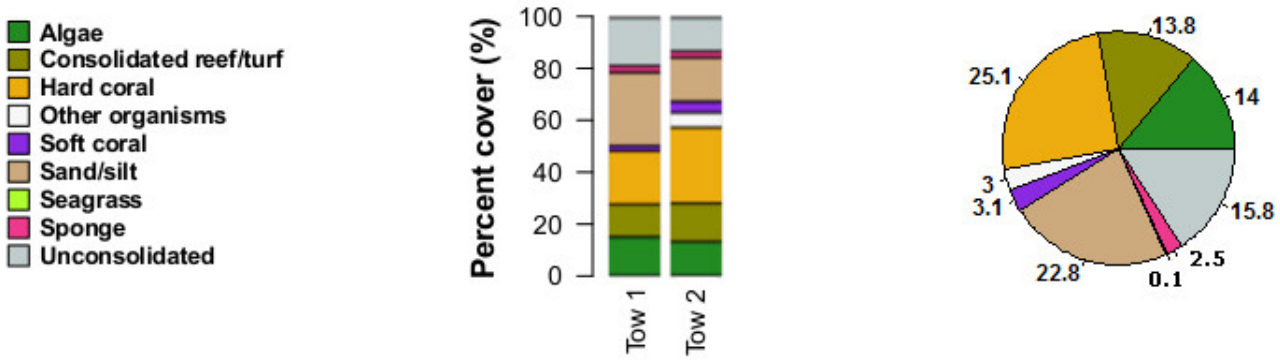

Figure 26: Summary of the abundance (% cover) of the broad-scale categories of benthos at Blackwood Shoal, derived from image analysis of high resolution still photos taken using the AIMS towvideo system. Data for individual transects are shown in the bar plots and overall image level percentages for the shoal in the pie diagram.

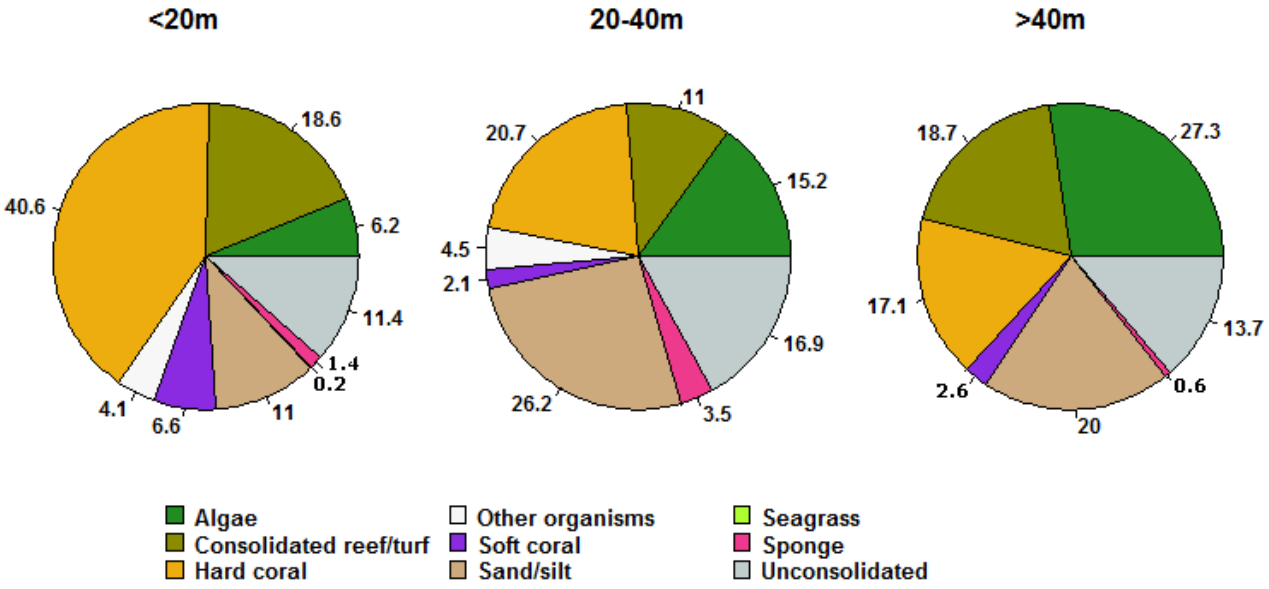

Figure 27: Summary of the relative proportion of each of the broad-scale categories of benthos across depths at Blackwood Shoal.

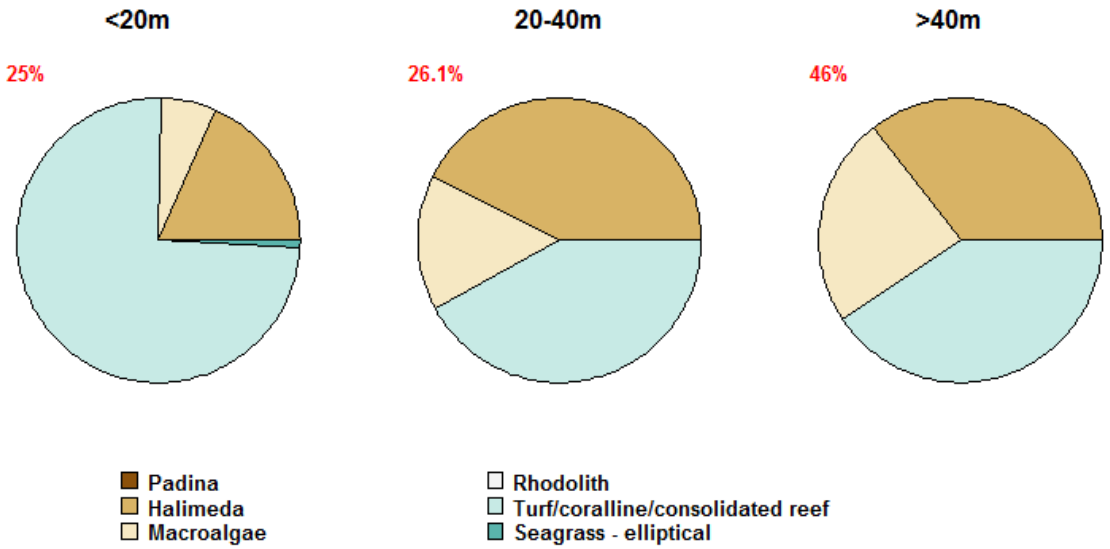

Figure 28: Summary of the proportion of each of the fine-scale categories of algae and seagrass occurring across Blackwood Shoal grouped by depth. The proportion of all benthos within each grouping that was represented by alage and seagrass is denoted alongside each pie diagram.

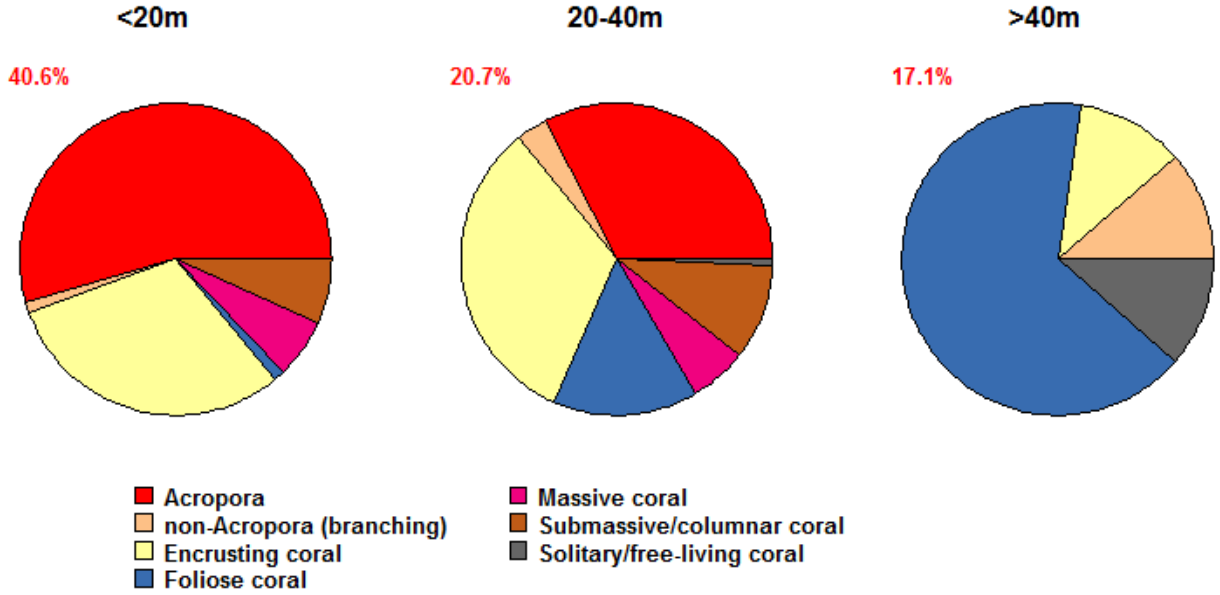

Figure 29: Summary of the proportion of each of the fine-scale categories of hard coral occurring across Blackwood Shoal grouped by depth. The proportion of all benthos within each grouping that was represented by hard coral is denoted alongside each pie diagram.

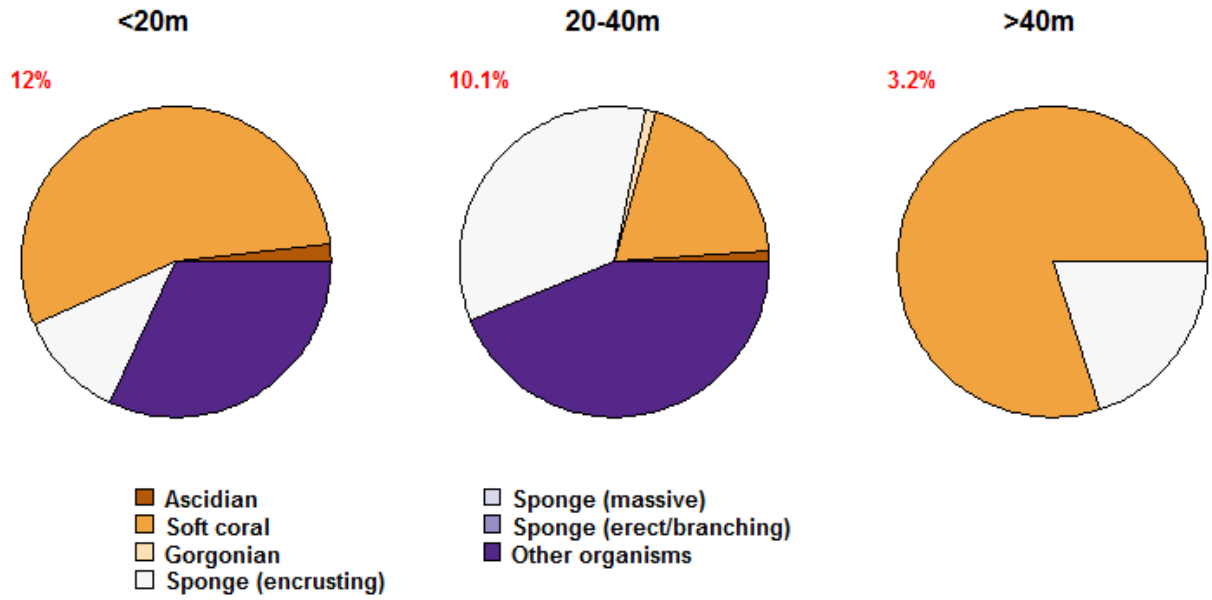

Figure 30: Summary of the proportion of each of the fine-scale categories of other organisms occurring across Blackwood Shoal grouped by depth. The proportion of all benthos within each grouping that was represented by other organisms is denoted alongside each pie diagram.

2.4.1.3 Shoal Benthic Habitat Modelling results

Accuracy estimates for benthic modelling based on downward facing still images and forward facing real time towed video showed each approach performed quite differently. The real time towed video benthic model test indicated very high accuracy results with AUC values all greater than 0.95 (Table 7). Digital still image model performance was much poorer than the real time towed video, with only two of the seven models tested having AUC values over 0.6 (Table 7).

The discrepancy in model accuracy comparing the two image methods is most likely due to biases in the way the biotic habitats are sampled (both based on spatial scale and canopy verses fragmented understory communities). Forward facing towed video provides a broad-scale landscape measure of habitat, well matched to the spatial scale of the multibeam depth and derived habitat metrics (scale 10s-100s of metres, Table 3). Thus the model based on real-time video is sensitive to large three dimensional habitat forming communities such as mature corals, algae and sponges; however understory communities and areas of bare substrate are typically under-represented. In contrast, the downward facing camera picks up fine scale patterns (sub metre) in understory communities, and larger mature three dimensionally complex habitats are under underrepresented. In the model based on digital still data encrusting and juvenile benthic groups are better represented and areas of bare substrate with no-biota (rubble/sand) can make up a very large representation of the points sampled. The combination of broad scale (forward facing real time towed video) and fine scale (downward facing digital stills) provide a holistic and less biased view of community composition. To aid this interpretation a couple of measures could be used to increase the model accuracy of the towed video digital stills; for example for each image, thresholding the five points per image to classify each image into one habitat type based on a majority rule. The second method would be to aggregate habitat classifications based on a range of neighbouring images. The appropriate size of the neighbourhood can be determined based on a spatial autocorrelation metric such as a variogram and may vary based on the spatial pattern and patchiness of different biotic groups (see Holmes et al 2007 for methods and interpretation).

Spatial representations of probabilistic models from real time video and digital stills are shown for Evans Shoal in Figure 32 and 33, for Tassie Shoal in Figures 35 and 36 and for Blackwood Shoal in Figures 38 and 39. A heat map with Euclidian distance based cluster analysis was used to summarise relative variable importance (scaled model accuracy "Gain" index) for model prediction of biotic groups from multibeam is shown in Figure 40 for digital stills and Figure 41 for real time towed video. More detailed information on model accuracy (AUC plot), variable importance (plot of gain index for all multibeam variables) and the partial response of each biotic group to the most important six variables are detailed in Appendix 3 (Figures A3.1-A3.6 for digital stills and Figures A3.7-A3.12 for real time towed video).

For habitat models based on digital stills (Figures 32, 35 and 38), some caution must be used when interpreting the relationships between the habitat variables and biotic groups as poor model performance effects the accuracy of these relationships compared to the real time towed video. As a result, the relationship between multibeam variables and each biotic group is quite variable and the cluster analysis (Figure 40) identified four main groups in the dendogram. Firstly there is the "Macroalage and Sponge group" where two variables "plan" and "rng50" dominate. These variables are both measures of rugosity and for this group, identify a correlation with areas that are flatter with low rugosity. The second cluster "Tabulate acropora" is highly correlated with the variable mean50, which is a broad scale indicator of depth dependence with probability of occurrence increasing with depths up to 50 m (Figure A3.3). The third cluster contains "Branching acropora" and "All hard corals", and are most highly correlated to mean50, asp and rng50. This cluster shows a broad-scale depth relationship (mean 50) found between 20-60 meters, in areas of higher rigosity (rng50) and more commonly on the east and west edges of the shoals (asp) (Figures A3.1 and A3.4). The final cluster contains "Turf and coralline algae", "Soft corals" and "other corals" (such as free living species). This group is typified by its relationship with rng50 and rng25 plus asp showing correlation with slopes (indicated by rng values) particularly a north facing aspect (Figures A3.2, A3.6 and A3.7).

For habitat models based on real time towed video (Figures 33, 36 and 39) the relationships between multibeam variables and each biotic group identified two distinct clusters (Figure 41). The first cluster contains the main coral groups (dense, medium and sparse) where the most important predictor variables are mean50 and rng50. The patterns here show an increase in coral probability over certain depth distributions (less than 50 m and greater than 50 m to 75 m; Figures A3.10, A3.12 and A3.13) which are likely to be indicative of two different types of coral communities and may also reflect the different depth profiles at each shoal. The probability of coral occurrence increases with broad scale rugosity indicative of three dimensionally complex areas and slopes. The second cluster contains the "medium" and "sparse filter feeder" communities as well as the "Medium hard coral and Halimeda community". This cluster is also characterised by the importance of mean50 and rng50 with an increase in probability of occurrence with a decrease in depth from 50 m but this is contrasted in most cases (the exception being Medium hard coral and Halimeda community) in areas of lower rugosity (rng50) typified by flatter lagoon and rubble zone areas (Figures A3.8, A3.9 and A3.11).

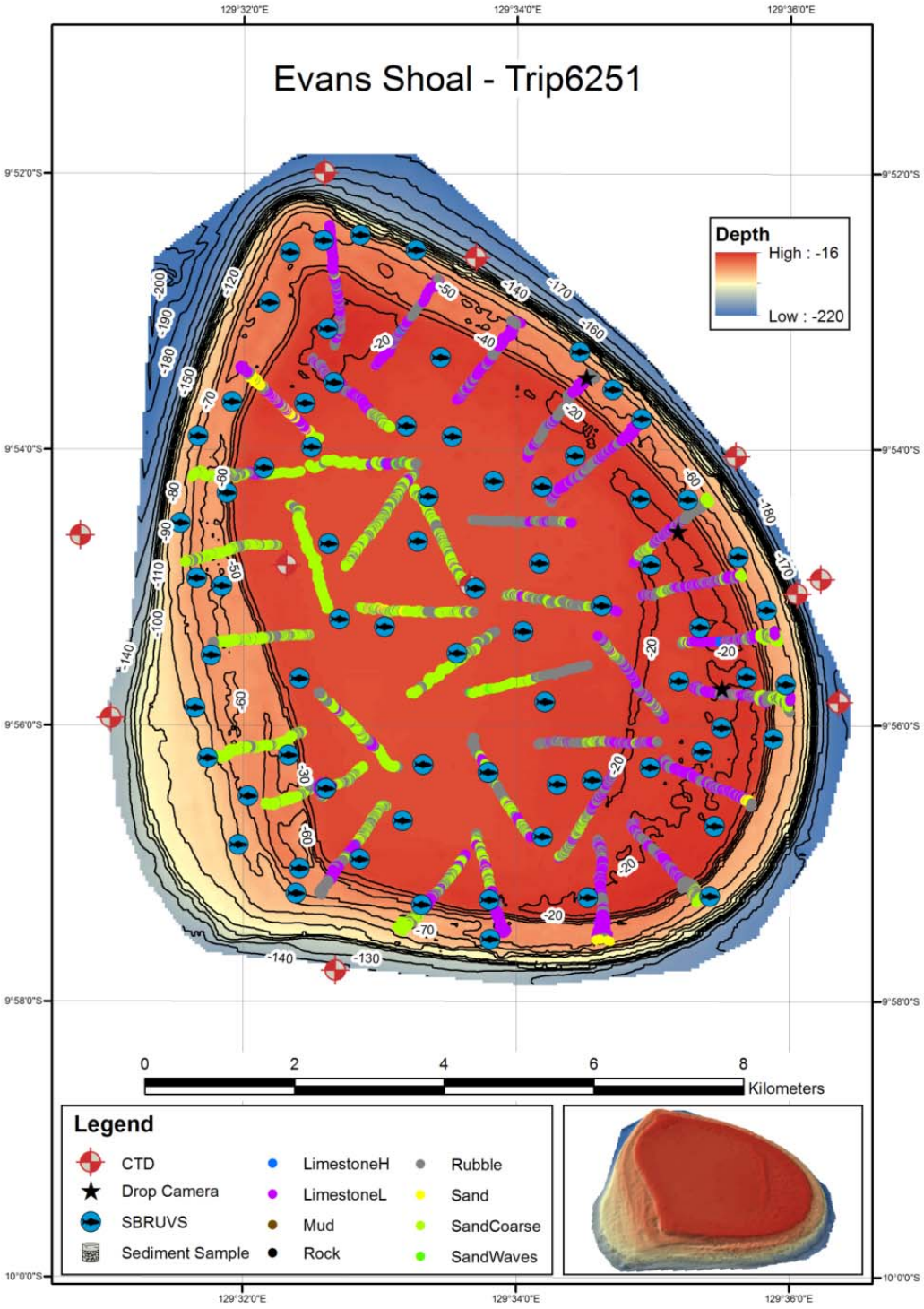

Figure 31: Sampling completed at Evans Shoal. Towed video and SBRUVS stations are overlaid on bathymetry of the shoal produced from the expedition's multibeam data. A 3D representation of the shoal is shown in the lower right box. Warmer colours associated with shallower depths.

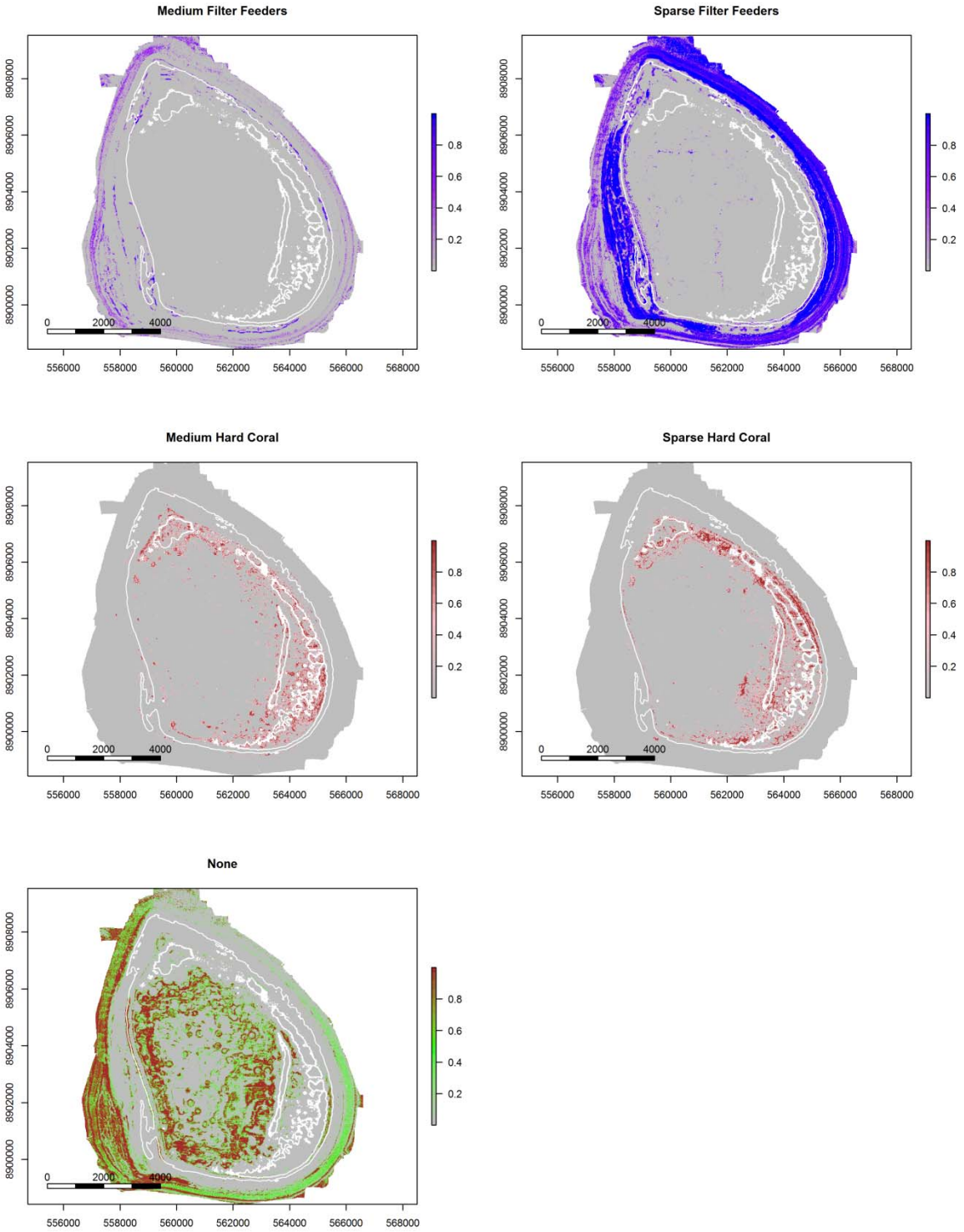

Figure 32: Evans Shoal - modelled spatial distributions describing the presence/absence probabilities for major benthic habitat classes generated using oblique forward facing real-time scored towed video. The 20 m & 50 m depth contours shown in white.

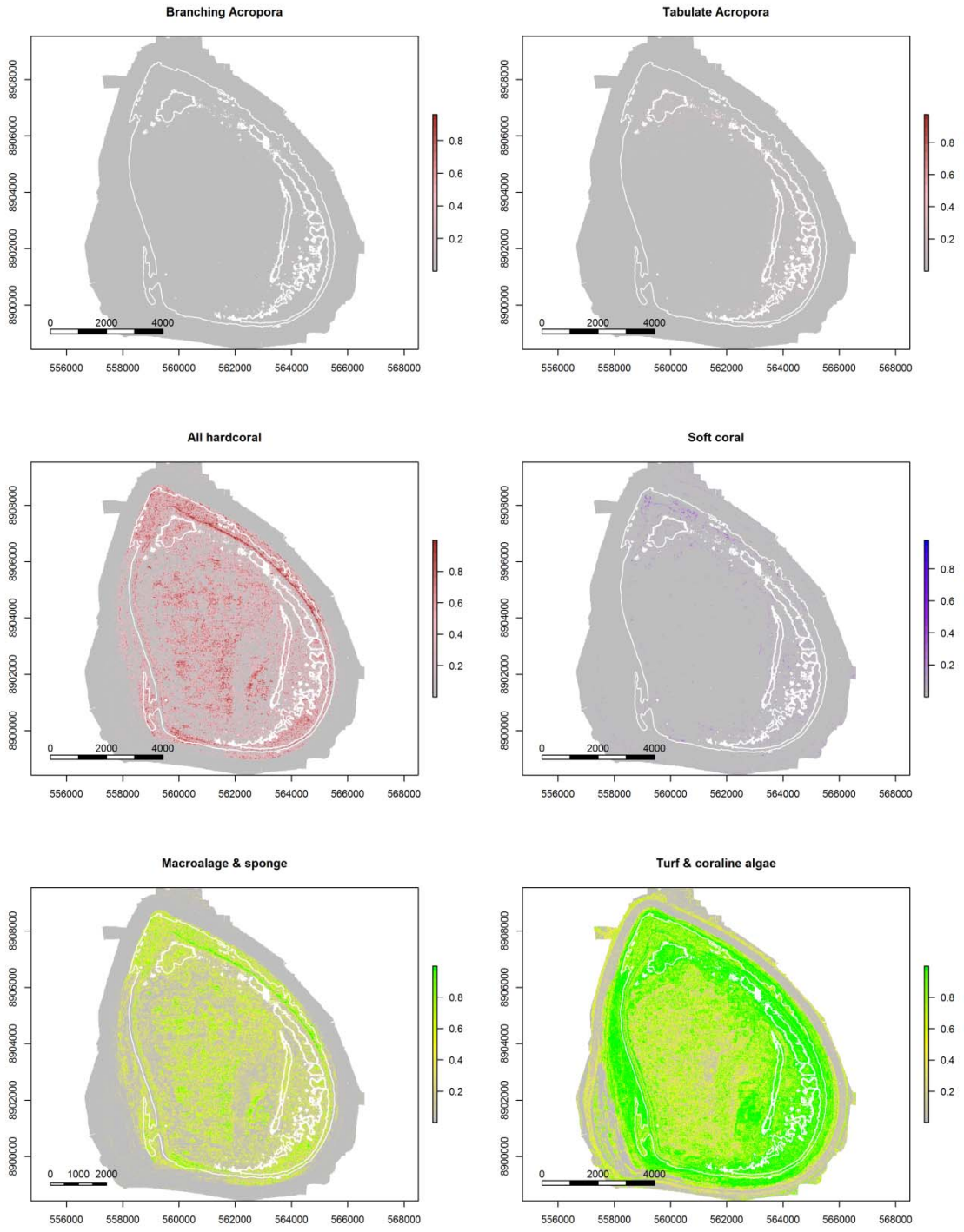

Figure 33: Evans Shoal - modelled spatial distributions describing the presence/absence probabilities for major benthic habitat classes generated using post processed downward facing digital stills. The 20 m & 50 m depth contours shown in white

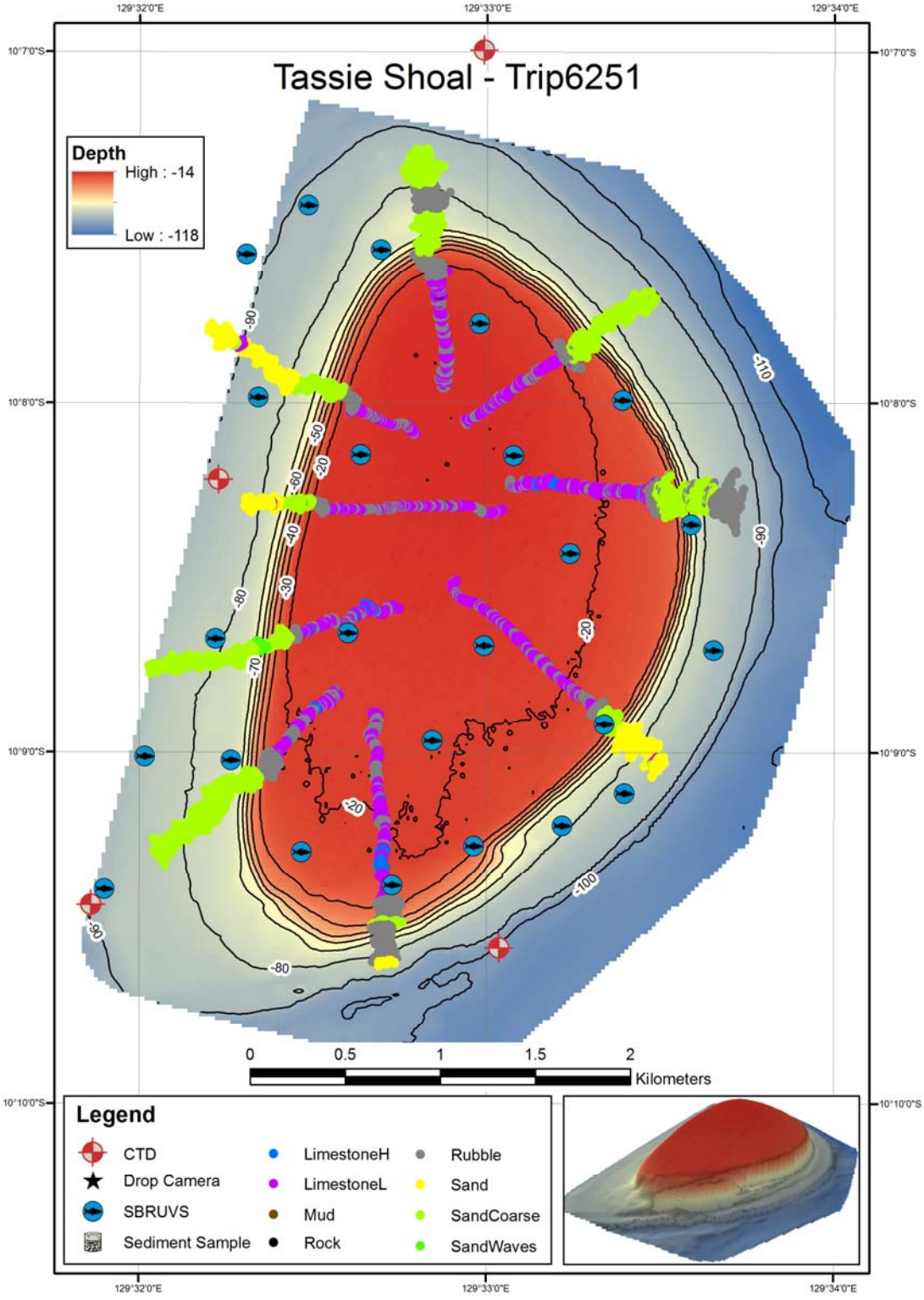

Figure 34: Sampling completed at Tassie Shoal. Towed video and SBRUVS stations are overlaid on bathymetry of the shoal produced from the expedition's multibeam data. A 3D representation of the shoal is shown in the lower right box. Warmer colours associated with shallower depths.

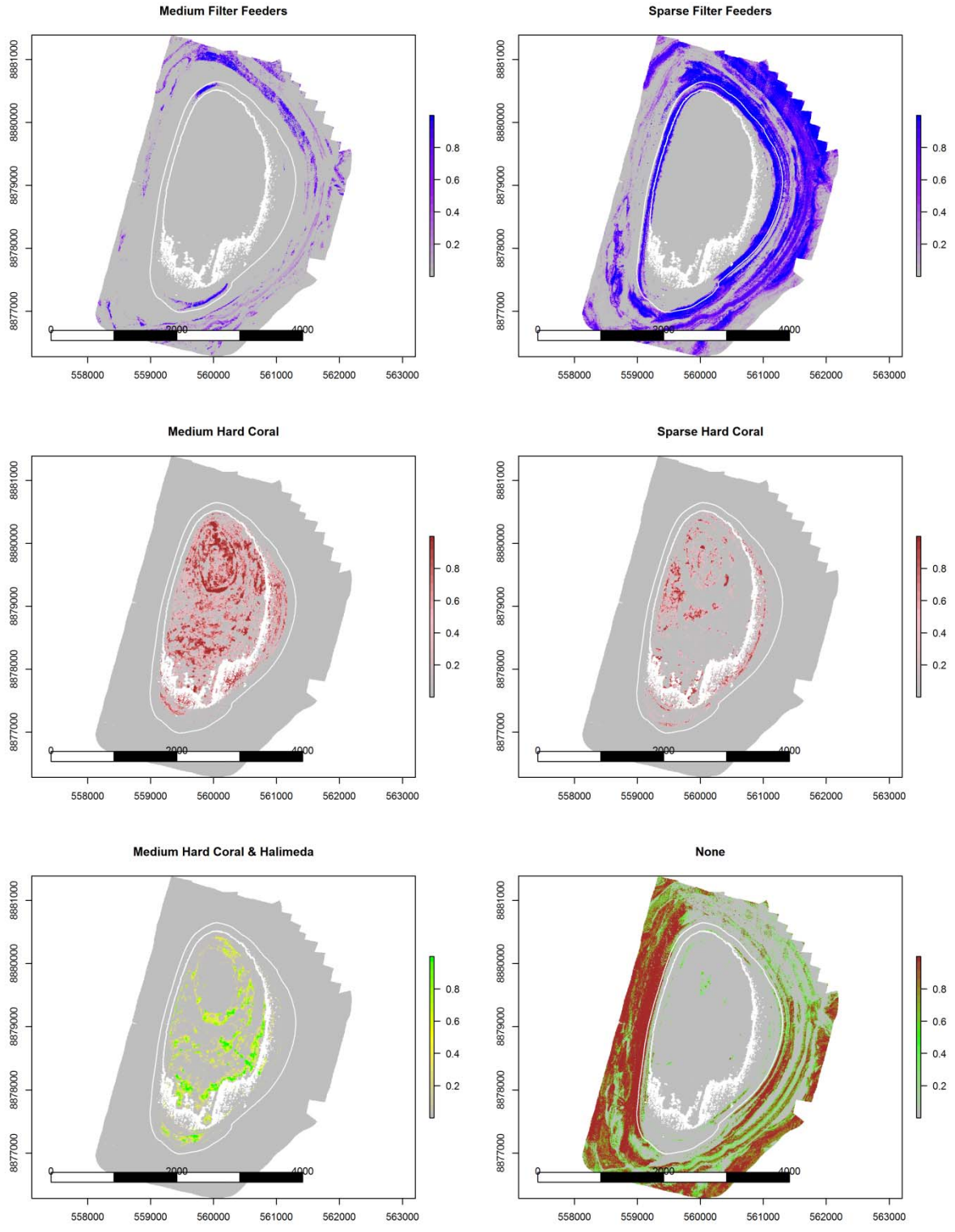

Figure 35: Tassie Shoal - modelled spatial distributions describing the presence/absence probabilities for major benthic habitat classes generated using oblique forward facing real-time scored towed video. The 20 m & 50 m depth contours shown in white.

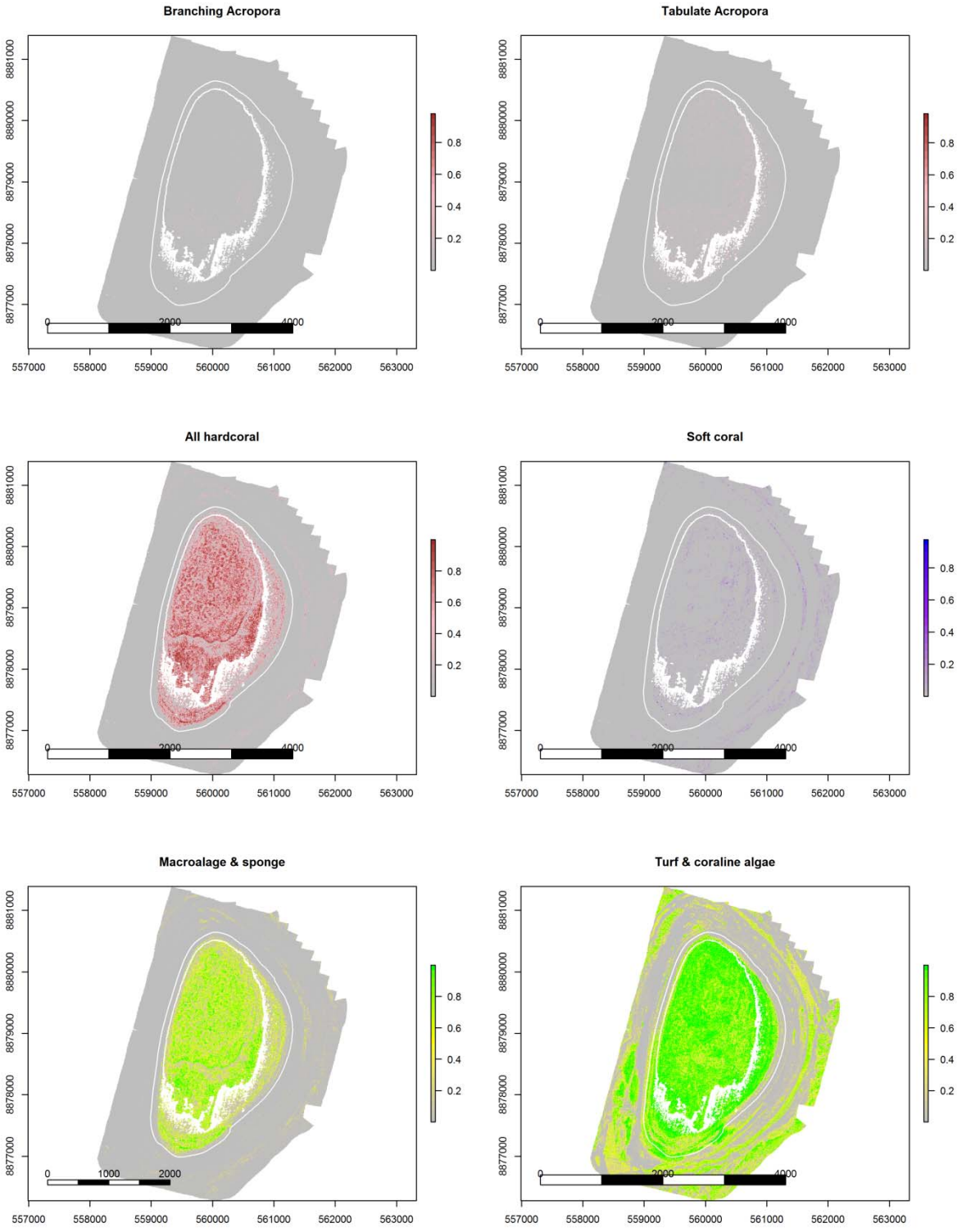

Figure 36: Tassie Shoal - modelled spatial distributions describing the presence/absence probabilities for major benthic habitat classes generated using post processed downward facing digital stills. The 20 m & 50 m depth contours shown in white.

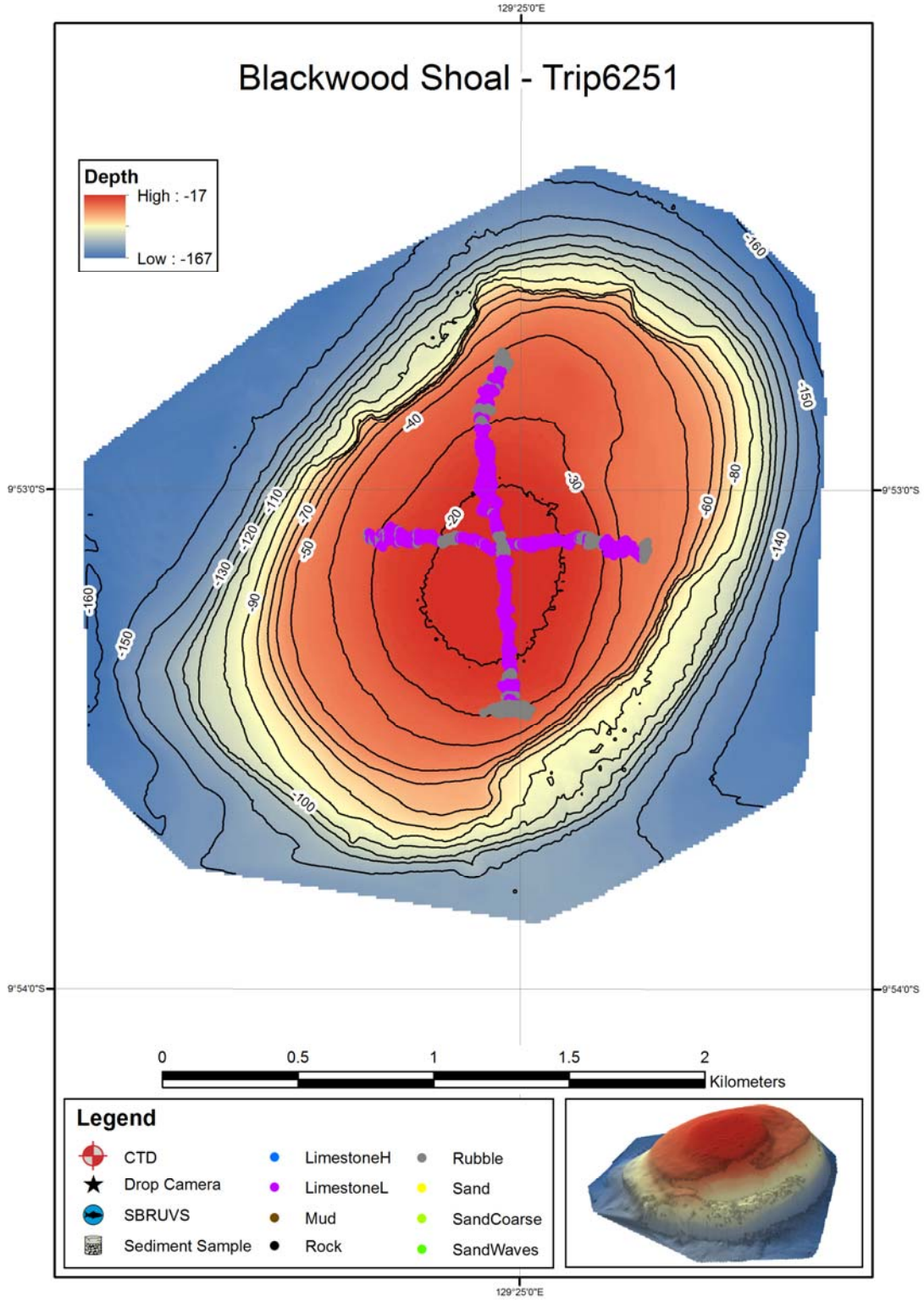

Figure 37: Sampling completed at Blackwood Shoal, which consisted of multibeam mapping and two towed video transects across central plateau region. The bathymetric representation of the shoal was produced from the expedition's multibeam data. A 3D representation of the shoal is shown in the lower right box. Warmer colours associated with shallower depths.

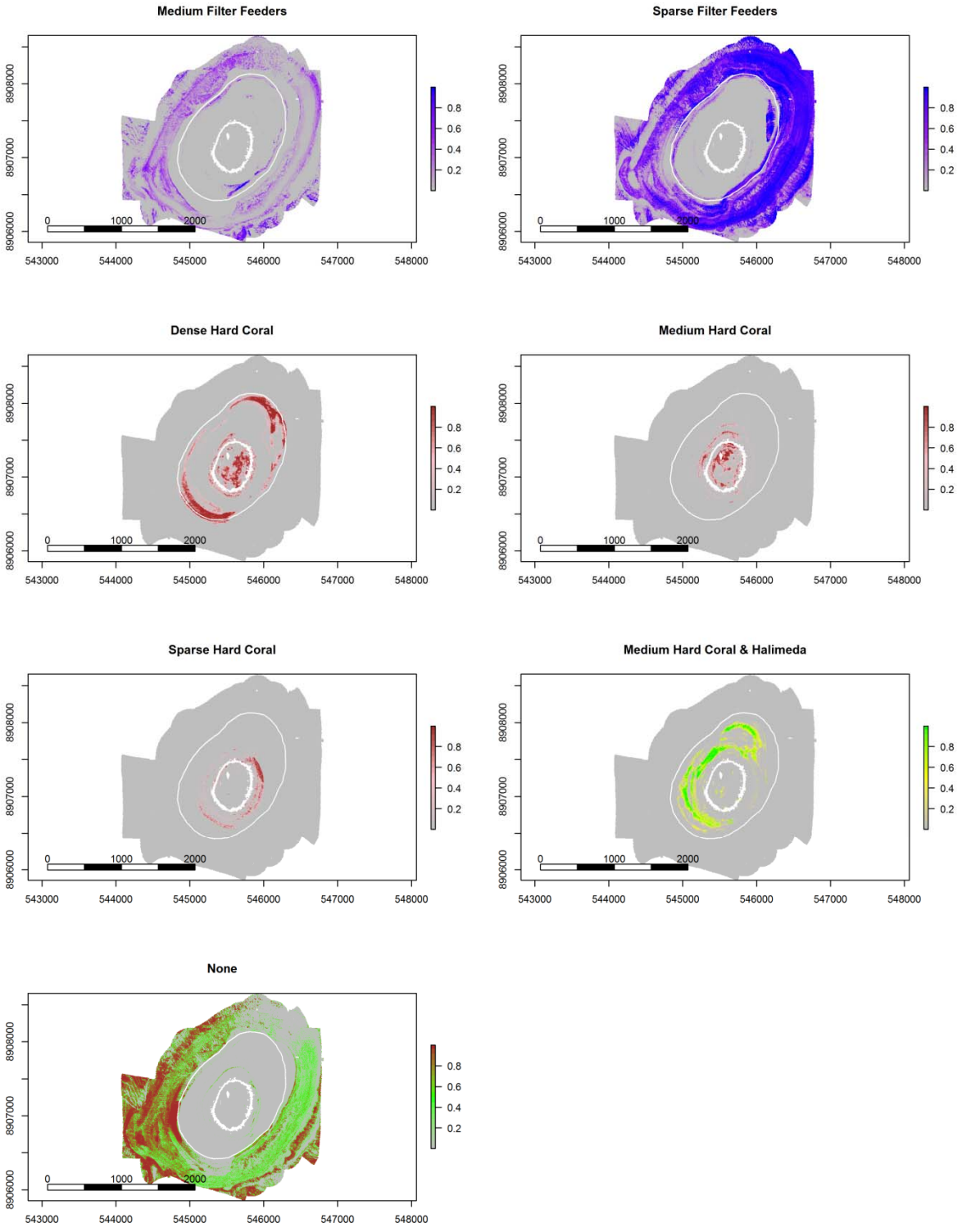

Figure 38: Blackwood Shoal - modelled spatial distributions describing the presence/absence probabilities for major benthic habitat classes generated using oblique forward facing real-time scored towed video. The 20 m & 50 m depth contours shown in white.

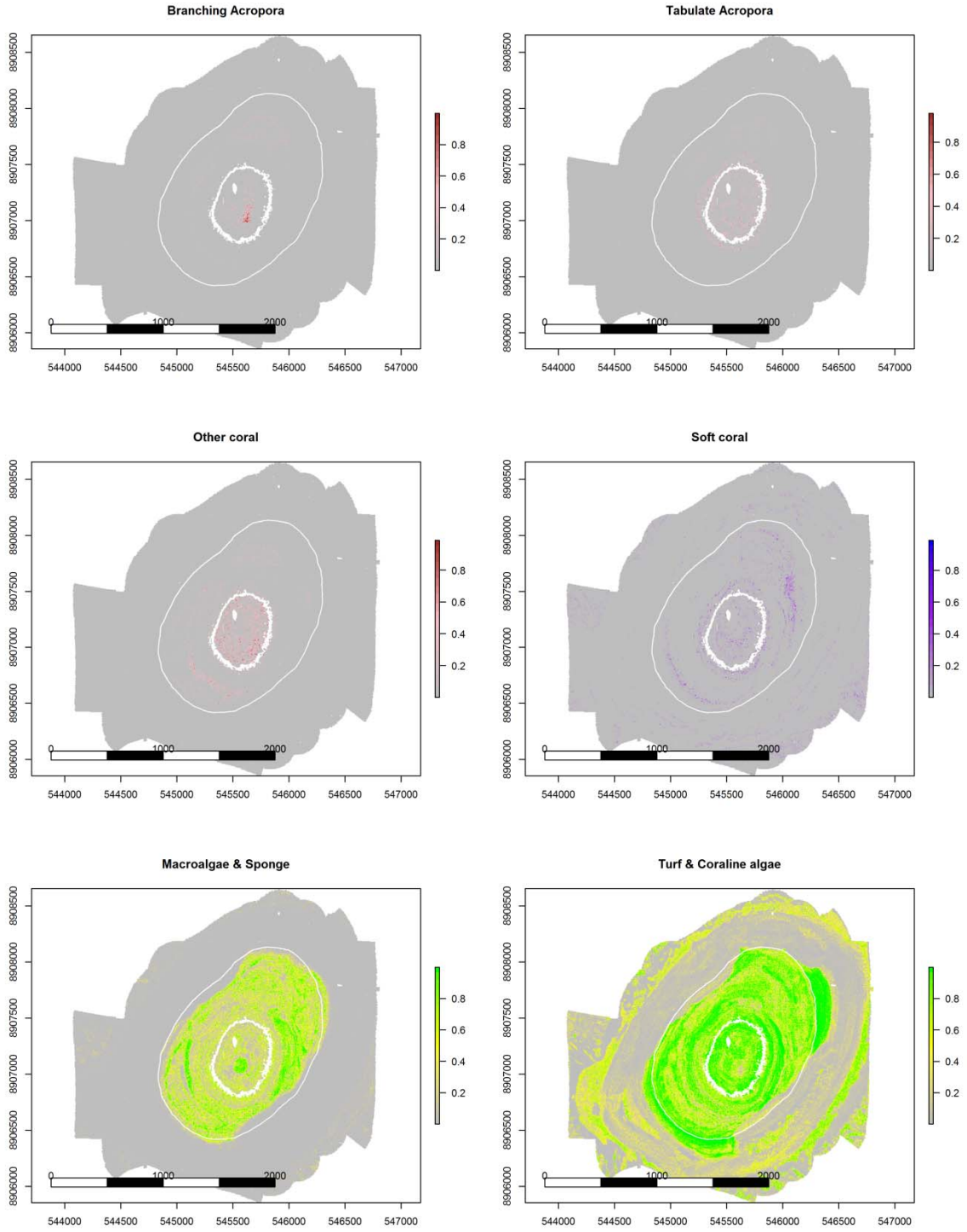

Figure 39: Blackwood Shoal - modelled spatial distributions describing the presence/absence probabilities for major benthic habitat classes generated using post processed downward facing digital stills. The 20 m & 50 m depth contours shown in white.

Table 7. Boosted model (xgboost) model accuracy estimates (AUC and Kappa) comparing towed video and digital stills biota measurement with full resolution multibeam depth and derivatives (2 m pixel at Blackwood, Evans and Tassie shoal) and interpolated multibeam depth and derivatives (50 m pixel at Cape Helveticus and Goodrich Bank).

Method	Sites	Biotic Group	Threshold	% correct	sensitivity	specificity	Kappa	AUC
Digital Stills 2 m bin multibeam	Blackwood, Evans & Tassie	All hard corals	0.50	0.50	0.56	0.49	0.03	0.50
Digital Stills 2 m bin multibeam	Blackwood, Evans & Tassie	Soft corals	0.50	0.95	0.00	1.00	0.00	0.50
Digital Stills 2 m bin multibeam	Blackwood, Evans & Tassie	Tabulate acropora	0.50	0.95	0.00	1.00	0.00	0.64
Digital Stills 2 m bin multibeam	Blackwood, Evans & Tassie	Branching Acropora	0.50	0.98	0.00	1.00	0.00	0.66
Digital Stills 2 m bin multibeam	Blackwood, Evans & Tassie	Macroalgae and sponge	0.50	0.76	0.01	0.98	0.20	0.51
Digital Stills 2 m bin multibeam	Blackwood, Evans & Tassie	Other corals	0.50	0.97	0.00	1.00	0.00	0.55
Digital Stills 2 m bin multibeam	Blackwood, Evans & Tassie	Turf and coralline algae	0.50	0.47	1.00	0.00	0.00	0.50
Real-time towed video 2 m bin multibeam	Blackwood, Evans & Tassie	Medium Filter feeders	0.50	0.99	0.60	1.00	0.69	0.99
Real-time towed video 2 m bin multibeam	Blackwood, Evans & Tassie	Sparse filter feeders	0.50	0.97	0.85	0.98	0.84	0.99
Real-time towed video 2 m bin multibeam	Blackwood, Evans & Tassie	Dense Hard Coral	0.50	0.98	0.77	1.00	0.83	0.99
Real-time towed video 2 m bin multibeam	Blackwood, Evans & Tassie	Medium Hard Coral & Halimeda	0.50	0.98	0.73	1.00	0.80	0.99
Real-time towed video 2 m bin multibeam	Blackwood, Evans & Tassie	Medium Hard Coral	0.50	0.95	0.76	0.98	0.78	0.97
Real-time towed video 2 m bin multibeam	Blackwood, Evans & Tassie	Sparce Hard Coral	0.50	0.95	0.75	0.98	0.78	0.97
Real-time towed video 2 m bin multibeam	Blackwood, Evans & Tassie	None	0.50	0.96	0.89	0.98	0.87	0.99
Real-time towed video 50 m bin multibeam	Cape Helveticus & Goodrich Bank	Burrowers	0.50	0.99	0.46	1.00	0.55	0.99
Real-time towed video 50 m bin multibeam	Cape Helveticus & Goodrich Bank	Dense filter feeders	0.50	1.00	0.38	1.00	0.34	0.85
Real-time towed video 50 m bin multibeam	Cape Helveticus & Goodrich	Medium filter feeders	0.50	0.95	0.74	0.98	0.77	0.98

	Bank							
Real-time towed video 50 m bin multibeam	Cape Helveticus & Goodrich Bank	Sparse filter feeders	0.50	0.90	0.79	0.94	0.74	0.96
Real-time towed video 50 m bin multibeam	Cape Helveticus & Goodrich Bank	No modelled benthos	0.50	0.93	0.95	0.91	0.86	0.98

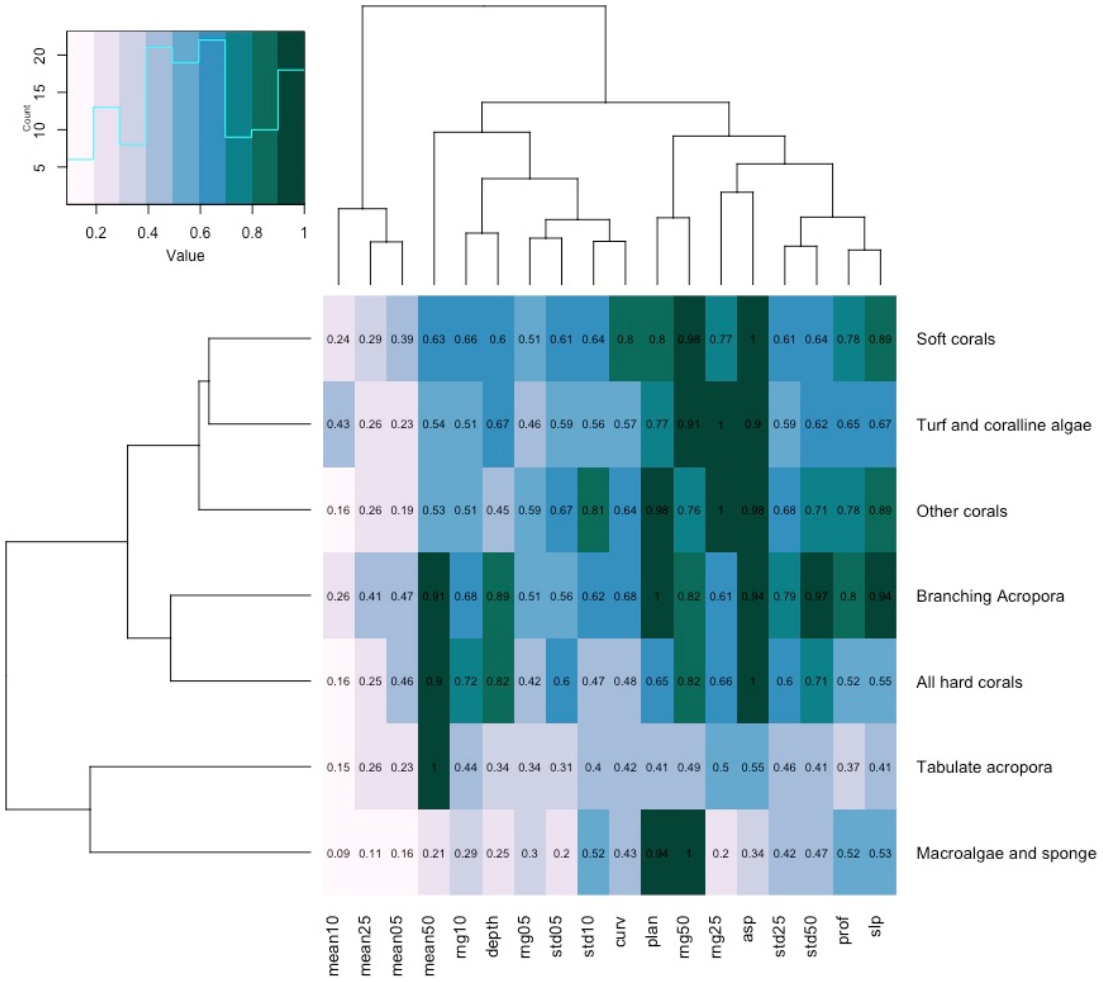

Figure 40: Heatmap with Euclidean distance cluster analysis showing the relative importance for predictor variables (0-1 from least to most important) for towed digital still based benthic habitat models of Blackwood, Evans and Tassie shoal. Benthic groups are on the y-axis and 2 m multibeam depth and derivatives (see Table 3 for descriptions) are on the x-axis.

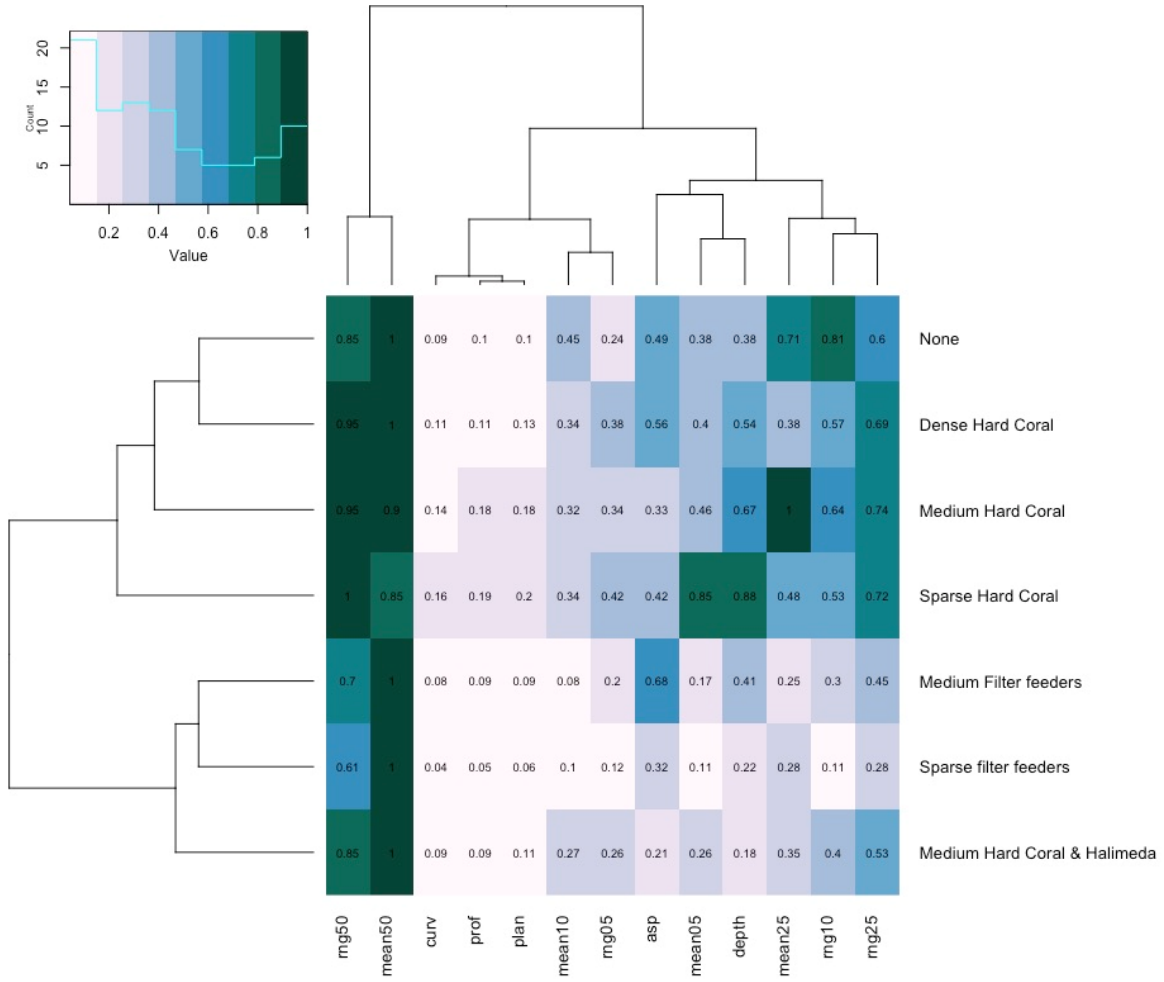

Figure 41: Heatmap with Euclidean distance cluster analysis showing the relative importance for predictor variables (0-1 from least to most important) for towed video real-time classification based benthic habitat models of Blackwood, Evans and Tassie shoal. Benthic groups are on the y-axis and 2 m multibeam depth and derivatives (see Table 3 for descriptions) are on the x-axis.

2.4.1.4. Fish communities

A total of 7282 fish from 304 species were recorded in interrogation of 95 SBRUVS videos (72 from Evans shoal and 23 from Tassie shoal). These included a diverse range of demersal and semi-pelagic fishes, sharks, rays and sea snakes (see Appendix 1 for full list). The bony fishes were most numerous (Actinopterygii; 7175 individuals) followed by the sharks and rays (Chondrichthyes; 81 individuals) and sea snakes (Reptilia; 26 individuals) (Table 8).

Table 8 Summary of each taxonomic Order recorded on 95 SBRUVS samples from Evans Shoal and Tassie Shoal, in decreasing order of diversity.

	Order	Common Name	*n* families	*n* genera	*n* species	*n* individuals
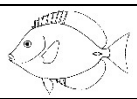	Perciformes	Perch-like fishes	30	102	261	6565
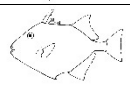	Tetraodontiformes	Puffers and triggerfish	3	13	21	396
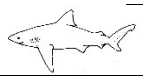	Carcharhiniformes	Sharks	2	5	6	62
	Anguilliformes	Moray eels	1	3	5	8
	Beryciformes	Squirrelfish	1	1	1	3
	Clupeiformes	Herrings	1	1	1	200
	Gasterosteiformes	Flutemouths	1	1	1	3
	Myliobatiformes	Rays	1	2	2	10
	Orectolobiformes	Wobbegong sharks	1	1	1	8
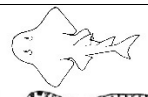	Rajiformes	Shovelnose rays	1	1	1	1
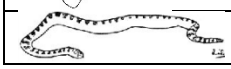	Squamata	Sea snakes	1	4	4	26

Models of richness and abundance as a function of "habitat"

The most parsimonious models of richness and transformed abundance were additive (including only main effects, not any interactions). The final models included only 10 environmental predictors each, but only the first few of these had relatively high influence on the univariate responses.

Species richness was influenced most by the calcareous reef composition of the substratum, and the percentage cover of hard coral on this substratum (Figure 42). The mean species richness in the entire dataset was 21.38 species, with a variance of 258.8 species. The model explained about 62% of this variation in species richness. Species richness was above average for SBRUVS where %calcareous substrata was about 40%, and where %coral cover was about 20%. The partial effects plots show the single influence of one predictor with all other predictors held to their mean value. These influences were about eight extra species above average (~21) once seabed composition exceeded 60% calcareous reef, and about five extra species once %coral cover exceeded 40% (Figure 44). Depths shallower than ~30 m had higher, steeply rising, richness, and bare seabeds had lower than average richness.

Transformed fish abundance was influenced most by the presence of any epibenthos on the seafloor (%bare) and by calcareous reef composition of the substratum. Low values of %bare indicated that the field of view of the SBRUVS was largely covered by epipenthos of any category (e.g. macroalgae, filter feeders) – not just coral. High values of %bare were open seafloors of sand, gravel, or rubble with little or no epibenthic cover. The model explained about half (50.7%) of the variation in transformed fish abundance. Abundance was above average for SBRUVS where there was more than 20% of the seabed in the field of view covered by any category of epibenthos. At this coverage, transformed fish abundance rose above the average transformed abundance by about 0.4 units, or 15%. Back-transformation of the slopes in Figure 45 showed that samples where %bare~20% had ~60-70 fish (about 20-40%) more than the mean (~50 fish). The seabed classifications where %calcareous substrata exceeded 40% also had above average fish abundance (Figure 43). Depth had a lesser influence, but fish abundance was below average in deeper waters and above average in shallows under 30 m.

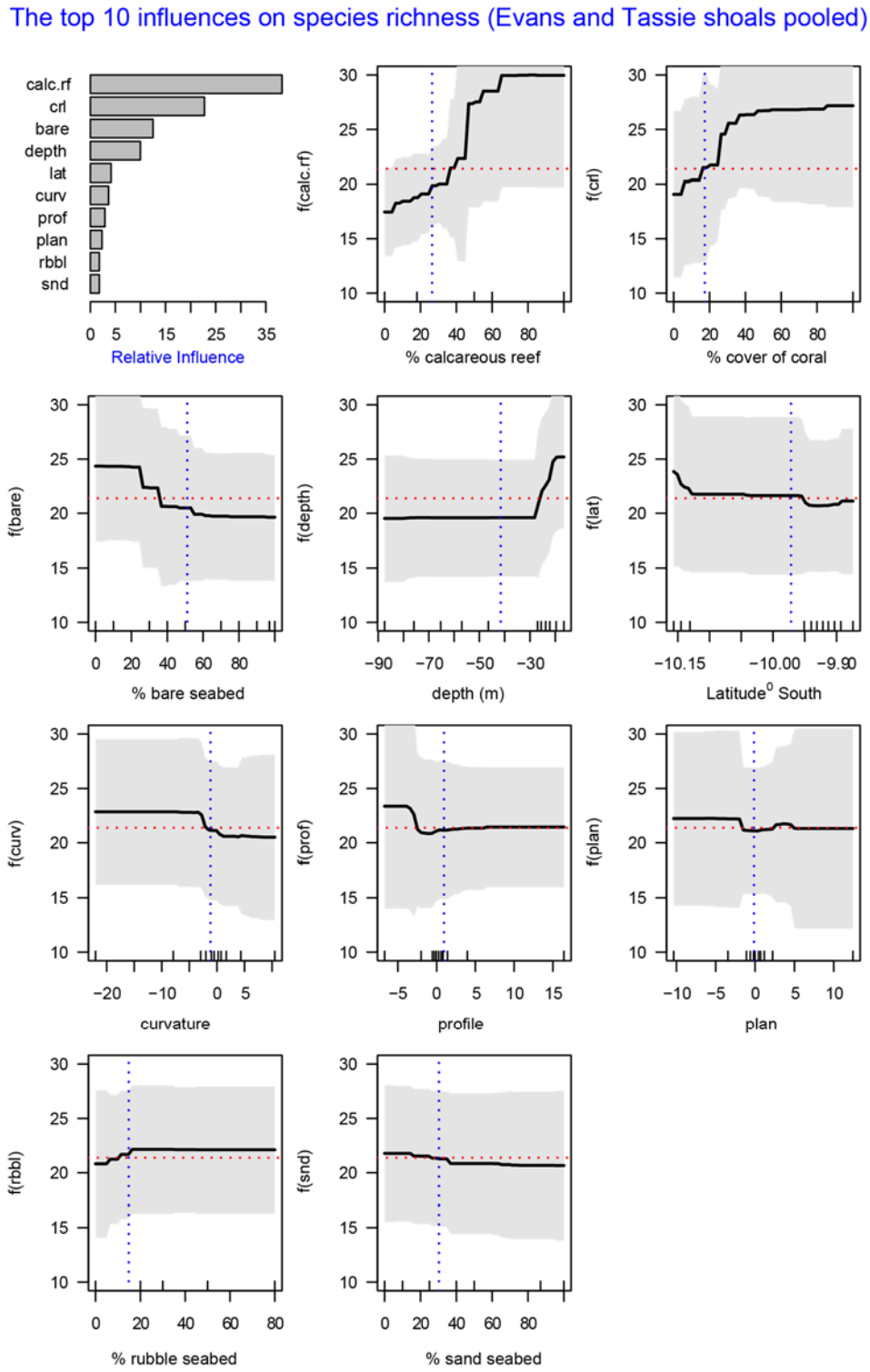

Figure 42: Partial dependency plots of the 10 major influences on species richness. The reduced model of 10 covariates was applied. Horizontal dotted lines (red) show the mean richness across all SBRUVS drops. Vertical dotted lines (blue) show the mean value for each predictor. The response lines shown the relationship of richness as a function of each predictor, with the influence of all other predictors held to a constant (ie accounted for). Shading around the response lines are 2 standard errors. Calcareous composition of the seabed, and percentage cover of coral, were the major drivers of species richness.

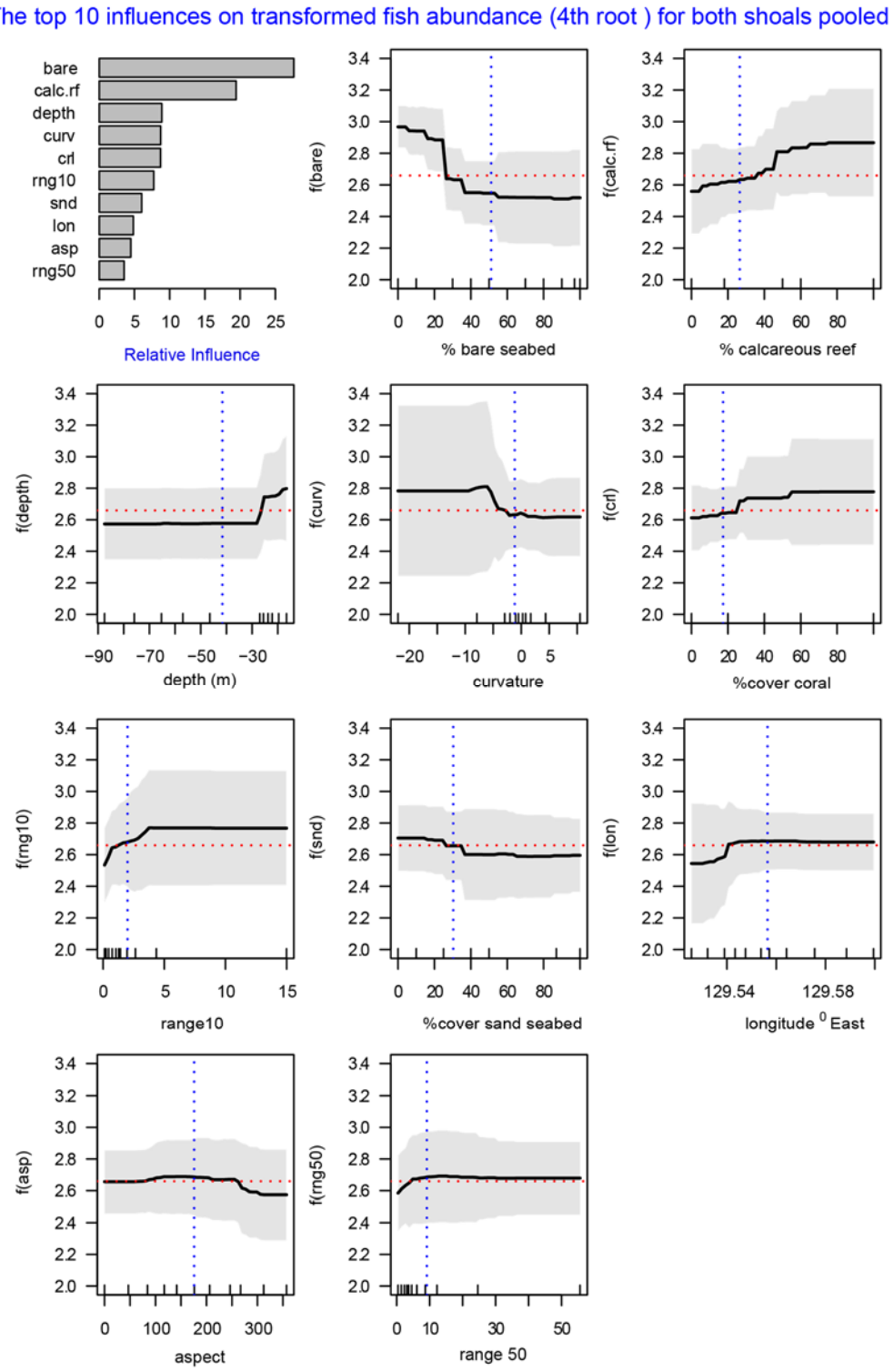

Figure 43: Partial dependency plots of the 10 major influences on total abundance (MaxN 4th root transformed). All conventions follow Figure 42. The y-scale is in the transformed units of abundance. SBRUVS with low %bare seabed (ie higher cover of any type of epibenthos), and those with higher % calcareous composition of the substratum in the field of view, had higher fish abundances.

Community assemblage structure as a function of "habitat"

Clustering of the Bray-Curtis dissimilarity matrix of transformed abundance of 98 fish genera by 95 SBRUVS sites revealed 14 significant clusters of data (Figure 44 A). Assigning these samples to four depth categories showed higher diversity of clusters in the shallower categories (nine clusters in waters less than 23 m deep, and eight in 23-42 m) (Figure 44 B). An unconstrained ordination of the same matrix explained about 31% of the distance variation in the dissimilarity matrix. The first two principal components (axes) in Figure 45 explained ~35% of this total. The site scores showed that the highest species richness occurred in the shallowest sites along the first axis, whereas the deeper sites were separated mainly along both axes (Figure 47).

The species scores in Figure 46 showed there was a high correlation between the first axis and the abundance of many "reef associated" fish genera, such as *Plectropomus* (coral trouts), *Pomacentrus* and *Dascyllus* (damselfishes), *Scarus* (parrot fish), *Chaetodon* (butterflyfish) and *Cirrhilabrus* (wrasses). In contrast, "sand associated" genera were highly correlated with the second axis. These were larger-bodied fish in the genera *Lethrinus* and *Gymnocranius* (emperors), *Abalistes* (trigger fish) and *Symphorus* (a snapper). The biplot in Figure 47 shows the clustering in multidimensional space of shallow sites highly correlated with "reef associated" genera.

These three representations of the unconstrained clustering and ordination show that "reef associated" genera were highly correlated with shallow sites with richest species diversity. However, there are numerous other dimensions accounting for the other 65% of the "structure" in the dissimilarity matrix that cannot be visualised or interpreted this way.

This multivariate variation is best explored with multivariate prediction and regression trees where we modelled the transformed abundance of 179 species as a response to shoal name, site depth, the seven categories of epibenthic cover, and the six categories of substratum (see Table 4). The first split in the tree distinguished sites with %coral cover (in the field of view) less than or greater than 35% (Figure 48). Two thirds of the sites (n=63) grouped together, irrespective of shoal name, in one terminal node we termed "Barer seabed". The other third of the data was split into Tassie and Evans Shoal sites based on depth, where shoal tops and shoal bases separated. Just three of the shallowest Tassie Shoal sites (<17.9m) formed a distinct assemblage where species were both numerous and abundant. The shallowest shoal tops with >35% coral cover had the highest species richness and abundance at both shoals in the histograms at the bottom of Figure 48.

Inspection of the DLI species values shows groups of species ubiquitous amongst assemblages (such as some large mobile carangid trevallies), at the root node (Figure 48), and assemblages of "reef associated" species characteristic of the shallow sites where coral cover was 35% or more. The full list of indicator species is detailed in Table 9. It is important to note that some of the species characterising "Barer seabed" are also found on coral reefs sometimes (e.g. silvertip whaler sharks *Carcharhinus albimarginatus*), but all other "reefy" nodes are distinguished by high DLI values for species that are only found on Indo-Pacific coral reefs (not inter-reefal shelf plains) (Figure 48 and Table 9). These include species such as corallivorous butteflyfishes (*Chaetodon lunula, C. ornatissimus*), coral-scraping parrotfish (*Scarus forsteni*), reef planktivores (*Pterocaesio marri*), reef herbivores (*Kyphosus cinerascens*) and cleaner fish (*Labroides bicolor*).

The "Barer seabed" node had an average richness of ~12 species and average abundance of ~37 fish, but these parameters doubled, tripled or quadrupled for the "reefy" nodes as the depth decreased (Table 10). It was clear that most of the "pattern" in diversity and abundance in the dataset was concentrated in the one-third of the SBRUVS set in shallow shoal waters where coral cover was highest.

Species accumulation curves for the five assemblages showed that all were still rising toward an asymptote of much higher diversity (Figure 49 A). More SBRUVS sets in all habitats would produce more species. The maps in Figure 49 (Inset B) show that only the "Barer seabed" assemblage is shared between shoals. Tassie Shoal is much smaller than Evans Shoal, yet they both supported only three distinct assemblages in the analysis. This may be because of the under-sampling of latent fish diversity evident from the species accumulation curves. It is also important to note that many sites on the top of Evans Shoal were classified by the analysis in the "Barer seabed" node with coral cover <35%. The tree analysis and the assemblage maps support further the notion that diversity increases sharply with coral cover and with decreasing depth.

The model had high error predicting the node membership of sites (only 7% success rate), and explained only 25% of the multivariate variation, but the best fit recognised five fish assemblages amongst the two shoals, based on depth, shoal name, and the percentage composition of calcareous reefal substrata in the field of view. Histograms on the "leaves" show abundance of each species, and the number of sites (*n*) are given with node names and node numbers. The species indicators (DLI) characterising each branch and each terminal node (leaf) are an index of fidelity and specificity of a species to a tree node. The hierarchical nature of the tree allows examination of which species are ubiquitous amongst Tassie and Evans Shoals with DLI at the "stump", and which species characterise the terminal assemblages. Only the top 10 DLI are shown for each node. The full list is given in Table 9.

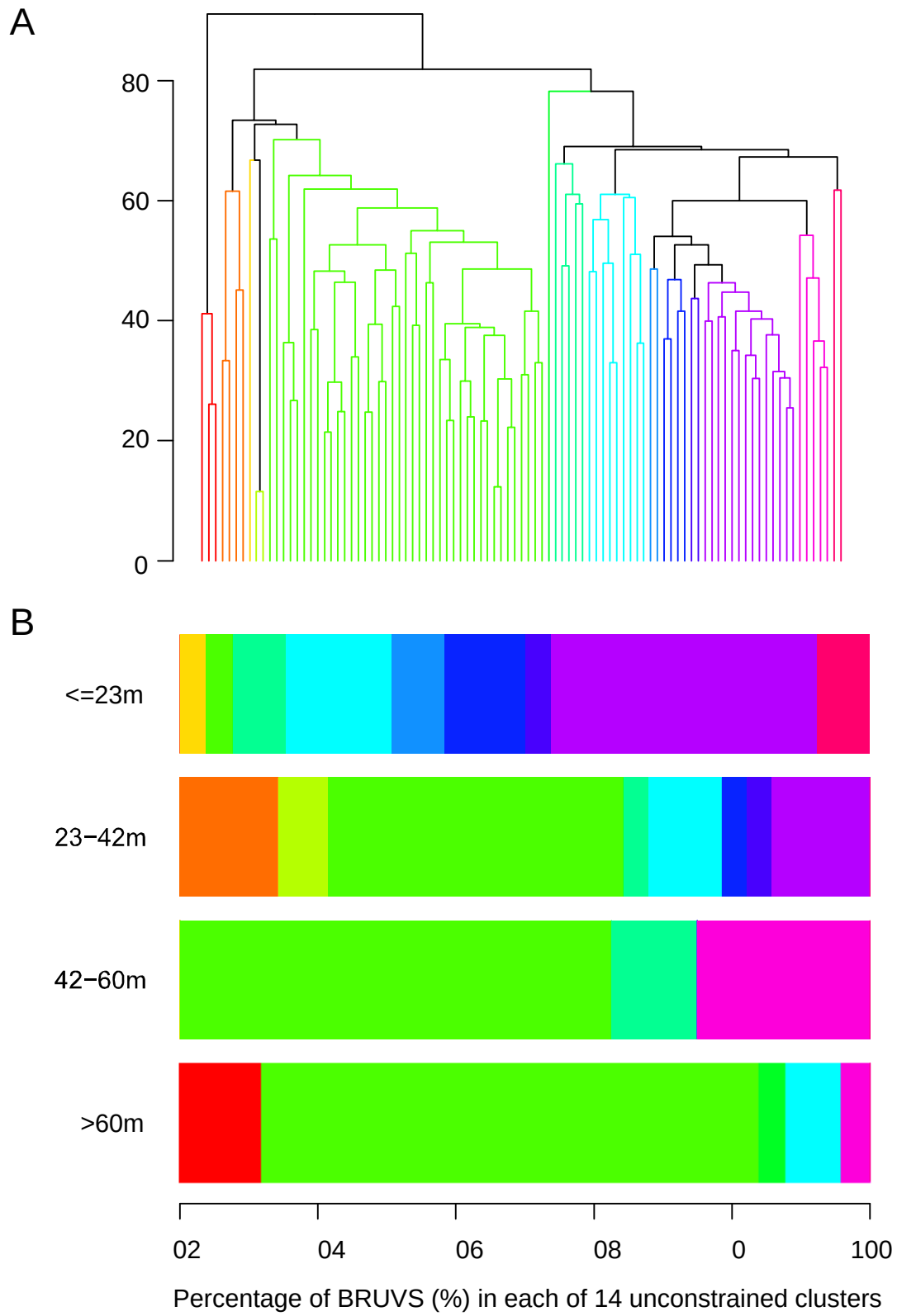

Figure 44: Unconstrained cluster analysis of transformed abundance (4th root MaxN) of 98 fish genera from 95 SBRUVS surveyed on Tassie and Evans Shoals (A), including a visual representation of the proportion of the 14 significant clusters that occurred in each of four nominal depth strata (B). Shallow SBRUVS sites had most clusters of fish genera.

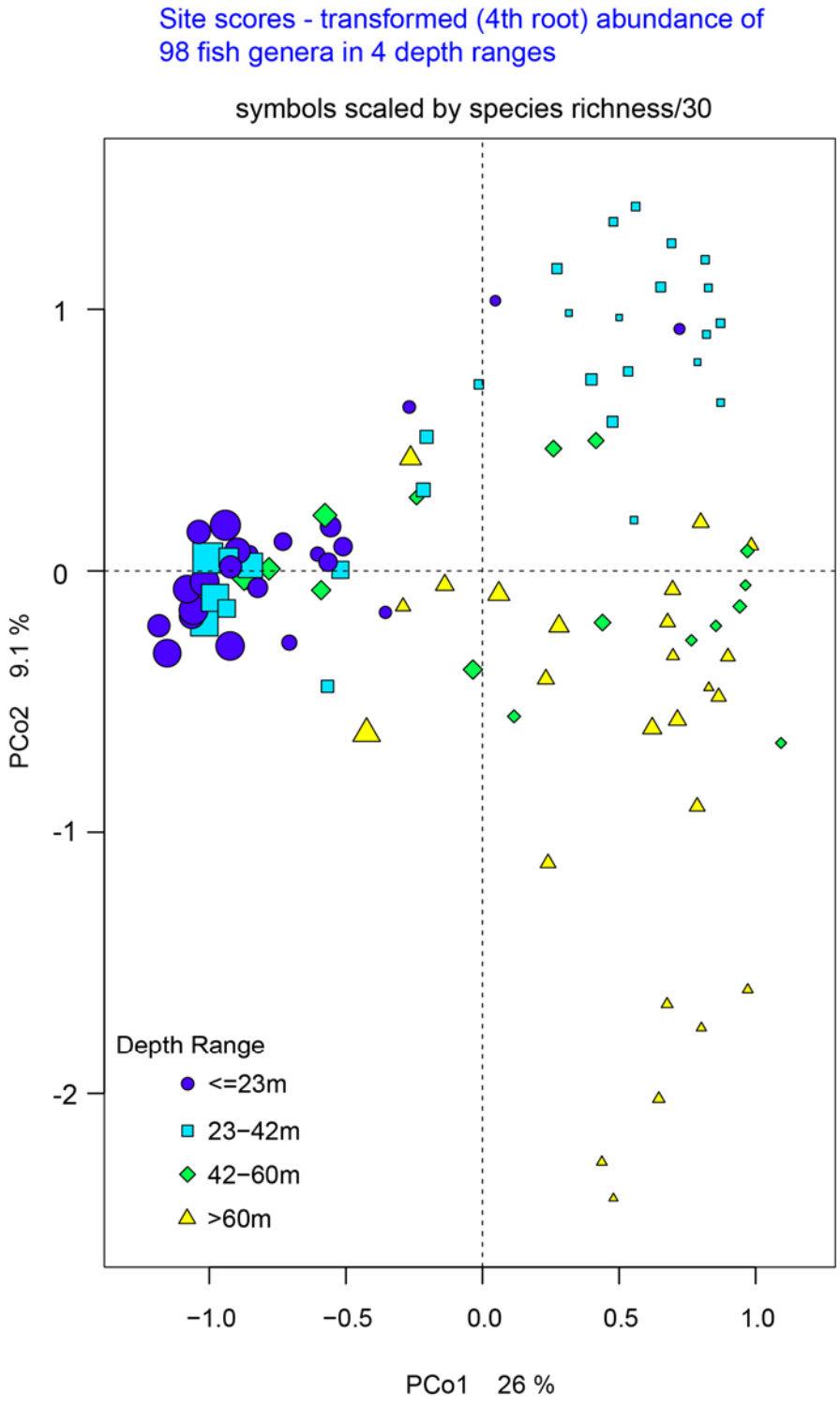

Figure 45: Unconstrained ordination of the Bray-Curtis dissimilarity matrix produced for all 95 SBRUVS sets using the transformed abundance (4th root MaxN) of 98 fish genera. The first 2 principal components accounted for 35% of the total variation explained (31%) in the abundance of these genera. The separation of BRUVS sets in 4 nominal depth categories is most evident in the scores along the first axis. Site symbols are scaled by species richness/30. Shallow sites had more species.

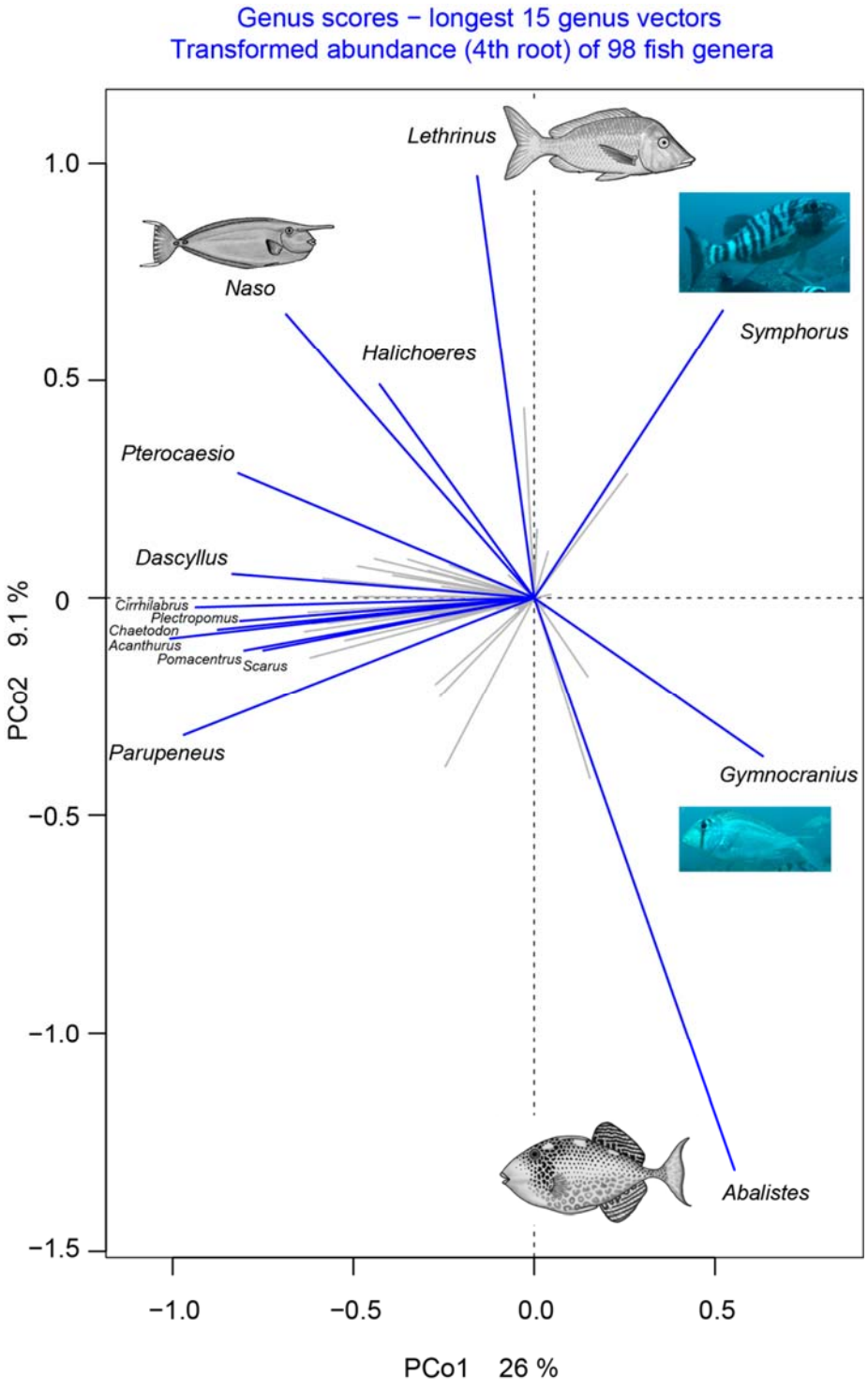

Figure 46: Unconstrained ordination of the Bray-Curtis dissimilarity matrix produced for all 95 SBRUVS sets using the transformed abundance (4th root MaxN) of 98 fish genera. The top 15 genera correlated with these 2 principal components are shown by blue vectors. Grey vectors represent the remainder in these first 2 dimensions. "Reef-associated" genera were correlated with the first axis, and fewer, "sand-associated", genera were correlated with the second axis.

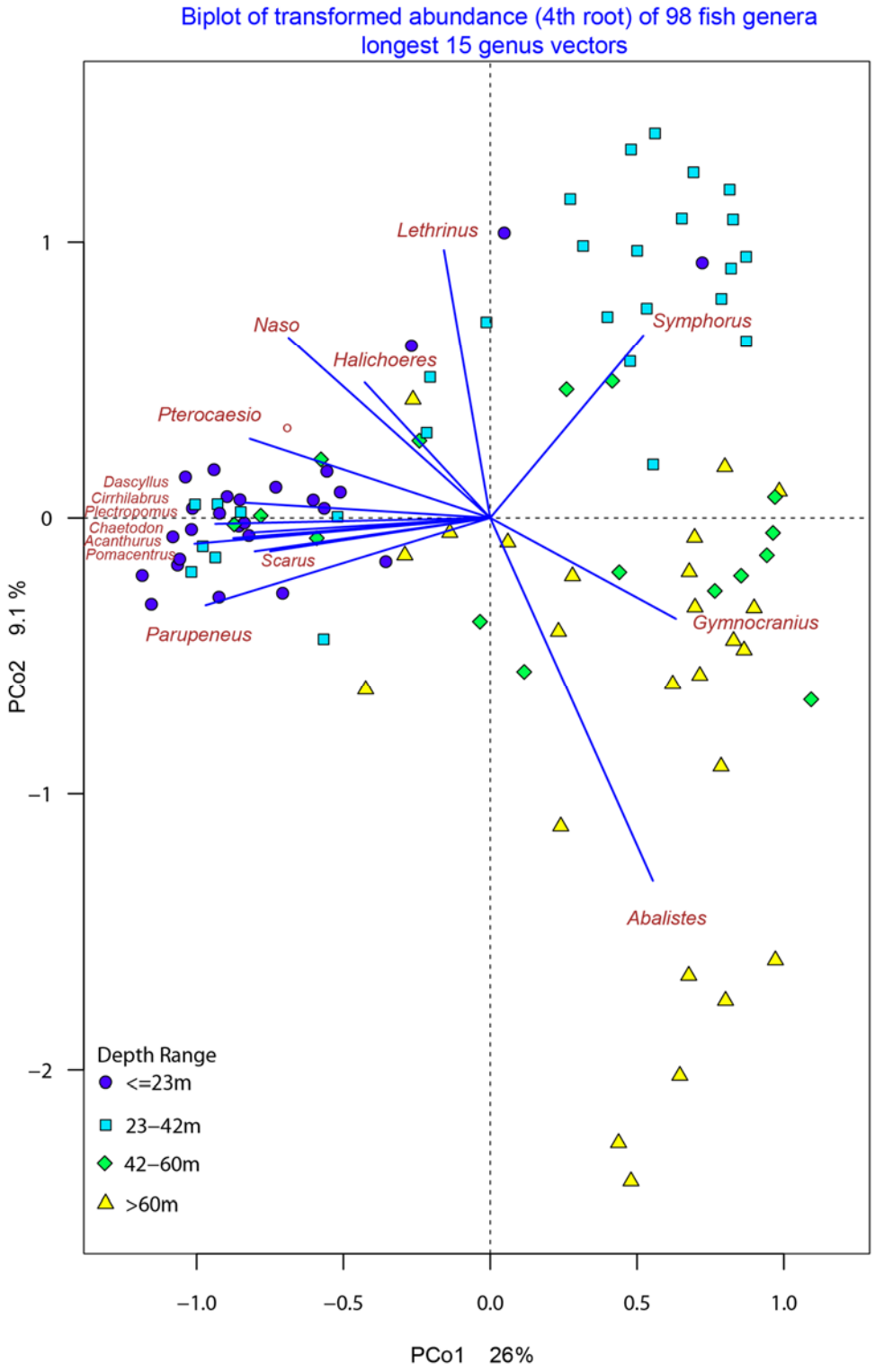

Figure 47: Biplot of an unconstrained ordination of the Bray-Curtis dissimilarity matrix produced for all 95 SBRUVS sets using the transformed abundance (4th root MaxN) of 98 fish genera. The top 15 genera correlated with these 2 principal components are shown by blue vectors. "Reef-associated" genera were correlated with shallow sites on the first axis, and fewer, "sand-associated", genera were correlated along the second axis with deeper sites.

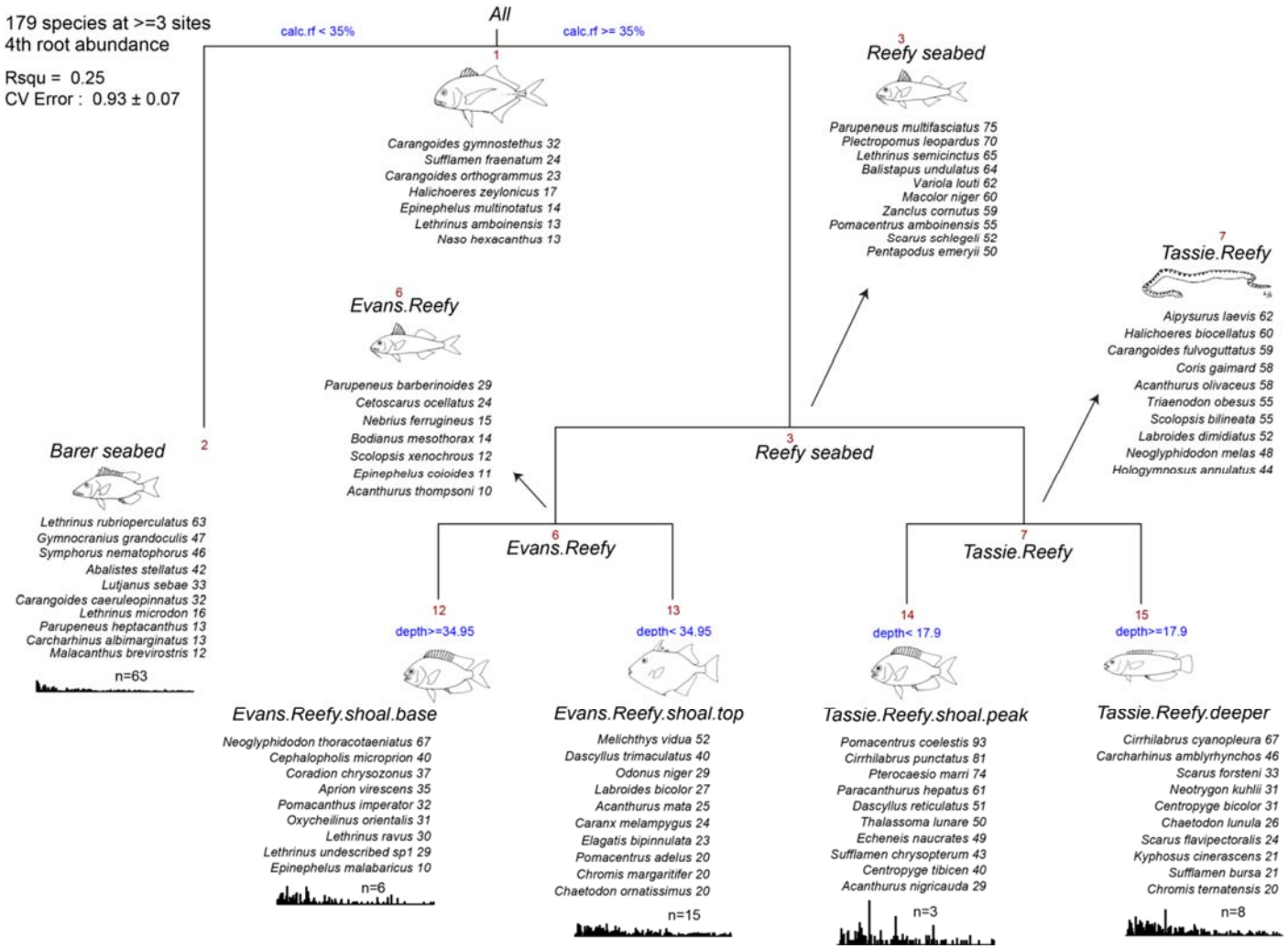

Figure 48: The best tree structure from a multivariate analysis of the transformed abundance (4th root MaxN) of 179 species predicted by the biotic explanatory covariates.This subset of 179 fish species were present on at least 3 SBRUVS.

Table 9. The Dufrene-Legendre indices (DLI) for each of the 179 species analysed as the multivariate response in Figure 50. The DLI species, and their values, are shown for each node of the tree. These nodes include the hierarchical branches, and the terminal nodes comprising the 5 fish assemblages (in bold italics).

Nodename	node	DLI values
All	1	*Carangoides gymnostethus(32), Sufflamen fraenatum(24), Carangoides orthogrammus(23), Halichoeres zeylonicus(17), Epinephelus multinotatus(14), Lethrinus amboinensis(13), Naso hexacanthus(13), Lutjanus lemniscatus(4), Pseudobalistes fuscus(4)*
Barer_seabed	*2*	*Lethrinus rubrioperculatus(63), Gymnocranius grandoculis(47), Symphorus nematophorus(46), Abalistes stellatus(42), Lutjanus sebae(33), Carangoides caeruleopinnatus(32), Lethrinus microdon(16), Parupeneus heptacanthus(13), Carcharhinus albimarginatus(13), Malacanthus brevirostris(12), Parupeneus barberinus(10), Aluterus monoceros(10), Pristipomoides filamentosus(10), Naso mcdadei(10), Lagocephalus sceleratus(10), Oxycheilinus bimaculatus(8), Carangoides ferdau(8), Carangoides chrysophrys(8), Lethrinus nebulosus(8), Naso fageni(7), Lethrinus lentjan(6), Decapterus sp(6), Epinephelus areolatus(5), Parupeneus cyclostomus(5), Pristipomoides typus(5), Xyrichtys melanopus(5), Pseudojuloides severnsi(5), Cirrhilabrus sp(5), Naso tonganus(5)*
Reefy_seabed	3	*Parupeneus multifasciatus(75), Plectropomus leopardus(70), Lethrinus semicinctus(65), Balistapus undulatus(64), Variola louti(62), Macolor niger(60), Zanclus cornutus(59), Pomacentrus amboinensis(55), Scarus schlegeli(52), Pentapodus emeryii(50), Naso lituratus(47), Apolemichthys trimaculatus(46), Aethaloperca rogaa(45), Lutjanus bohar(43), Parupeneus pleurostigma(42), Lethrinus erythracanthus(41), Chaetodon kleinii(40), Oxycheilinus celebicus(38), Ctenochaetus striatus(38), Naso vlamingii(28), Cephalopholis miniata(27), Chlorurus bleekeri(25), Pygoplites diacanthus(25), Monotaxis grandoculis(25), Chaetodon lunulatus(25), Naso brevirostris(24), Chromis weberi(22), Amblyglyphidodon leucogaster(22), Forcipiger longirostris(22), Chaetodon trifascialis(19), Acanthurus grammoptilus(17), Lutjanus rivulatus(12), Chaetodon adiergastos(12), Choerodon jordani(11), Heniochus singularius(9), Naso caesius(9)*
Evans_Reefy	6	*Parupeneus barberinoides(29), Cetoscarus ocellatus(24), Nebrius ferrugineus(15), Bodianus mesothorax(14), Scolopsis xenochrous(12), Epinephelus coioides(11), Acanthurus thompsoni(10)*
Tassie_Reefy	7	*Aipysurus laevis(62), Halichoeres biocellatus(60), Carangoides fulvoguttatus(59), Coris gaimard(58), Acanthurus olivaceus(58), Triaenodon obesus(55), Scolopsis bilineata(55), Labroides dimidiatus(52), Neoglyphidodon melas(48), Hologymnosus annulatus(44), Acanthurus pyroferus(43), Hologymnosus doliatus(43), Coris batuensis(36), Balistoides viridescens(35), Chaetodon auriga(34), Genicanthus lamarck(32), Halichoeres chrysus(31), Carangoides plagiotaenia(29), Parapercis xanthozona(28), Cirrhilabrus exquisitus(24)*
Evans_Reefy shoal_base	*12*	*Neoglyphidodon thoracotaeniatus(67), Cephalopholis microprion(40), Coradion chrysozonus(37), Aprion virescens(35), Pomacanthus imperator(32), Oxycheilinus orientalis(31), Lethrinus ravus(30), Lethrinus undescribedsp1(29), Epinephelus malabaricus(10), Lethrinus olivaceus(9)*
Evans_Reefy shoal_top	*13*	*Melichthys vidua(52), Dascyllus trimaculatus(40), Odonus niger(29), Labroides bicolor(27), Acanthurus mata(25), Caranx melampygus(24), Elagatis bipinnulata(23), Pomacentrus adelus(20), Chromis margaritifer(20), Chaetodon ornatissimus(20), Acanthurus nigros(20), Acanthurus nigricans(19), Plectorhinchus vittatus(19), Lutjanus gibbus(18), Acanthurus blochii(16), Zebrasoma scopas(13), Oxycheilinus digrammus(13), Coris pictoides(5), Heniochus acuminatus(5), Naso unicornis(4)*
Tassie_Reefy shoal_peak	*14*	*Pomacentrus coelestis(93), Cirrhilabrus punctatus(81), Pterocaesio marri(74), Paracanthurus hepatus(61), Dascyllus reticulatus(51), Thalassoma lunare(50), Echeneis naucrates(49), Sufflamen chrysopterum(43), Centropyge tibicen(40), Acanthurus nigricauda(29), Acanthurus dussumieri(28), Siganus punctatus(25), Thalassoma amblycephalum(25), Naso brachycentron(24), Caranx ignobilis(23), Chaetodon baronessa(23), Cantherhines dumerilii(22), Melichthys niger(22), Caesio teres(21), Plectroglyphidodon johnstonianus(21), Cephalopholis urodeta(20), Leptojulis cyanopleura(20), Chromis xanthura(19), Plectropomus laevis(19), Hydrophis sp(18), Acanthurus leucocheilus(18), Aluterus scriptus(17), Cirrhilabrus temminckii(14)*
Tassie_Reefy deeper	*15*	*Cirrhilabrus cyanopleura(67), Carcharhinus amblyrhynchos(46), Scarus forsteni(33), Neotrygon kuhlii(31), Centropyge bicolor(31), Chaetodon lunula(26), Scarus flavipectoralis(24), Kyphosus cinerascens(21), Sufflamen bursa(21), Chromis ternatensis(20), Chaetodon lineolatus(19), Acanthurus nigrofuscus(19), Pomacentrus philippinus(18), Balistoides conspicillum(18), Hemitaurichthys polylepis(17), Epinephelus maculatus(15), Arothron stellatus(10), Novaculichthys taeniourus(8), Scarus ghobban(7), Siganus argenteus(7)*

Table 10 Summaries of the overall abundance and species richness in the 5 fish assemblages identified in the multivariate tree (Figure 48). Each SBRUVS station was assigned to an assemblage. The range in species richness (S) and abundance (∑MaxN) for each of the n BRUVS sites within an assemblage was then tallied as S and ∑∑MaxN. The node number and assemblage name, from Figure 48, is accompanied by the total number of DLI species (nDLI) from Table 9.

nodes	*n* sites	Node name	Richness *S*	∑∑ *MaxN*	*n* DLI	*S* range	*S* mean	∑*MaxN* range	∑*MaxN* mean
2	63	Barer seabed	180	2368	29	(1 - 34)	(12.2 ± 7.2)	(3 - 318)	(37.6 ± 46.2)
12	6	Evans.Reefy shoal.base	86	502	10	(13 - 36)	(25.3 ± 8.1)	(49 - 112)	(83.7 ± 22.5)
13	15	Evans.Reefy shoal.top	216	2181	20	(15 - 59)	(40.5 ± 14.5)	(37 - 343)	(145.4 ± 90.2)
14	3	Tassie.Reefy shoal.peak	82	989	28	(38 - 45)	(40.3 ± 4)	(123 - 626)	(329.7 ± 263.2)
15	8	Tassie.Reefy deeper	135	1242	20	(32 - 66)	(45.8 ± 12.6)	(68 - 257)	(155.2 ± 74)

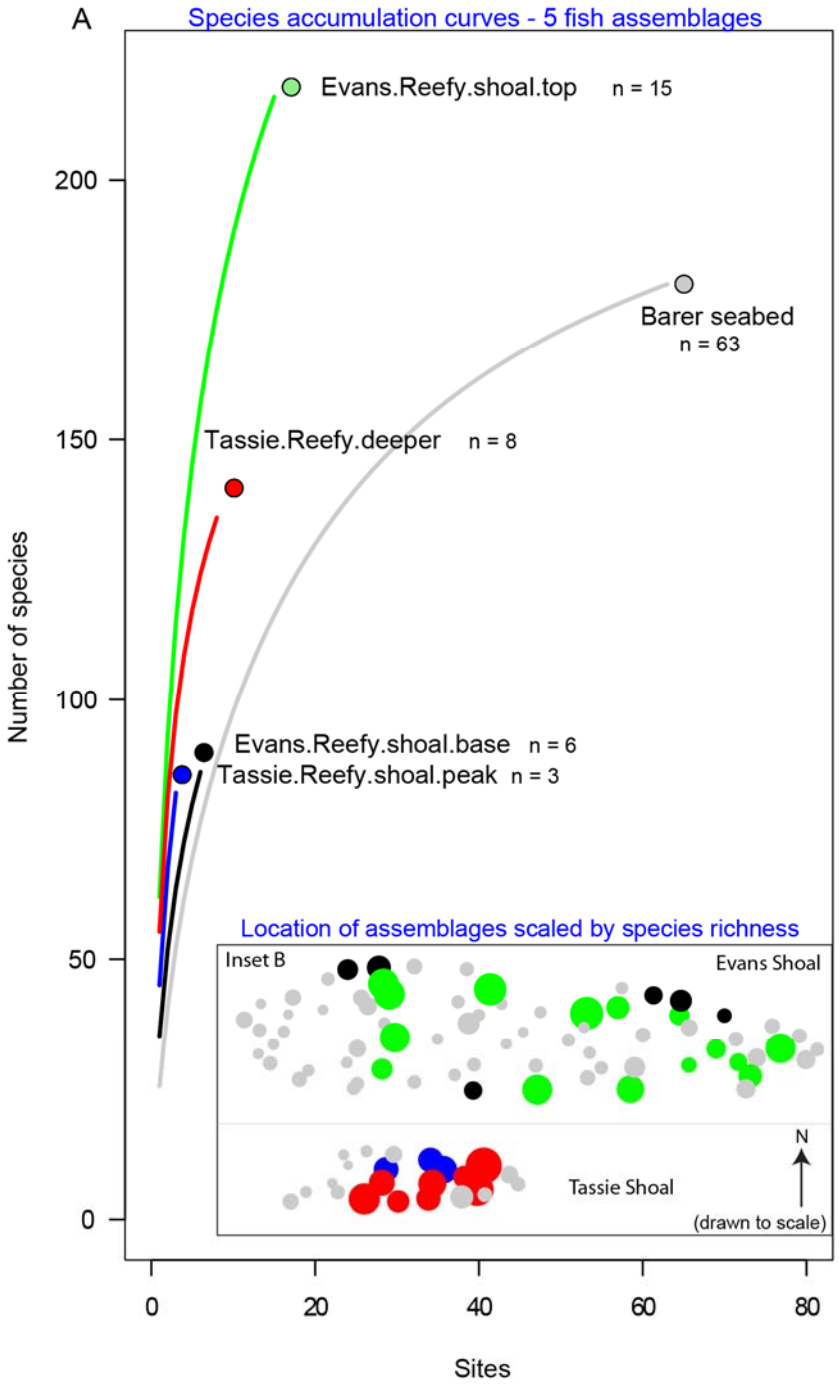

Figure 49: Species accumulation curves (A) derived for the 5 assemblages identified in Figure 50. The numbers and node names are shown. In general the curves were still ascending toward an asymptote, indicating that there remained much latent fish diversity in the assemblages. The colour-coded location of sites in each assemblage are shown on maps of the shoals as an inset (B). Shoals are drawn to scale with each other, but the latitudinal scale has been broken to place the maps next to each other. Symbols are scaled by species richness/40. Tassie Shoal top was the most diverse and comprised two fish assemblages based on depth.

2.5. Regional comparisons

2.5.1 Benthos

A cluster analysis using the coarse scale habitat data from real-time towed video data collected during this survey and the AIMS dataset from similar surveys across the Timor Sea and Bonaparte Gulf region showed similarities in benthic community composition among shelf edge shoals, such as Evans, Tassie and Blackwood, the Sahul Shoals and Eugene McDermott Shoal far to the west (Figure 50) but also differences between some close neighbouring sites, for example between Vulcan and Goeree Shoals. There is also a clear differentiation across the shelf, with the current study sites at Goodrich Bank and Cape Helvetius grouping with more coastal locations, likely influenced by the presence of bare soft substrate and a greater contribution from filter feeders and burrowing infauna (Figure 50). Notably, this analysis grouped Evans, Tassie and Blackwood Shoals together, along with other shoals in the central and western ends of the bioregion, based on the relative contribution of sparse to medium density hard coral habitats on all three shoals and similarities in the amount of bare substrate observed between Evans and Tassie Shoals (Figure 51).

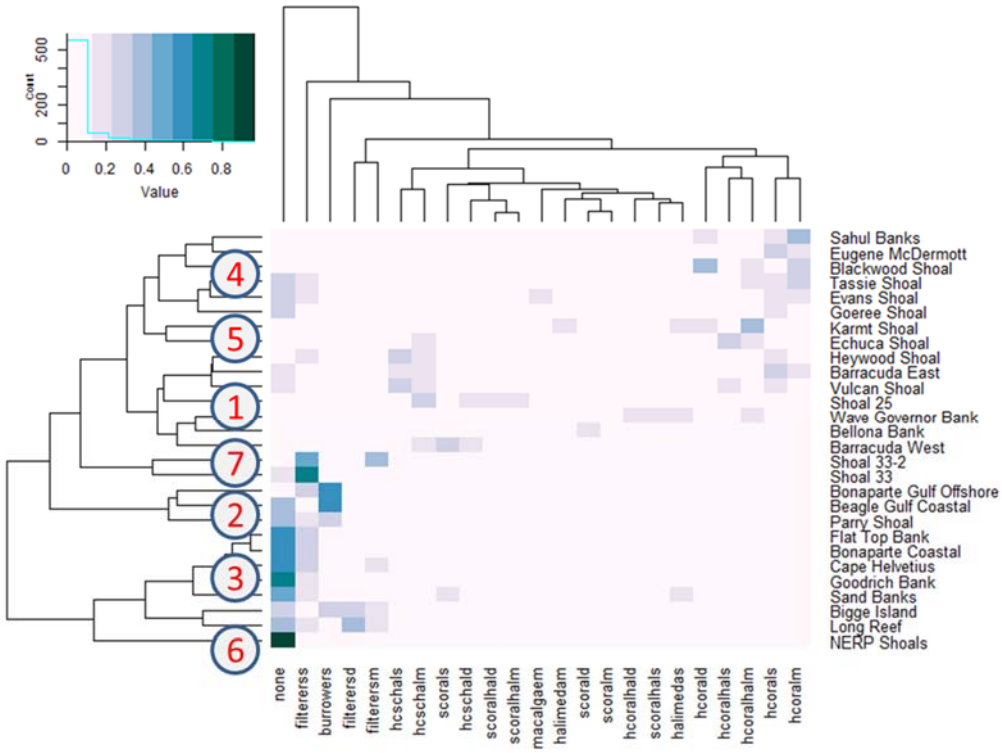

Figure 50: Cluster analysis from real time towed-video data showing the contribution of major habitat classifications to seabed communities surveyed on shoals and shelf areas throughout the region.

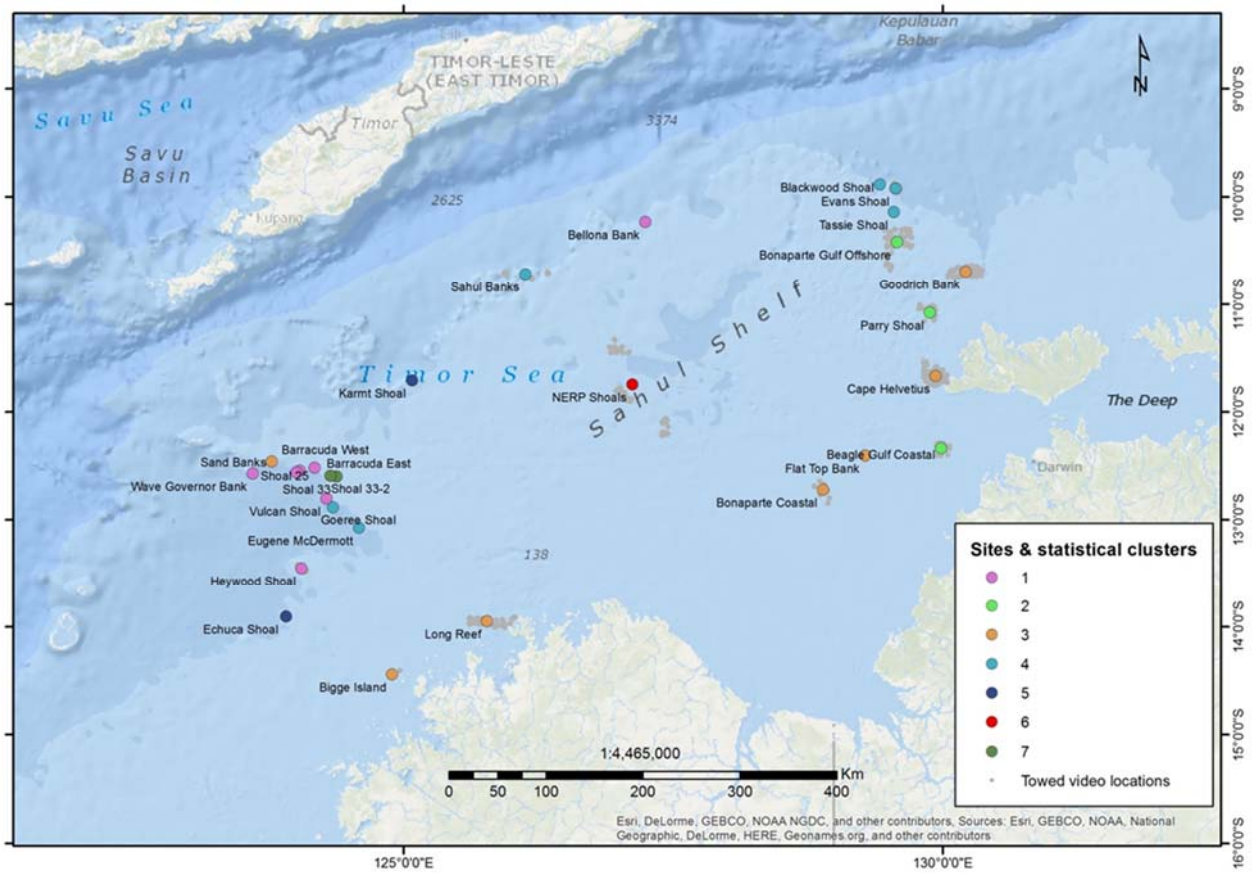

Figure 51: Colour coded regional similarities and differences in shelf and shoal locations based on initial analysis of coarse level benthic habitat classes, produced by realtime classification of video during towvid transects.

The realtime classification data has a limited range of categories into which to place particular habitats as they are viewed during a towed video transect. Corals, for example, may be classed as high medium or low density habitats, which can limit the ability to resolve more subtle differences. The use of still photo derived data removes these limitations. Hence a second cluster analysis based on fine-scale point intercept classification of all still images collected at Evans, Tassie and Blackwood Shoals with other AIMS data was performed. This provided a more stringent analysis of regional similarities and differences among 20 shoals across the NW Shelf. The relative proportion of each of the categories of benthos across depths (Figure 52), confirms the presence of the same major benthic categories, but some variability in the relative importance of these, on each shoal. These data represent submerged shoals distributed across more than 600 km of the North and North-west marine regions and a variety of shelf positions. Bare sand and consolidated reef, often supporting turfing algae, are major features of all shoals. Hard corals and macroalgae are ubiquitous but variable in abundance, with soft corals and sponges often important components of the benthos. Evans and Tassie Shoals are in the middle of the range for categories such as hard corals. Evans Shoal is notable for the large areas of sand, and similar to one of the three Margaret Harries Banks, though with more hard coral overall and notably with one of the higher abundances of deep coral between 30-60 m on the shoal slopes. The deep coral community at Evans Shoal consists of foliaceous corals, such as *Montipora* spp. and *Pachyseris* spp. which were encountered in a discrete depth band between approximately 40-60 m deep at the northern and southern ends of the shoal. By comparison Tassie Shoal had slightly less hard coral, but also a more even contribution from all the benthic biota, which relates to the presence of a greater proportion of consolidated substrate across the plateau, often in

the form of small patch reefs and outcrops. The foliaceous community observed at Evans Shoal was also found on Tassie Shoal but was more limted in extent and shallower in depth distribution. No hard coral was found on Tassie Shoal below 30 m, which is unusual for these shoals.

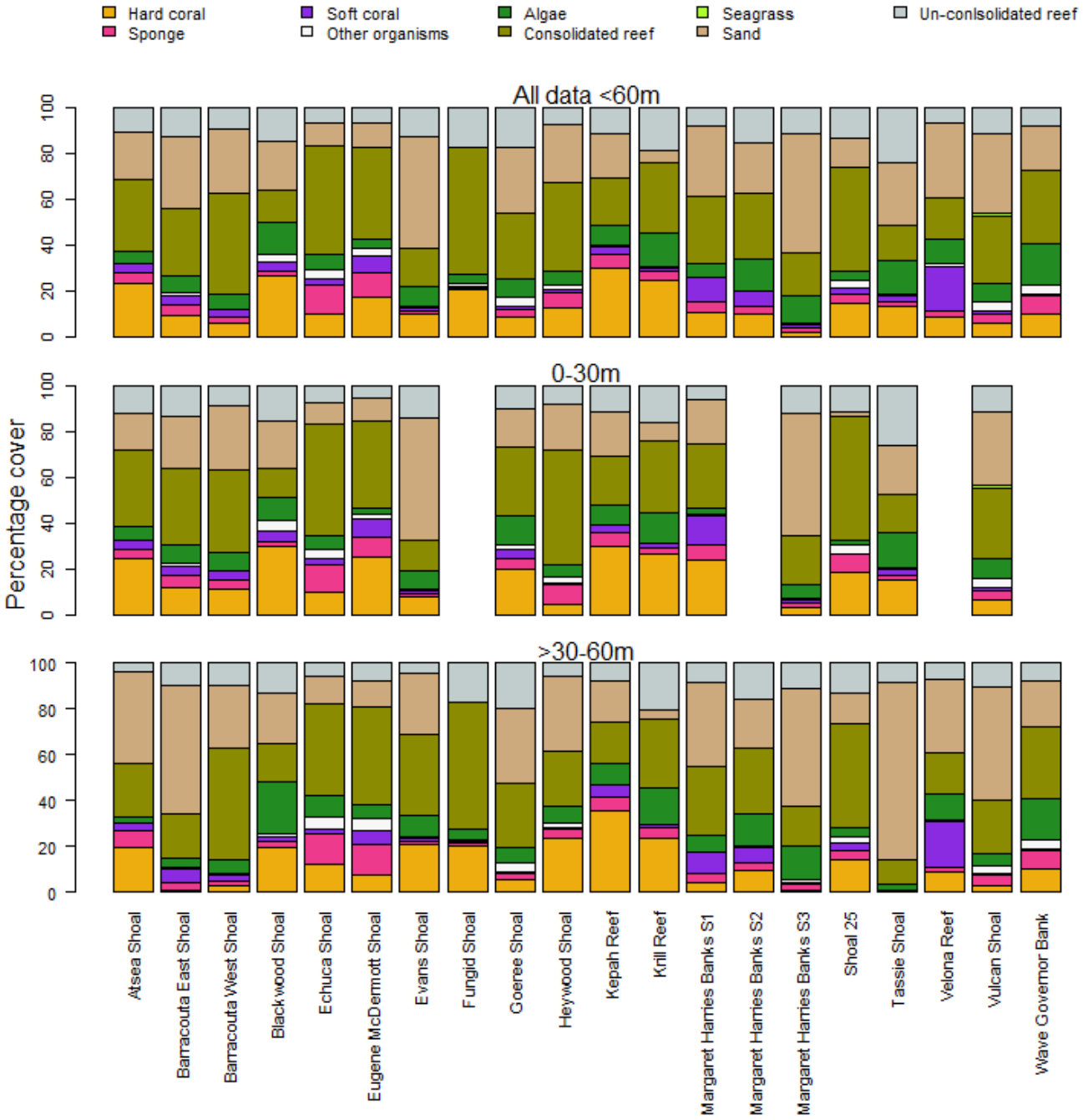

Figure 52: Summary of quantitative data derived from point intercept photo analysis: 20 shoals across the region showing the relative proportion of each of the broad-scale categories of benthos across depths.

The high level habitat comparisons (Figure 52) do not, however, reveal some of the fine scale complexities in the composition of broad scale habitats found within and between shoals. For example, the abundance of coral is similar at Fungid Shoal and Evans Shoal, but the composition of the two shoal coral communities is quite different. Evans Shoal corals are diverse and various branching and massive species in the Families Acroporidae, Poitidae and Favidae make major contributions to coral habitats across the shallower regions of the plateau. However there is also a substantial presence of hard coral on the deeper edges of the plateau, in the 30-60 m depth range, consisting mainly of foliaceous species in the Families Acroporidae and Agaricidae. In contrast Fungid Shoal in the middle of the bioregion, while having a similar abundance of hard coral, is dominated by the Fungidae and Agaricidae between 30-60 m.

The regional comparison of shoals, using the quantitative data derived from high resolution still image interpretation, confirms the similarity of benthic communities at Tassie Shoal and Blackwood Shoal, in particular with regard to the abundance of sand and unconsolidated reef areas and some similarity in coral cover. However, Evans Shoal groups most strongly with one of the Margaret Harries Banks, which lies approximately 100 km to the south west, rather than with the nearby Tassie and Blackwood Shoals (Figures 53 & 54).

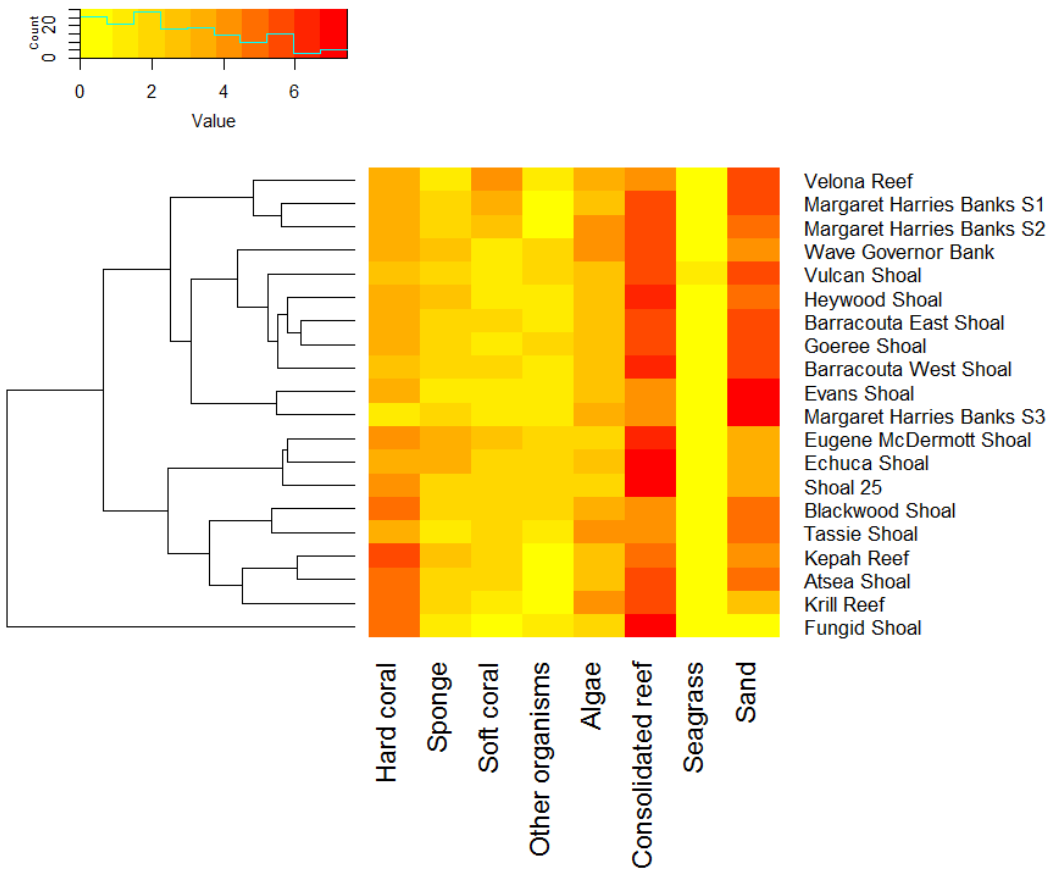

Figure 53: Cluster analysis, based on the quantitative data derived from high resolution imagery analysis, showing the contribution of major habitat classifications to seabed communities surveyed on shoals throughout the region.

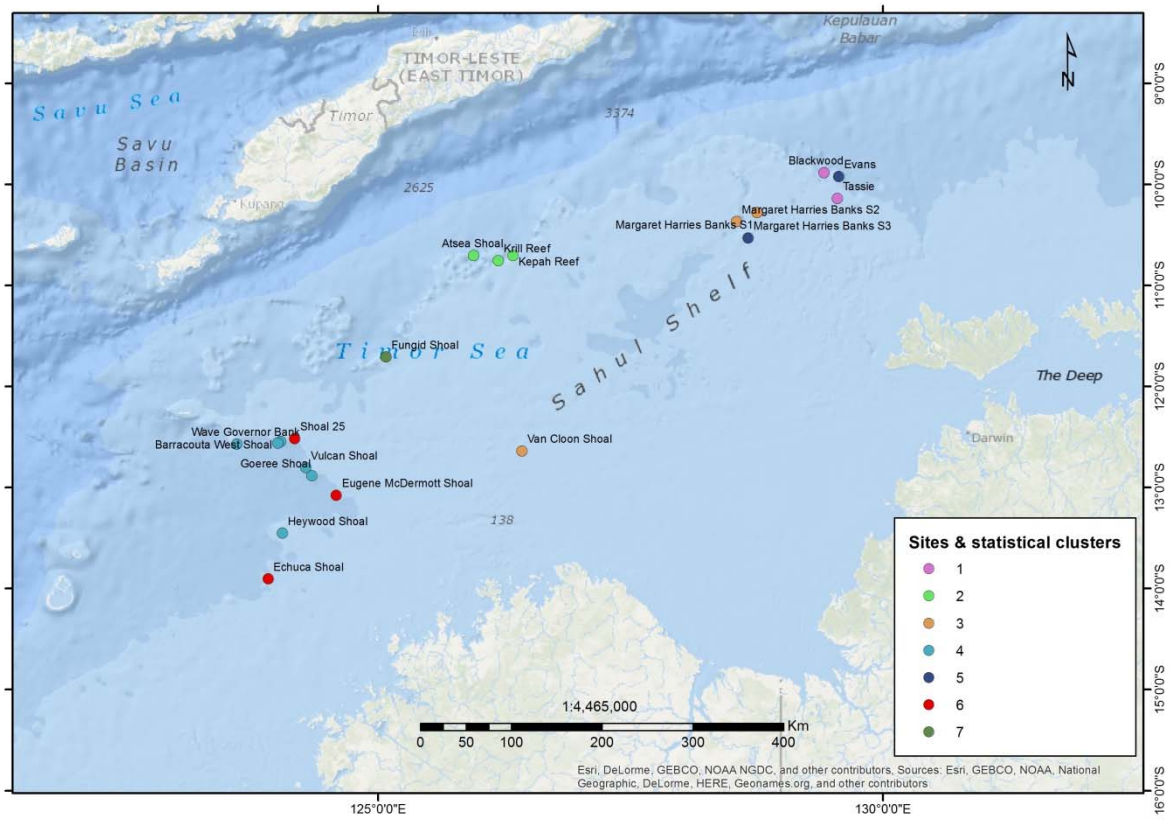

Figure 54: Colour coded regional similarities and differences shoal locations based on cluster analysis of fine scale benthic habitat classes, produced by point intercept analysis of high resolution benthic still imagery.

The coral composition found on shoals across the region (Figure 55) varies among shoals, sometimes substantially, but many general attributes are shared. Acroporid corals in a mix of branching, corymbose and tabulate growth forms are widespread throughout the region. Together with other branching and encrusting species they contribute a major proportion of the hard corals found on the shallowest areas of the shoals, particularly in depths less than 30 m. While these groups do extend into greater depths, the shoal regions between 30-60 m also support sometimes dense patches of foliose coral and/or solitary corals in the family Fungiidae. Unlike the majority of reef building coral species found on the shoal plateaus, these free living corals have the ability to colonise areas of unconsolidated substrate and also appear to thrive across a range of depths, including areas below 30 m.

While overall habitat composition suggests Evans Shoal is most similar to one of the Margaret Harries Banks (Figure 54), comparison of just coral assemblages across the region (Figure 56), indicates Evans Shoal to be most similar to Echuca, Goree and Barracouta West Shoals, while Tassie Shoal is most similar to Eugene McDermott Shoal. All of these shoals are situated at the western end of the bioregion, and the Blackwood Shoal coral community is most similar to two shoals, Atsea and Kepah, in the central area of the bioregion.

Overall these results suggest that while many attributes and species are shared throughout the region, individual shoals have their own character and the status of their benthic communities may reflect different disturbance and recruitment histories, as well as potentially different ecosystem trajectories.

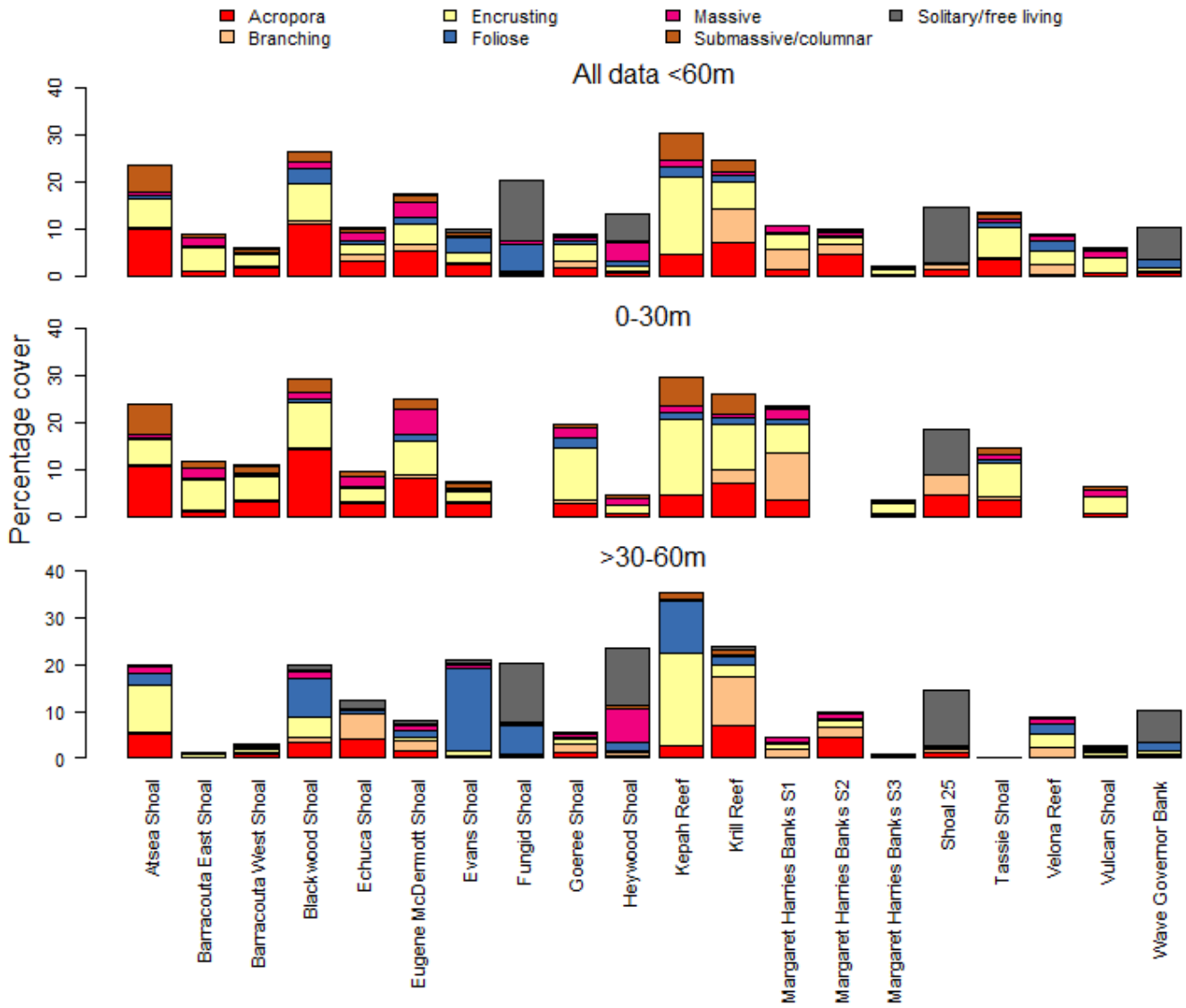

Figure 55: Relative proportion of each of the hard coral categories across depths; summary from 20 shoals distributed across 750 km of the submerged shoals region (see Figure 54 for locations).

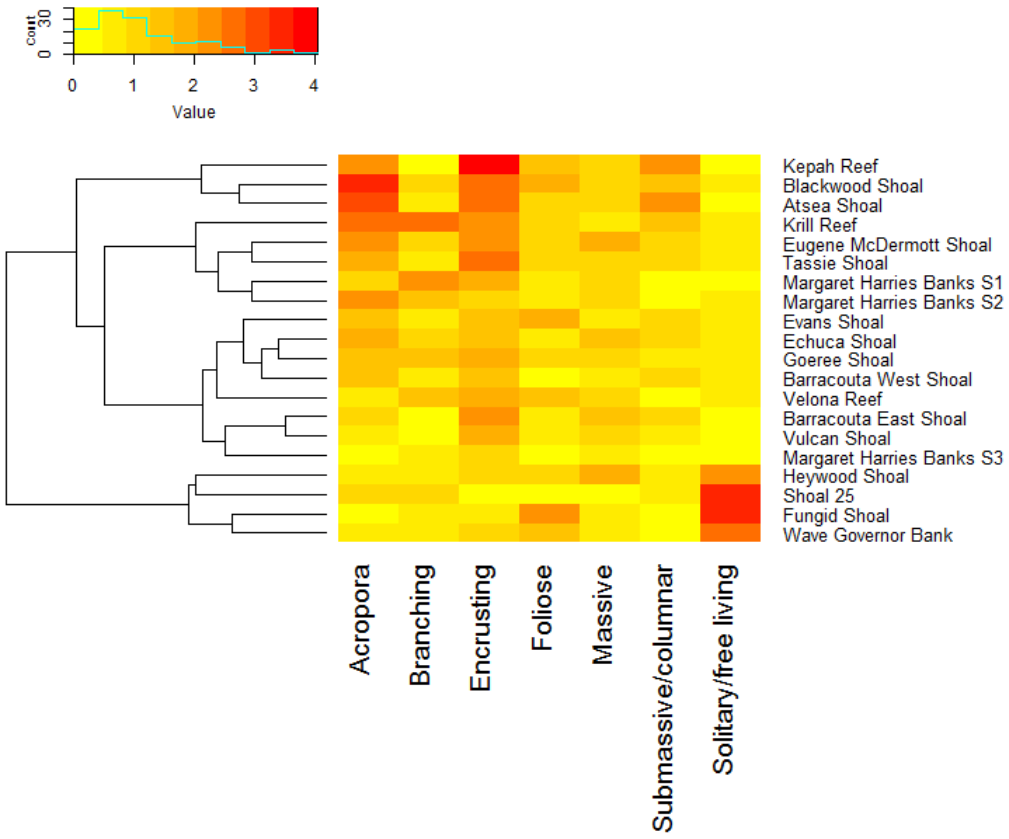

Figure 56: Cluster analysis of the contribution of hard coral categories to towed video benthic surveys at 20 shoals in the region.

2.5.2 Regional scale habitat model

The regional scale habitat model (Figure 57) results cover ~46,810 sq km and show a mosaic of habitats throughout the model domain. These habitats are dominated by Burrower/Crinoid soft sediment communities (Table 5, making up ~23% of the total area) interspersed with no modelled biota present (category "None" making up ~ 69% of the total areas). There was also a lesser but significant amount of filter feeder communities (~6%) most commonly found in the east of the model domain within the bounds of the Oceanic Shoals Commonwealth Marine Reserve (OSCMR). Hard corals (including free living forms), soft corals, macroalgae and gorgonians all make up less than one percent of regional scale model by area. Their distribution is largely associated with the shoals, banks and emergent reefs in the northern extent of the study domain. However, hard coral also extends into areas of the OSCMR, with towed video analysis suggesting that this is most likely associated with isolates and free leaving coral forms. Alycon, seagrass, whips and *Halimeda* are marginal environments through the model domain with less than or equal to 0.1% by area.

Overall model accuracy was assessed using Kappa (Table 6) with the outcome showing a good level of accuracy (Kappa >= 0.7, Hosmer and Lemeshow 2000). The confusion matrix showed that the majority of habitats are accurately classified (~80%) with the exception of "None" which is the weakest class with only ~50% accuracy. While all reasonable efforts are made to make model results as representative and accurate as possible, interpreting the regional habitat model results should be done with caution particularly at fine scales. It is also important to note that large areas of the model outside the sites detailed in Figure 57 have no validation data and model accuracy cannot be assessed in these regions. A detailed ecological interpretation of drivers of each modelled benthic group in the

regional scale model is beyond the scope of this report. It should also be noted with caution that while over the entire regional model performed well for most habitat categories, the "None" category had the poorest performance most frequently under predicting filter feeder (including whips) and Halimedia communities which by their nature can be discrete, stochastic and challenging to model.

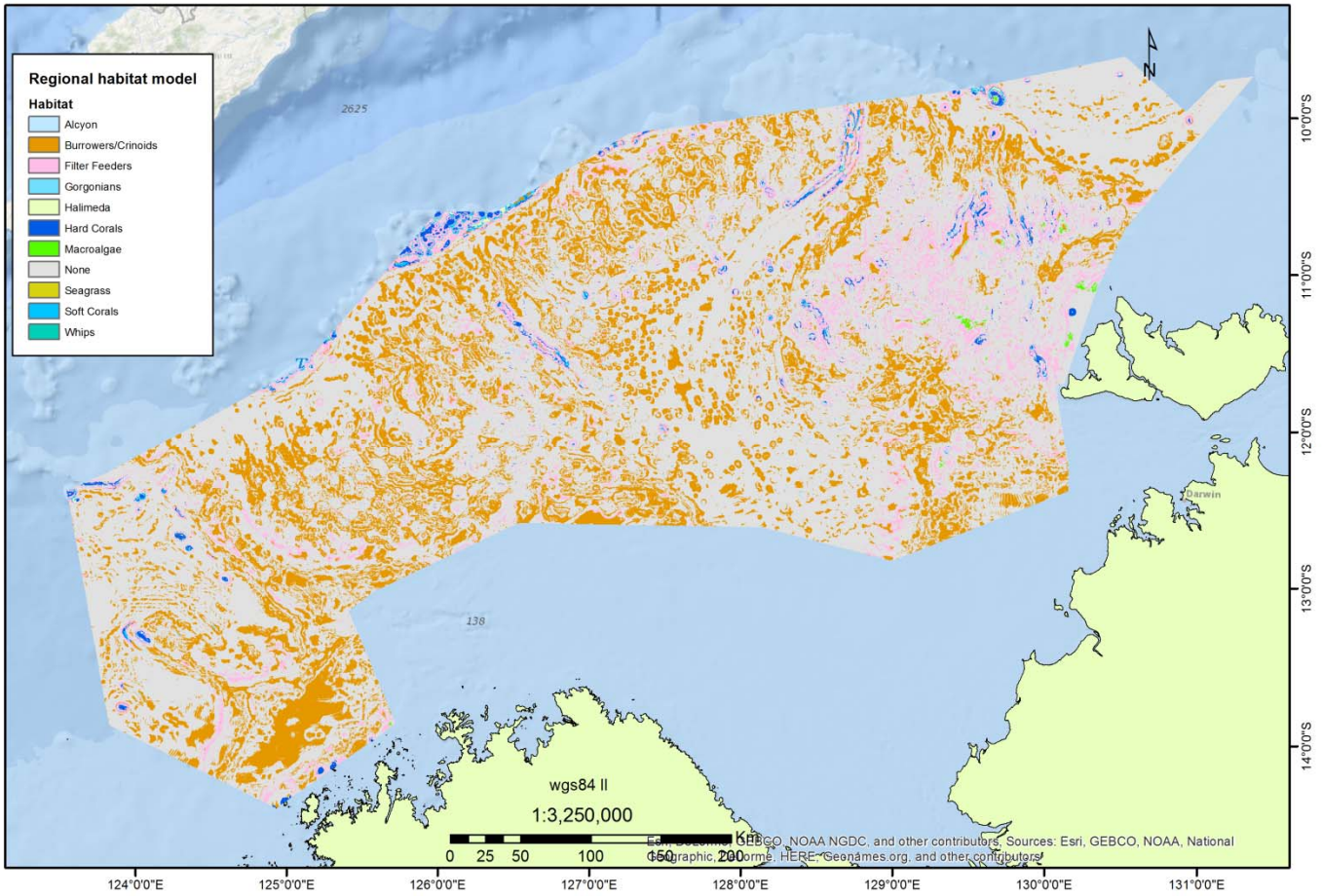

Figure 57. Regional habitat model (v 5) based on Geosciences Australia National 250 m bathymetry and derived variables modelled with coarse level benthic habitat classes, produced by realtime classification of video during towvid transects, as shown in Figure 14.

Table 5. Proportion broad scale benthic habitat class model area by type for regional model.

Habitat	Percent
Alcyon	0.10%
Burrowers/Crinoids	22.91%
Filter Feeders	6.44%
Gorgonians	0.18%
Halimeda	0.10%
Hard Corals	0.65%
Macroalgae	0.09%
Soft Corals	0.28%
Seagrass	0.00%
Whips	0.00%
None	69.24%

Table 6. Accuracy confusion matrix and statistics for regional habitat model (based on 33% blind validation n 113822)

		Predicted											
		None	Alcyon	Burrowers/Crinoids	Filter Feeders	Gorgonians	Halimeda	Hard Corals	Macroalgae	Soft Corals	Seagrass	Sponges	Whips
Observed	None	1040	1	96	225	0	185	22	35	3	7	433	51
	Alcyon	0	4942	174	0	0	0	0	0	1	0	390	2
	Burrowers/Crinoids	1	119	13042	0	8	1461	48	162	0	0	1708	7
	Filter Feeders	183	0	31	1268	0	37	1	6	0	22	371	101
	Gorgonians	0	0	42	0	383	410	4	36	0	0	314	0
	Halimeda	203	0	747	1	73	42194	66	633	47	0	1468	0
	Hard Corals	8	0	61	0	0	21	1419	0	0	0	184	0
	Macroalgae	9	0	145	0	75	1081	22	2341	0	0	241	0
	Soft Corals	0	0	0	0	0	607	0	0	169	0	24	0
	Seagrass	66	0	3	132	0	63	0	0	0	54	71	15
	Sponges	188	182	1522	357	12	2906	252	302	5	29	27085	19
	Whips	241	22	161	206	0	0	0	0	0	0	212	506
	Total Accuracy	82.97%											
	Kappa	0.76											

2.5.3 Fish community comparisons

Tassie Shoal has notably higher fish diversity in comparison with shoals and reefs at similar depths around Australia, and relatively high levels of fish abundance (Figure 57). Tassie shoal has the highest median species richness yet recorded by AIMS at any location using BRUVS techniques. The geographically closest shoals for comparison are the Margaret Harries Banks, which also have higher fish species richness and abundance compared with the global mean. In contrast, Evans Shoal has fish species richness and abundance much closer to the global mean.

The highly diverse fish communities at Tassie Shoal include three new species records for Australia in the data. These were an undescribed emperor (*Lethrinus* sp1), not yet classified in the scientific literature, and two parrotfish known to occur in Indonesia – *Scarus hypselopterus* and *Scarus*

fuscodocaudalis (see Appendix 2). There were a number of other species recorded for the first time in AIMS sampling of the north-western bioregions, such as the Pinjalo snapper (*Pinjalo lewisi*).

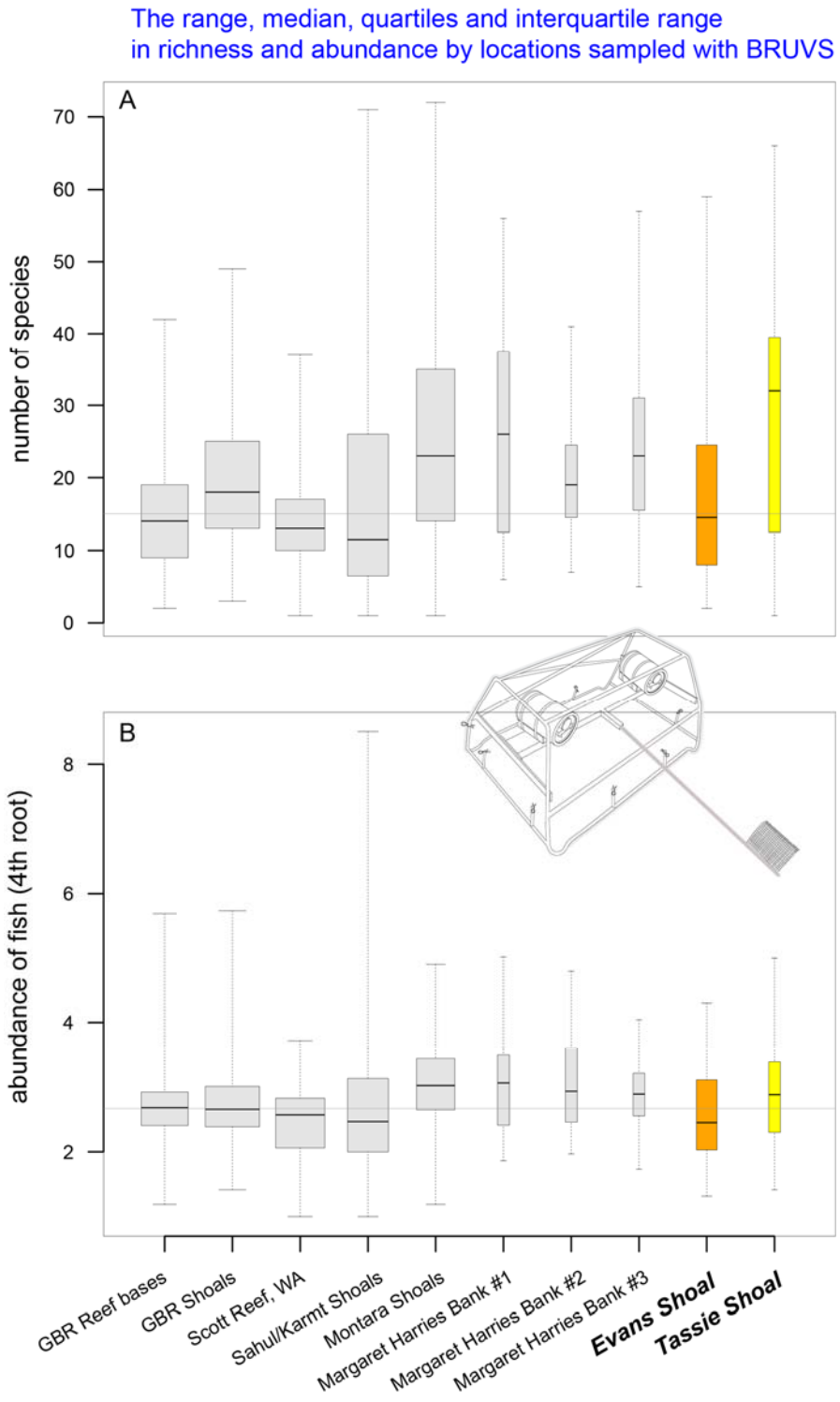

Figure 57: Comparison of species richness and transformed abundance (4th root) of fishes, sharks, rays and sea snakes pooled among baited videos (BRUVS) set in different regions. The samples from each region were selected to have similar depths and habitats as the BRUVS imagery analysed from Evans and Tassie Shoals. The box and whisker plots show the ranges, medians, and interquartile ranges in data. The box widths are proportional to the square root of the sample size

(number of SBRUVS drops). Horizontal lines show the global medians in richness and transformed abundance across the 10 regions compared. Tassie shoal has the highest diversity and abundance of any region sampled by AIMS.

3 Discussion

On both Tassie and Evans Shoals, the presence of extensive carbonate sand fields down a proportion of the shoal slope is suggestive of sediments being moved from the plateau regions and accumulating on the slopes. This feature was particularly noticeable on the western margins, but could be found on both eastern and western sides of the shoals, though less extensive or absent at northern and southern ends. This distribution of unconsolidated sand may reflect an approximate east-west sediment transport environment associated with prevailing currents and wave regimes. Clearer water along the outer shelf allowed light dependent organisms to dominate the upper regions of all shoals in the region. Coral cover was more consistent and increased its contribution to the shallow plateau habitats as shoal depth and plateau size decreased. However, the mechanism responsible for this possible trend is not clear and it may merely reflect the level of consolidated substrate available to support coral recruitment and growth. Similarly, it is unclear why some, but not all parts of the upper plateau rim and slopes, supported dense areas of foliaceous coral. The biota observed on all three shoals appeared to be in healthy condition. It is notable that only two giant clams were observed in total on the transects surveyed at the three shoals. Although the detectability of clams using towed video is not known, clams of the sizes represented by those confiscated from illegal fishing boats in the area in recent years should be clearly visible and the lack of clams may reflect a general loss of these larger specimens from the shallower and more accessible areas. Other than the lack of clams, there was little or no mortality seen amongst the coral species and on all shoals the presence of large table corals greater than a metre in diameter suggests no recent major disturbances from storms.

The three shoals shared similar habitats and species, but the relative contribution of key biota and associated habitat complexity varied on each. The benthic community on Tassie Shoal was more similar to Blackwood, although with less hard coral overall, while Evans Shoal was most comparable for benthic community structure with one of the Margaret Harries Banks shoals. In terms of hard corals, overall coral cover was similar at Tassie and Evans Shoal, at approximately 9% cover, while Blackwood was significantly higher at a mean cover of 25%. This relates to Blackwood Shoal having coral dominated habitat more consistently spread across much of its small plateau, while on Tassie and Evans Shoals a variety of other habitat types are more common. An analysis of coral cover on individual transects revealed that maximum coral cover within coral dominated habitats was more similar between these three shoals, typically ranging between 21-32%. This level of coral cover is typical of coral dominated habitats on healthy coral reefs. An AIMS analysis of individual transects featuring moderate to high coral cover over distances of 250-900 m, found that maximum coral cover at Evans, Tassie and Blackwood Shoals, within a single transect, was in the middle ranking of the twenty shoals for which AIMS has comparable data. The one exception to this mid-ranking level of coral abundance was in the deeper foliaceous coral habitats found at Evans Shoal, where corals appeared to be closely packed and coral cover reached a maximum of 63% over approximately 300 m on one transect during its transit across that coral community. This type of coral community is not unique to Evans Shoal, however, having also been observed, but much more limited extent on Tassie Shoal, as well as during 2004 AIMS surveys at Barton Shoal to the west and in the deeper lagoon habitat at south Scott Reef (Heyward, pers.obs.).

The larger Evans Shoal had very extensive areas of sand and rubble across large proportions of it plateau, with corals patchy and variable in abundance and diversity. Some areas of medium to high coral density were noted, including the presence in selected areas between 40-60 m, of foliaceous coral habitat very similar to that observed further west in the Sahul Shoals and within the deeper lagoon at Scott Reef. The steepening slopes at the shoal edges saw an increase in the presence of coarse sand, likely being transported off the plateaus, with filter feeding biota becoming more prevalent on any rocky outcrops beyond around 60 m.

The benthic habitats at all three shoals were consistent with other outer-shelf shoals observed by AIMS across the North and North-west bioregions. The quantitative measures of major habitat types and fine scale detail of coral abundance and diversity point to strong regional similarities between shoals. The available information indicates that each shoal has its own characteristic benthic community but that there are many species that are in common among shoals. The fish communities encountered at Evans and Tassie Shoals were similarly comparable to other shoals in the region in terms of abundance and diversity, sharing many species, although the Tassie Shoal data was notably more diverse than several others and features three species not recorded elsewhere by AIMS. It is a feature of all BRUVS sampling conducted on shoals by AIMS in this region that the fish data from a single survey captures a majority of species present, but species accumulation curves fall well short of reaching an asymptote. The 300 species of finfish, sharks and rays encountered in this study is typical of the diversity seen during initial survey of shoals in this region. Where repeat surveys have been conducted on other shoals by AIMS, additional species have been observed, with total recorded fish species incrementing around 10% with each additional survey. Records of fish diversity would increase if further BRUVS deployments were made at Evans and Tassie Shoals, particularly in the reefy habitat areas.

Levels of ecological connectivity among the shoals remain to be demonstrated, but the strong surface currents tracked using satellite drifters throughout this bioregion (AIMS, unpublished data), indicate transport rates of 20km/day under light to moderate wind conditions and much higher during storms or seasonal tradewind periods. Consequently connectivity, at least on evolutionary timescales, between shoal features is expected. The status of the biota on each shoal may reflect varying connectivity, to some degree, but also disturbance events such as cyclone and storm damage and coral bleaching.

The two mid-shelf areas investigated were much more turbid than the shelf-edge shoals and did not support notable benthic primary producer habitat, other than the occasional coral on the very shallowest transects <30 m. Sparse to moderate density filter feeders, dominated by small sponges, were observed on areas of bare rock or sand covered pavement, with larger organisms observed on outcropping low relief reef or rocks where the seabed slope changed around the edge of deeper channels. In general, epibenthic biota was sparse and initial observations suggest the dominant species present are consistent with what has been seen during other surveys of similarly turbid waters in the region, e.g. Kelly & Prezlawski (2012). Most of these areas were found to have a seabed covered in unconsolidated sediments such as coarse sand and mud, but occasionally gravels, with epibenthic fauna present at low densities attached to areas of consolidated pavement covered in fine sediment, or on low relief rock outcropping, most commonly present around ridges and sharp drop offs. These patterns were also consistent with the regional community analysis and regional spatial model (Figure 57) where large areas were sparsely populated with epibenthic fauna (Burrows/Crinoids; 22.91%) and to a lesser extent filter feeder communities (6.44%). Coral reef communities were associated with the shallower reefs, shoals and banks particularly as they moved away from the turbid coastal fringe. No benthic habitat was predicted for a substantial portion of the area (69.24%). These areas will contain various organisms, but in general insufficient biota to allow a discrete category to be modelled as a habitat class. However caution should be used interpreting the extrapolations in the regional model beyond the extent of the surveyed data. The "none" habitat category is most likely to represent areas with little or no habitat forming biota, but is less well predicted by the model that the other categories. Caution should be used interpreting the regional model beyond the extent of the surveyed data. There are large areas where there is no validation information available so estimates of model accuracy and error are not possible to calculate without additional field data. It should also be noted with caution that while over the entire regional model performed well for most habitat categories, the "None" category had the poorest performance most frequently under predicting filter feeder (including whips) and Halimedia communities which by their nature can be discrete, stochastic and challenging to model.

The complex seabed bathymetry gives rise to turbulence associated with tidal flows and resuspension of fine sediments, which is a feature of these mid- and inner shelf areas. Spring tides with associated high turbidity and strong tidal currents were encountered during the field survey, particularly when surveying

across some of the submerged channel features adjacent to Cape Helvetius. The limited sediment data collected during this project and the review of sediment data for the region suggest a complex spatial pattern of reworked old terrigenous sediments and *in situ* production of carbonates, which may increase in importance in shallow waters and in particular with distance from the coast.

In summary, this report represents the final results from the October 2015 study and establishes baseline information relevant to the Barossa Field and surrounds. It provides a general characterisation of habitat distributions and dominant biota on shoals and mid-shelf areas surveyed. Both the mid-shelf areas and the shoals displayed biological communities consistent with other similar areas in the broader region. The patchy distribution of filter feeder communities on the mid-shelf suggests a pattern linked to the underlying geology and complex bathymetry that are a legacy of the drowned coastal shelf area. The outer shelf shoals support filter feeding communities, but their most striking feature is a rich biodiversity more similar to coral reefs, driven by light in the upper regions and across the plateaux.

While the survey recorded the major habitat types and a large portion of the species present, it is clear that the biodiversity will continue to be further defined as part of additional regional survey efforts over time. Future repeats of this survey would likely produce a very similar broad characterisation of the seabed biodiversity, although change in abundance of dominant species and distribution of habitats is possible, with variability over time likely to be a natural attribute of these ecosystems. These systems, particularly the shallower habitats, may also be subject to larger scale changes from acute, but less predictable natural disturbances, such as a severe storms or elevated seawater temperature anomalies.

4 References

Anderson, T.J., Nichol, S., Radke, L., Heap, A.D., Battershill, C., Hughes, M., Siwabessy, J., Barrie, V., Alvarez de Glasby, B., Daniell, J., Tran, M. & Shipboard Party, 2011. Seabed Environments of the Eastern Joseph Bonaparte Gulf, Northern Australia. Record 2011/008. Geoscience Australia, Canberra

Allen GR, Swainston R (1988) The marine fishes of north-western Australia. A field guide for anglers and divers. Western Australian Museum, Perth, Western Australia. 201 pp

Becker, R. A., Chambers, J. M. and Wilks, A. R. (1988) The New S Language. Wadsworth & Brooks/Cole.

Breiman L (2001) Random Forests. Machine Learning 45: 5-32.

Cappo M, De'ath G & Speare P (2007a) Inter-reef vertebrate communities of the Great Barrier Reef Marine Park determined by baited remote underwater video stations. Marine Ecology Progress Series 350: 209-221

Cappo M, Harvey E & Shortis M (2007b) Counting and measuring fish with baited video techniques – An overview. Australian Society for Fish Biology 2006 Workshop Proceedings, p. 101-114.

Cappo M, Stowar M, Syms C, Johansson C & Cooper T (2011) Fish-habitat associations in the region offshore from James Price Point – a rapid assessment using Baited Remote Underwater Video Stations (BRUVS). Journal of the Royal Society of Western Australia, 94. 303-321. Kimberley Special Issue

Cappo M, Stowar M, Stieglitz T, Lawrey E, Johansson C & Macneil, A (2012) Measuring and communicating effects of MPAs on deep "shoal" fisheries. In: Proceedings of the 12th International Coral Reef Symposium, pp. 1-5. From: 12th International Coral Reef Symposium, 9-13 July 2012, Cairns, QLD, Australia.

Chen, T. and He, T., 2015. xgboost: eXtreme Gradient Boosting. R package version 0.4-2.

Colton MA & Swearer SE (2012) Locating faunal breaks in the nearshore fish assemblage of Victoria, Australia. Marine and Freshwater Research 63: 218-231.

Cutler, D. R. Edwards T.C, Beard, K.H, Cutler, A,Hess, K.T, Gibson, J, and Lawler, J. J. (2007) "Random Forests for Classification in Ecology." *Ecology* 88: 2783–2792.

De'ath G (2002) Multivariate regression trees: A new technique for modeling species-environment relationships. Ecology 83: 1105-1117.

De'ath G (2007) Boosted trees for ecological modeling and prediction. Ecology 88: 243-251.

De'ath G & Fabricius KE (2000) Classification and regression trees: A powerful yet simple technique for ecological data analysis. Ecology 81: 3178-3192.

Denny CM, Willis TJ & Babcock RC (2004) Rapid recolonisation of snapper *Pagrus auratus*: Sparidae within an offshore island marine reserve after implementation of no-take status. Marine Ecology Progress Series 272: 183-190.

Dufrêne M, Legendre P (1997) Species assemblages and indicator species: the need for a flexible asymmetrical approach. Ecological Monographs 67:345-366

Elith J, Leathwick JR & Hastie T (2008) A working guide to boosted regression trees. Journal of Animal Ecology 77: 802-813.

Elith, J. and J.R. Leathwick, 2009. Species Distribution Models: Ecological Explanation and Prediction Across Space and Time. Annual Review of Ecology, Evolution, and Systematics 40: 677-697. http://dx.doi.org/ 10.1146/annurev.ecolsys.110308.120159

Elith, J., C.H. Graham, R.P. Anderson, M. Dudik, S. Ferrier, A. Guisan, R.J. Hijmans, F. Huettmann, J. Leathwick, A. Lehmann, J. Li, L.G. Lohmann, B. Loiselle, G. Manion, C. Moritz, M. Nakamura, Y. Nakazawa, J. McC. Overton, A.T. Peterson, S. Phillips, K. Richardson, R. Scachetti-Pereira, R. Schapire, J. Soberon, S. Williams, M. Wisz and N. Zimmerman. 2006. Novel methods improve prediction of species' distributions from occurrence data. Ecography 29: 129-151. http://dx.doi.org/10.1111/j. 2006.0906-7590.04596.x

Elith, J., S.J. Phillips, T. Hastie, M. Dudik, Y.E. Chee, C.J. Yates. 2011. A statistical explanation of MaxEnt for ecologists. Diversity and Distributions 17:43-57. http://dx.doi.org/10.1111/j.1472-4642.2010.00725.x Elith, J., J.R. Leathwick and T. Hastie, 2009. A working guide to boosted regression trees. Journal of Animal Ecology 77: 802-81

Espinoza M, Cappo M, Heupel MR, Tobin AJ, Simpfendorfer CA (2014) Quantifying shark distribution patterns and species-habitat associations: implications of marine park zoning. PLoSONE. DOI: 10.1371/journal.pone.0106885

Fitzpatrick BM, Harvey ES, Heyward AJ, Twiggs EJ & Colquhoun J (2012) Habitat specialization in tropical continental shelf demersal fish assemblages. PLOS ONE 7(6): e39634. doi:10.1371/journal.pone.0039634

Harvey ES, Cappo M, Kendrick GA & McLean DL (2013) Coastal fish assemblages reflect geological and oceanographic gradients within an Australian zootone. PLoS ONE 8(11): e80955

Heyward, A., Pinceratto, E., and L. Smith. (Eds). 1997. Big Bank Shoals of the Timor Sea: An Environmental Resource Atlas. Australian Institute of Marine Science, Townsville and BHP Petroleum: Melbourne. 115p.

Heyward, A., Jones, R., Meeuwig, J., Burns, K., Radford, B., Colquhoun, J., Cappo, M., Case, M., O'Leary, R.A., Fisher, R., Meekan, M., and M. Stowar. 2012. Monitoring Study S5. Montara: 2011 Offshore Banks Assessment Survey. Final report prepared by the Australian Institute of Marine Science for PTTEP Australasia (Ashmore Cartier) Pty. Ltd. in accordance with Contract No. 000/2011/02-04. Perth, May 2012. 257p.

Heyward, A. et al. 2015. Barossa Environmental Baseline Study 2015 Interim Report for Conoco Philips (Browse Basin) Pty Ltd. Australian Institute of Marine Science, Perth 2015. 55p.

Holmes, K. W., K. P. Van Niel, G. A. Kendrick, and B. Radford. (2007) "Probabilistic Large-Area Mapping of Seagrass Species Distributions." *Aquatic Conservation: Marine and Freshwater Ecosystems* 17: 385–407.

Hosmer, D.W. and Lemeshow S. (2000) "Interpretation of the Fitted Logistic Regression Model." *Applied Logistic Regression, Second Edition*, pp 47–90.

Kelly, T. & Przeslawski, R., 2012. The ecology and morphology of sponges and octocorals in the northeastern Joseph Bonaparte Gulf. Record 2012_067. Geoscience Australia, Canberra

Mallet D & Pelletier D (2014) Underwater video techniques for observing coastal marine biodiversity: A review of sixty years of publications (1952–2012). Fisheries Research 154:44-62.

Mardia, K. V., Kent, J. T. and Bibby, J. M. (1979) Multivariate Analysis. Academic Press.

McLean DL, Harvey ES, Fairclough DV & Newman SJ (2010) Large decline in the abundance of a targeted tropical lethrinid in areas open and closed to fishing. Marine Ecology Progress Series 418, 189-199.

Nichol, S.L., Howard, F.J.F., Kool, J., Siwabessy, J. & Przeslawski, R., Picard, K., Alvarez de Glasby, B., Colquhoun, J., Letessier, T. and Heyward., A. (2013). Oceanic Shoals Commonwealth Marine Reserve (Timor Sea) Biodiversity Survey: GA0339/SOL5650 Post-Survey Report. Record 2013/038. Geoscience Australia, Canberra

Ridgeway G (2007) gbm: Generalized Boosted Regression Models. URL: http://wwwi-pensiericom/gregr/gbmshtml

'R' Development Core Team (2006) R: A language and environment for statistical computing. Reference Index. R Foundation for Statistical Computing: http://cran.r-project.org/doc/manuals/refman.pdf

Schobernd ZH, Bacheler NM & Conn PB (2014) Examining the utility of alternative video monitoring metrics for indexing reef fish abundance. Canadian Journal of Fisheries and Aquatic Sciences, 2014, 71(3): 464-471.

Stevens, D. L., Jr., and A.R. Olsen. 2004. Spatially-balanced sampling of natural resources. Journal of American Statistical Association 99(465):262-278

Udyawer V, Cappo M, Simpfendorfer CA, Heupel MR, & Lukoschek V (2013) Distribution of sea snakes in the Great Barrier Reef Marine Park: observations from 10 yrs of baited remote underwater video station (BRUVS) sampling. Coral Reefs 33: 777-791

Willis TJ, Millar RB & Babcock RC (2000) Detection of spatial variability in relative density of fishes: comparison of visual census, angling, and baited underwater video. Marine Ecology Progress Series 198: 249-260.

Yearsley GK, Last PR & Morris GB (1997) Codes for Australian Aquatic Biota (CAAB): An upgraded and expanded species coding system for Australian fisheries databases, CSIRO, Australia, Hobart, Tasmania.

Appendix 1

Date	Technique	Site	Name	Data	Latitude	Longitude	Depth
14-Sep-15	Towed Video	Goodrich Bank	Goodrich Bank_Tow19	Real Time Benthic Classification, Video, HD Images	-10.6803	130.1968	27.3
14-Sep-15	Towed Video	Goodrich Bank	Goodrich Bank_Tow15	Real Time Benthic Classification, Video, HD Images	-10.6816	130.2113	28.3
14-Sep-15	Towed Video	Goodrich Bank	Goodrich Bank_Tow13	Real Time Benthic Classification, Video, HD Images	-10.7094	130.2238	26.4
14-Sep-15	Towed Video	Goodrich Bank	Goodrich Bank_Tow14	Real Time Benthic Classification, Video, HD Images	-10.6960	130.2476	52.1
14-Sep-15	Towed Video	Goodrich Bank	Goodrich Bank_Tow11	Real Time Benthic Classification, Video, HD Images	-10.7066	130.2615	77.2
14-Sep-15	Towed Video	Goodrich Bank	Goodrich Bank_Tow8	Real Time Benthic Classification, Video, HD Images	-10.7379	130.2664	77.6
14-Sep-15	Towed Video	Goodrich Bank	Goodrich Bank_Tow4	Real Time Benthic Classification, Video, HD Images	-10.7081	130.3045	42.1
14-Sep-15	CTD	Goodrich Bank	Trip6251_CTD1	CTD	-10.7377	130.3110	66.7
14-Sep-15	Towed Video	Goodrich Bank	Goodrich Bank_Tow7	Real Time Benthic Classification, Video, HD Images	-10.7371	130.3111	66.1
15-Sep-15	Towed Video	Goodrich Bank	Goodrich Bank_Tow28	Real Time Benthic Classification, Video, HD Images	-10.6972	130.0634	103.8
15-Sep-15	Towed Video	Goodrich Bank	Goodrich Bank_Tow27	Real Time Benthic Classification, Video, HD Images	-10.7219	130.0527	29
15-Sep-15	Towed Video	Goodrich Bank	Goodrich Bank_Tow26	Real Time Benthic Classification, Video, HD Images	-10.7301	130.0583	28.8
15-Sep-15	Towed Video	Goodrich Bank	Goodrich Bank_Tow25	Real Time Benthic Classification, Video, HD Images	-10.7385	130.0963	52.3
15-Sep-15	Towed Video	Goodrich Bank	Goodrich Bank_Tow21	Real Time Benthic Classification, Video, HD Images	-10.7277	130.1395	73.9
15-Sep-15	CTD	Goodrich Bank	Trip6251_CTD2	CTD	-10.7293	130.1669	77
15-Sep-15	Towed Video	Goodrich Bank	Goodrich Bank_Tow20	Real Time Benthic Classification, Video, HD Images	-10.7369	130.1633	75.8
15-Sep-15	Towed Video	Goodrich Bank	Goodrich Bank_Tow29	Real Time Benthic Classification, Video, HD Images	-10.6855	130.0917	42.7
15-Sep-15	Towed Video	Goodrich Bank	Goodrich Bank_Tow22	Real Time Benthic Classification, Video, HD Images	-10.6872	130.0949	34

15-Sep-15	Towed Video	Goodrich Bank	Goodrich Bank_Tow24	Real Time Benthic Classification, Video, HD Images	-10.6730	130.1415	30.6
15-Sep-15	CTD	Goodrich Bank	Trip6251_CTD3	CTD	-10.6797	130.0777	74.8
16-Sep-15	Towed Video	Goodrich Bank	Goodrich Bank_Tow5	Real Time Benthic Classification, Video, HD Images	-10.7132	130.3262	20.6
16-Sep-15	Towed Video	Goodrich Bank	Goodrich Bank_Tow3	Real Time Benthic Classification, Video, HD Images	-10.6817	130.3153	19.3
16-Sep-15	Towed Video	Goodrich Bank	Goodrich Bank_Tow9	Real Time Benthic Classification, Video, HD Images	-10.6808	130.3572	64.9
16-Sep-15	Towed Video	Goodrich Bank	Goodrich Bank_Tow2	Real Time Benthic Classification, Video, HD Images	-10.6681	130.3429	56.7
16-Sep-15	CTD	Goodrich Bank	Trip6251_CTD4	CTD	-10.6498	130.3209	53.7
16-Sep-15	Towed Video	Goodrich Bank	Goodrich Bank_Tow1	Real Time Benthic Classification, Video, HD Images	-10.6451	130.3038	71
16-Sep-15	Towed Video	Goodrich Bank	Goodrich Bank_Tow12	Real Time Benthic Classification, Video, HD Images	-10.6407	130.2588	80.4
16-Sep-15	Towed Video	Goodrich Bank	Goodrich Bank_Tow10	Real Time Benthic Classification, Video, HD Images	-10.6610	130.2928	78.9
16-Sep-15	Towed Video	Goodrich Bank	Goodrich Bank_Tow17	Real Time Benthic Classification, Video, HD Images	-10.6509	130.2222	52.5
16-Sep-15	CTD	Goodrich Bank	Trip6251_CTD5	CTD	-10.6696	130.2658	84.7
17-Sep-15	Smith McIntryre Grab	Goodrich Bank	Goodrich Bank_Stn01Gr01	Sediment Samples	-10.7187	130.2625	80.8
17-Sep-15	Smith McIntryre Grab	Goodrich Bank	Goodrich Bank_Stn02Gr02	Sediment Samples	-10.6918	130.2629	67.6
17-Sep-15	Smith McIntryre Grab	Goodrich Bank	Goodrich Bank_Stn03Gr03	Sediment Samples	-10.6643	130.2631	83.5
17-Sep-15	Towed Video	Goodrich Bank	Goodrich Bank_Tow16	Real Time Benthic Classification, Video, HD Images	-10.6686	130.2092	28.2
17-Sep-15	Towed Video	Goodrich Bank	Goodrich Bank_Tow18	Real Time Benthic Classification, Video, HD Images	-10.6580	130.1789	49.4
17-Sep-15	Towed Video	Goodrich Bank	Goodrich Bank_Tow23	Real Time Benthic Classification, Video, HD Images	-10.6493	130.1436	34.3
17-Sep-15	CTD	Evans Shoal	Trip6251_CTD6	CTD	-9.9305	129.6060	179.3
18-Sep-15	Towed Video	Evans Shoal	EvansShoal_Tow31	Real Time Benthic Classification, Video, HD Images	-9.9476	129.5767	
18-Sep-15	Towed Video	Evans Shoal	EvansShoal_Tow21	Real Time Benthic Classification, Video, HD Images	-9.9455	129.5811	19.7

18-Sep-15	Towed Video	Evans Shoal	EvansShoal_Tow20	Real Time Benthic Classification, Video, HD Images	-9.9377	129.5846	19.3
18-Sep-15	Towed Video	Evans Shoal	EvansShoal_Tow19	Real Time Benthic Classification, Video, HD Images	-9.9289	129.5887	18.7
18-Sep-15	Towed Video	Evans Shoal	EvansShoal_Tow18	Real Time Benthic Classification, Video, HD Images	-9.9234	129.5873	22.1
18-Sep-15	CTD	Evans Shoal	Trip6251_CTD7	CTD	-9.9156	129.6038	190
18-Sep-15	Towed Video	Evans Shoal	EvansShoal_Tow14	Real Time Benthic Classification, Video, HD Images	-9.9176	129.5823	18.9
18-Sep-15	Towed Video	Evans Shoal	EvansShoal_Tow13	Real Time Benthic Classification, Video, HD Images	-9.9134	129.5811	18
18-Sep-15	Towed Video	Evans Shoal	EvansShoal_Tow6	Real Time Benthic Classification, Video, HD Images	-9.9058	129.5711	25.5
18-Sep-15	Towed Video	Evans Shoal	EvansShoal_Tow5	Real Time Benthic Classification, Video, HD Images	-9.9005	129.5682	26.2
18-Sep-15	Towed Video	Evans Shoal	EvansShoal_Tow4	Real Time Benthic Classification, Video, HD Images	-9.8936	129.5596	22.7
18-Sep-15	CTD	Evans Shoal	Trip6251_CTD8	CTD	-9.8665	129.5432	169.9
19-Sep-15	SBRUVS	Evans Shoal	EvansShoal_CAM1RIG1	Stereo Video	-9.8882	129.5743	68
19-Sep-15	SBRUVS	Evans Shoal	EvansShoal_CAM2RIG2	Stereo Video	-9.8927	129.5783	56.6
19-Sep-15	SBRUVS	Evans Shoal	EvansShoal_CAM3RIG3	Stereo Video	-9.8963	129.5819	56.2
19-Sep-15	SBRUVS	Evans Shoal	EvansShoal_CAM4RIG4	Stereo Video	-9.9060	129.5875	49.7
19-Sep-15	SBRUVS	Evans Shoal	EvansShoal_CAM5RIG5	Stereo Video	-9.9129	129.5937	60.9
19-Sep-15	SBRUVS	Evans Shoal	EvansShoal_CAM6RIG6	Stereo Video	-9.9194	129.5971	64.9
19-Sep-15	SBRUVS	Evans Shoal	EvansShoal_CAM7RIG7	Stereo Video	-9.9283	129.5995	68.1
19-Sep-15	SBRUVS	Evans Shoal	EvansShoal_CAM8RIG9	Stereo Video	-9.9349	129.5980	60.8
19-Sep-15	SBRUVS	Evans Shoal	EvansShoal_CAM9RIG9	Stereo Video	-9.8889	129.5573	19.6
19-Sep-15	SBRUVS	Evans Shoal	EvansShoal_CAM10RIG7	Stereo Video	-9.9008	129.5738	20.7
19-Sep-15	SBRUVS	Evans Shoal	EvansShoal_CAM11RIG6	Stereo Video	-9.9059	129.5817	18
19-Sep-15	SBRUVS	Evans Shoal	EvansShoal_CAM12RIG5	Stereo Video	-9.9139	129.5830	21.1
19-Sep-15	SBRUVS	Evans Shoal	EvansShoal_CAM13RIG4	Stereo Video	-9.9214	129.5890	19.6
19-Sep-15	SBRUVS	Evans Shoal	EvansShoal_CAM14RIG3	Stereo Video	-9.9275	129.5947	18.3
19-Sep-15	SBRUVS	Evans Shoal	EvansShoal_CAM15RIG2	Stereo Video	-9.9336	129.5917	19.1
19-Sep-15	SBRUVS	Evans Shoal	EvansShoal_CAM16RIG1	Stereo Video	-9.9455	129.5908	17.5
19-Sep-15	SBRUVS	Evans Shoal	EvansShoal_CAM17RIG1	Stereo Video	-9.8972	129.5532	24.5
19-Sep-15	SBRUVS	Evans Shoal	EvansShoal_CAM18RIG2	Stereo Video	-9.8984	129.5588	25.9

19-Sep-15	SBRUVS	Evans Shoal	EvansShoal_CAM19RIG3	Stereo Video	-9.9038	129.5638	26.3
19-Sep-15	SBRUVS	Evans Shoal	EvansShoal_CAM20RIG4	Stereo Video	-9.9045	129.5698	25
19-Sep-15	SBRUVS	Evans Shoal	EvansShoal_CAM21RIG5	Stereo Video	-9.9137	129.5694	25.6
19-Sep-15	SBRUVS	Evans Shoal	EvansShoal_CAM22RIG6	Stereo Video	-9.9189	129.5770	24.5
19-Sep-15	SBRUVS	Evans Shoal	EvansShoal_CAM23RIG7	Stereo Video	-9.9280	129.5864	22.2
19-Sep-15	SBRUVS	Evans Shoal	EvansShoal_CAM24RIG9	Stereo Video	-9.9365	129.5893	20.9
19-Sep-15	Panda	Evans Shoal	EvansShoal_Drop1	Oblique Images	-9.9288	129.5917	19.6
19-Sep-15	Panda	Evans Shoal	EvansShoal_Drop2	Oblique Images	-9.8913	129.5751	53.3
19-Sep-15	Panda	Evans Shoal	EvansShoal_Drop3	Oblique Images	-9.9099	129.5863	19.9
19-Sep-15	CTD	Evans Shoal	Trip6251_CTD9	CTD	-9.9008	129.5934	181.4
20-Sep-15	Towed Video	Evans Shoal	EvansShoal_Tow36	Real Time Benthic Classification, Video, HD Images	-9.9471	129.5619	26.8
20-Sep-15	Towed Video	Evans Shoal	EvansShoal_Tow22	Real Time Benthic Classification, Video, HD Images	-9.9491	129.5604	24.7
20-Sep-15	Towed Video	Evans Shoal	EvansShoal_Tow24	Real Time Benthic Classification, Video, HD Images	-9.9433	129.5504	26.8
20-Sep-15	Towed Video	Evans Shoal	EvansShoal_Tow33	Real Time Benthic Classification, Video, HD Images	-9.9387	129.5476	26.7
20-Sep-15	Towed Video	Evans Shoal	EvansShoal_Tow23	Real Time Benthic Classification, Video, HD Images	-9.9346	129.5395	41.5
20-Sep-15	Towed Video	Evans Shoal	EvansShoal_Tow11	Real Time Benthic Classification, Video, HD Images	-9.9224	129.5410	24.5
20-Sep-15	CTD	Evans Shoal	Trip6251_CTD10	CTD	-9.9103	129.5135	168.2
20-Sep-15	CTD	Evans Shoal	Trip6251_CTD11	CTD	-9.9139	129.5386	24.7
20-Sep-15	Towed Video	Evans Shoal	EvansShoal_Tow10	Real Time Benthic Classification, Video, HD Images	-9.9117	129.5375	24.1
20-Sep-15	Towed Video	Evans Shoal	EvansShoal_Tow9	Real Time Benthic Classification, Video, HD Images	-9.9027	129.5400	25.1
20-Sep-15	Towed Video	Evans Shoal	EvansShoal_Tow2	Real Time Benthic Classification, Video, HD Images	-9.8985	129.5422	23.9
20-Sep-15	Towed Video	Evans Shoal	EvansShoal_Tow3	Real Time Benthic Classification, Video, HD Images	-9.8871	129.5445	18.3
20-Sep-15	Towed Video	Evans Shoal	EvansShoal_Tow1	Real Time Benthic Classification, Video, HD Images	-9.8897	129.5496	22.9
20-Sep-15	CTD	Evans Shoal	Trip6251_CTD12	CTD	-9.8768	129.5617	151.2
21-Sep-15	SBRUVS	Evans Shoal	EvansShoal_CAM25RIG1	Stereo Video	-9.8759	129.5543	75.4
21-Sep-15	SBRUVS	Evans	EvansShoal_CAM26RIG2	Stereo Video	-9.8741	129.5475	56.9

		Shoal					
21-Sep-15	SBRUVS	Evans Shoal	EvansShoal_CAM27RIG3	Stereo Video	-9.8747	129.5430	47.2
21-Sep-15	SBRUVS	Evans Shoal	EvansShoal_CAM28RIG4	Stereo Video	-9.8762	129.5390	43.8
21-Sep-15	SBRUVS	Evans Shoal	EvansShoal_CAM29RIG5	Stereo Video	-9.8822	129.5364	44.7
21-Sep-15	SBRUVS	Evans Shoal	EvansShoal_CAM30RIG6	Stereo Video	-9.8942	129.5319	56.4
21-Sep-15	SBRUVS	Evans Shoal	EvansShoal_CAM31RIG7	Stereo Video	-9.8984	129.5278	66.6
21-Sep-15	SBRUVS	Evans Shoal	EvansShoal_CAM32RIG9	Stereo Video	-9.9052	129.5313	39.9
21-Sep-15	SBRUVS	Evans Shoal	EvansShoal_CAM33RIG9	Stereo Video	-9.9089	129.5256	71.6
21-Sep-15	SBRUVS	Evans Shoal	EvansShoal_CAM34RIG7	Stereo Video	-9.9155	129.5277	57.1
21-Sep-15	SBRUVS	Evans Shoal	EvansShoal_CAM35RIG6	Stereo Video	-9.9249	129.5294	56.4
21-Sep-15	SBRUVS	Evans Shoal	EvansShoal_CAM36RIG5	Stereo Video	-9.9312	129.5275	75.1
21-Sep-15	SBRUVS	Evans Shoal	EvansShoal_CAM37RIG4	Stereo Video	-9.9373	129.5290	79.4
21-Sep-15	SBRUVS	Evans Shoal	EvansShoal_CAM38RIG3	Stereo Video	-9.9419	129.5339	56.9
21-Sep-15	SBRUVS	Evans Shoal	EvansShoal_CAM39RIG2	Stereo Video	-9.9478	129.5328	73.4
21-Sep-15	SBRUVS	Evans Shoal	EvansShoal_CAM40RIG1	Stereo Video	-9.9536	129.5398	62.4
21-Sep-15	SBRUVS	Evans Shoal	EvansShoal_CAM41RIG1	Stereo Video	-9.9276	129.5402	23.8
21-Sep-15	SBRUVS	Evans Shoal	EvansShoal_CAM42RIG2	Stereo Video	-9.9369	129.5389	54.5
21-Sep-15	SBRUVS	Evans Shoal	EvansShoal_CAM43RIG3	Stereo Video	-9.9506	129.5402	52.3
21-Sep-15	SBRUVS	Evans Shoal	EvansShoal_CAM44RIG4	Stereo Video	-9.9495	129.5476	22.5
21-Sep-15	SBRUVS	Evans Shoal	EvansShoal_CAM45RIG5	Stereo Video	-9.9550	129.5551	46.8
21-Sep-15	SBRUVS	Evans Shoal	EvansShoal_CAM46RIG6	Stereo Video	-9.9592	129.5635	58.1
21-Sep-15	SBRUVS	Evans Shoal	EvansShoal_CAM47RIG7	Stereo Video	-9.9541	129.5754	18.2
21-Sep-15	SBRUVS	Evans Shoal	EvansShoal_CAM48RIG9	Stereo Video	-9.9539	129.5903	65.8
21-Sep-15	Towed Video	Evans Shoal	EvansShoal_Tow32	Real Time Benthic Classification, Video, HD Images	-9.9489	129.5722	23.6
21-Sep-15	Towed Video	Evans Shoal	EvansShoal_Tow29	Real Time Benthic Classification, Video, HD Images	-9.9356	129.5696	23.2
21-Sep-15	Towed Video	Evans Shoal	EvansShoal_Tow25	Real Time Benthic Classification, Video, HD Images	-9.9327	129.5847	21.5
21-Sep-15	CTD	Evans Shoal	Trip6251_CTD13	CTD	-9.9174	129.6009	161.9
22-Sep-15	Towed Video	Evans Shoal	EvansShoal_Tow7	Real Time Benthic Classification, Video, HD Images	-9.8893	129.5420	18.7
22-Sep-15	Towed Video	Evans Shoal	EvansShoal_Tow8	Real Time Benthic Classification, Video, HD Images	-9.9019	129.5417	26.3

22-Sep-15	Towed Video	Evans Shoal	EvansShoal_Tow15	Real Time Benthic Classification, Video, HD Images	-9.9031	129.5539	27.4
22-Sep-15	Towed Video	Evans Shoal	EvansShoal_Tow12	Real Time Benthic Classification, Video, HD Images	-9.9067	129.5393	25.2
22-Sep-15	Towed Video	Evans Shoal	EvansShoal_Tow16	Real Time Benthic Classification, Video, HD Images	-9.9192	129.5483	27.1
22-Sep-15	Towed Video	Evans Shoal	EvansShoal_Tow17	Real Time Benthic Classification, Video, HD Images	-9.9049	129.5543	26.8
22-Sep-15	CTD	Evans Shoal	Trip6251_CTD14	CTD	-9.9164	129.5610	26.3
22-Sep-15	Towed Video	Evans Shoal	EvansShoal_Tow26	Real Time Benthic Classification, Video, HD Images	-9.9085	129.5618	26.2
22-Sep-15	Towed Video	Evans Shoal	EvansShoal_Tow27	Real Time Benthic Classification, Video, HD Images	-9.9178	129.5655	25.1
22-Sep-15	Towed Video	Evans Shoal	EvansShoal_Tow30	Real Time Benthic Classification, Video, HD Images	-9.9223	129.5636	25.4
22-Sep-15	Towed Video	Evans Shoal	EvansShoal_Tow28	Real Time Benthic Classification, Video, HD Images	-9.9293	129.5614	25.6
22-Sep-15	Towed Video	Evans Shoal	EvansShoal_Tow35	Real Time Benthic Classification, Video, HD Images	-9.9353	129.5615	25.9
22-Sep-15	Towed Video	Evans Shoal	EvansShoal_Tow34	Real Time Benthic Classification, Video, HD Images	-9.9382	129.5517	27.1
22-Sep-15	CTD	Evans Shoal	Trip6251_CTD15	CTD	-9.9324	129.5172	138.2
23-Sep-15	SBRUVS	Evans Shoal	EvansShoal_CAM49RIG1	Stereo Video	-9.8854	129.5436	18.5
23-Sep-15	SBRUVS	Evans Shoal	EvansShoal_CAM50RIG2	Stereo Video	-9.8919	129.5443	21.3
23-Sep-15	SBRUVS	Evans Shoal	EvansShoal_CAM51RIG3	Stereo Video	-9.8944	129.5408	23.4
23-Sep-15	SBRUVS	Evans Shoal	EvansShoal_CAM52RIG4	Stereo Video	-9.8997	129.5416	24.8
23-Sep-15	SBRUVS	Evans Shoal	EvansShoal_CAM53RIG5	Stereo Video	-9.9022	129.5358	23.3
23-Sep-15	SBRUVS	Evans Shoal	EvansShoal_CAM54RIG6	Stereo Video	-9.9114	129.5437	27.4
23-Sep-15	SBRUVS	Evans Shoal	EvansShoal_CAM55RIG7	Stereo Video	-9.9111	129.5546	26.8
23-Sep-15	SBRUVS	Evans Shoal	EvansShoal_CAM56RIG9	Stereo Video	-9.9056	129.5558	27.9
23-Sep-15	SBRUVS	Evans Shoal	EvansShoal_CAM57RIG9	Stereo Video	-9.9165	129.5307	59
23-Sep-15	SBRUVS	Evans Shoal	EvansShoal_CAM58RIG7	Stereo Video	-9.9205	129.5450	26.1
23-Sep-15	SBRUVS	Evans Shoal	EvansShoal_CAM59RIG6	Stereo Video	-9.9214	129.5505	27.6
23-Sep-15	SBRUVS	Evans Shoal	EvansShoal_CAM60RIG5	Stereo Video	-9.9246	129.5594	26.3
23-Sep-15	SBRUVS	Evans Shoal	EvansShoal_CAM61RIG4	Stereo Video	-9.9168	129.5616	26.8
23-Sep-15	SBRUVS	Evans Shoal	EvansShoal_CAM62RIG3	Stereo Video	-9.9220	129.5674	25.2

23-Sep-15	SBRUVS	Evans Shoal	EvansShoal_CAM63RIG2	Stereo Video	-9.9305	129.5701	23.9
23-Sep-15	SBRUVS	Evans Shoal	EvansShoal_CAM64RIG1	Stereo Video	-9.9390	129.5632	25.7
23-Sep-15	Panda	Evans Shoal	EvansShoal_Drop4	Oblique Images	-9.9407	129.5434	18.5
23-Sep-15	Panda	Evans Shoal	EvansShoal_Drop5	Oblique Images	-9.9408	129.5435	18.5
23-Sep-15	SBRUVS	Evans Shoal	EvansShoal_CAM65_RIG1	Stereo Video	-9.9410	129.5434	18.6
23-Sep-15	SBRUVS	Evans Shoal	EvansShoal_CAM66_RIG2	Stereo Video	-9.9448	129.5528	26.4
23-Sep-15	SBRUVS	Evans Shoal	EvansShoal_CAM67_RIG3	Stereo Video	-9.9381	129.5553	27
23-Sep-15	SBRUVS	Evans Shoal	EvansShoal_CAM68_RIG4	Stereo Video	-9.9544	129.5634	19.8
23-Sep-15	SBRUVS	Evans Shoal	EvansShoal_CAM69_RIG5	Stereo Video	-9.9467	129.5699	23.5
23-Sep-15	SBRUVS	Evans Shoal	EvansShoal_CAM70_RIG6	Stereo Video	-9.9404	129.5716	21.7
23-Sep-15	SBRUVS	Evans Shoal	EvansShoal_CAM71_RIG7	Stereo Video	-9.9399	129.5759	21.4
23-Sep-15	SBRUVS	Evans Shoal	EvansShoal_CAM72_RIG9	Stereo Video	-9.9384	129.5829	21.3
23-Sep-15	Towed Video	Evans Shoal	EvansShoal_Pavona1	Real Time Benthic Classification, Video, HD Images	-9.9406	129.5417	26.6
23-Sep-15	Towed Video	Evans Shoal	EvansShoal_Pavona2	Real Time Benthic Classification, Video, HD Images	-9.9415	129.5430	24.8
23-Sep-15	CTD	Evans Shoal	Trip6251_CTD16	CTD	-9.9629	129.5447	135.8
24-Sep-15	Towed Video	Blackwood Shoal	BlackwoodShoal_Tow1	Real Time Benthic Classification, Video, HD Images	-9.8849	129.4120	28.6
24-Sep-15	Towed Video	Blackwood Shoal	BlackwoodShoal_Tow2	Real Time Benthic Classification, Video, HD Images	-9.8789	129.4159	38.9
24-Sep-15	CTD	Tassie Shoal	Trip6251_CTD17	CTD	-10.1166	129.5499	113.7
24-Sep-15	Towed Video	Tassie Shoal	TassieShoal_Tow4	Real Time Benthic Classification, Video, HD Images	-10.1341	129.5493	15.3
24-Sep-15	Towed Video	Tassie Shoal	TassieShoal_Tow3	Real Time Benthic Classification, Video, HD Images	-10.1324	129.5480	14.7
24-Sep-15	Towed Video	Tassie Shoal	TassieShoal_Tow5	Real Time Benthic Classification, Video, HD Images	-10.1363	129.5501	14.9
24-Sep-15	Towed Video	Tassie Shoal	TassieShoal_Tow5a	Real Time Benthic Classification, Video, HD Images	-10.1373	129.5512	14.3
24-Sep-15	Towed Video	Tassie Shoal	TassieShoal_Tow9	Real Time Benthic Classification, Video, HD Images	-10.1472	129.5429	18.3
24-Sep-15	CTD	Tassie Shoal	Trip6251_CTD18	CTD	-10.1572	129.5310	89.4
25-Sep-15	SBRUVS	Tassie Shoal	TassieShoal_CAM1_RIG9	Stereo Video	-10.1239	129.5414	88.2
25-Sep-15	SBRUVS	Tassie Shoal	TassieShoal_CAM2_RIG7	Stereo Video	-10.1263	129.5385	95.9
25-Sep-15	SBRUVS	Tassie Shoal	TassieShoal_CAM3_RIG6	Stereo Video	-10.1331	129.5390	84.9

25-Sep-15	SBRUVS	Tassie Shoal	TassieShoal_CAM4_RIG5	Stereo Video	-10.1358	129.5439	16.3
25-Sep-15	SBRUVS	Tassie Shoal	TassieShoal_CAM5_RIG4	Stereo Video	-10.1443	129.5434	18.8
25-Sep-15	SBRUVS	Tassie Shoal	TassieShoal_CAM6_RIG3	Stereo Video	-10.1446	129.5370	81.1
25-Sep-15	SBRUVS	Tassie Shoal	TassieShoal_CAM7_RIG2	Stereo Video	-10.1502	129.5336	85
25-Sep-15	SBRUVS	Tassie Shoal	TassieShoal_CAM8_RIG1	Stereo Video	-10.1565	129.5317	88.5
25-Sep-15	SBRUVS	Tassie Shoal	TassieShoal_CAM9_RIG1	Stereo Video	-10.1261	129.5449	77.2
25-Sep-15	SBRUVS	Tassie Shoal	TassieShoal_CAM10_RIG2	Stereo Video	-10.1296	129.5496	17
25-Sep-15	SBRUVS	Tassie Shoal	TassieShoal_CAM11_RIG3	Stereo Video	-10.1359	129.5513	16.1
25-Sep-15	SBRUVS	Tassie Shoal	TassieShoal_CAM12_RIG4	Stereo Video	-10.1405	129.5540	19.1
25-Sep-15	SBRUVS	Tassie Shoal	TassieShoal_CAM13_RIG5	Stereo Video	-10.1449	129.5499	18.8
25-Sep-15	SBRUVS	Tassie Shoal	TassieShoal_CAM14_RIG6	Stereo Video	-10.1494	129.5474	19.6
25-Sep-15	SBRUVS	Tassie Shoal	TassieShoal_CAM15_RIG7	Stereo Video	-10.1547	129.5411	22.3
25-Sep-15	SBRUVS	Tassie Shoal	TassieShoal_CAM16_RIG9	Stereo Video	-10.1504	129.5377	77.6
25-Sep-15	CTD	Tassie Shoal	Trip6251_CTD19	CTD	-10.1593	129.5506	101.3
25-Sep-15	SBRUVS	Tassie Shoal	TassieShoal_CAM17_RIG9	Stereo Video	-10.1332	129.5565	24.1
25-Sep-15	SBRUVS	Tassie Shoal	TassieShoal_CAM18_RIG7	Stereo Video	-10.1391	129.5598	61.3
25-Sep-15	SBRUVS	Tassie Shoal	TassieShoal_CAM19_RIG6	Stereo Video	-10.1451	129.5609	85.6
25-Sep-15	SBRUVS	Tassie Shoal	TassieShoal_CAM20_RIG5	Stereo Video	-10.1486	129.5556	23.3
25-Sep-15	SBRUVS	Tassie Shoal	TassieShoal_CAM21_RIG4	Stereo Video	-10.1519	129.5566	85.1
25-Sep-15	SBRUVS	Tassie Shoal	TassieShoal_CAM22_RIG3	Stereo Video	-10.1535	129.5536	74.3
25-Sep-15	SBRUVS	Tassie Shoal	TassieShoal_CAM23_RIG2	Stereo Video	-10.1544	129.5494	26
25-Sep-15	SBRUVS	Tassie Shoal	TassieShoal_CAM24_RIG1	Stereo Video	-10.1563	129.5455	25.3
25-Sep-15	Towed Video	Tassie Shoal	TassieShoal_TowBommie	Real Time Benthic Classification, Video, HD Images	-10.1547	129.5418	20.3
25-Sep-15	Towed Video	Tassie Shoal	TassieShoal_Tow7	Real Time Benthic Classification, Video, HD Images	-10.1485	129.5446	18.3
25-Sep-15	Towed Video	Tassie Shoal	TassieShoal_Tow8	Real Time Benthic Classification, Video, HD Images	-10.1432	129.5454	16.7
25-Sep-15	CTD	Tassie Shoal	Trip6251_CTD20	CTD	-10.1370	129.5371	96.7
26-Sep-15	Towed Video	Tassie Shoal	TassieShoal_Tow1	Real Time Benthic Classification, Video, HD Images	-10.1346	129.5462	15.1
26-Sep-15	Towed Video	Tassie Shoal	TassieShoal_Tow2	Real Time Benthic Classification, Video, HD Images	-10.1384	129.5504	16.5
26-Sep-15	Towed Video	Tassie Shoal	TassieShoal_Tow6	Real Time Benthic Classification, Video, HD Images	-10.1421	129.5486	

26-Sep-15	Towed Video	Tassie Shoal	TassieShoal_Panda1		-10.1575	129.5447	29.6
26-Sep-15	Towed Video	Tassie Shoal	TassieShoal_Kanga2	Real Time Benthic Classification, Video, HD Images	-10.1572	129.5442	28.2
26-Sep-15	Towed Video	Tassie Shoal	TassieShoal_Kanga3	Real Time Benthic Classification, Video, HD Images	-10.1577	129.5450	33.1
26-Sep-15	Towed Video	Tassie Shoal	TassieShoal_Kanga4	Real Time Benthic Classification, Video, HD Images	-10.1362	129.5485	15.8
26-Sep-15	Towed Video	Tassie Shoal	TassieShoal_Kanga5	Real Time Benthic Classification, Video, HD Images	-10.1364	129.5500	16.4
26-Sep-15	Towed Video	Tassie Shoal	TassieShoal_Kanga6	Real Time Benthic Classification, Video, HD Images	-10.1351	129.5577	28
27-Sep-15	Towed Video	Cape Helvetius	CapeHelvetius_Tow32	Real Time Benthic Classification, Video, HD Images	-11.5852	129.9353	41.7
27-Sep-15	Towed Video	Cape Helvetius	CapeHelvetius_Tow14	Real Time Benthic Classification, Video, HD Images	-11.6045	129.9506	38.7
27-Sep-15	Towed Video	Cape Helvetius	CapeHelvetius_Tow24	Real Time Benthic Classification, Video, HD Images	-11.6054	129.9285	52.7
27-Sep-15	Towed Video	Cape Helvetius	CapeHelvetius_Tow27	Real Time Benthic Classification, Video, HD Images	-11.6224	129.9159	81.7
27-Sep-15	Towed Video	Cape Helvetius	CapeHelvetius_Tow29	Real Time Benthic Classification, Video, HD Images	-11.6300	129.8694	34.7
27-Sep-15	CTD	Cape Helvetius	Trip6251_CTD23	CTD	-11.6301	129.8972	162.5
27-Sep-15	Towed Video	Cape Helvetius	CapeHelvetius_Tow25	Real Time Benthic Classification, Video, HD Images	-11.6288	129.9353	44.2
27-Sep-15	Towed Video	Cape Helvetius	CapeHelvetius_Tow11	Real Time Benthic Classification, Video, HD Images	-11.6441	129.9576	48.9
27-Sep-15	Towed Video	Cape Helvetius	CapeHelvetius_Tow20	Real Time Benthic Classification, Video, HD Images	-11.6790	129.9772	45.3
27-Sep-15	Towed Video	Cape Helvetius	CapeHelvetius_Tow5	Real Time Benthic Classification, Video, HD Images	-11.6567	130.0414	19
27-Sep-15	CTD	Cape Helvetius	Trip6251_CTD22	CTD	-10.6648	130.1088	93.9
27-Sep-15	CTD	Cape Helvetius	Trip6251_CTD24	CTD	-11.5659	129.9693	
27-Sep-15	CTD	Cape Helvetius	Trip6251_CTD25	CTD	-11.5729	129.8700	180.5
27-Sep-15	CTD & 2 DRIFTERS	Cape Helvetius	Trip6251_CTD21	CTD, GPS Locations	-9.4817	129.4184	131
28-Sep-15	Towed Video	Cape Helvetius	CapeHelvetius_Tow7	Real Time Benthic Classification, Video, HD Images	-11.6123	130.0016	26.6
28-Sep-15	Towed Video	Cape Helvetius	CapeHelvetius_Tow6	Real Time Benthic Classification, Video, HD Images	-11.6470	129.9995	31.4

28-Sep-15	Towed Video	Cape Helvetius	CapeHelvetius_Tow8	Real Time Benthic Classification, Video, HD Images	-11.6751	129.9678	45
28-Sep-15	Towed Video	Cape Helvetius	CapeHelvetius_Tow22	Real Time Benthic Classification, Video, HD Images	-11.6787	129.9315	55.3
28-Sep-15	Towed Video	Cape Helvetius	CapeHelvetius_Tow12	Real Time Benthic Classification, Video, HD Images	-11.6625	129.9239	76.8
28-Sep-15	CTD	Cape Helvetius	Trip6251_CTD26	CTD	-11.6701	129.9098	136
28-Sep-15	Towed Video	Cape Helvetius	CapeHelvetius_Tow3	Real Time Benthic Classification, Video, HD Images	-11.7172	130.0045	31.2
28-Sep-15	CTD	Cape Helvetius	Trip6251_CTD27	CTD	-11.6778	129.9825	77.8
29-Sep-15	Towed Video	Cape Helvetius	CapeHelvetius_Tow10	Real Time Benthic Classification, Video, HD Images	-11.7296	129.9603	46.1
29-Sep-15	Towed Video	Cape Helvetius	CapeHelvetius_Tow2	Real Time Benthic Classification, Video, HD Images	-11.7279	130.0460	11.5
29-Sep-15	Towed Video	Cape Helvetius	CapeHelvetius_Tow1	Real Time Benthic Classification, Video, HD Images	-11.6944	130.0324	17
29-Sep-15	Towed Video	Cape Helvetius	CapeHelvetius_Tow19	Real Time Benthic Classification, Video, HD Images	-11.7054	129.9379	45.8
29-Sep-15	Towed Video	Cape Helvetius	CapeHelvetius_Tow18	Real Time Benthic Classification, Video, HD Images	-11.7204	129.9169	75.8
29-Sep-15	CTD	Cape Helvetius	Trip6251_CTD28	CTD	-11.7354	129.9054	82.3
29-Sep-15	Smith McIntyre Grab	Cape Helvetius	Cape Helvetius_Stn04Gr04	Sediment Samples	-11.7356	129.9248	76
29-Sep-15	Smith McIntyre Grab	Cape Helvetius	Cape Helvetius_Stn05Gr05	Sediment Samples	-11.6942	129.9283	57.1
29-Sep-15	Smith McIntyre Grab	Cape Helvetius	Cape Helvetius_Stn06Gr06	Sediment Samples	-11.6178	129.9329	42
29-Sep-15	Smith McIntyre Grab	Cape Helvetius	Cape Helvetius_Stn07Gr07	Sediment Samples	-11.6968	129.9610	55.6
29-Sep-15	Smith McIntyre Grab	Cape Helvetius	Cape Helvetius_Stn08Gr08	Sediment Samples	-11.6974	130.0032	33.2
29-Sep-15	Smith McIntyre Grab	Cape Helvetius	Cape Helvetius_Stn09Gr09	Sediment Samples	-11.6937	130.0442	16
29-Sep-15	Towed Video	Cape Helvetius	CapeHelvetius_Tow4	Real Time Benthic Classification, Video, HD Images	-11.6863	130.0018	33.2
29-Sep-15	Towed Video	Cape Helvetius	CapeHelvetius_Tow23	Real Time Benthic Classification, Video, HD Images	-11.6550	129.8695	51.5
29-Sep-15	CTD	Cape Helvetius	Trip6251_CTD29	CTD	-11.5698	129.9303	58.5
30-Sep-15	Towed Video	Cape Helvetius	CapeHelvetius_Tow9	Real Time Benthic Classification, Video, HD Images	-11.7428	129.9621	50.1

30-Sep-15	Towed Video	Cape Helvetius	CapeHelvetius_Tow15	Real Time Benthic Classification, Video, HD Images	-11.7543	129.9213	81
30-Sep-15	Towed Video	Cape Helvetius	CapeHelvetius_Tow16	Real Time Benthic Classification, Video, HD Images	-11.7476	129.8712	75.4
30-Sep-15	Towed Video	Cape Helvetius	CapeHelvetius_Tow28	Real Time Benthic Classification, Video, HD Images	-11.6691	129.8875	105.1
30-Sep-15	Towed Video	Cape Helvetius	CapeHelvetius_Tow28a	Real Time Benthic Classification, Video, HD Images	-11.6689	129.8875	105.6
30-Sep-15	Towed Video	Cape Helvetius	CapeHelvetius_Tow13	Real Time Benthic Classification, Video, HD Images	-11.7013	129.8865	115.6

Appendix 2

Total counts (sum *MaxN*) of each fish taxa recorded on 95 video files from Evans Shoal (n=72) and Tassie Shoal (n=23), in phylogenetic order. Families, genera and species are listed in alphabetical order within phylogenetic orders. Species marked with an asterisk are new records for Australia.

Order/Family	Common name	Scientific name	Evans	Tassie
Carcharhiniformes				
 Carcharhinidae	Silvertip whaler shark	*Carcharhinus albimarginatus*	5	5
	Grey reef shark	*Carcharhinus amblyrhynchos*	12	10
	White tip reef shark	*Triaenodon obesus*	13	13
	Slit-eye shark	*Loxodon macrorhinus*	0	1
	Lemon shark	*Negaprion acutidens*	1	0
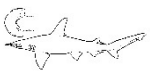 Sphyrnidae	Great Hammerhead	*Sphyrna mokarran*	2	0
Orectolobiformes				
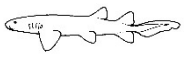 Ginglymostomatidae	Tawny nurse shark	*Nebrius ferrugineus*	8	0
Rajiformes				
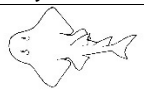 Rhynchobatidae	Shovelnose ray	*Rhynchobatus australiae*	1	0
Myliobatiformes				
 Dasyatidae	Blue-spotted stingray	*Neotrygon kuhlii*	5	4
	Blotched fantail ray	*Taeniurops meyeni*	1	0
Anguilliformes				
 Muraenidae	Grayface moray eel	*Siderea thrysoidea*	2	1
		Echidna nebulosa	1	0
		Gymnothorax javanicus	0	1
		Gymnothorax sp	2	0
		Gymnothorax zonipectis	1	0
Clupeiformes				
 Clupeidae	Blue sprat	*Spratelloides delicatulus*	200	0
Beryciformes				
 Holocentridae	Squirrelfish	*Sargocentron caudimaculatum*	3	0
Gasterosteiformes				
 Fistulariidae	Flutemouth	*Fistularia petimba*	3	0

Order/Family	Common name	Scientific name	Evans	Tassie
Perciformes				
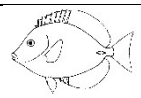 Acanthuridae	Ringtail surgeonfish	*Acanthurus blochii*	9	3
	Eyestripe surgeonfish	*Acanthurus dussumieri*	2	1
	Finelined Surgeonfish	*Acanthurus grammoptilus*	11	7
	Surgeonfish	*Acanthurus leucocheilus*	4	5
	Elongate Surgeonfish	*Acanthurus mata*	142	11
		Acanthurus nigricans	9	0
	Blackstreak Surgeonfish	*Acanthurus nigricauda*	3	3
	Brown Surgeonfish	*Acanthurus nigrofuscus*	3	8
	Bluelined Surgeonfish	*Acanthurus nigros*	8	0
	Orange band Surgeonfish	*Acanthurus olivaceus*	13	11
	Mimic Surgeonfish	*Acanthurus pyroferus*	14	14
		Acanthurus sp	0	1
		Acanthurus thompsoni	26	0
	Yellowfin Surgeonfish	*Acanthurus xanthopterus*	6	0
	Bristletooth Surgeonfish	*Ctenochaetus sp*	1	0
	Bristletooth surgeonfish	*Ctenochaetus striatus*	11	8
	Whitemargin unicornfish	*Naso annulatus*	1	0
	Humpback unicornfish	*Naso brachycentron*	14	1
	Spotted unicornfish	*Naso brevirostris*	10	2
	Thorpe's unicornfish	*Naso caesius*	6	1
	Fagen's unicornfish	*Naso fageni*	16	0
	Sleek unicornfish	*Naso hexacanthus*	130	0
	Orangespine unicornfish	*Naso lituratus*	12	10
		Naso lopezi	7	0
	McDade's unicornfish	*Naso mcdadei*	33	0
	Slender unicornfish	*Naso minor*	3	0
		Naso tonganus	3	0
	Bluespine unicornfish	*Naso unicornis*	4	0
	Vlaming's unicornfish	*Naso vlamingii*	14	3
	Palette surgeonfish	*Paracanthurus hepatus*	5	3
	Brushtail tang	*Zebrasoma scopas*	5	1
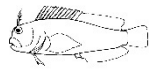 Blenniidae		*Meiacanthus lineatus*	1	1
	Bluestriped fangblenny	*Plagiotremus rhinorhynchos*	3	0
		Plagiotremus tapeinosoma	1	1
 Caesionidae	Blue and gold fusilier	*Caesio teres*	67	21
		Caesio lunaris	4	0
	Black-tipped fusilier	*Pterocaesio marri*	481	680
		Pterocaesio trilineata	80	0
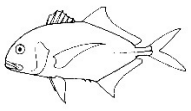		*Atule mate*	12	0

Order/Family	Common name	Scientific name	Evans	Tassie
Carangidae				
	Onion trevally	*Carangoides coeruleopinnatus*	40	18
	Longnose trevally	*Carangoides chrysophrys*	0	31
		Carangoides dinema	0	2
	Blue trevally	*Carangoides ferdau*	8	0
	Goldspot trevally	*Carangoides fulvoguttatus*	2	8
	Bludger trevally	*Carangoides gymnostethus*	55	46
	Coachwhip trevally	*Carangoides orthogrammus*	31	2
	Trevally	*Carangoides plagiotaenia*	5	6
		Carangoides sp	6	0
	Blue-spotted trevally	*Caranx bucculentus*	1	0
	Giant trevally	*Caranx ignobilis*	3	1
	Bluefin trevally	*Caranx melampygus*	25	1
	Scad	*Decapterus sp*	317	0
	Rainbow runner	*Elagatis bipinnulata*	46	0
	Queenfish	*Scomberoides lysan*	0	7
	Queenfish	*Scomberoides tol*	7	0
	Highfin amberjack	*Seriola rivoliana*	0	1
 Chaetodontidae	Butterflyfish	*Chaetodon adiergastos*	5	1
	Threadfin butterflyfish	*Chaetodon auriga*	8	10
	Triangular butterflyfish	*Chaetodon baronessa*	4	1
		Chaetodon ephippium	2	0
	Klein's butterflyfish	*Chaetodon kleinii*	16	9
		Chaetodon leucopleura	3	0
	Lined butterflyfish	*Chaetodon lineolatus*	4	3
	Raccoon butterflyfish	*Chaetodon lunula*	6	3
	Redfin butterflyfish	*Chaetodon lunulatus*	9	6
		Chaetodon meyeri	1	2
	Ornate butterflyfish	*Chaetodon ornatissimus*	4	0
		Chaetodon speculum	1	0
	Chevroned butterflyfish	*Chaetodon trifascialis*	4	4
		Chaetodon trifasciatus	1	0
	Double-saddled butterflyfish	*Chaetodon ulietensis*	0	1
	Teardrop butterflyfish	*Chaetodon unimaculatus*	2	2
		Chaetodon vagabundus	1	0
	Orange-banded coralfish	*Coradion chrysozonus*	5	1
		Forcipiger flavissimus	2	0
	Longnose butterflyfish	*Forcipiger longirostris*	7	2
	Pyramid butterflyfish	*Hemitaurichthys polylepis*	6	2
		Heniochus acuminatus	2	2
	Singular bannerfish	*Heniochus singularius*	4	1
		Heniochus varius	2	0
 Cirrhitidae	Blackside hawkfish	*Paracirrhites forsteri*	2	0

Order/Family	Common name	Scientific name	Evans	Tassie
 Echeneidae	Suckerfish	*Echeneis naucrates*	18	10
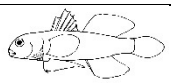 Gobiidae		*Amblygobius phalaena*	2	0
 Ephippidae	Orbicular batfish	*Platax orbicularis*	1	0
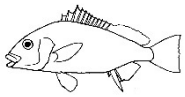 Haemulidae	Painted sweetlips	*Diagramma pictum*	3	0
		Plectorhinchus vittatus	3	1
 Kyphosidae	Topsail drummer	*Kyphosus cinerascens*	1	3
 Labridae		*Anampses meleagrides*	1	0
		Anampses neoguinaicus	1	0
		Anampses twistii	2	0
		Biochoeres biocellatus	2	0
		Bodianus anthioides	0	1
		Bodianus mesothorax	3	0
	Redbreasted maori wrasse	*Cheilinus fasciatus*	1	0
		Choerodon cephalotes	1	0
	Gomon's wrasse	*Choerodon gomoni*	1	0
	Jordan's wrasse	*Choerodon jordani*	12	1
	Zamboanga tuskfish	*Choerodon zamboangae*	3	1
	Blueside wrasse	*Cirrhilabrus cyanopleura*	26	386
	Exquisite wrasse	*Cirrhilabrus exquisitus*	1	11
	Morrison's wrasse	*Cirrhilabrus morrisoni*	60	0
	Dotted wrasse	*Cirrhilabrus punctatus*	54	101
	Wrasse	*Cirrhilabrus sp*	16	0
	Temminck's wrasse	*Cirrhilabrus temminckii*	61	10
	Goldline coris	*Coris aurilineata*	3	0
	Schroeder's coris	*Coris batuensis*	9	8
		Coris dorsomacula	1	0
	Yellowtail coris	*Coris gaimard*	4	8
	Black-striped wrasse	*Coris pictoides*	6	0
		Gomphosus varius	2	0
	Red-lined wrasse	*Halichoeres biocellatus*	1	14
	Golden wrasse	*Halichoeres chrysus*	5	13
		Halichoeres hortulanus	2	0
		Halichoeres margaritaceus	1	0
	Nebulous wrasse	*Halichoeres nebulosus*	1	1
	Twotone wrasse	*Halichoeres prosopeion*	2	0
	Goldstripe wrasse	*Halichoeres zeylonicus*	56	0

Order/Family	Common name	Scientific name	Evans	Tassie
		Hemigymnus fasciatus	2	0
	Ringwrasse	*Hologymnosus annulatus*	2	7
	Pastel ringwrasse	*Hologymnosus doliatus*	4	8
	Bicolour cleaner wrasse	*Labroides bicolor*	4	0
	Cleaner wrasse	*Labroides dimidiatus*	21	14
	Shoulderspot wrasse	*Leptojulis cyanopleura*	10	2
		Labropsis xanthonota	1	0
	Rockmover wrasse	*Novaculichthys taeniourus*	3	2
		Oxycheilinus arenatus	1	0
	Twospot maori wrasse	*Oxycheilinus bimaculatus*	13	0
	Celebes maori wrasse	*Oxycheilinus celebicus*	32	3
	Cheeklined maori wrasse	*Oxycheilinus digrammus*	4	1
		Oxycheilinus orientalis	15	0
	wrasse	*Pseudojuloides severnsi*	5	0
	Gunther's wrasse	*Pseudolabrus guentheri*	2	0
	Bluntheaded wrasse	*Thalassoma amblycephalum*	9	5
	Jansen's wrasse	*Thalassoma jansenii*	4	0
	Moon wrasse	*Thalassoma lunare*	30	29
		Xyrichtys melanopus	6	0
	Pavo razorfish	*Xyrichtys pavo*	2	0
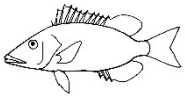 Lethrinidae	Robinson's seabream	*Gymnocranius grandoculis*	75	33
	Ambon emperor	*Lethrinus amboinensis*	27	3
	Yellow-tailed emperor	*Lethrinus atkinsoni*	0	1
	Yellow-spotted emperor	*Lethrinus erythracanthus*	7	6
	Pink-eared emperor	*Lethrinus lentjan*	0	10
	Smalltooth emperor	*Lethrinus microdon*	12	3
	Spangled emperor	*Lethrinus nebulosus*	4	1
	Orange-striped emperor	*Lethrinus obsoletus*	2	0
	Long-nose emperor	*Lethrinus olivaceus*	7	0
	Drab emperor	*Lethrinus ravus*	52	41
	Spotcheek emperor	*Lethrinus rubrioperculatus*	119	3
	Emperor	*Lethrinus semicinctus*	151	49
	Unidentified emperor	*Lethrinus sp*	8	0
*	Undescribed emperor	*Lethrinus undescribed sp1**	10	5
	Bigeye bream	*Monotaxis grandoculis*	11	3
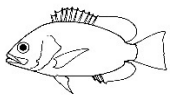 Lutjanidae		*Aphareus furca*	1	0
	Ironjaw jobfish	*Aphareus rutilans*	7	0
	Green jobfish	*Aprion virescens*	31	0
	Red bass	*Lutjanus bohar*	79	8
	Crimson seaperch	*Lutjanus erythropterus*	3	0
	Paddle-tail	*Lutjanus gibbus*	7	0
		Lutjanus kasmira	100	0

Order/Family	Common name	Scientific name	Evans	Tassie
	Dark-tailed seaperch	*Lutjanus lemniscatus*	3	3
	Saddletail seaperch	*Lutjanus malabaricus*	1	0
	Onespot snapper	*Lutjanus monostigma*	0	1
	Maori seaperch	*Lutjanus rivulatus*	3	1
		Lutjanus rufolineatus	1	2
	Red emperor	*Lutjanus sebae*	26	11
	Brown-stripe snapper	*Lutjanus vitta*	0	3
	Midnight seaperch	*Macolor macularis*	0	1
	Midnight seaperch	*Macolor niger*	22	24
		Pinjalo lewisi	0	8
	Rosy jobfish	*Pristipomoides filamentosus*	3	6
	Goldband snapper	*Pristipomoides multidens*	0	3
		Pristipomoides typus	0	10
	Chinaman fish	*Symphorus nematophorus*	41	11
 Malacanthidae	Dusky tilefish	*Hoplolatilus cuniculus*	3	0
	Quakerfish	*Malacanthus brevirostris*	18	0
 Microdesmidae	Flagtail dartfish	*Ptereleotris uroditaenia*	2	0
 Mullidae		*Mulloidichthys flavolineatus*	3	0
	Swarthy-headed goatfish	*Parupeneus barberinoides*	28	1
	Dash-and-dot goatfish	*Parupeneus barberinus*	9	0
	Gold-saddled goatfish	*Parupeneus cyclostomus*	6	0
	Spotted golden goatfish	*Parupeneus heptacanthus*	25	13
	Manybar goatfish	*Parupeneus multifasciatus*	55	30
	Sidespot goatfish	*Parupeneus pleurostigma*	36	7
 Nemipteridae	Purple threadfin bream	*Pentapodus emeryii*	61	22
	Western butterfish	*Pentapodus vitta*	2	0
		Scolopsis affinis	3	0
	Bridled monocle bream	*Scolopsis bilineata*	13	11
		Scolopsis margaritifer	1	0
	Monocle bream	*Scolopsis monogramma*	1	1
	Pearl-streaked monocle bream	*Scolopsis xenochrous*	38	0
 Pinguipedidae	Spothead grubfish	*Parapercis clathrata*	0	3
		Parapercis nebulosa	0	1
		Parapercis sp	2	0
		Parapercis tetracantha	2	0
	Yellowbar sandperch	*Parapercis xanthozona*	7	4
 Pomacanthidae	Three-spot angelfish	*Apolemichthys trimaculatus*	18	11
	Bicolor angelfish	*Centropyge bicolor*	11	6

Order/Family	Common name	Scientific name	Evans	Tassie
	Keyhole angelfish	*Centropyge tibicen*	3	9
	Pearlscale angelfish	*Centropyge vroliki*	0	2
	Lamarck's angelfish	*Genicanthus lamarck*	6	14
		Genicanthus melanospilos	2	0
	Emperor angelfish	*Pomacanthus imperator*	21	6
	Regal angelfish	*Pygoplites diacanthus*	8	4
 Pomacentridae	Spiny chromis	*Acanthochromis polyacanthus*	1	0
	Golden damselfish	*Amblyglyphidodon aureus*	5	0
	Staghorn damselfish	*Amblyglyphidodon curacao*	3	1
	Yellowbelly damselfish	*Amblyglyphidodon leucogaster*	15	3
	Black-banded demoiselle	*Amblypomacentrus breviceps*	2	0
	Anemone fish	*Amphiprion clarkii*	2	0
	Bicolor chromis	*Chromis margaritifer*	6	0
	Ternate chromis	*Chromis ternatensis*	6	5
	Weber's chromis	*Chromis weberi*	47	102
	Paletail chromis	*Chromis xanthura*	6	2
		Chrysiptera caeruleolineata	5	0
	Reticulate dascyllus	*Dascyllus reticulatus*	54	109
	Threespot dascyllus	*Dascyllus trimaculatus*	17	0
	Black damselfish	*Neoglyphidodon melas*	5	7
	Barhead damsel	*Neoglyphidodon thoracotaeniatus*	6	0
	Johnston Island damsel	*Plectroglyphidodon johnstonianus*	3	4
		Plectroglyphidodon lacrymatus	2	0
		Pomacentrus adelus	8	0
	Ambon damsel	*Pomacentrus amboinensis*	23	27
	Goldbelly damsel	*Pomacentrus auriventris*	3	0
	Charcoal damsel	*Pomacentrus brachialis*	3	0
	Neon damsel	*Pomacentrus coelestis*	4	25
		Pomacentrus lepidogenys	6	0
	Miller's damselfish	*Pomacentrus milleri*	1	0
		Pomacentrus nagasakiensis	1	1
		Pomacentrus nigromanus	0	3
	Philippine damsel	*Pomacentrus philippinus*	7	6
	Ocellate damselfish	*Pomacentrus vaiuli*	0	1
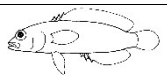 Pseudochromidae	Firetail Dottyback	*Labracinus cyclophthalmus*	1	0
		Labracinus japonicus	2	0
		Pseudochromis fuscus	2	0
		Pseudochromis perspicillatus	1	0
 Rachycentridae	Cobia	*Rachycentron canadum*	2	2

Order/Family	Common name	Scientific name	Evans	Tassie
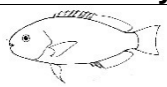 Scaridae	Red-speckled parrotfish	*Cetoscarus ocellatus*	5	0
	Bleeker's parrotfish	*Chlorurus bleekeri*	6	5
		Chlorurus capistratoides	3	0
	Blunt-head parrotfish	*Chlorurus microrhinos*	0	1
	Bullethead parrotfish	*Chlorurus sordidus*	1	1
	Yellowfin parrotfish	*Scarus flavipectoralis*	1	5
	Forsten's parrotfish	*Scarus forsteni*	2	3
		Scarus frenatus	2	0
*	Darktail parrotfish	*Scarus fuscocaudalis**	6	0
		Scarus ghobban	3	4
		Scarus globiceps	1	1
*	Yellowtail parrotfish	*Scarus hypselopterus**	0	1
	Dark-capped parrotfish	*Scarus oviceps*	0	2
		Scarus psittacus	1	0
	Schlegel's parrotfish	*Scarus schlegeli*	50	20
	Unidentified parrotfish	*Scarus sp*	0	2
		Scarus xanthopleura	0	1
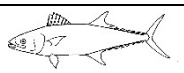 Scombridae	Shark mackerel	*Grammatorcynus bilineatus*	9	0
	Dogtooth tuna	*Gymnosarda unicolor*	1	0
	Spanish mackerel	*Scomberomorus commerson*	2	0
	School mackerel	*Scomberomorus queenslandicus*	1	0
	Unidentified mackerel	*Scomberomorus sp*	2	0
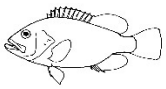 Serranidae	Redflushed rockcod	*Aethaloperca rogaa*	13	7
		Anyperodon leucogrammicus	2	0
	Bluelined rockcod	*Cephalopholis formosa*	0	1
		Cephalopholis leopardus	2	0
	Freckled rockcod	*Cephalopholis microprion*	4	1
	Coral cod	*Cephalopholis miniata*	11	7
	Tomato cod	*Cephalopholis sonnerati*	4	0
	Strawberry grouper	*Cephalopholis spiloparaea*	3	0
	Flagtailed rockcod	*Cephalopholis urodeta*	4	4
	Yellow-spotted rockcod	*Epinephelus areolatus*	2	9
		Epinephelus bleekeri	1	0
	Goldspot cod	*Epinephelus coioides*	6	0
	Flowery cod	*Epinephelus fuscoguttatus*	1	0
	Trout cod	*Epinephelus maculatus*	4	7
	Blackspot cod	*Epinephelus malabaricus*	2	3
	Rankin cod	*Epinephelus multinotatus*	17	4
	Maori cod	*Epinephelus undulatostriatus*	0	3
	Bluespot coral trout	*Plectropomus laevis*	6	1
	Common coral trout	*Plectropomus leopardus*	35	19
	Undientified fairy basslet	*Pseudanthias sp*	4	0

Order/Family	Common name	Scientific name	Evans	Tassie
	Lyretail trout	*Variola albimarginata*	4	0
	Coronation trout	*Variola louti*	26	14
	Unidentified coronation trout	*Variola sp*	1	0
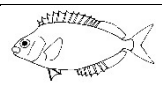 Siganidae	Spinefoot	*Siganus argenteus*	19	2
	Masked spinefoot	*Siganus puellus*	0	2
	Goldspotted spinefoot	*Siganus punctatus*	5	2
		Siganus vulpinus	2	0
 Sparidae	Frying-pan snapper	*Argyrops spinifer*	0	5
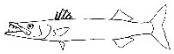 Sphyraenidae	Great barracuda	*Sphyraena barracuda*	1	1
 Zanclidae	Moorish idol	*Zanclus cornutus*	31	13
Tetraodontiformes				
 Balistidae	Starry triggerfish	*Abalistes stellatus*	20	39
	Red-lined triggerfish	*Balistapus undulatus*	20	16
	Clown triggerfish	*Balistoides conspicillum*	2	2
	Titan triggerfish	*Balistoides viridescens*	1	4
	Spotted oceanic triggerfish	*Canthidermis maculatus*	1	0
		Melichthys niger	7	1
	Pinktail triggerfish	*Melichthys vidua*	16	0
	Redtooth triggerfish	*Odonus niger*	155	6
		Pseudobalistes flavimarginatus	1	0
	Dusky triggerfish	*Pseudobalistes fuscus*	4	0
	Pallid triggerfish	*Sufflamen bursa*	1	2
	Black triggerfish	*Sufflamen chrysopterum*	10	4
	Brown triggerfish	*Sufflamen fraenatum*	21	9
		Sufflamen sp	1	0
		Xanthichthys auromarginatus	1	0
 Monacanthidae		*Aluterus monoceros*	17	1
	Scribbled leatherjacket	*Aluterus scriptus*	7	2
	Yelloweye leatherjacket	*Cantherhines dumerilii*	2	3
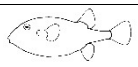 Tetraodontidae		*Arothron firmamentum*	1	0
	Stars and stripes puffer	*Arothron hispidus*	0	1
		Arothron nigropunctatus	2	0
	Starry pufferfish	*Arothron stellatus*	1	2

Order/Family	Common name	Scientific name	Evans	Tassie
	Silver toadfish	*Lagocephalus sceleratus*	7	6
Squamata				
 Hydrophiidae	Olive sea snake	*Aipysurus laevis*	0	9
	Turtle-headed sea snake	*Emydocephalus annulatus*	2	0
	Unidentified sea snake	*Hydrophis sp*	7	5
	Unidentified sea snake	*Seasnake sp*	0	1
	Unidentified sea snake	*seasnake sp_banded*	0	2

Appendix 3

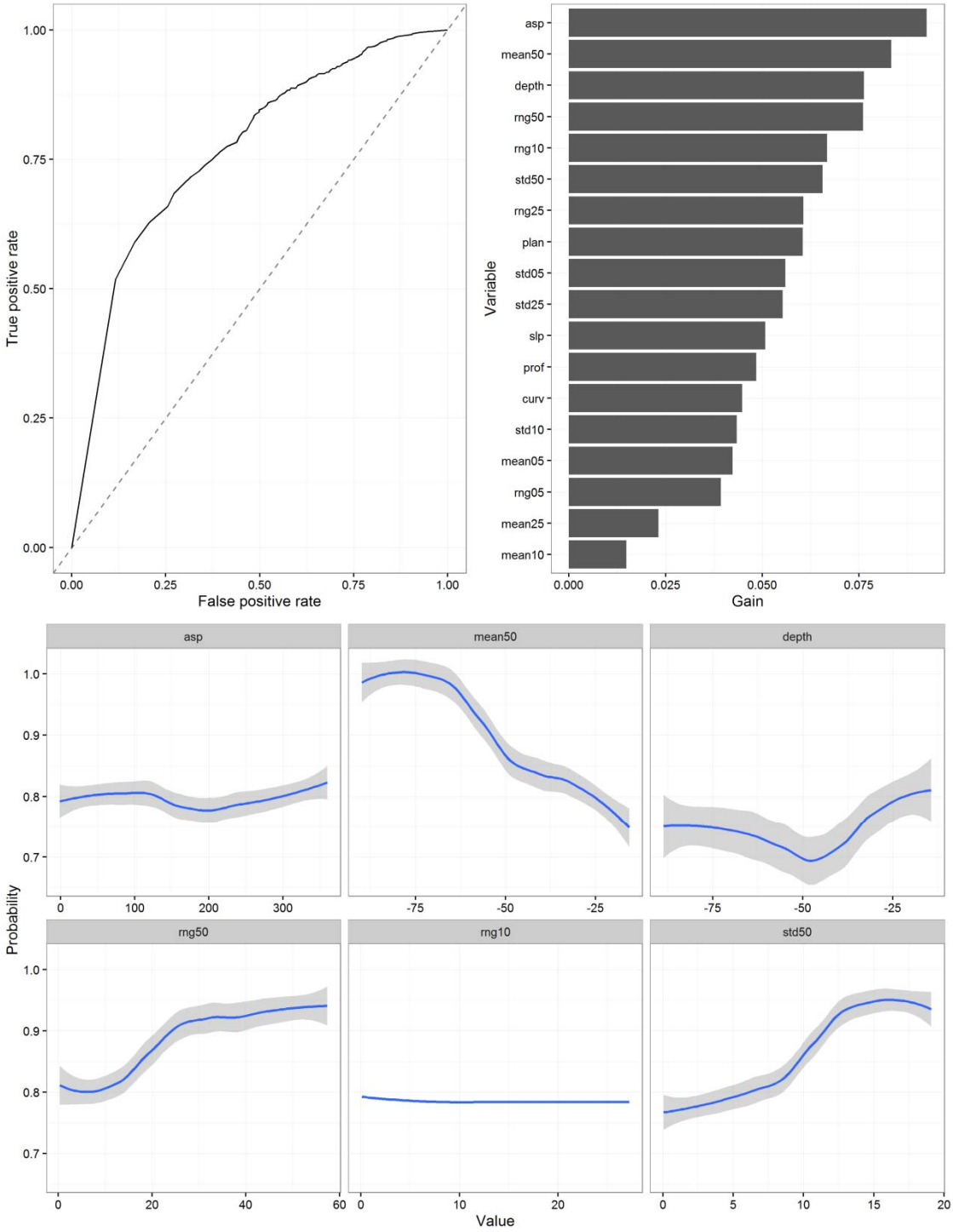

Figure A3.1: All hard coral - Towed digital still image model AUC performance plot (top left), relative measure of variable influence ("Gain") for improvement on model performance (top right) and partial response plots for the top 6 most influential model variables (bottom panel). For variable descriptions see Table 3 in the main report).

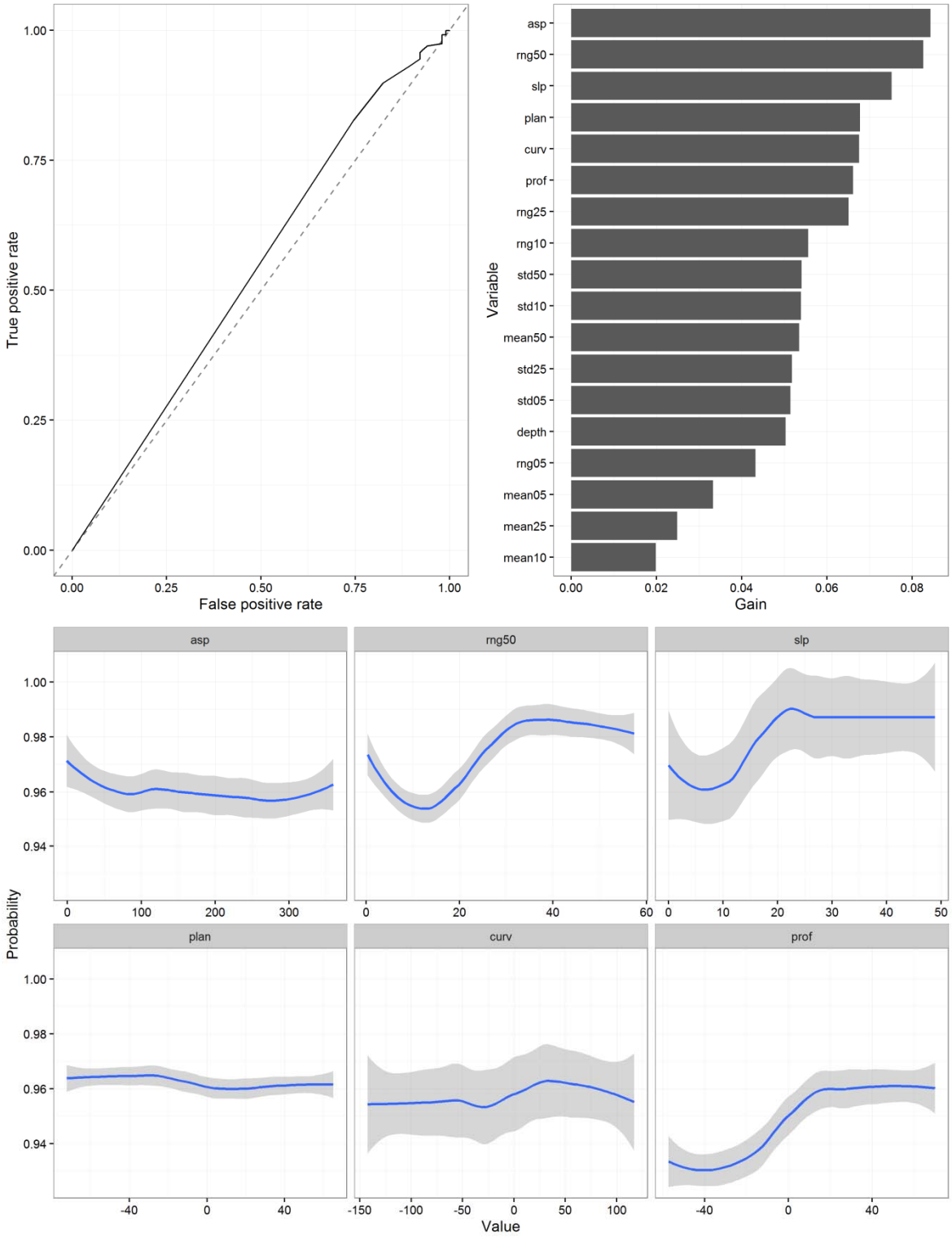

Figure A3.2: Soft corals - Towed digital still image model AUC performance plot (top left), relative measure of variable influence ("Gain") for improvement on model performance (top right) and partial response plots for the top 6 most influential model variables (bottom panel). For variable descriptions see Table 3 in the main report).

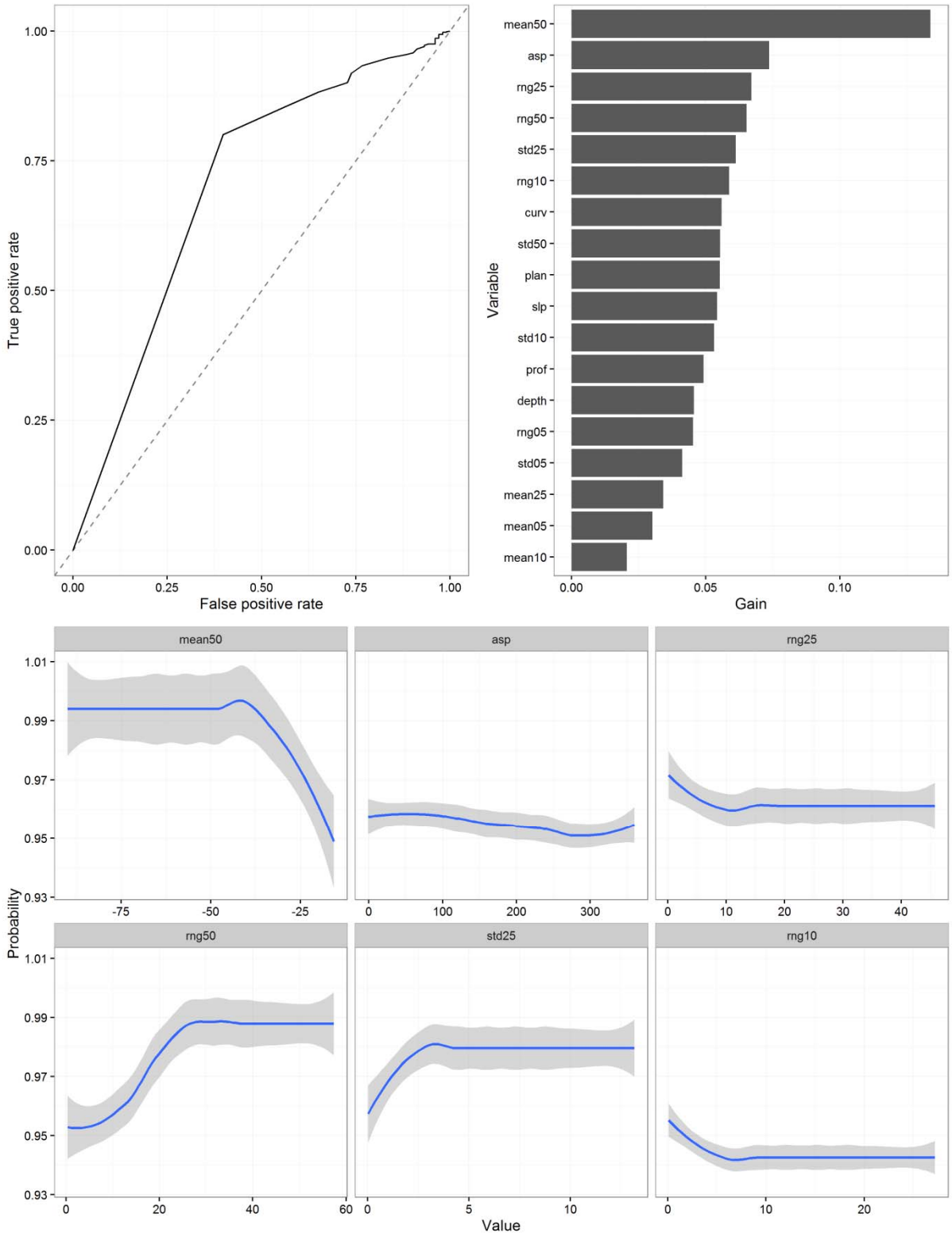

Figure A3.3 Tabulate Acropora - Towed digital still image model AUC performance plot (top left), relative measure of variable influence ("Gain") for improvement on model performance (top right) and partial response plots for the top 6 most influential model variables (bottom panel). For variable descriptions see Table 3 in the main report).

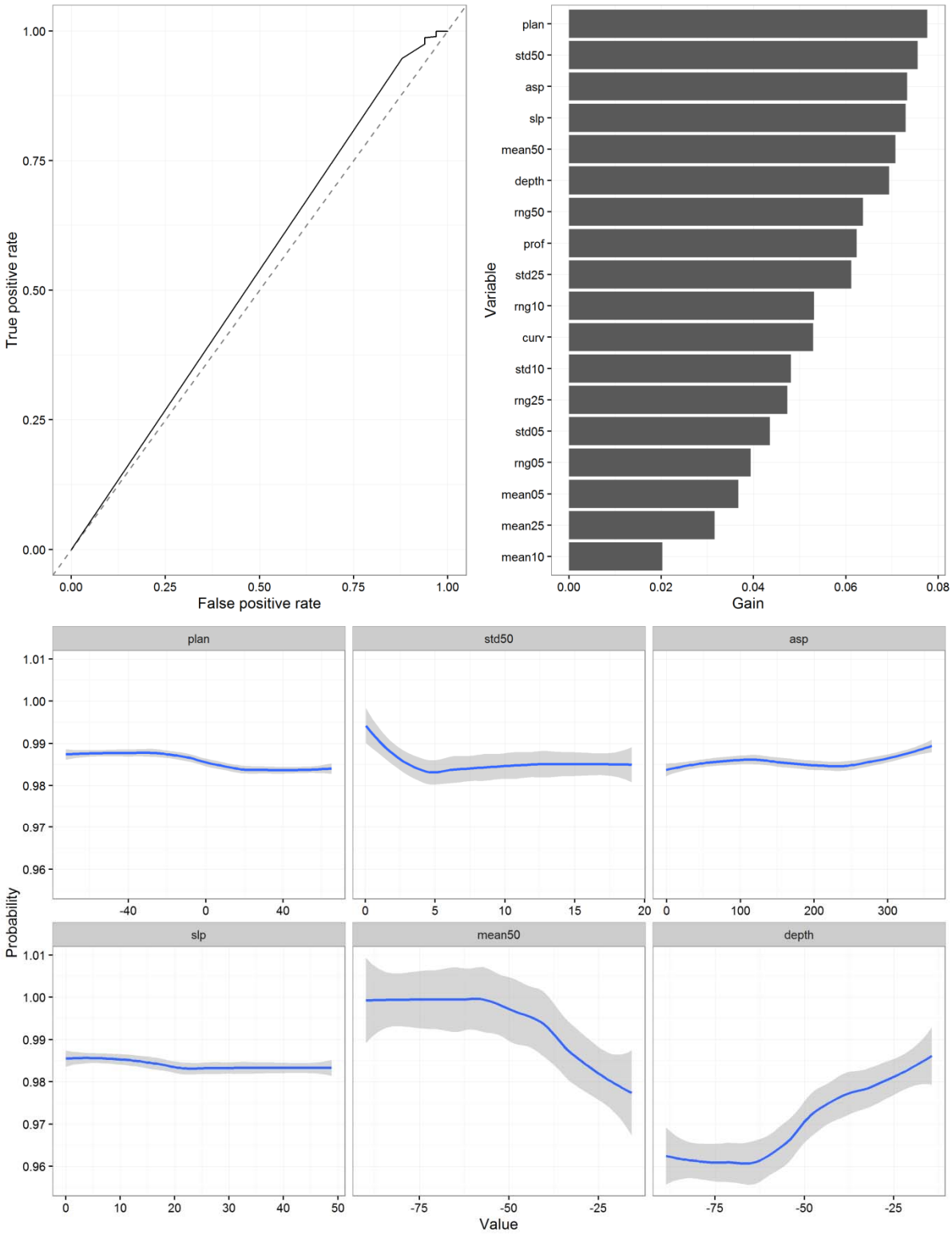

Figure A3.4: Branching Acropora - Towed digital still image model AUC performance plot (top left), relative measure of variable influence ("Gain") for improvement on model performance (top right) and partial response plots for the top 6 most influential model variables (bottom panel). For variable descriptions see Table 3 in the main report).

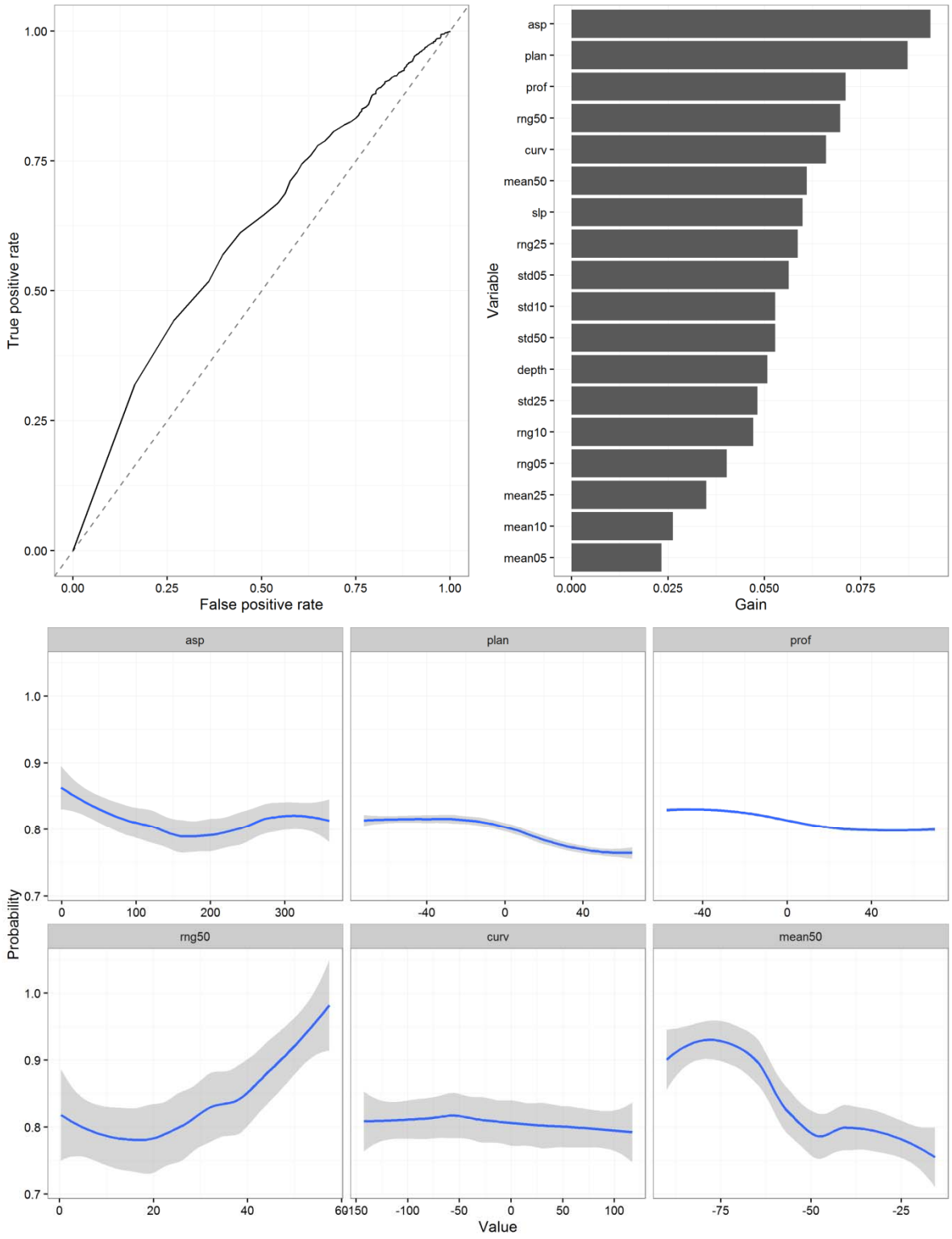

Figure A3.5: Macroalgae and sponge - Towed digital still image model AUC performance plot (top left), relative measure of variable influence ("Gain") for improvement on model performance (top right) and partial response plots for the top 6 most influential model variables (bottom panel). For variable descriptions see Table 3 in the main report).

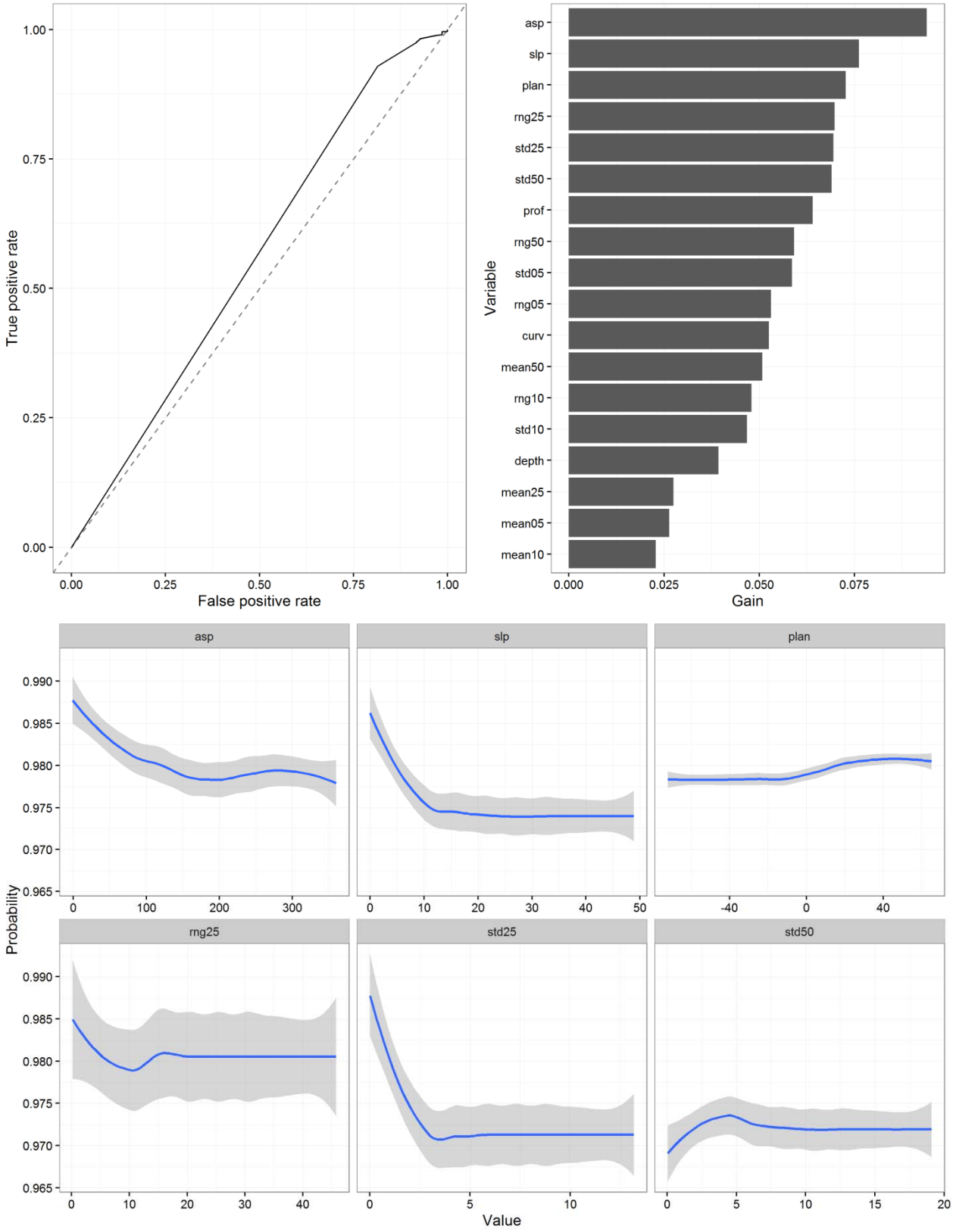

Figure A3.6: Other corals - Towed digital still image model AUC performance plot (top left), relative measure of variable influence ("Gain") for improvement on model performance (top right) and partial response plots for the top 6 most influential model variables (bottom panel). For variable descriptions see Table 3 in the main report).

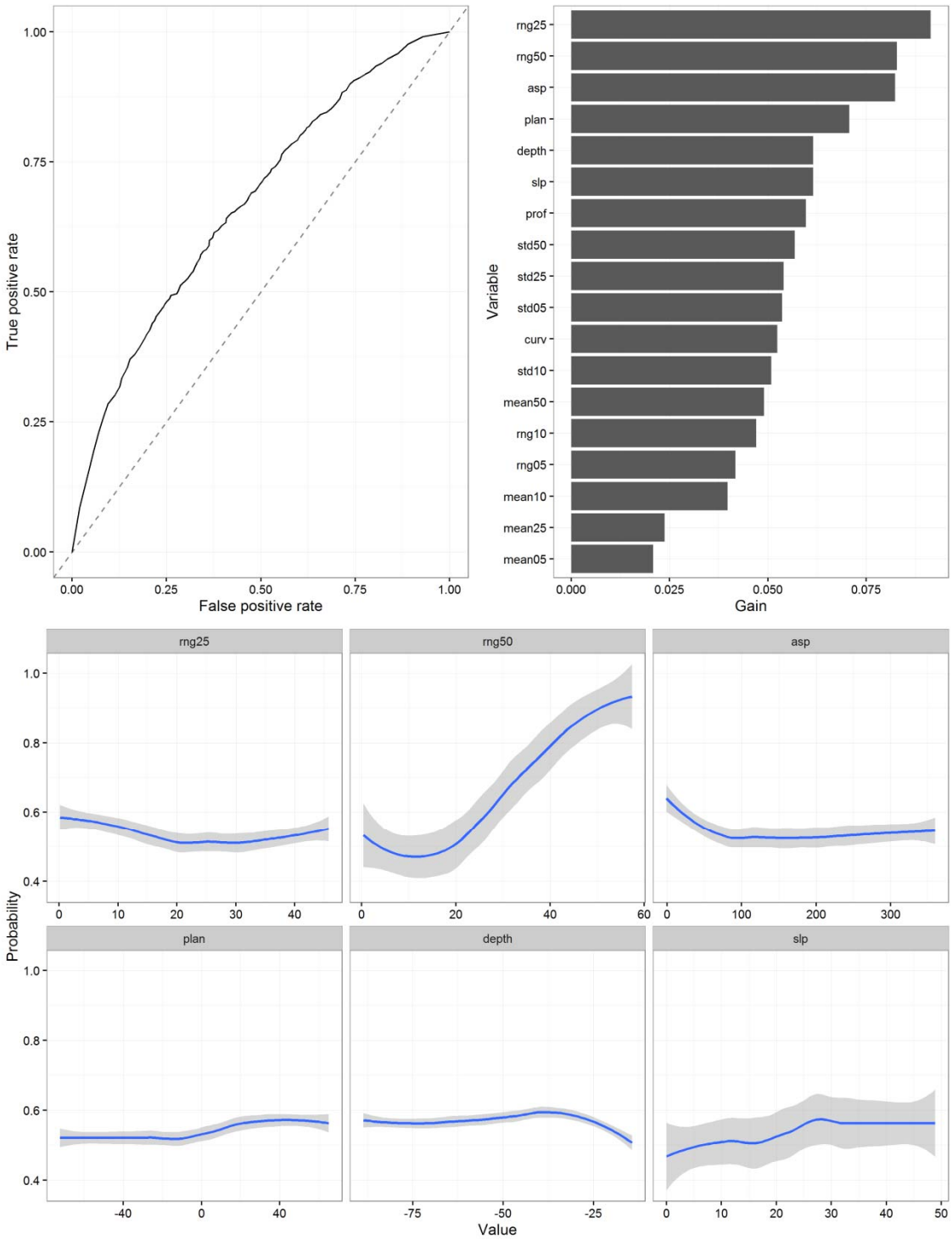

Figure A3.7: Turf and coralline algae - Towed digital still image model AUC performance plot (top left), relative measure of variable influence ("Gain") for improvement on model performance (top right) and partial response plots for the top 6 most influential model variables (bottom panel). For variable descriptions see Table 3 in the main report).

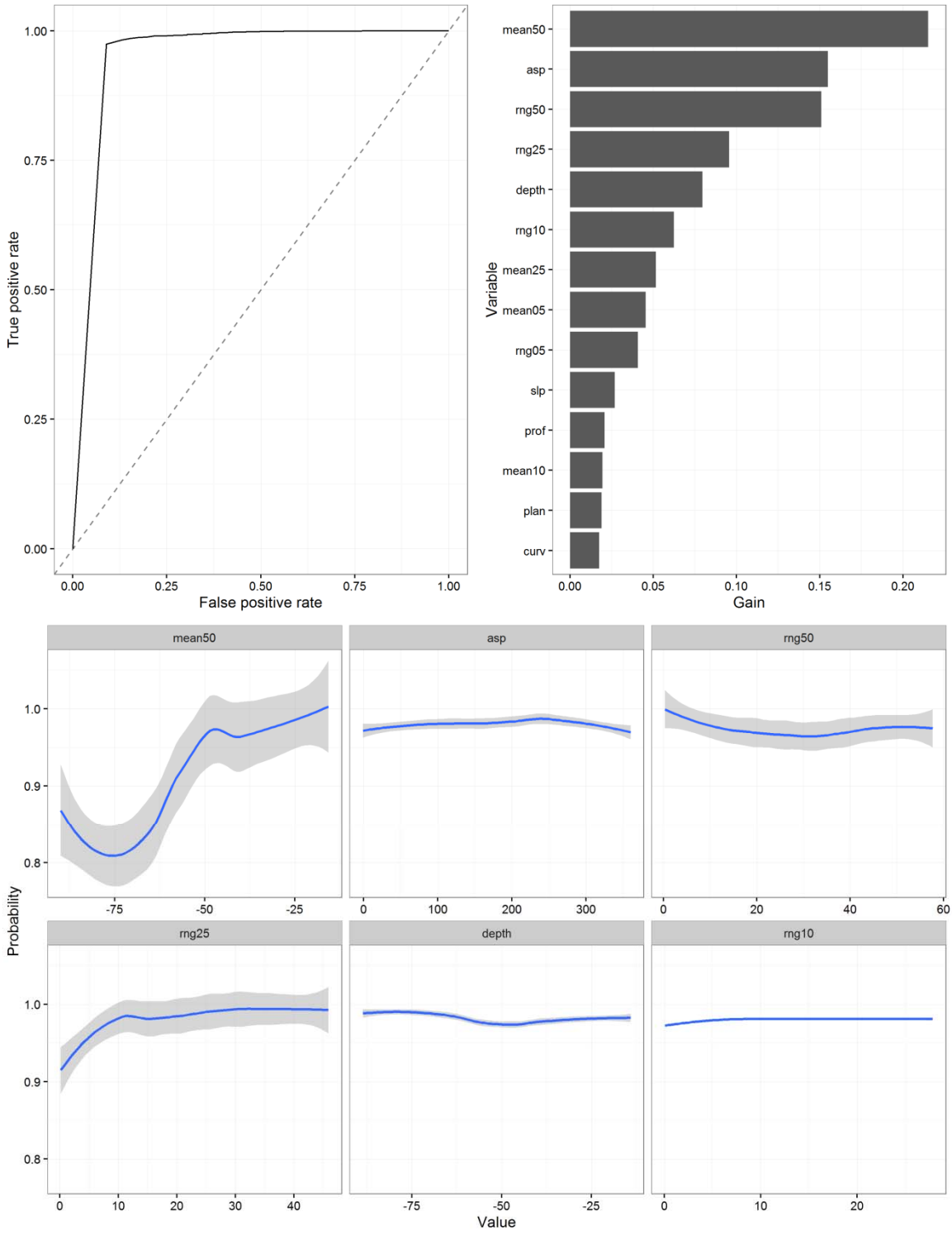

Figure A3.8 Medium filter feeders - Towed real-time video model (with 2m binned multibeam and covariates) AUC performance plot (top left), relative measure of variable influence ("Gain") for improvement on model performance (top right) and partial response plots for the top 6 most influential model variables (bottom panel). For variable descriptions see Table 3 in the main report).

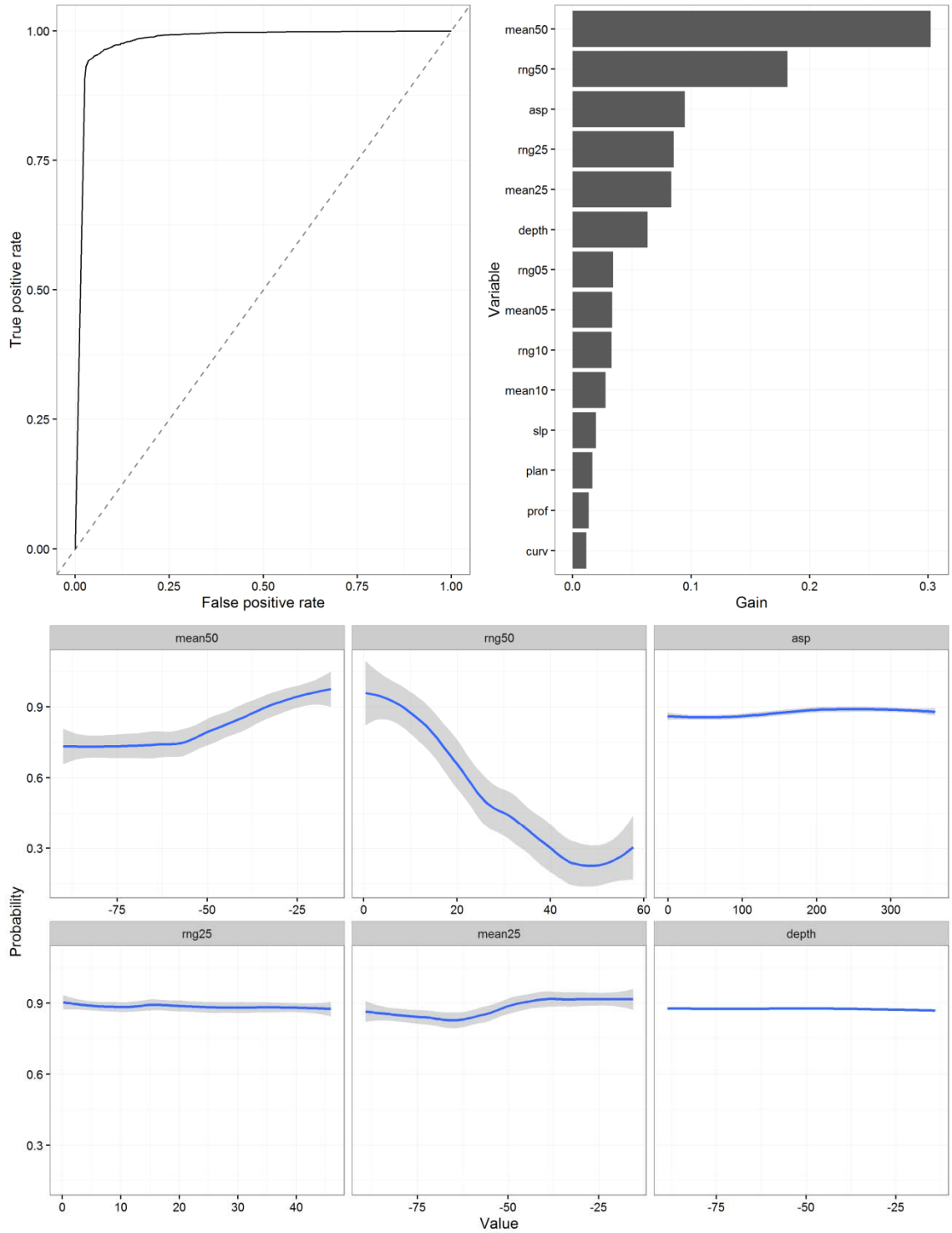

Figure A3.9: Sparse filter feeders - Towed real-time video model (with 2m binned multibeam and covariates) AUC performance plot (top left), relative measure of variable influence ("Gain") for improvement on model performance (top right) and partial response plots for the top 6 most influential model variables (bottom panel). For variable descriptions see Table 3 in the main report).

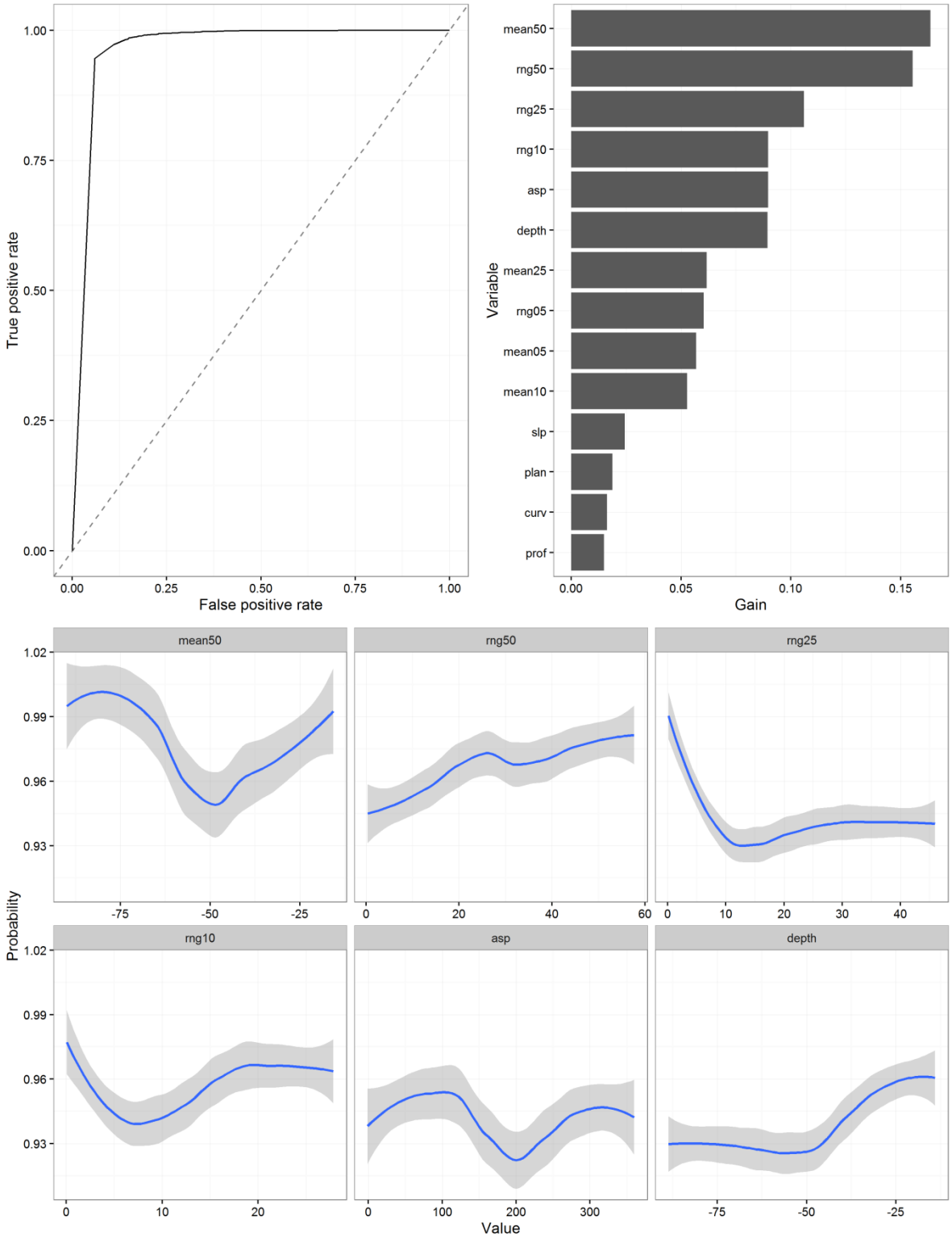

Figure A3.10: Dense hard coral - Towed real-time video model for shoals (with 2m binned multibeam and covariates) AUC performance plot (top left), relative measure of variable influence ("Gain") for improvement on model performance (top right) and partial response plots for the top 6

most influential model variables (bottom panel). For variable descriptions see Table 3 in the main report).

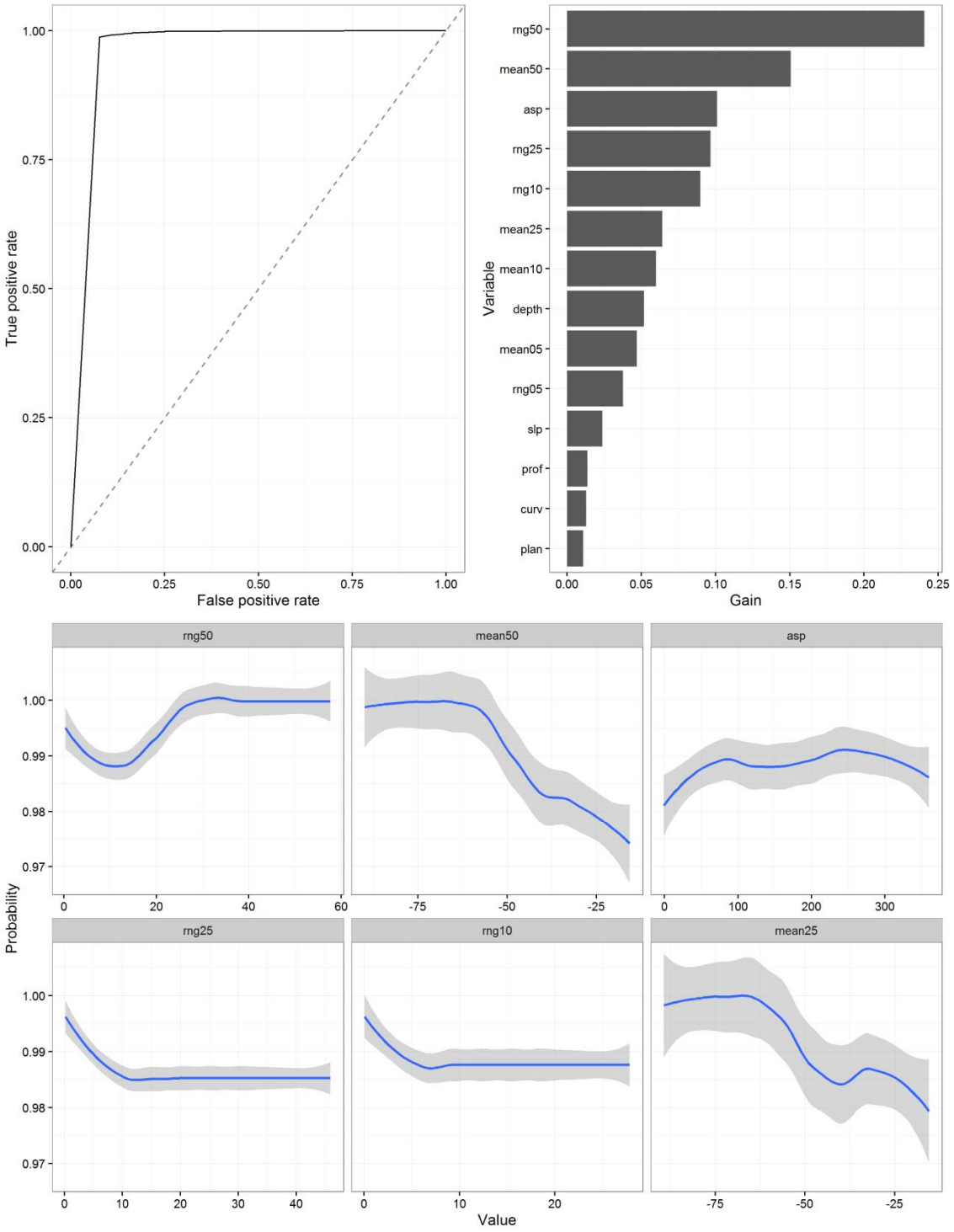

Figure A3.11 Medium hard coral and Halimeda - Towed real-time video model for shoals (with 2m binned multibeam and covariates) AUC performance plot (top left), relative measure of variable influence ("Gain") for improvement on model performance (top right) and partial response plots for the top 6 most influential model variables (bottom panel). For variable descriptions see Table 3 in the main report).

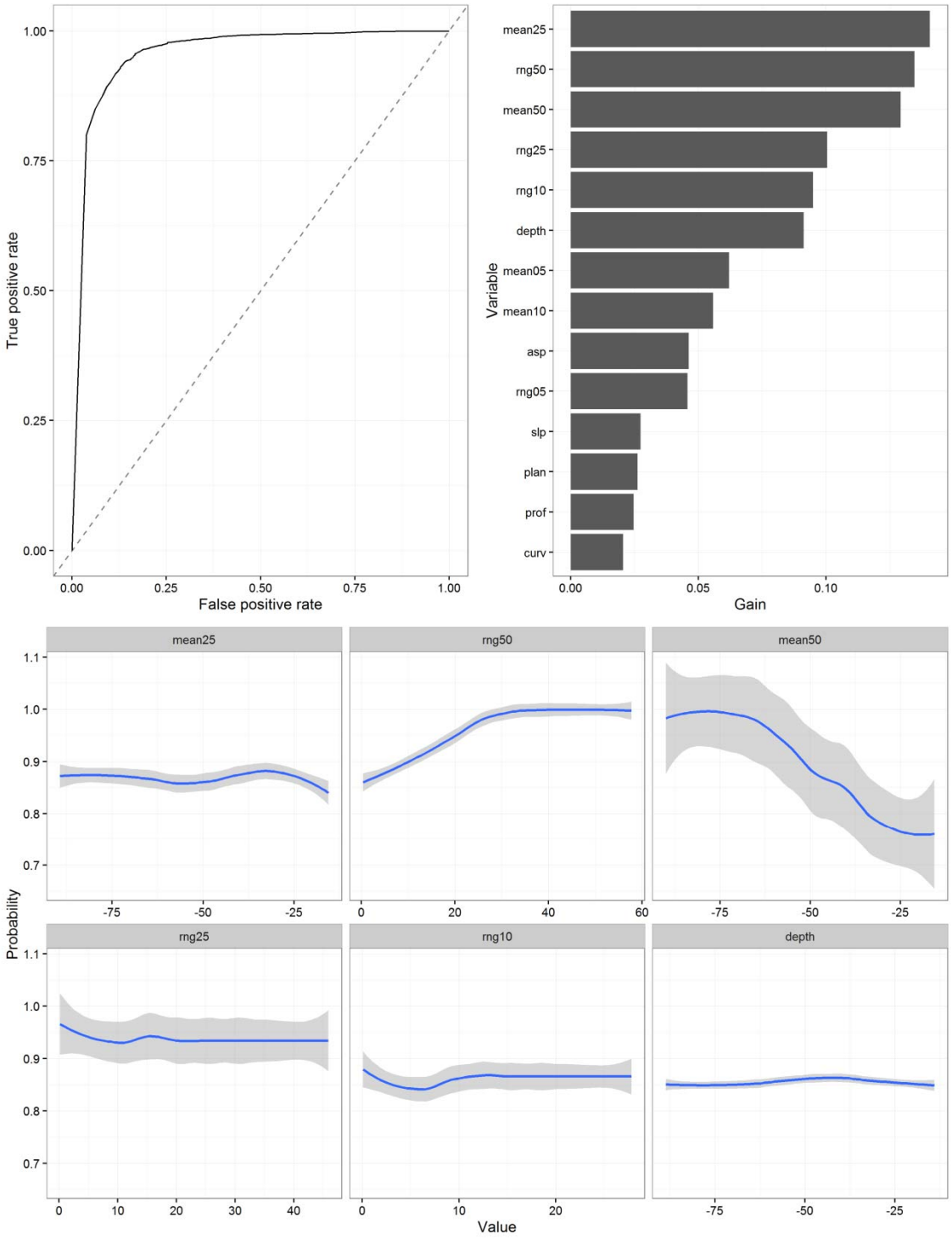

Figure A3.12: Medium hard coral - Towed real-time video model for shoals (with 2m binned multibeam and covariates) AUC performance plot (top left), relative measure of variable influence ("Gain") for improvement on model performance (top right) and partial response plots for the top 6 most influential model variables (bottom panel). For variable descriptions see Table 3 in the main report).

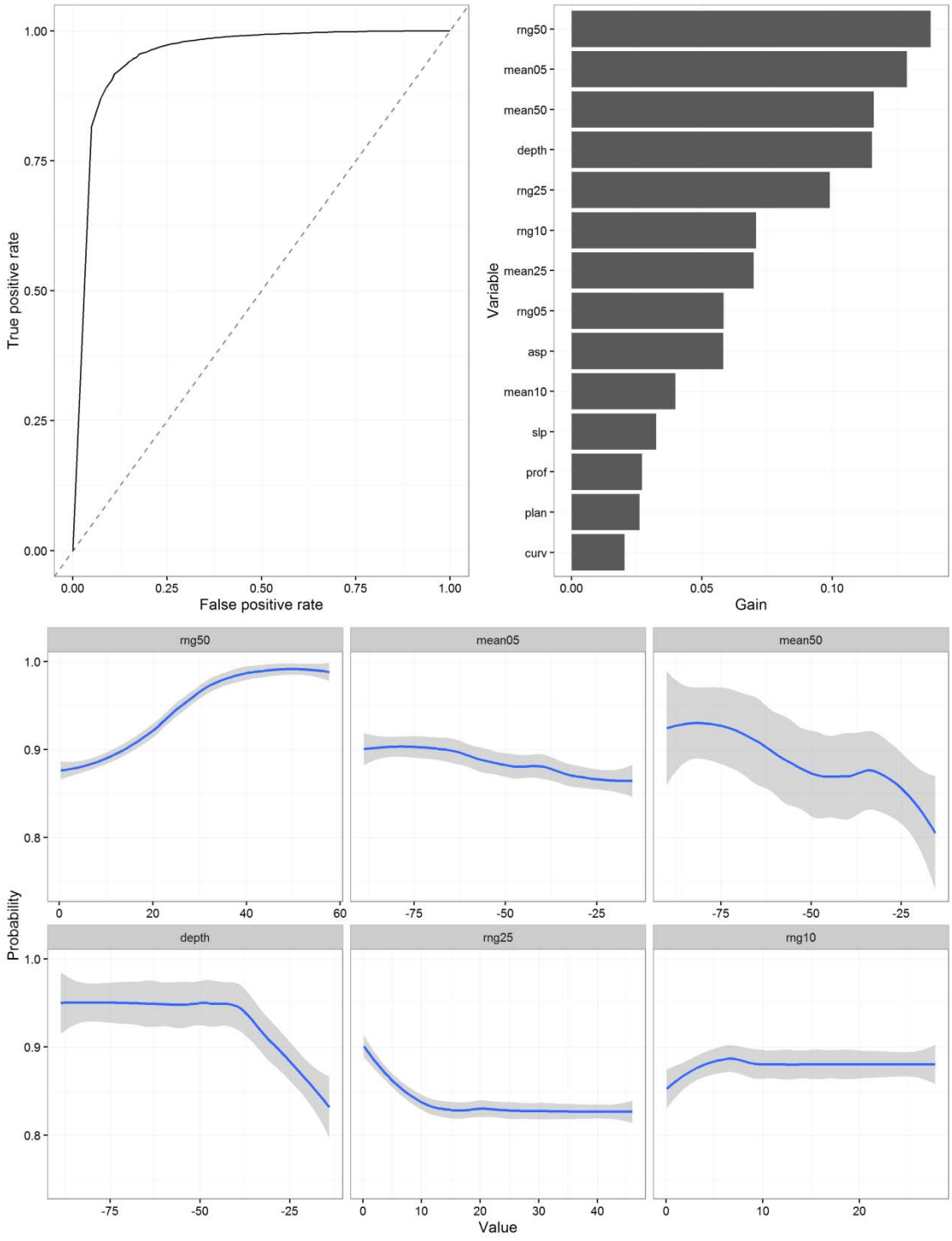

Figure A3.13: Sparse hard coral - Towed real-time video model for shoals (with 2m binned multibeam and covariates) AUC performance plot (top left), relative measure of variable influence ("Gain") for improvement on model performance (top right) and partial response plots for the top 6 most influential model variables (bottom panel). For variable descriptions see Table 3 in the main report).

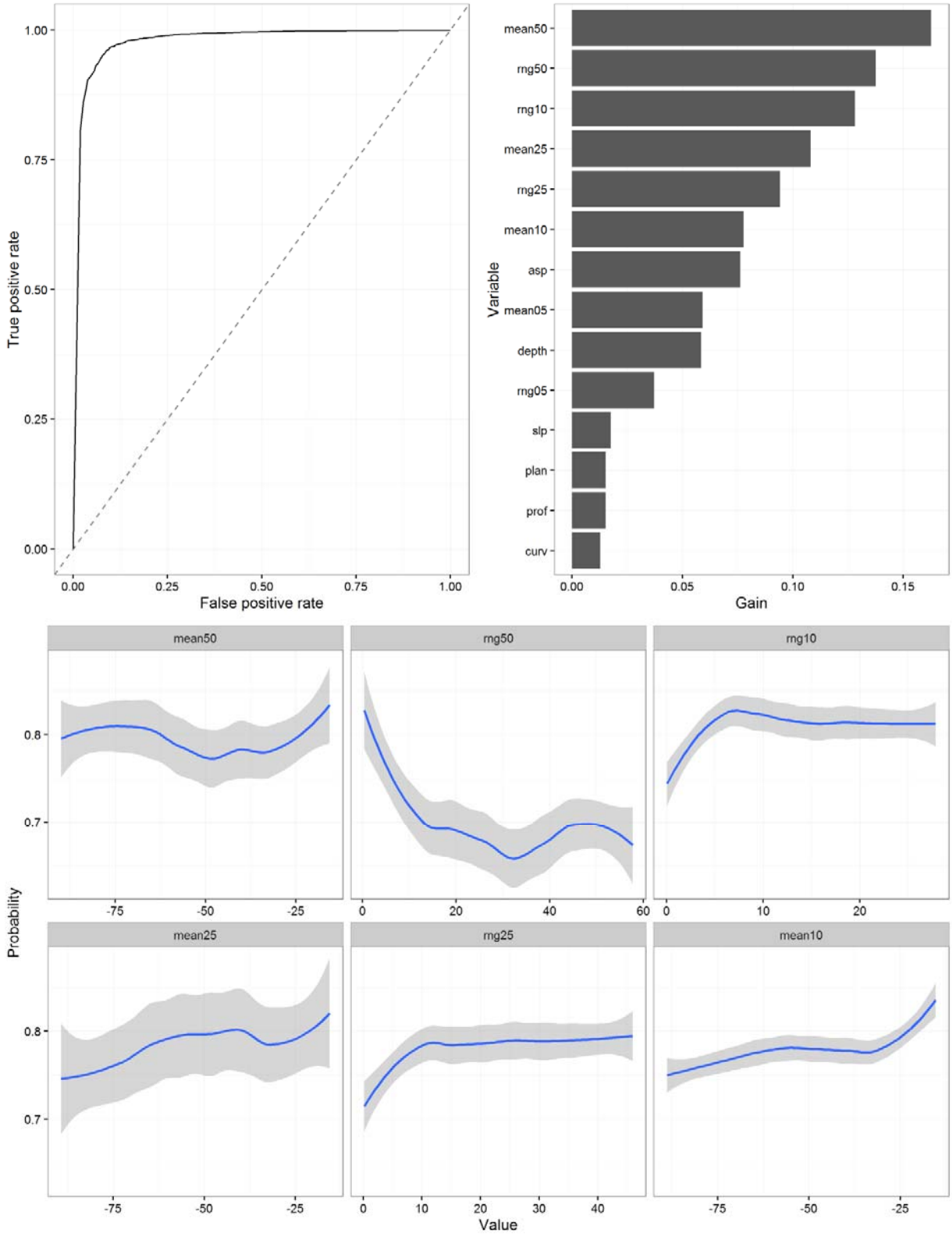

Figure A3.14: None (no modelled benthos) - Towed real-time video model for shoals (with 2m binned multibeam and covariates) AUC performance plot (top left), relative measure of variable influence ("Gain") for improvement on model performance (top right) and partial response plots for the top 6 most influential model variables (bottom panel). For variable descriptions see Table 3 in the main report).

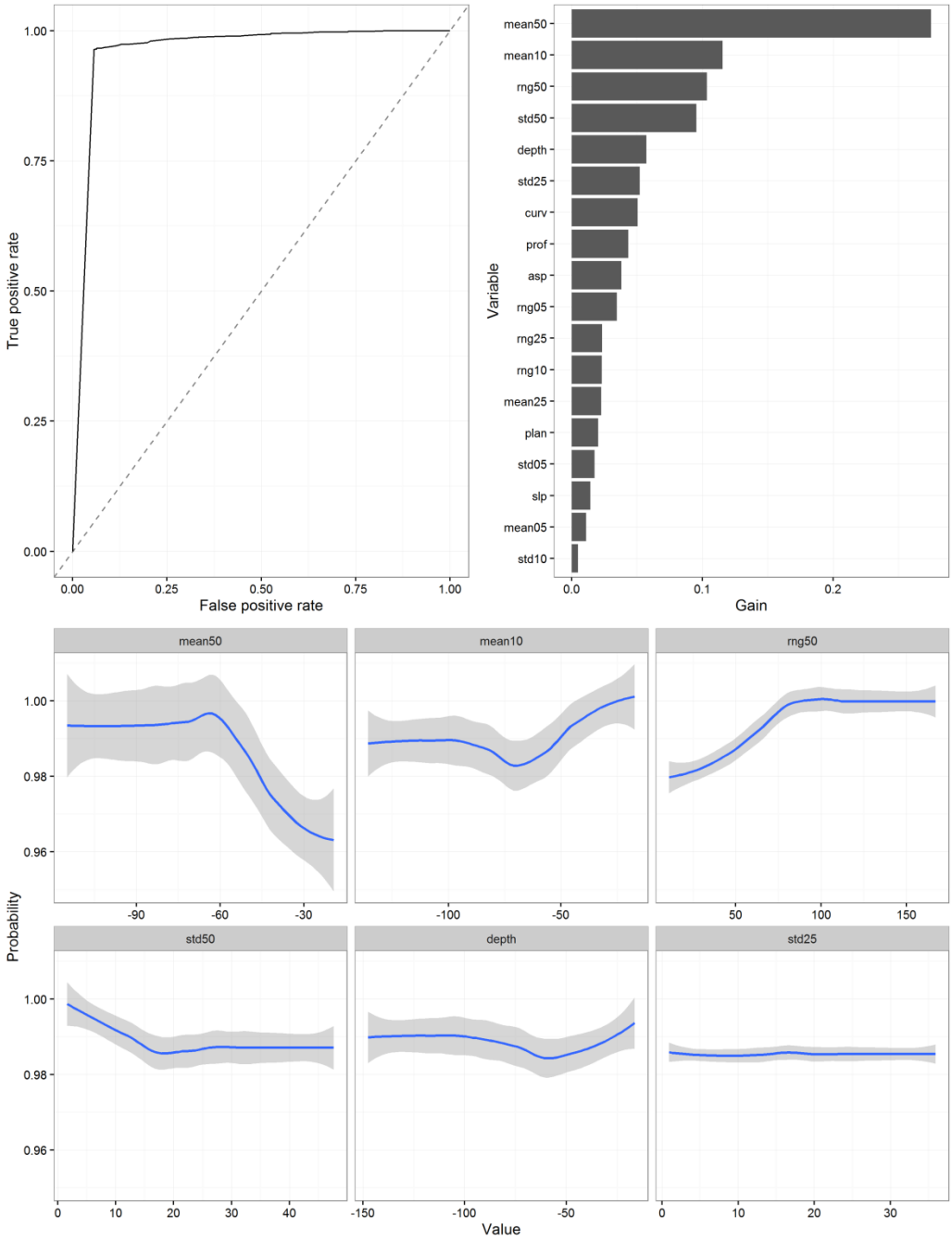

Figure A3.15: Burrows - Towed real-time video model for shelf regions (with 50 m binned multibeam and covariates) AUC performance plot (top left), relative measure of variable influence ("Gain") for improvement on model performance (top right) and partial response plots for the top 6 most influential model variables (bottom panel). For variable descriptions see Table 3 in the main report).

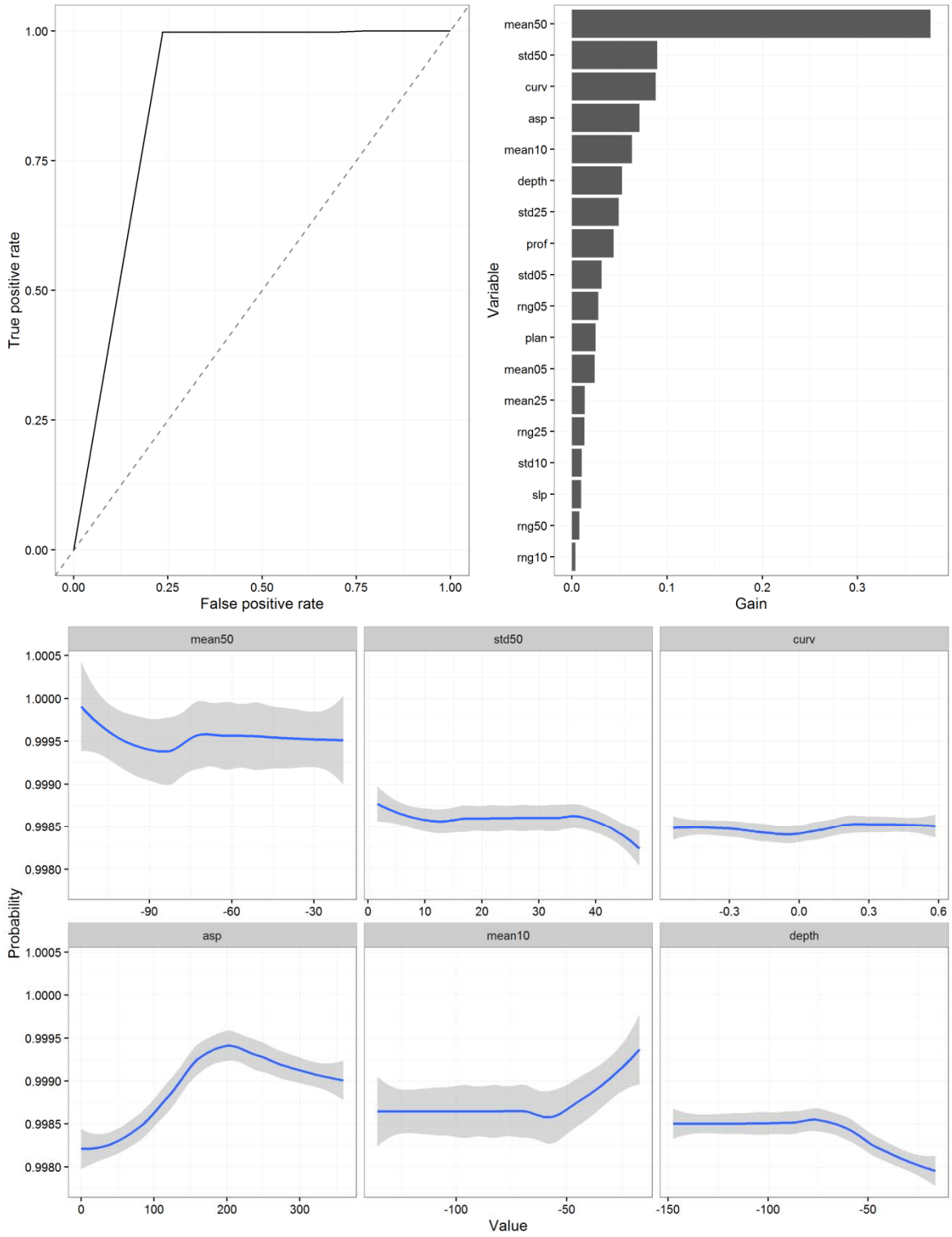

Figure A3.16: Dense filter feeders - Towed real-time video model for shelf regions (with 50m binned multibeam and covariates) AUC performance plot (top left), relative measure of variable influence ("Gain") for improvement on model performance (top right) and partial response plots for the top 6 most influential model variables (bottom panel). For variable descriptions see Table 3 in the main report).

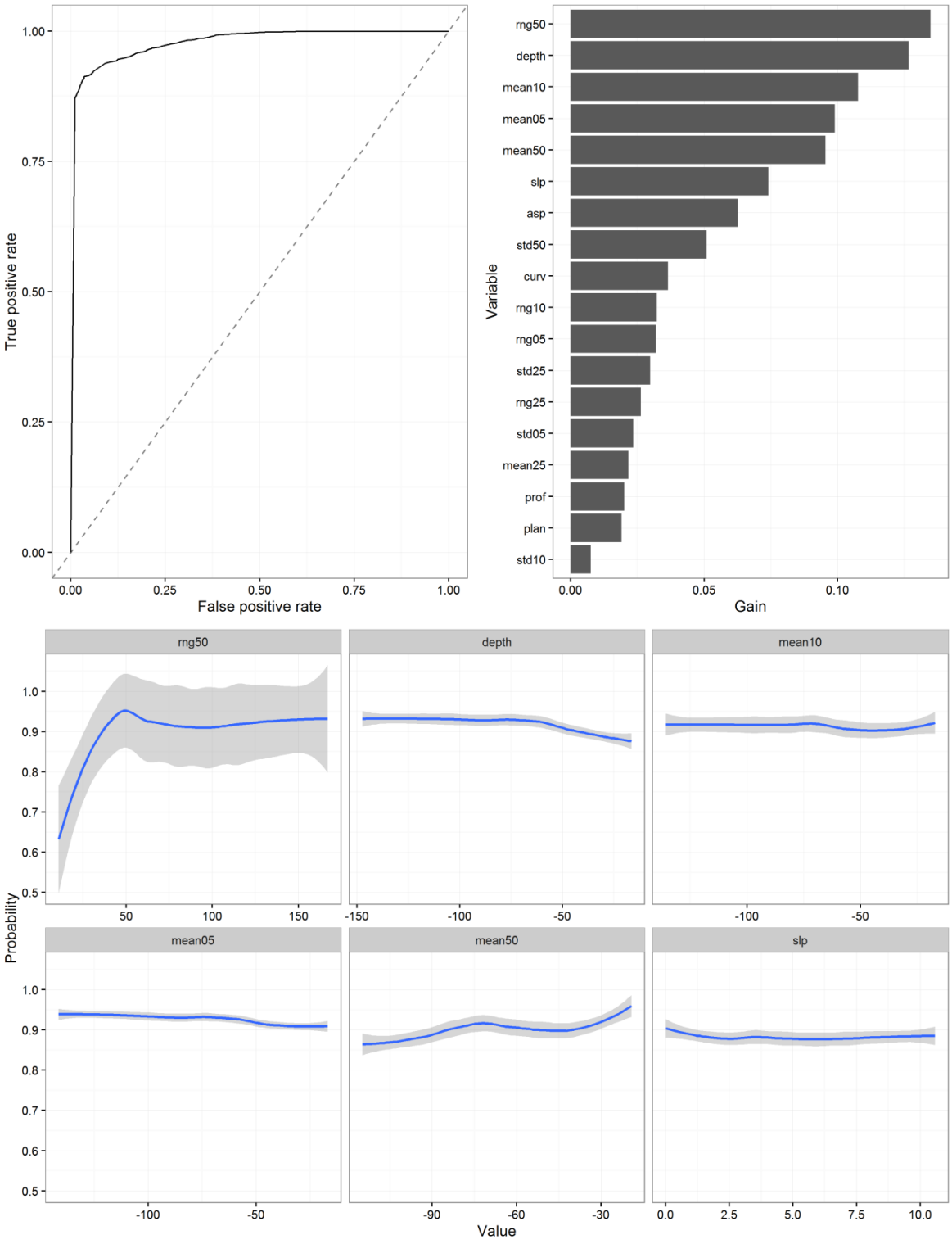

Figure A3.17: Medium filter feeders - Towed real-time video model for shelf regions (with 50m binned multibeam and covariates) AUC performance plot (top left), relative measure of variable influence ("Gain") for improvement on model performance (top right) and partial response plots for the top 6 most influential model variables (bottom panel). For variable descriptions see Table 3 in the main report).

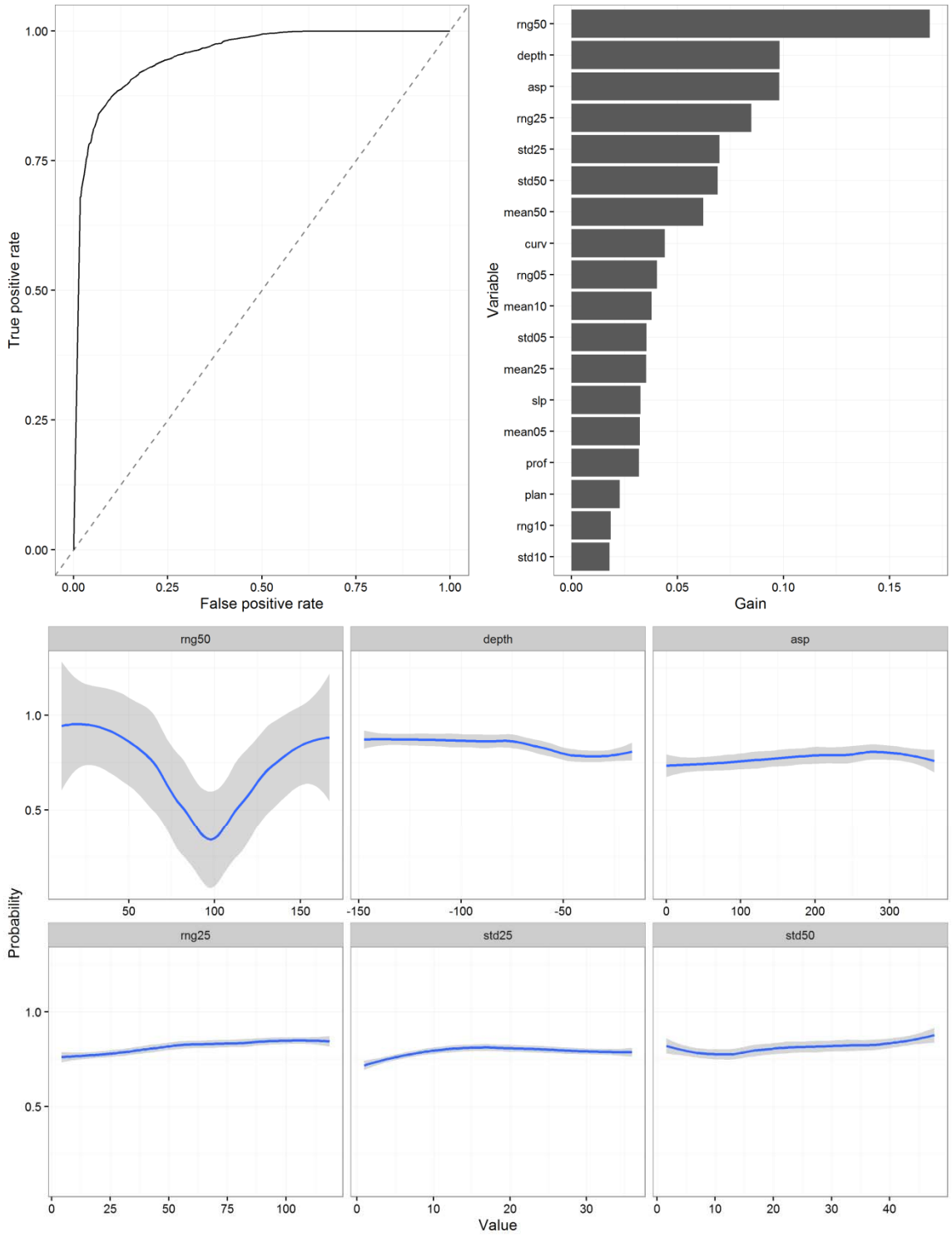

Figure A3.18: Sparse filter feeders - Towed real-time video model for shelf regions (with 50m binned multibeam and covariates) AUC performance plot (top left), relative measure of variable influence ("Gain") for improvement on model performance (top right) and partial response plots for the top 6 most influential model variables (bottom panel). For variable descriptions see Table 3 in the main report).

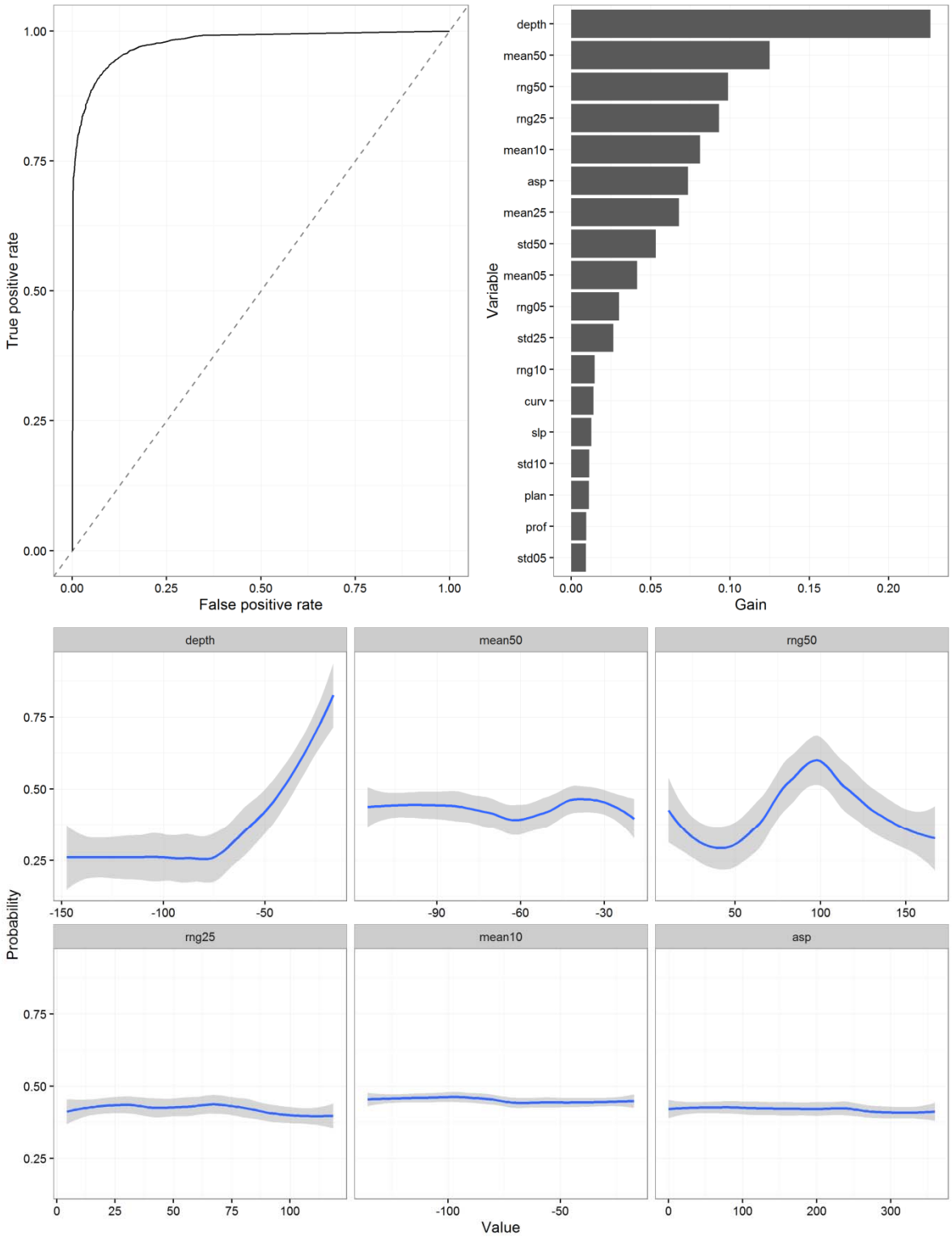

Figure A3.19: No modelled benthos - Towed real-time video model for shelf regions (with 50m binned multibeam and covariates) AUC performance plot (top left), relative measure of variable influence ("Gain") for improvement on model performance (top right) and partial response plots for the top 6 most influential model variables (bottom panel). For variable descriptions see Table 3 in the main report).

Addendum to the AIMS Barossa Environmental Baseline Study, Regional Shoals and Shelf Assessment Report[1]: regional biodiversity patterns and connectivity amongst the submerged shoals and banks in relation to the area of influence from a hypothetical uncontrolled release.

Connectivity

The shoals/banks in the Timor Sea and broader region share a tropical marine biota consistent with that found on emergent reef systems of the Indo West Pacific. Based on larval development rates, current speeds and the distance between various shoals, banks and reefs, a high level of interconnectivity is likely (1).

While larvae of many species are likely to actively influence their dispersal to some extent, usually in the direction of greater local retention, passive larval dispersal in surface currents is often used in the analysis of prevailing larval transport routes (1,2). Surface currents at the eastern and western end of the Sahul Shelf ,measured by AIMS using satellite tracked drifters (Heyward, unpublished data), demonstrate common speeds of 20-30 km/day during mild weather in the monsoonal periods, with much faster speeds measured during winter or modelled under cyclone modified conditions (1). Given the peak reproductive season for corals and many fish occurs over warmer months and noting that larvae may easily be competent for days to weeks (2,3), a planktonic dispersal range of 50-100 km is very plausible for many species in this region. The distribution of >150 shoal features across the Sahul Shelf, with individual shoals often separated by 5-20 km, suggests an extensive series of stepping stone habitats are available to recruit larvae from the plankton and connect these ecosystems at ecological time scales.

The bank and shoal features in Australian water within the modelled 'area of influence' from a large scale hydrocarbon release (Figure 1) are present at highest density west of the Barossa offshore development area along the outer portion of the continental shelf. These shoals and banks are likely to be highly interconnected by surface currents carrying species that produce pelagic larvae. Sources of larvae supply to the east would include a number of seabed features in Australian waters such as Lynedoch Bank, but importantly this region sits within the strong Indonesian Throughflow, providing a source of larvae from tropical benthic habitats from the Coral Triangle region (5).

Shoal and bank attributes - Ubiquity and Uniqueness

The submerged shoals and banks of the Sahul Shelf surveyed by AIMS to date (2, 6, Figure 1) have all supported a range of tropical biota typical throughout the region (6). A hierarchical cluster analysis of benthic communities in the Barossa Environmental Baseline Study 2015 Final Report showed that neighbouring shoals and banks (i.e. within 100s of km's) frequently share approximately 80% of benthic community composition whereas cross shelf (>200 km) there is less similarity (approximately 60%) between turbidity inshore areas and clearer water offshore shoals (Figure 1, 2 a and b). This pattern is driven by variation in the dominance of key habitats and species. The shallower depths, where sufficient light reaches the seabed, support benthic primary producers. These include various algae, corals and occasionally seagrass. Beyond those depths, usually at the margins on the steeper slopes of shoals and banks, filter feeders and detritivores become more prominent. In the clearer

oceanic waters of the outer continental shelf, consolidated substrate can support hard coral habitat in 10-60 m depths, with filter feeding fauna like sponges and seafans becoming dominant on rocky substrates below these depths. In mid-shelf locations where water clarity is reduced, the transition between primary producers and heterotrophic habitats is often observed at shallower depths due to reduced light reaching the seabed. The most influential determinants of the biota observed to date appear to be depth associated light intensity, substrate consolidation and substrate three dimensional complexity. Each of the shoals is likely to have the potential to support similar types of benthic habitats, dependent on extent of these underlying variables and the influence of the ecology of particular species and the local history of recruitment events and natural disturbances. Each shoal and bank has its own character in terms of species abundance and the relative contribution key taxa may make to the benthic community, but the same suite of habitats have been observed on multiple shoals and banks. Consequently the shoals and banks across the region represent a mosaic of benthic habitats, with variations in the abundance and distribution of both substrates and key species, but sharing many species in common.

While temporal datasets for the region's shoals are limited, changes from year to year on individual shoals have been observed (6). Available observations are consistent with the composition of the benthic assemblages being dynamic, in much the same way the bioregion's emergent coral reefs are (7) in response to natural disturbances such thermal stress events, storms and cyclones.

Cycles of natural disturbances and subsequent founder effects, particularly involving species that can propagate locally via asexual reproduction, may explain some of the variability between shoals. For example, monospecific stands of soft corals, seagrass or hard corals seen in some shoals but markedly lower levels of abundance of the same species have been observed on neighbouring shoals.

At the regional scale, therefore, the shoals and banks all support high levels of seabed biodiversity, but vary in the abundance and diversity of dominant benthic species, with subsets of species featuring more prominently on some than others. Similarly the associated fish fauna is highly diverse but variable between shoals (8), being influenced by depth, substrate and exposure to prevailing weather, though with all shoals sharing many species.

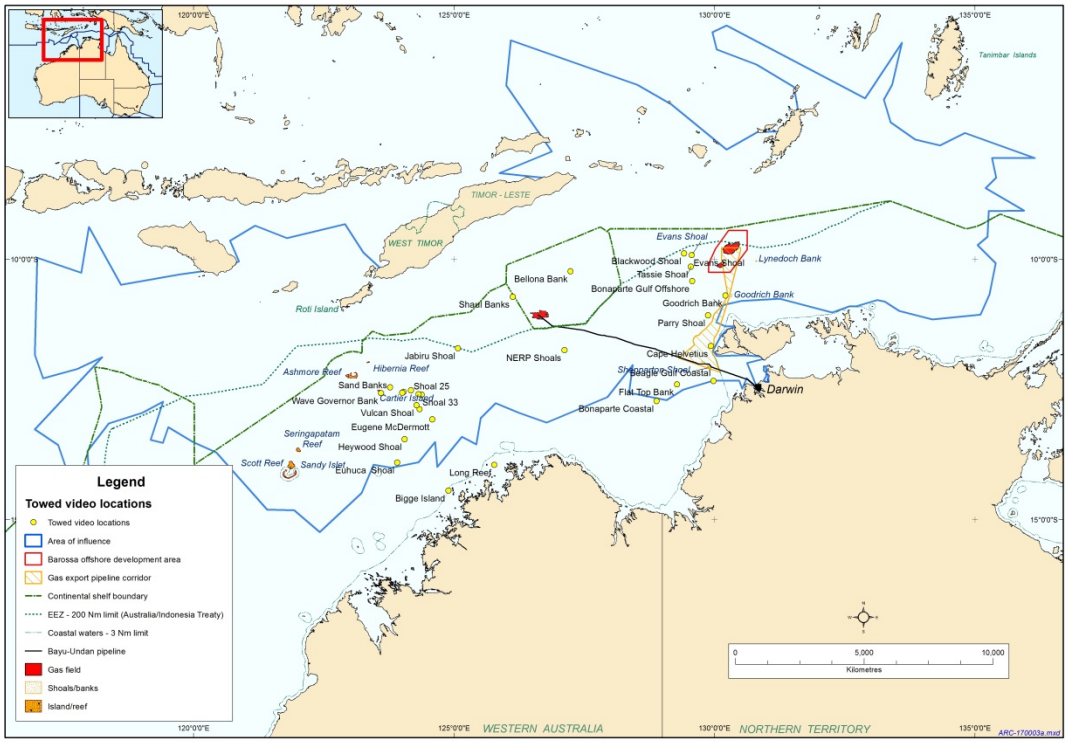

Figure 1: Regional towed video sites across the Sahul Shelf and adjacent coastal sites used in the "Barossa Environmental Baseline Study 2015 Final Report".

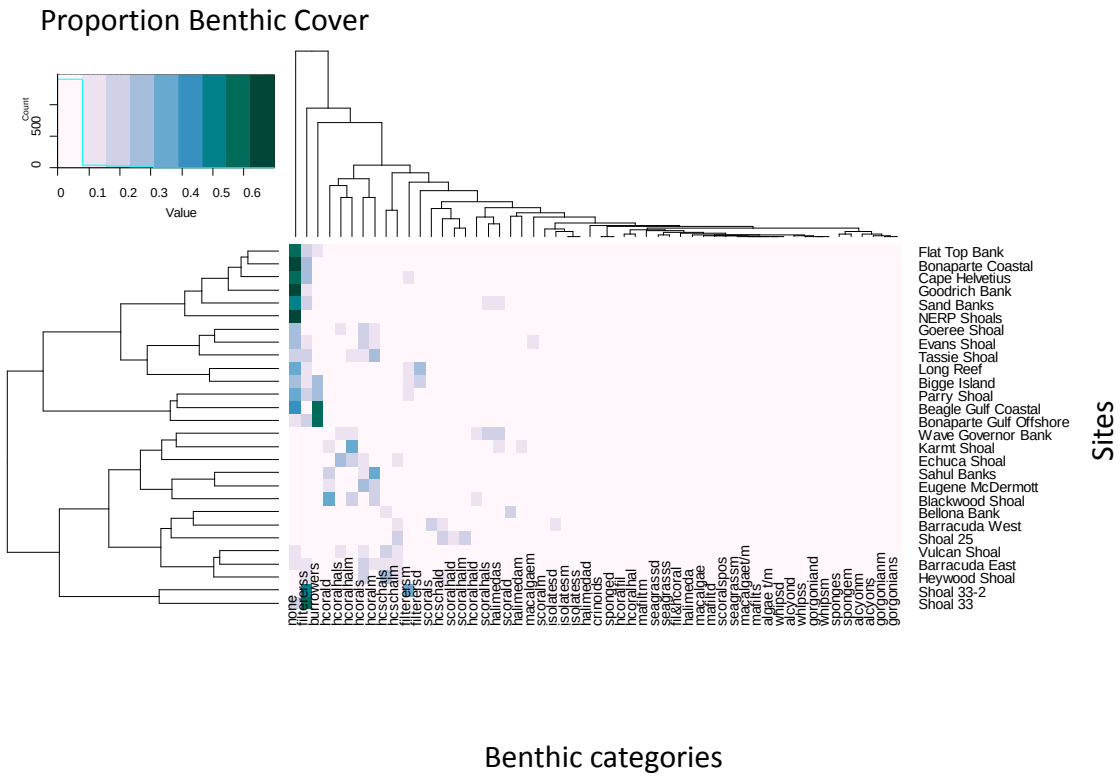

Figure 2 a) Euclidian distance based hierarchical cluster analysis of benthic categories and cover type from 20 towed video site surveys spanning ~900 km the Sahul Shelf and adjacent coastal sites.

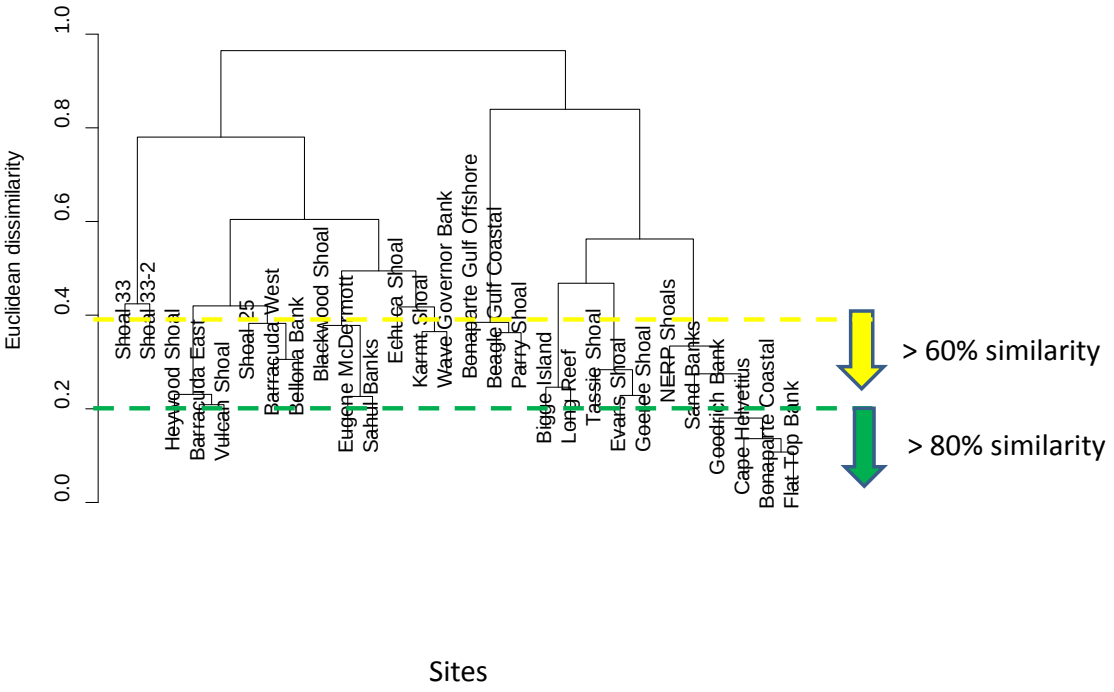

Figure 2 b) Annotation of cluster analysis in Figure a) clustering Sahul Shelf and adjacent coastal sites of sites based on 80% similarity and 60% similarity.

Connectivity has high potential between shoals and banks across the bioregion, with nearest neighbour shoals or banks likely to act as source reefs for shoals downstream. The coral triangle region to the north of the Barossa offshore development area, beyond the Australian Exclusive Economic Zone, is also a probable upstream source of tropical larvae for the region. With steady recruitment of marine larvae onto the region's shoals and banks, the key factors influencing the biodiversity and assemblage structures observed at any point in time on a particular shoal will include the depth, substrate type and complexity, hydrodynamic environment and position on the continental shelf. Some shoals or banks may be notable for the abundance of particular biota, but that status can be dynamic and available data points to many species being shared in common across the region. In terms of biodiversity all shoals and banks should be regarded as sensitive receptors.

Therefore, in the event of a large-scale hydrocarbon release, the spill response measures implemented to protect shoals would the same for all of these features, as the direct impact pathway is the same (i.e. contact with in-water hydrocarbons and/or dispersants), with the predominant factor determining the scale of potential impact being water depth. As was the case in the Montara uncontrolled release (6), an entrained pollutant potentially intersecting with the shoal and bank habitats would be a reasonable trigger for assessment and monitoring.

The Barossa Environmental Baseline Study 2015 findings and links to the CMR Benthic Habitat Model.

To infer a regional scale distribution of coarse benthic categories a habitat model was produced covering both the study area and the broader Bonaparte Basin. The regional habitat model was developed based on the Oceanic Shoals Commonwealth Marine Reserve benthic habitat model produced as part of the Australian National Environmental Science Programme (http://northwestatlas.org/node/1710). Both the Oceanic Shoals Commonwealth Marine Reserve benthic habitat model and the regional habitat model were developed as part of the National Environmental Research Project D1 (as descripted here http://maps.northwestatlas.org/files/montara/ html_popups_oceanic_shoals/ Spatial_benthic_habitat_model_for_the_Oceanic_Shoals_CMR_6dec16.pdf). This contains comprehensive habitat assessments at 18 field sites spanning 800 km of the oceanic shoals of the Sahul Shelf. The extension of the model included additional benthic habitat data held by AIMS and data collected as part of Barossa Environmental Baseline Study 2015 Final Report [2] and extends the model beyond the Oceanic Shoals Commonwealth Marine Reserve.

The regional scale habitat model results cover approximately 46,810 sq km and show a mosaic of habitats throughout the model domain. These habitats are dominated by Burrower/Crinoid soft sediment communities (making up ~23% of the total area) interspersed with no modelled biota present (category "None" making up ~ 69% of the total areas). There was also a lesser but significant amount of filter feeder communities (~6%) most commonly found in the east of the model domain within the bounds of the Oceanic Shoals Commonwealth Marine Reserve (OSCMR). Hard corals (including free living forms), soft corals, macroalgae and gorgonians all make up less than one percent of regional scale model by area. Their distribution is largely associated with the shoals, banks and emergent reefs in the northern extent of the study domain. However, hard coral also extends into areas of the OSCMR, with towed video analysis suggesting that this is most likely associated with isolates and free living coral forms. Alycon, seagrass, whips and Halimeda are marginal environments through the model domain with less than or equal to 0.1% by area.

A description of the how the model was developed and assessment of the model accuracy is provided in the Barossa Environmental Baseline Study 2015 Final Report (2). While all reasonable efforts are made to make model results as representative and accurate as possible, it's important to understand the assumptions and limitations when interpreting the regional habitat model results. For example a caution approach should be applied when interpreting results at fine scales (< 300 m), where validation information is not available and where the model performs poorly (Kappa values < 0.7). Model interpretation guidelines and limitations are detailed in Environmental Baseline Study 2015 Final Report (2).

References cited

1. Radford, Ben, Russ Babcock, Kimberly Niel, and Terry Done. "Are Cyclones Agents for Connectivity between Reefs?" Journal of Biogeography 41, no. 7 (2014): 1367–1378.

2. Heyward et al. 2016; Barossa Environmental Baseline Study 2015 Final Report. A report for ConocoPhillips Australia Exploration Pty Ltd by the Australian Institute of Marine Science, Perth 2016. 124pp

3. Roberts, C. 1997. Connectivity and management of Caribbean coral reefs. Science. 278(5342):1454-7

4. Heyward AJ, Negri AP (2010) Plasticity of larval pre-competency in response to temperature: observations on multiple broadcast spawning coral species. Coral Reefs 29: 631-636

5. Location map of the Coral Triangle. https://en.wikipedia.org/wiki/Coral_Triangle

6. Heyward, A et al 2011a; Monitoring Study S5 Banks and Shoals, Montara 2011 Offshore Banks Assessment Survey.: Report for PTTEP Australasia (Ashmore Cartier) Pty Ltd. Australian Institute of Marine Science, Townsville.

7. Gilmour et al (2013). Recovery of an isolated coral reef system following severe disturbance. 340(6128):69-71

8. Moore, C., Cappo, M., Radford, B. et al. (2017). Submerged oceanic shoals of north Western Australia are a major reservoir of marine biodiversity. Coral Reefs doi:10.1007/s00338-017-1564-y

9. Hosmer, D.W. and Lemeshow S. (2000) "Interpretation of the Fitted Logistic Regression Model." Applied Logistic Regression, Second Edition, pp 47–90.